Models and Methods for GTOC2

Analysis of a Multiple Asteroid Rendezvous Mission

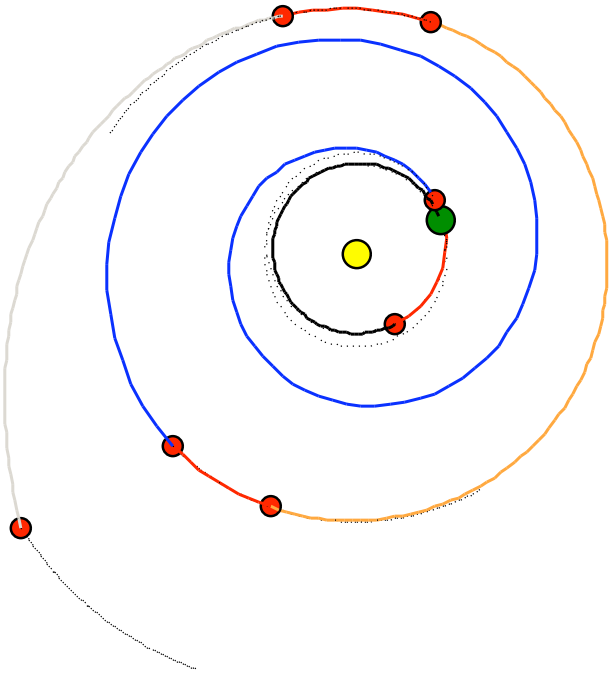

Hessel Gorter

22 February 2010

TU Delft
Delft University of Technology

Models and Methods for GTOC2

Analysis of a Multiple Asteroid Rendezvous Mission

Hessel Gorter

22 February 2010

Astrodynamics & Satellite Systems
Faculty of Aerospace Engineering
Delft University of Technology
Kluyverweg 1, 2629 HS Delft
The Netherlands

Astrodynamics & Satellite systems

Preface

It's 0:21 a.m., I am sitting behind my desk writing and streaming some tunes, as I have been doing for the past year or so. This report is finished but for the few lines you are reading now. Although a number of revisions still lay ahead, writing this provides a sense of closure. When I started a year ago, I had the naive and somewhat arrogant conviction that I would easily solve the complex problem that is being scrutinized in this report. This proved to be a healthy batch of optimism on my behalf. Problems piled up, errors were made and the amount of results obtained seemed inversely proportional to the amount of effort put into getting them. But choices were made, timetables adjusted and source code was debugged. Looking back, I am happy with the choices I made. They resulted in a solid research process, that was completed in time, and provided useful results.

On a personal note, I would like to thank a number of people without whom this project would not have been the same. First of all, of course, my supervisors Ron Noomen and Erwin Mooij. They were there when I needed them, and helped me with whatever I was stuck with. Also, their consideration and support for my future plans is much appreciated. Second, I would like to thank Marc Naeije for providing support on all IT related matters. Third, I would like to thank my friends from the ninth floor. The darts we played, coffee we had and especially the cake we ate made this thesis project apart from interesting also a lot of fun. Finally, I would like to thank the bunch of people with whom I consumed a huge amount of coffees, you know who you are. These coffee breaks helped me to reassess what I was doing and get frustrations out of my system.

I hope this report will be an interesting and informative read, and that it will kindle the same enthusiasm for the various topics that has driven me this past year.

Delft, January 26, 2010

Summary

The Global Trajectory Optimization Competition (GTOC) is a competition that seeks to stimulate improvements in the fields of mission analysis and optimization. Due to the increase in interest, the competition has become a good way to measure one's skills in solving complex mission analysis problems. In this report the problem posed in the second version of the competition, GTOC2, is investigated. The problem concerns an asteroid tour mission. Starting from Earth, four asteroids selected out of a total of 910, have to be visited. The total set of asteroids is divided into four groups, based on their physical and orbit characteristics. One asteroid from each set needs to be visited. Minimization of final mass over time of flight is sought.
At the point of departure of this thesis project, the Mission Analysis Department at the Faculty of Aerospace Engineering of the Delft University of Technology is efficient in coping with GTOC-like problems, and therefore can not successfully compete in the GTOC competition. This situation calls for a study of the GTOC2 problem and relevant solution methods. With this purpose in mind, the main research question is therefore formulated as follows:

What is the best way to handle the GTOC2 problem in order to find the optimal solution with the least amount of computational effort?

It is emphasized that the research focuses on finding a solution technique, rather than a solution of GTOC2. To answer this question as accurately as possible, the GTOC2 problem has been divided into three parts. The first part concerns the asteroid selection and sequencing. This problem is identified as an Exact Generalized Traveling Salesman Problem (EGTSP), which is a variant of a classic problem in combinatorial analysis, the Traveling Salesman Problem. To convert this problem into a GTOC2 model, the cities are replaced by asteroids, and the salesman by a spacecraft. The distances between the cities are calculated using three alternatives. One is a cost function based on the velocity budget, ΔV, required to match the orbital elements of the departure and arrival orbit, the second on the energy difference between the departure and arrival orbit, and the last cost function is the one implemented by ESA when participating in GTOC2. The cost function implemented by ESA is based on a three-burn transfer. Two methods will be employed to solve the EGTSP, the Nearest Neighbor Heuristic (NNH) and the Branch and Bound Method (B&B).
The second part of the problem concerns a phasing assessment of the sequences that were found after solving the first part of the problem. For this purpose, a continuous method based on exponential sinusoids was developed. Finding optimal solutions, using the exponential sinusoid model, was done by applying a Monte Carlo search, a Genetic Algorithm and an Interior Point Method consecutively.

The third part of the problem is to find a trajectory that fulfills the stringent constraints of the GTOC2 assignment. Due to time constraints, the third part will not be addressed in this research.

The results show that the B&B method outperforms the NNH on the same search space. Due to its efficiency, however, the NNH is able to cope with the complete set of 910 asteroids, whilst the B&B Method could only cope with a reduced set, with a size of about 60 asteroids. For, the cost function based on energy, the B&B results did outperform the results obtained by applying the NNH to the complete set.
When a selection of the sequences obtained by the GTOC2 participants was analyzed using a continuous method, it was found that such a continuous method could only be used to perform very rough assessments of the quality of the phasing of a sequence. Only the sequence ranking last, according to the GTOC2 results, was classified significantly worse than the sequences obtained by the other participants, including the winner.
The continuous method was applied to the sequences obtained by the NNH and B&B methods, using the three different cost functions, as well. This makes a total of six sets of asteroid sequences that were analyzed. The continuous results show that both methods, in combination with any of the cost functions, are able to come up with good solutions, except for the NNH in combination with the cost function used by ESA. The solutions obtained with a cost function based on energy proved to be the most volatile. The continuous results for the sequences obtained using the B&B method in combination with the ΔV and ESA cost functions produced results similar to those for the sequences obtained by the GTOC2 participants. The continuous results for the sequences obtained using the NNH in combination with the cost function based on ΔV slightly outperformed the continuous results for the sequences obtained by the GTOC2 participants.

Of the methods analyzed in this report, the NNH method applied to the complete cost matrix, in combination with a cost function based on ΔV, proved to be the most efficient in consistently finding good asteroid sequences. The developed B&B algorithm was not able to cope with the complete cost matrix. Results suggest, however, that if a more advanced B&B approach is developed, one that is able to cope with the complete cost matrix, it will most likely outperform the NNH method.
The continuous method, was, in its current state, unable to perform an accurate phasing assessment of asteroid sequences. The obtained solutions contained large constraint violations, which makes it impossible to make any accurate observation regarding phasing. The developed method can only be used to confirm the sequences obtained when solving the first part of the problem. Improvements of the continuous method are needed to increase the accuracy of the model and solution method.
Although the third part of the main question was not cover by the research in this report, the order of magnitude of the constraint violations do indicate that finding a trajectory fulfilling the GTOC2 constraints requires a far more accurate and powerful solution method than the ones investigated here.
It is advised not to attempt to solve the GTOC2 problem in the framework of one MSc thesis. The required solution methods are quite involved and require significant amounts of time to develop and test. Instead it is advised to divide the problem in two or three parts.

It is also advised to not participate in the GTOC competition until a toolbox containing the basic mission analysis tools is available. The time available to solve the GTOC assignment (one month) is far too short to develop the required tools.

Contents

List of Figures

List of Symbols

Latin Symbols

a	Semi-major axis	$[m]$
a	Acceleration	$[m/s^2]$
c	Cost of an individual transfer	$[-]$
c	Cosine	
$\mathbf{C}$	Cost matrix	$[-]$
d	Distance	$[m]$
e	Eccentricity	$[-]$
E	Set of edges in a graph	$[-]$
$\mathcal{E}$	Energy	$[J]$
f	Function	$[-]$
F	Thrust	$[N]$
g	Constraint function	$[-]$
g_0	Gravitational acceleration at Earth's surface	$[m/s^2]$
G	Graph	$[-]$
H	Hamiltonian	$[-]$
i	Inclination	$[deg]$
i	Counter, identifier	$[-]$
I_{sp}	Specific impulse	$[s]$
j	Counter, identifier	$[-]$
J	Objective/Cost function	$[-]$
k	Counter, identifier	$[-]$
k_0	Scaling parameter for exponential sinusoid	$[-]$
k_1	Dynamic range parameter for exponential sinusoid	$[-]$
k_2	Winding parameter for exponential sinusoid	$[-]$
L	Lagrangian	$[-]$
L	Linear	$[-]$
M	Mass	$[kg]$
N	Number of edges	$[-]$
N	Number larger than the sum of all elements in a cost matrix	$[-]$
N	Number of vertices	$[-]$

P	Specific problem	$[-]$
P	Penalty function	$[-]$
$\mathbb{P}$	Problem set	$[-]$
Q	Quadratic	$[-]$
r	Position	$[m]$
s	Sine	$[-]$
s	Slack variable	$[-]$
V	Velocity	$[m/s]$
V	Set of vertices in a graph	$[-]$
ΔV	Velocity mismatch or increment	$[m/s]$
$\mathbf{V}_\infty$	Hyperbolic excess velocity	$[m/s]$
x	Input variable	$[-]$
Z	Zero in the cost matrix	$[-]$

Greek Symbols

α	Difference in argument of pericenter	$[deg]$
α	Thrust angle w.r.t. flight path	$[deg]$
γ	Flight-path angle	$[deg]$
λ	Lagrange multiplier	$[-]$
μ	Gravitational Parameter, GM	$[m^3/s^2]$
μ	Barrier parameter	$[-]$
φ	Angular distance in departure orbit	$[deg]$
ψ	Angular distance in arrival orbit	$[deg]$
ω	Argument of pericenter	$[deg]$
Ω	Right Ascension of the Ascending Node (RAAN)	$[deg]$
θ	True Anomaly	$[deg]$
θ	Transfer angle	$[deg]$

Coordinates

x, y, z	Cartesian coordinates
r, θ	Polar coordinates

Indices

0	At initial time
1	At departure
2	At arrival
a	At apoapsis
f	At final time
p	At periapsis
sub	Subgraph
$\dot{}$	Derivative w.r.t. time
$\ddot{}$	Double derivative w.r.t. time
$*$	Optimum
$'$	Transformed variable
$\bar{}$	Repeating every 2π
$\odot$	Sun

General Notations

$\mathbf{x}$	Vectors are indicated by bold lower case letters
$\mathbf{X}$	Matrices are indicated by bold capitals
$\frac{\partial f}{\partial x}$	Partial derivative of function f with respect to x
$x \in \{S\}$	x is an element of set S
$deg(i)$	Degree of vertex i
∇	Gradient operator

List of Acronyms

Abbreviations and Acronyms

AP	Assignment Problem
ACT	Advanced Concepts Team
AU	Astronomical Unit
B&B	Branch and Bound algorithm
BC	Boundary Condition
BFS	Best First Search
CNES	Centre National d'Etudes Spatiales
DFS	Depth First Search
DV	ΔV
DUT	Delft University of Technology
EGTSP	Exact Generalized Traveling Salesman Problem
ESA	European Space Agency
ESTEC	European Space Technology Center
GA	Genetic Algorithm
GMV	Grupo Mechanica Vuelo
GTOC	Global Trajectory Optimization Competition
GTSP	Generalized Traveling Salesman Problem
HA	Hungarian Algorithm
HQP	Huge Quadratic Programming
JPL	Jet Propulsion Laboratory
LB	Lower Bound
LIFO	Last In First Out
MC	Monte Carlo
MJD	Modified Julian Date
NNH	Nearest Neighbor Heuristic
OC	Optimality Condition
PC	Process Count
PSO	Particle Swarm Optimization
SQP	Sequential Quadratic Programming
TOF	Time Of Flight
TOS	Time Of Stay
TSP	Traveling Salesman Problem
UB	Upper Bound

Chapter 1

Introduction

The Global Trajectory Optimization Competition (GTOC) is a competition that seeks to stimulate improvements in the fields of mission analysis and optimization. It was first organized in 2005 by ESA's Advanced Concept Team [*ESA*, 2005]. Over the past few years, the interest in the GTOC competition has increased significantly. The large number of participants makes this competition a good way to directly measure one's skills in solving complex mission analysis problems.
This research is performed under the auspices of the Mission Analysis Department at the Faculty of Aerospace Engineering of the Delft University of Technology (DUT). At this point the department is not efficient in coping with GTOC-like problems, and therefore cannot successfully compete in the GTOC competition. MSc students have been attempting to solve the second version of the competition, GTOC2, but were unsuccessful. Large constraint violations were still present in the solutions obtained by [*Evertsz*, 2008]. This situation calls for a study of the GTOC2 problem and relevant solution methods.
In this report the GTOC2 will be investigated. The problem concerns an asteroid tour mission. Starting from Earth, four asteroids selected out of a total of 910, have to be visited. The total set of asteroids is divided into four groups, based on their physical and orbit characteristics. One asteroid from each set has to be visited. This problem was selected by JPL, the organizer of GTOC2, not only because of its complexity, but also because of a more practical reason. Asteroids have earned an increase in interest from the scientific community, because it is expected they provide information about the formation of our solar system.

The research presented in this report sets out to gain more understanding of the GTOC2 problem and to formulate an advise on how to solve it. With this purpose in mind, the main research question is formulated:

What is the best way to handle the GTOC2 problem in order to find the optimal solution with the least amount of computational effort?

To answer this question as accurately as possible, the GTOC2 problem will be divided into three parts. The first part concerns the discrete aspect of the problem, being the asteroid selection and sequencing. This problem is identified as a variant of the Exact Generalized Traveling Salesman Problem (EGTSP), where the cities are being replaced by asteroids, and the salesman by a spacecraft. The distances between these cities will be determined using three different cost functions. The first cost function is based on the velocity budget required to match all orbit

elements of the departure orbit with the elements of the target orbit. It was selected as an attempt to improve the results of the other two cost functions. The second cost function is based on an energy difference between two asteroid orbits. It was selected because of an observation made about the GTOC results. This will be explained in chapter 2. The last cost function is the cost function implemented by ESA when solving the GTOC2 problem. It is based on a three-burn transfer and was selected here to compare the sequences obtained by the other methods used in this research and the sequences obtained by ESA when participating in GTOC2. Note that the cost functions do not consider the phasing aspect of the transfers. Now that the asteroid selection and sequencing problem is identified as a combinatorial analysis problem, solution techniques from this field can be employed to solve this problem. Two solution methods will be investigated. The Nearest Neighbor Heuristic (NNH), for its low computational cost, and a more involved Branch and Bound (B&B) algorithm, because it generally outperforms the NNH. For the latter method, the problem needs to be transformed from an EGTSP into a standard Traveling Salesman Problem (TSP).
The second part of the problem considers the continuous aspect of the problem, being a phasing assessment of the sequences that were found after solving the first part of the problem. There are two options for the orbit model when performing such an assessment, one is a numerical model, the other an analytical model. Since it is known beforehand that this method will have to cover a lot of ground, it is opted to use the computationally more efficient analytical orbit model. There are three options for the analytic model, being the exponential sinusoids [*Petropoulos et al.*, 2004], the inverse polynomials [*Wall and Conway*, 2009] and a pseudo-spectral model [*Vogeleer*, 2008]. Parallel to the research performed in this report, another project at the Faculty of Aerospace Engineering of the Delft University of Technology was performed in which a multileg exponential sinusoid orbit model was developed. In order to save time, this model was converted to the needs of this research, thereby automatically choosing for an exponential sinusoid model. The MATLAB optimizer toolbox will be used to solve the continuous aspect of the problem.
The last part of the problem is finding a trajectory that fulfills the stringent constraints of the assignment. Due to project time constraints, the third part will not be addressed in this research.

This report is written under the assumption that the reader is familiar with the fields of astrodynamics and optimization. For an introduction in both fields the reader is referred to [*Gorter*, 2009]. Theory that is needed to perform this research, and is not typically part of an undergraduate mission analysis program, will be introduced.
To answer the main question, first the GTOC2 assignment will be presented and analyzed in Chapter 2. In this chapter the topics that will be scrutinized in this report are identified as well. Because basic knowledge about combinatorial problems and analysis is required, relevant topics from this field are included in Chapter 3. With the concepts presented here, it is possible to construct a model for the discrete aspect of the GTOC2 problem. This discrete model, as well as a model for the continuous aspect of the GTOC2 problem, will be constructed in Chapter 4. Chapter 5 will present the techniques used to solve both the discrete and the continuous aspect of the problem. In order to assess the validity of the designed models and methods, a number of benchmark tests are performed in Chapter 6. The results of the performed analyses will be presented in Chapter 7 and chapter

8 will draw conclusions based on these results. Recommended starting points for future research will be included in Chapter 8 as well.

Chapter 2

GTOC2 Analysis

This chapter will introduce the GTOC2 competition [*NASA*, 2006]. First, the assignment will be described. Second, the models and solution methods used by the GTOC 2 participants will be stated. The chapter concludes with a number of observations relevant to the research presented in this report.

2.1 The GTOC2 Assignment

To make sure the goal of the GTOC competition is reached (improving mission analysis tools) certain criteria are imposed on the design of the assignment itself [*Petropoulos*, 2007]. First, the global design space has to be large, including a large number of local minima. Second, the objective function or constraints has to be unusual, so no existing software can tackle the problem. Third, the problem needs to be solvable within 3 or 4 weeks. The last criterion is that the solutions need to be verifiable easily [*Petropoulos*, 2006]. The winner of the competition befalls the honor of organizing the next round of the competition and with that, also the definition of the new assignment. The winners of GTOC over the years are [*ESA*, 2005]:

GTOC1 (2005): JPL
GTOC2 (2006): Politecnico di Torino
GTOC3 (2007): CNES
GTOC4 (2009): Moscow State University

The assignment for GTOC2, handed out by JPL, will provide the framework for the research in this report.

The assignment of GTOC2 concerns the design of a multiple asteroid rendezvous mission, using low-thrust propulsion only. The spacecraft has to rendezvous with one asteroid out of each of the four predefined groups of asteroids. Maximization of the final spacecraft mass over flight time is sought, which leads to the objective function given by 2.1 [*Petropoulos*, 2006]:

$$J = \frac{m_f}{t_f} \tag{2.1}$$

The constraints of the problem are:

- A hyperbolic excess velocity when leaving Earth, $\mathbf{V}_\infty$, of no more than 3.5 km/s in any direction.
- Launch window is between 2015 to 2035.
- A stay time of at least 90 days is required at the first three asteroids; only a flyby at the fourth asteroid is required.
- The time of flight of the total mission must be less than 20 years.
- No gravity assists are permitted.
- Initial spacecraft mass is 1500 kg of which 1000 kg is propellant. The truster has an I_{sp} of 4000 s and has a maximum thrust level of 0.1 N.
- A rendezvous is considered successful when the spacecraft is within 1000 km of the asteroid and matches its velocity within 1 m/s for 90 days, upon departure and arrival. The flyby is successful when the position is matched within 1000 km of the fourth asteroid.

The orbits of all asteroids of the GTOC2 assignment are presented in Figure 2.1.

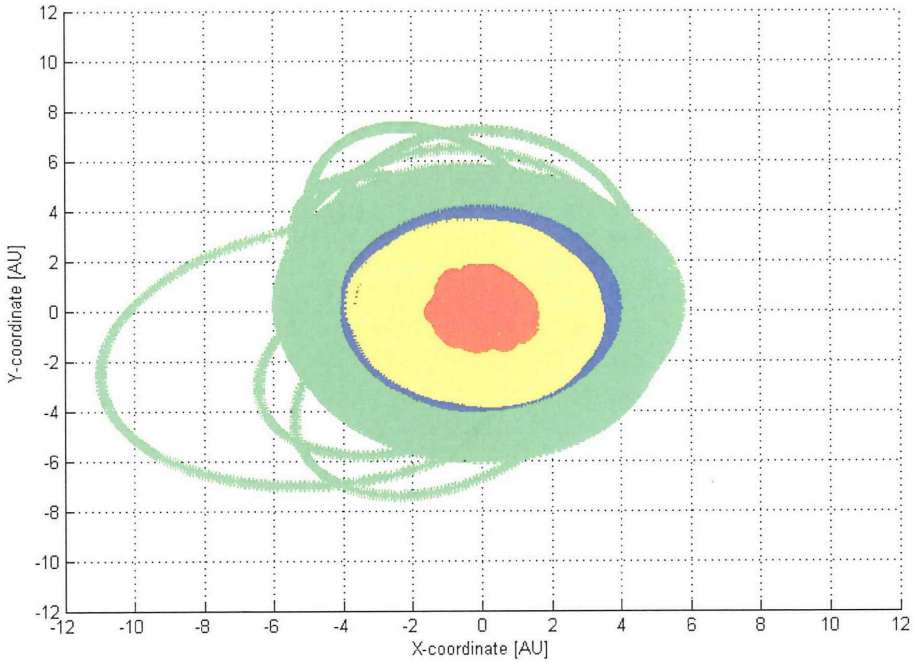

Figure 2.1 Visualization of the asteroid orbits. The image is a top view of the ecliptic plane. The different colors indicate the different asteroid groups. Group 1 = green, group 2= blue, group 3 = yellow, group 4 = red [*Evertsz*, 2008].

2.2 GTOC2 Models, Methods and Results

The models and methods used by the different teams during the competition are summarized in Figures 2.2 and 2.3. Because the different participating teams all tackled the problem in at least two steps, two figures are presented. Figure 2.2 shows models and methods for finding the asteroid sequence. Figure 2.3 shows models and methods used for finding the final low-thrust orbit. The rank numbers

in each of the two figures correspond with each other. Thus, for each competitor (with a certain rank) the method for the first step is presented in Figure 2.2 and the method for the second step is presented in Figure 2.3. The tables are constructed based on a discussion of the GTOC2 results presented in [*Petropoulos*, 2007]. Unfortunately, openness and sharing of knowledge is not part of the nature of the mission analysis community and only brief statements of the models and methods used during GTOC2 are available, with the exception of ESA, who published their cost function used for asteroid selection in the paper [*Izzo et al.*, 2007]. Other than that, only the information about the used methods in Figures 2.2 and 2.3 is available. Extensive descriptions of the models and methods mentioned in Figures 2.2 and 2.3 are given in [*Gorter*, 2009].

Rank	Asteroid selection and sequencing
1	Heuristics and Edelbaum approximation using phasing.
2	High-thrust Lambert solutions between asteroids.
3	Branch- and Prune with and without phasing. Model: Lambert arcs and exposins.
4	Use one leg as reference and check phasing with other asteroids for other legs.
5	1: Phase free based on variation of orbital elements and high-thrust. 2: Low-thrust on one leg including phasing.
6	Low-thrust model analyzed with neural networks.
7	GA and PSO on Lambert arcs, exposin for 2nd leg.
8	Dynamic programming, three consecutive times on diffent criteria.
9	High-thrust Lambert arcs.
10	Unknown
11	Heuristics on inclination and semi-major axis

Figure 2.2 GTOC2: Models and methods for analyzing mission scenarios.

Rank	Trajectory optimization
1	Indirect method solved with multiple shooting.
2	Pontryagin's Maximum principle and continuation.
3	First Differential Evolution, followed by Nonlinear Programming.
4	1: Impulsive model evaluated using direct method. 2: Low-thrust solved by maximum principle.
5	Lawden's implicit guidance scheme, local optimization by Genetic Algorithm or Simplex.
6	Nonlinear Programming, solved with software package (SNOPT).
7	Direct method using either multiple shooting or collocation.
8	Unknown
9	Pontryagin's Maximum principle using multiple shooting.
10	GA and MATLAB optization toolbox (fminsearch).
11	Direct transcription

Figure 2.3 GTOC2: Models and methods for obtaining final low-thrust orbit.

The results of the competition are included in Appendix A. The attained objective values range from a little under 30 to almost 100 kg/year. The corresponding total time of flights are for the best 8 candidates near 10 years and the corresponding fuel budgets range from about 580 kg to 680 kg. Ranks 9 to 11 have, relatively speaking, longer time of flights and higher fuel consumptions. The group order of the best results obtained by each participant is 4-3-2-1, with the exception of GMV, that found a group order of 4-2-3-1. Not all participants use the 3.5 km/s available when departing Earth.

2.3 Observations Regarding the Results of the GTOC2 Participants

The first thing that becomes obvious from looking at the applied models and methods is that, as mentioned before, every team divided the problem into two parts. The first part of the problem is to establish the asteroid sequences. This is the discrete aspect of the GTOC2 problem. These sequences are mainly obtained using low-fi methods. Often these methods are not based on low-thrust characteristics, but use impulsive, high-thrust models and Lambert targeting-like techniques, which are easier and quicker to evaluate than a low-thrust trajectory.

An important part of the asteroid selection and sequencing procedure is assessing the phasing characteristics of an asteroid sequence. A sequence that is considered promising without considering its phasing characteristic might become unattractive when its phasing characteristics are considered. Assessing phasing characteristics further decreases the set of candidate solution sequences. Most teams combined the asteroid selection, sequencing and phasing analysis process. Of teams ranking 1st, 3rd, 5th and 11th it is known, however, that they separated the asteroid selection and sequencing from the phasing analysis. Because this research focuses on analyzing the GTOC2 problem itself and is trying to determine what it is that makes this problem so complex, it is chosen to split the asteroid selection and sequencing analysis from the phasing analysis.

The second part in the solution procedure is to find the actual trajectory passing the selected asteroids in the determined order, without violating the mission constraints. The method of choice to solve the trajectory was, for most participants, a calculus-based method. Either a direct or an indirect approach was adopted. The time frame imposed on the research performed in this report, unfortunately, did not permit an accurate analysis of the actual trajectory. Implementing an accurate direct or indirect method is not straightforward and should be the subject of a separate research project.

It was observed that the group sequences obtained by the winners is either 4-3-2-1 or 4-2-3-1. Together with the asteroid orbits shown in Figure 2.1, this shows that the optimal trajectories obtained by the participants travel outward with respect to the Sun. In other words the group sequences are ordered with increasing amount of orbital energy. This makes sense because travelling to a sequence with lower orbital energy followed by one with a higher orbital energy is inefficient. For this reason, one of the cost functions analyzed in this report is based on energy.

Another observation is that using heuristics is only useful when applied modestly and carefully. Although the winner applied heuristics, there is a number of other teams that applied heuristics too but were not as successful. In Figures 2.2 and 2.3, only the teams that found valid solutions are listed. There were a few other teams (including the Delft University of Technology team) that used heuristics on orbital elements (for example plane changes larger than a certain limit were discarded) to determine the asteroid sequence, but were not very successful by doing so. The winners used heuristics to establish bounds on parameters. For example, the winner of the second competition used the observation that a group of asteroids with low energy and low inclination passed through their perihelia

within a window of two years, repeated every 8 years [*Petropoulos*, 2007]. The second heuristic they used was a stepping approach in determining the scenario. This means that they gave preference to sequences of which the apoapsis of the previous leg was close to periapsis of the next leg.

Chapter 3

Combinatorial Problems and Analysis

The problem of determining which asteroids to visit and in what order classifies as a combinatorial optimization problem. This chapter will introduce the relevant problems and solution methods from the field of combinatorial analysis.

When the phasing characteristics of the asteroid sequence are disregarded (i.e. a time-independent formulation is chosen) the sequencing problem reduces to an Exact Generalized Traveling Salesman Problem, or EGTSP. To describe the EGTSP, two other combinatorial problems will be introduced. The first is the most general of combinatorial problems, called the Assignment Problem (AP). Based on the AP another classic problem in combinatorial mathematics, the Traveling Salesman Problem (TSP), will be introduced. The EGTSP is a variant of the TSP.
Three methods that will be useful when analyzing the discrete aspect of the GTOC2 problem will be described. The Hungarian Algorithm (HA) is used to solve APs. The Branch-and-Bound algorithm (B&B) and the Nearest Neighbor Heuristic (NNH) can be used to solve TSPs. Since the AP and TSP are closely related, it is not surprising that the solution methods for these problems will be related as well. The B&B calls the HA once every iteration.
An overview of the relations between the combinatorial problems and the solution methods is given in Figure 3.1. It is emphasized that the figure is not exhaustive and it does not give a solution procedure, but merely an overview of relations. The total solution procedure of the EGTSP will be discussed in section 5.1.1.

3.1 Basic Graph Theory

This section will introduce relevant topics from the field of graph theory. This theory is used as a mathematical basis to formulate and solve a wide range of combinatorial problems. This section is written based on [*Hartmann and Weigt*, 2009]. For a more extensive introduction about graph theory the reader is referred to any introductory literature readily available on the topic, for example [*Hartmann and Weigt*, 2009] or [*Bondy and Murty*, 2009].

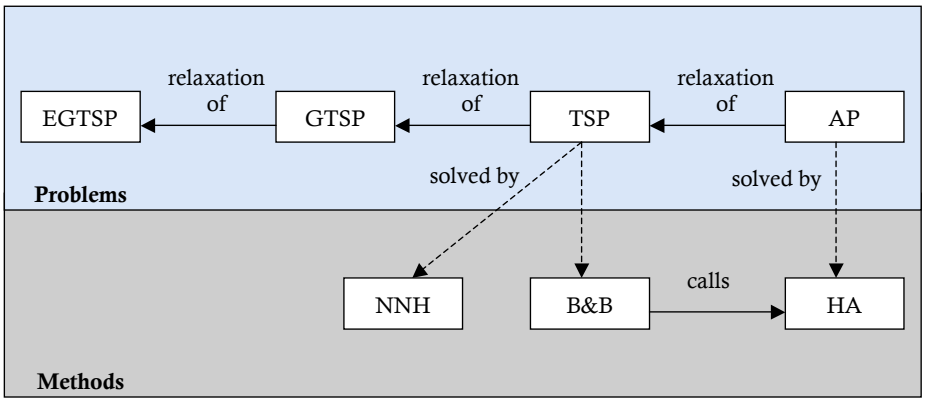

Figure 3.1 Relations between combinatorial problems and solution methods

A graph G is a mathematical identity given by its vertices $i \in V$ and its undirected edges $\{i, j\} \in E \subset V$:

$$G = (V, E) \tag{3.1}$$

Note that in a graph of this form $\{i, j\}$ and $\{j, i\}$ denote the same edge. A graph of this form is also known as an undirected graph, since the direction in which the edges have to be traversed is not prescribed. An edge for which the direction is fixed is called an arc. A visual example of a graph is given in Figure 3.2. Now

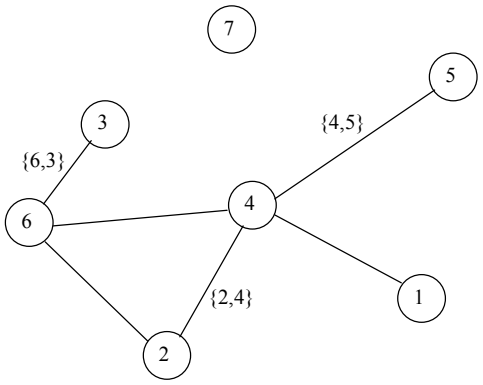

Figure 3.2 Example of a Graph. Vertices are denoted by circles, edges by lines.

that the concept of a graph has been introduced a number of characteristics can be described [*Hartmann and Weigt*, 2009].

- The order $N = |V|$ counts the number of vertices, and the size $M = |E|$ counts the number of edges.
- Two vertices are adjacent if $\{i, j\} \in E$ (for example, vertices 4 and 5 in Figure 3.2 are adjacent, 1 and 2 are not).

- The degree of vertex i, $deg(i)$, equals the number of adjacent vertices. Vertices of zero degree are called isolated (for example, vertex 7 in Figure 3.2 is isolated, and the degree of vertex 4 is four).

With a graph completely defined it is possible to introduce a few new concepts.

- A graph is called a subgraph G_{sub} of G if $V_{sub} \subset V$ and $E_{sub} \subset E$.
- A subgraph G_{sub} is a path of G if it has the form $V_{sub} = \{i_0, i_1, \ldots, i_l\}$, $E_{sub} = \{\{i_0, i_1\}, \{i_1, i_2\}, \ldots, \{i_{l-1}, i_l\}\}$. The length of the path is $l = |E_{sub}|$. i_0 and i_l are called endpoints.
- A path with $i_0 = i_l$ is called a cycle.
- A cycle visiting every vertex of a graph exactly once is called a Hamiltonian cycle. Note that a Hamiltonian cycle is a subgraph of the graph it cycles through.
- A weighted graph $G = (V, E, \mathbf{C})$ is a graph with edge weights described in $\mathbf{C}$. An edge weight describes the cost of traversing a certain edge. $\mathbf{C}$ is also known as the cost matrix.

The introduced characteristics and concepts will be useful when modeling the GTOC2 problem. Their physical meaning will be stated when applied.

3.2 The Assignment Problem

Suppose we have n agents and n tasks that need to be completed. Completing a specific task by a specific agent will have a certain cost. The assignment problem (AP) is the problem of assigning n tasks to n agents, such that the total cost of completing all tasks is minimal. Each agent is only allowed to complete one task. This problem can be described using a weighted graph and can be summarized in matrix form. In this case the agents and assignments are described by vertices and all possible combinations of agents and jobs are described by a set of edges. An example of an AP composed of three tasks (P,Q,R) and three agents (A,B,C) is shown in Figure 3.3 [*Pilgrim*, 2009]. The graph describing this problem is of order 6, because it involves 3 tasks and 3 assignments. There are 9 entries

	P	Q	R
A	1	2	3
B	2	4	6
C	3	6	9

Figure 3.3 Example of an AP with 3 tasks (horizontal) and 3 agents (vertical) [*Pilgrim*, 2009].

(9 possible combinations of agents and tasks), each representing an edge. This means that the size of the graph is 9. In this example, the entries in the matrix represent the cost of performing a certain task (weight of a certain edge) by a certain agent. For example, assigning task P to agent B will cost 2, assigning task Q to agent A will cost 2 and assigning task R to agent C will cost 9. The total cost

of completing all these tasks by the assigned agents is 13. This division of tasks between the different agents, however, is not the one with the lowest total cost. Trying different combinations of tasks and agents for this very simple example will lead to the result that the lowest cost is 10, which is obtained by assigning agent A to task R, agent B to task Q and agent C to task P. When the number of tasks and agents increases it becomes more difficult to solve this problem by trial and error. Fortunately there are algorithms available for solving APs. One of them is the Hungarian Algorithm, which will be discussed in section 3.4.

3.3 The Traveling Salesman Problem and its Variations

Suppose we have n cities each separated by a certain distance. Consider a salesman who has to visit each city exactly once to sell its merchandise. The salesman wants to find the shortest path connecting all cities such that he will have to travel the least amount of distance. This problem is adequately called the Traveling Salesman Problem (TSP) [*Winston*, 2004]. The TSP can also be described by a weighted graph and summarized in matrix form. In this case, the vertices represent the various cities and the edges describe the cost (e.g. distance, financial cost or time) of every possible transfer between any two cities. Each entry in the matrix represents an arc (each entry represents a directed edge between two vertices, i.e. each entry represents a connection between two cities that is traversed in a fixed direction). Since the diagonal represents irrelevant transfers to and from the same city, the diagonal entries are equal to infinity. An example of the problem is shown in Figure 3.4. The TSP can be regared as a constrained AP. The constraint that is

	A	B	C	D	E
A	∞	132	217	164	58
B	132	∞	290	201	79
C	217	290	∞	113	303
D	164	201	113	∞	196
E	58	79	303	196	∞

Figure 3.4 Example of a symmetric Traveling Salesman Problem with 5 cities [*Winston*, 2004].

added to the AP is that the solution of the AP has to be a Hamiltonian cycle: all vertices (cities A to E) need to be visited exactly once. Note that this implicitly means that the salesman returns to the city it started from. To give a physical meaning to this constraint, consider not just one salesman but one salesman in every city. Each salesman has to be assigned to go to one city. This is an AP. Adding the constraint that the solution to the AP has to be cyclic, means that all transfers by all agents (the salesmen) can be performed sequentially.
There is a characteristic of the TSP that deserves some attention. This characteristic is the (non-)uniqueness of the solution. It is possible to have multiple optimal solutions. In this case different paths exist with the same total cost (same total

distance, l, travelled). In Figure 3.4 it can be checked that there are multiple optimal solutions. The total cost of these solutions is 668, and the two corresponding cycles are: $A \rightarrow C \rightarrow D \rightarrow B \rightarrow E \rightarrow A$ and $A \rightarrow E \rightarrow B \rightarrow D \rightarrow C \rightarrow A$. Taking a closer look at these solutions reveals that the (Hamiltonian) cycles are identical but traversed in the opposite direction. These two solutions are both possible because this is a symmetric problem: the cost matrix is symmetric across its diagonal. Another way of looking at this is that although the entries in the matrix describe a set of arcs (a specific edge traversed in a specific direction) each arcs' opposite (the same edge but traversed in the opposite direction) is also present in the matrix. This basically reduces the TSP to an undirected graph. On such a graph Hamiltonian cycles exist that can be traversed in opposite directions. Concluding, if the problem is symmetric at least two solutions exist that describe the same Hamiltonian cycle but traverse it in opposite directions.
There are several variants of the TSP. Amongst others, the asymmetric TSP, where the cost matrix of the problem is not symmetric across its diagonal, or the bottleneck TSP where the distance the salesman is allowed to travel between two cities is limited. Due to these variants, the TSP has many very practical applications in real-life. For example the TSP can be used to model truck routing problems for transportation companies. The asymmetric TSP can be used when a truck is not allowed to go back to a city in exactly the same way (because of one way streets for example) and the bottleneck TSP can be practical when realizing that a truck has a limited amount of fuel, and that the distance it is allowed to travel between cities is limited by the distance it can cover on one tank of gas.
There is one variant of the TSP which considers the cities to be clustered. This variant is known as the Generalized Traveling Salesman Problem (GTSP) or Traveling Politician Problem. The GTSP is the problem of finding the shortest route visiting each *state* exactly once. The GTSP is thus a constrained TSP. There is a stronger formulation of this problem which not only demands that each state is visited exactly once, but also that exactly one city of each state is visited. This stronger form of the GTSP is called the Exact Generalized Traveling Salesman Problem or EGTSP. Note that it is not necessary for the groups to be detached. A city can belong to two groups. Although this is not possible when considering actual cities and states (a city is always located in either one state or the other), it can be of relevance for other real-life problems. Remember that the cities and connections refer to edges and vertices in a graph theory formulation, which are mathematical identities rather than physical objects.
The EGTSP can be stated in matrix form as well. An example is given in Figure 3.5. In this example city A and B belong to one state (state X), city C and D to a second state (state Y) and city E, F and G belong to a third state (state Z). In Figure 3.5 it is shown how these states are implemented in the cost matrix. Since the Salesman is not allowed to travel in between cities that are in the same state these connections are set to infinity (basically these edges are removed from the graph). In this way an optimal solution will never include any of these connections since the total cost of the solution would become infinity as well, which is of course a non-feasible solution. There are several methods to solve the TSP. Two of them are the NNH and the B&B algorithm. The B&B method in section 3.5, the NNH will be described in section 3.6.

	A	B	C	D	E	F	G
A	∞	∞	5	7	4	6	2
B	∞	∞	8	9	3	1	5
C	6	3	∞	∞	4	2	4
D	2	1	∞	∞	5	6	1
E	9	7	9	3	∞	∞	∞
F	8	4	6	5	∞	∞	∞
G	4	7	9	7	∞	∞	∞

Figure 3.5 Example of a Generalized Traveling Salesman Problem with 7 cities (A to G) divided over 3 states [*Behzad and Modarres*, 2002]

3.4 Hungarian Algorithm

The Hungarian Algorithm (HA), sometimes referred to as Munkres' Assignment Algorithm, is used to solve assignment problems. The algorithm presented here is a modification of the original algorithm presented by James Munkres in 1957 [*Munkres*, 1957] and makes it able to deal with rectangular cost matrices instead of square matrices. First, the actions for each step will be stated and the order in which they are executed. After the algorithm has been described, an example solution of an AP will be given that details the implementation of each step.

The steps presented are from [*Pilgrim*, 2009]. The algorithm describes the manual manipulation of a two-dimensional matrix by starring and priming zeros and by covering and uncovering rows and columns. The method is of polynomial runtime complexity, meaning it can solve an AP in $\mathcal{O}(M^k)$ steps, where M is the problem size (number of vertices) and k is some constant. This is opposed to exponential time where the problems are solved in $\mathcal{O}(k^M)$ steps. The steps of the algorithm will be stated here. For a more extensive description of the algorithm the reader is referred to [*Pilgrim*, 2009].

The algorithm contains six steps. These steps will not necessarily be performed in the presented order. Some of the steps will be repeated or executed in a different order if that is required to solve the problem. Figure 3.6 shows the process flow of these steps.

- **Step 0:** Create an n×m matrix called the cost matrix C in which each element represents the cost of assigning one of n workers to one of m jobs. If needed, rotate the matrix so that there are at least as many columns as rows and let K=min(n,m). Go to step 1.

- **Step 1:** For each row of the matrix, find the smallest element and subtract it

from every element in its row. Go to step 2.

- **Step 2:** Find a zero (Z) in the resulting matrix. If there is no starred zero in its row or column, star Z. Repeat for each element in the matrix. Go to step 3.

- **Step 3:** Cover each column containing a starred zero. If K columns are covered, the starred zeros describe a complete set of unique assignments. In this case, go to DONE, otherwise, go to step 4.

- **Step 4:** Find a noncovered zero and prime it. If there is no starred zero in the row containing this primed zero, go to step 5. Otherwise, cover this row and uncover the column containing the starred zero. Continue in this manner until there are no uncovered zeros left. Save the smallest uncovered value and go to step 6.

- **Step 5:** Construct a series of alternating primed and starred zeros as follows. Let Z_0 represent the uncovered primed zero found in step 4. Let Z_1 denote the starred zero in the column of Z_0 (if any). Let Z_2 denote the primed zero in the row of Z_1 (there will always be one). Continue until the series terminates at a primed zero that has no starred zero in its column. Unstar each starred zero of the series, star each primed zero of the series, erase all primes and uncover every line in the matrix. Return to step 3.

- **Step 6:** Add the value found in step 4 to every element of each covered row, and subtract it from every element of each uncovered column. Return to step 4 without altering any stars, primes, or covered lines.

- **DONE:** Assignment pairs are indicated by the positions of the starred zeros in the cost matrix. If C(i,j) is a starred zero, then the element associated with row i is assigned to the element associated with column j.

To illustrate the operations of the algorithm, all the steps of the solution of the AP example of Figure 3.3 are included in Figure 3.7. Some observations regarding the HA have to be made. The algorithm will work even when the minimum values in two or more rows are the same. It will also work when two or more rows contain the same values in the same order. In fact the algorithm is able to deal with a matrix in which all the values are the same, although this is not a very interesting problem. The most important thing, however, is that optimality is guaranteed [*Pilgrim*, 2009].

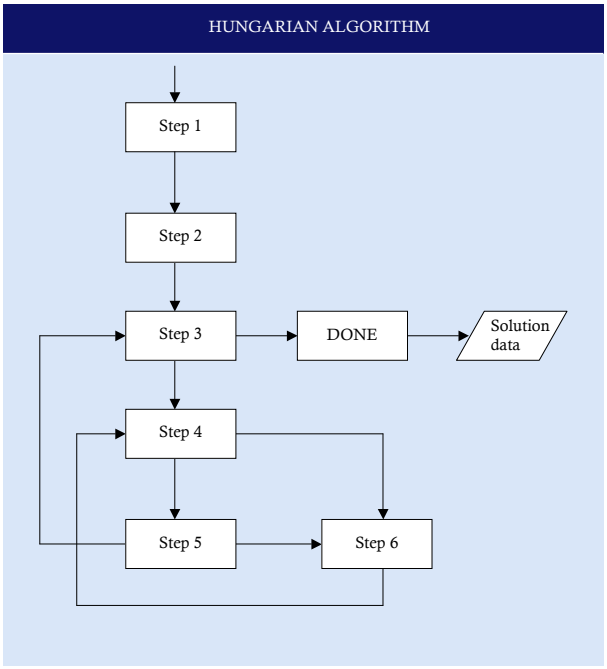

Figure 3.6 Process flow of the Hungarian Algorithm.

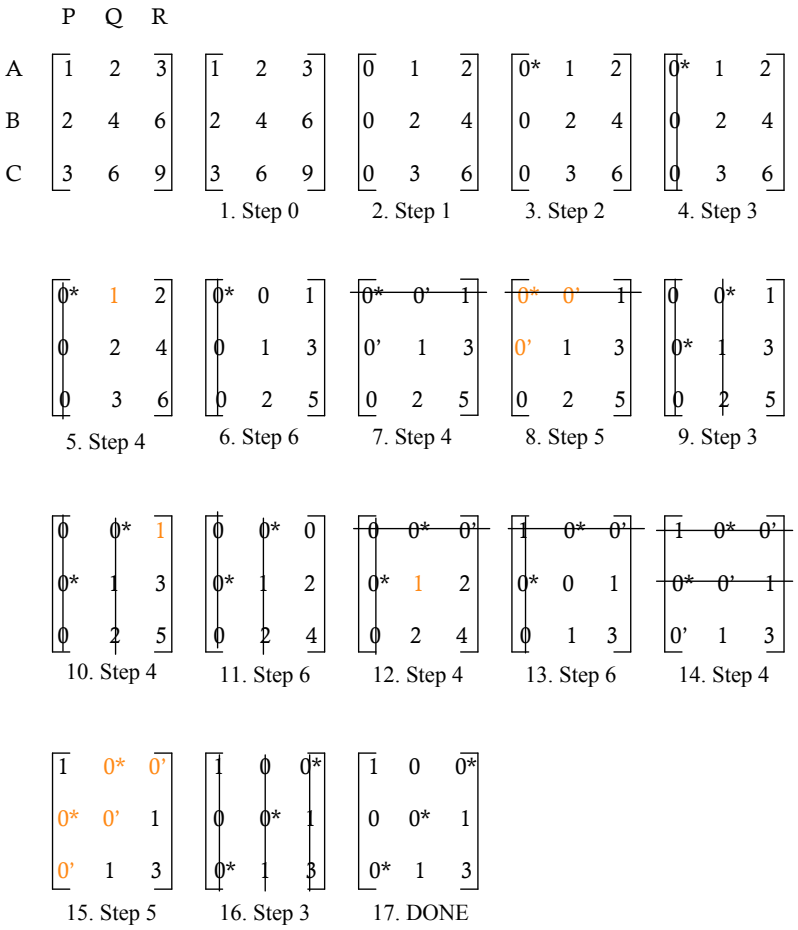

Figure 3.7 Example execution of the Hungarian Algorithm of problem presented in figure 3.3.

3.5 Branch-and-Bound Algorithm

A Branch-and-Bound (B&B) algorithm performs a structured search of the solution space. It is suitable for solving discrete (constrained) optimization problems. The B&B method starts with the initial problem and converts it to an easier subproblem. Then it starts solving and creating new subproblems until the original problem is solved. The algorithm only pursues options that meet a certain criterion. This criterion is usually the best objective value so far (the so-called upper bound). In section 3.5.1 a mathematical formulation of the BB algorithm will be presented. It is based on a survey performed by Lawler and Wood at the University of Michigan [*Lawler and Wood*, 1966]. In section 3.5.2 the example TSP from figure 3.4 will be solved using the B&B algorithm. Finally, some comments concerning the B&B will be given.

3.5.1 Mathematical Formulation and Solution Procedure

The general approach of the B&B algorithm is to substitute a 'difficult' problem by a sequence of smaller simpler problems. The benefit lies in the fact that subproblems with suboptimal results can be disregarded for further analysis and hence the search space is reduced. The starting point is a 'difficult' constrained optimization problem (problem P_0) also called node 0:

$$min\ J_0(x) \tag{3.2}$$

subject to:

$$\mathbf{g}_0(x) \geq 0 \tag{3.3}$$

$$x \in X_0 \tag{3.4}$$

Problem P_0 is replaced by a set of easier problems $\mathbb{P} = \{P_1, P_2, .., P_N\}$ that bounds problem P_0, such that the following boundary condition (BC) holds:

BC: There exists at least one optimal solution x_0^* of problem P_0, such that x_0^* is feasible for at least one problem $P_j \in \mathbb{P}$ and $J_j(x_0^*) \leq J_0(x_0^*)$

Suppose that an optimal solution x_j^* to each problem in $\mathbb{P}$ is obtained, and that x_k^* indicates the overall optimum:

$$J_k(x_k^*) = min_{P_j \in \mathbb{P}} J_j(x_j) \tag{3.5}$$

Then x_k^* is also an optimal solution of P_0 if the following optimality conditions (OC) are met:

OC1: x_k^* is a feasible solution to problem P_0.
OC2: $J_k(x_k^*) = J_0(x_k^*)$, i.e. the Objective value of the subproblem is the same as the objective value of the initial problem when using the same solution (x_k^*).

If not both of the optimality conditions are satisfied, the problem corresponding to the current optimal solution (P_k) is substituted by a new set of problems $\mathbb{P}_k$. These subproblems are represented by new nodes in the B&B tree.

Imposed on this new set of bounding problems is the requirement that the BC, as well as a convergence conditions, are still satisfied. The convergence condition can be formulated in a weak or strong way:

Weak Condition: For each problem $P_j \in \mathbb{P}_k$, either x_k^* is infeasible for P_j or $J_j(x_k^*) > J_k(x_k^*)$.
Strong Condition: For each problem $P_j \in \mathbb{P}_k$ and each feasible solution x to problem P_k, either x is infeasible or $J_j(x) > J_k(x)$.

These conditions state that the current optimal solution (of the parent problem) is either an unfeasible solution for the newly generated subproblems or that the current optimal solution will generate a worse objective value for the newly generated subproblems, compared to the solution value it returned for the parent problem. This way, the current optimal solution of the parent problem is not generated again by any of the subproblems. These conditions do not guarantee that an optimal solution will be found. However, they do represent a minimal condition such that progress towards a final solution is made. The process is visualized in Figure 3.8. During the B&B process it is possible to find

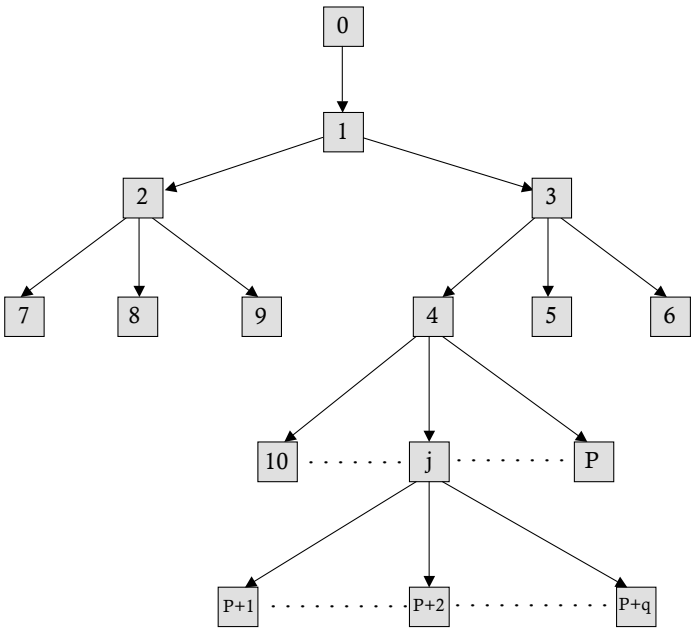

Figure 3.8 Branch-and-Bound Process.Each square indicates a node/subproblem. Based on [*Lawler and Wood*, 1966].

several subproblems that have equal optimal solutions and represent the overall optimum at a specific intermediate stage. These problems are classified as active, while problems who's optimum is larger than the intermediate overall optimum are designated as terminated. For example, in Figure 3.8, problem 4 is active while problems 5, 6, 7, 8 and 9 are terminated. The complete description of a B&B algorithm requires two more elements on top of the process described so far. One is the rule, which is used to select which of the currently active problems

is used for branching. The second is the method for deriving new bounding problems (the node splitting technique).

There is a limited amount of options for selecting which active problem is to be evaluated next. Three options are listed here [*Froushani and Yusuff*, 2009]:

- **Option 1:** Select an active problem at random.
- **Option 2:** Depth First Search (DFS), selects a problem of the last created set of subproblems. This option is also known as the Last-In-First-Out method, or LIFO.
- **Option 3:** Best First Search (BFS), selects one of the active problems which branch had the lowest cost so far. It is likely to have more than one active problem for which this holds, since each node will probably branch in more than one way.

The choice for using either DFS or BFS is made easier if experience with these methods was available. However, at the current state of the research, this experience is not available. Therefore, the choice is made based on logic. The DFS approach (option 2) will be implemented, because of two reasons. First, it requires less computer memory because storing the branch values is not needed (which is the case if the third option is chosen). Second, not every node of the tree represents a candidate solution. If the BFS method is chosen, it might get stuck in a maze of unfeasible solutions with good objective values.
Another method that is sometimes applied in B&B algorithms is including arcs with a low cost, because these arcs are considered to be good. This method fixes good arcs it comes across when solving the subproblems, such that they are a part of the solution of the newly generated subproblems. It is chosen not to implement this technique, because in the problem considered in this report good arcs are not necessarily present in the optimal solution.
The method for deriving new bounding problems (also know as the branching rule) is based on constraint addition. Whenever a new subproblem is created, the constraints of the parent subproblem are copied and an additional constraint, based on the result of the evaluation of the parent subproblem, is added.
To make the B&B algorithm more tangible, the next section will cover the solution procedure for the example TSP of Figure 3.4 using the B&B algorithm.

3.5.2 Example Solution of TSP

This section will detail the solution procedure of the TSP example of Figure 3.4 using the B&B algorithm. The entire process will require seven iterations of the B&B algorithm and thus a total of 7 subproblems will be generated and solved. The subproblems are APs and the HA is used to solve the APs. The process is shown in Figure 3.9. Every node (subproblem) contains the following information:

- PC: This is short for process count. It indicates the order in which the algorithms solves the various subproblems.
- J: Objective value obtained by HA when solving the corresponding subproblem.
- UB: This is short for upper bound. It is the best value found so far by the B&B algorithm.

- Assignment pairs: The right column contains the assignment pairs as determined by the HA.

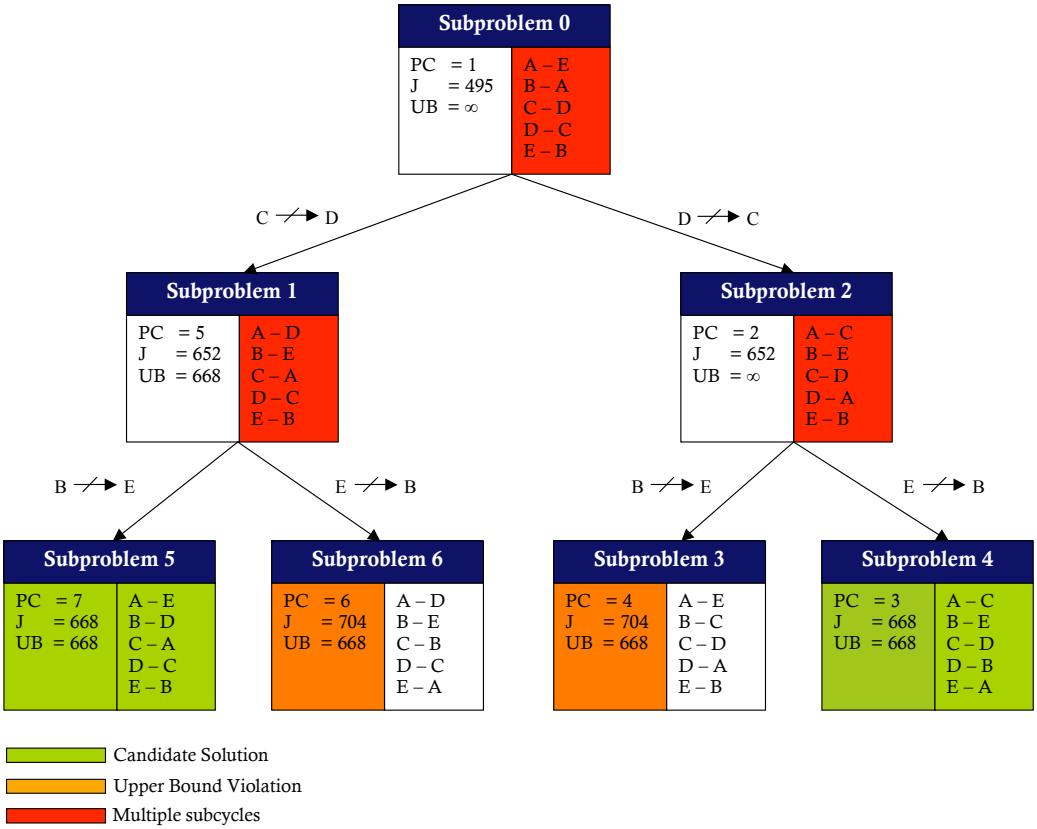

Figure 3.9 Branch-and-Bound process for TSP example of figure 3.4.

The cost matrices corresponding to these seven subproblems are included in Figure 3.10. Subproblem 0 is exactly the same as the TSP, with the exception that the solution does not have to be cyclic. This is the relaxation of the 'difficult' TSP into a 'simpler' AP. In fact the TSP corresponds to node 0 in Figure 3.8 and subproblem 0 corresponds to node 1 in Figure 3.8. The UB is set to infinity. This way, the UB will be updated when a candidate solution to the initial TSP is found, because the obtained candidate solution will certainly have a better objective value than infinity.

After the initial subproblem is formulated, it is solved using the HA. The solution consists of an objective value J, which is the sum of the costs of the assignment pairs as specified in the right column of each subproblem. If this solution of the AP is a valid solution of the original TSP (optimality condition 1 of section 3.5.1) and the cost of the of the solution of the AP is equal to the cost of the TSP (optimality condition 2) then the original TSP is solved. Optimality condition 1 demands that the solution of the AP is a valid solution for the TSP. This means that the solution of the AP should be cyclic. This is however not the case. If the assignment pairs of the solution of subproblem 0 are considered it is observed that they contain two subcycles: A→E→B→A and C→D→C. Optimality condition 1 is not satisfied by the solution of subproblem 0, because the solution is not a valid solution for the TSP (the solution is not a Hamiltonian cycle). Since no candidate solution is found for the initial problem the UB remains infinity.

The next step is to create a new set of subproblems ($\mathbb{P}$)in which the solution of

Subproblem 0

∞	132	217	164	58
132	∞	290	201	79
217	290	∞	113	303
164	201	113	∞	196
58	79	303	196	∞

Subproblem 1

∞	132	217	164	58
132	∞	290	201	79
217	290	∞	∞	303
164	201	113	∞	196
58	79	303	196	∞

Subproblem 2

∞	132	217	164	58
132	∞	290	201	79
217	290	∞	113	303
164	201	∞	∞	96
58	79	303	196	∞

Subproblem 3

∞	132	217	164	58
132	∞	290	201	∞
217	290	∞	113	303
164	201	∞	∞	196
58	79	303	196	∞

Subproblem 4

∞	132	217	164	58
132	∞	290	201	79
217	290	∞	113	303
164	201	∞	∞	196
58	∞	303	196	∞

Subproblem 5

∞	132	217	164	58
132	∞	290	201	∞
217	290	∞	∞	303
164	201	113	∞	96
58	79	303	196	∞

Subproblem 6

∞	132	217	164	58
132	∞	290	201	79
217	290	∞	∞	303
164	201	113	∞	196
58	∞	303	196	∞

Figure 3.10 Cost matrices for subproblems created during example solution of TSP problem of figure 3.4.

subproblem 0 (x_k^*) is infeasible. The solution of subproblem 0 consisted of two sub cycles. These sub cycles are not allowed in the TSP solution, hence the choice is made to select one of the sub cycles and use each link as a constraint for the new subproblems. In this way it is impossible for any future solutions to contain this subcycle and hence a step is made in the direction of finding one cycle containing all nodes, which is a valid solution of the original problem. The shortest cycle is chosen to create new subproblems. This choice is made because it will result in the least amount of subproblems (this is beneficial when the algorithm is implemented on a computer system). In this case the shortest subcycle is C→D→C. Since this cycle consists of two links, two new subproblems are created, one in which the link C→D is not allowed and one in which the link D→C is not allowed. These constraints are implemented by setting the corresponding assignment in the cost matrix to infinity.

To select the next subproblem that will be solved by the algorithm the DFS approach is used. This means that the latest created subproblem will be analyzed first. In this case subproblem 2 was created last and will be selected for the next iteration of the B&B algorithm.

Solving subproblem 2, by using the HA, also results in a optimal solution containing subcycles. In this case the shortest subcycle is B→E→B. Again these links are transformed into constraints for creating subproblems 3 and 4. According to the DFS approach subproblem 4 should be solved next.

The solution of subproblem 4 contains no subcycles and hence is a valid solution

for the original TSP. At this point it is not known if this solution is the best overall solution of the TSP. All that is known is that this solution is a valid solution for the TSP. The cost J of this solution is 668. This is the best solution value found so far and hence the upper bound (UB) is set to 668. This means that whenever a solution of a subproblem is higher, this branch will be excluded from further analysis. This is because the HA returns optimal solutions of the AP. Adding constraints to this AP will only make the problem more complex. Hence the cost J of any solution (obtained by the HA) of a similar AP with additional constraints will never improve.
DFS dictates that the next subproblem to be solved is subproblem 3. The optimal solution of this subproblem has a cost of 704. This is higher than the current upper bound of 668 and hence this branch will be excluded form further analysis. The only subproblem left for analysis is subproblem 1. The solution costs 652 which is less than the current upper bound of 668 and hence it is still possible to find a solution which better or equal to the current best of 668. Branching again on its shortest subcycle B→E→B, creates subproblems 5 and 6. Subproblem 6 is solved next, resulting in a valid solution. The cost is 704, which is no improvement of 668, and this branch is excluded from the tree. Subproblem 5 however, does result in a valid solution matching the current optimal solution of 668. Hence there are two valid optimal solutions of the TSP.

3.5.3 Comments

There exists no overall B&B application suited for all types of combinatorial problems. The B&B should be tailored to the problem at hand. The effectiveness of the B&B depends to a great extent on its node-splitting techniques. Creating overlapping subproblems should be avoided if possible. If overlapping problems are created, the search space is not pruned efficiently or not at all, in which case the B&B will get into an infinite process. The method of creating subproblems as detailed in the example of section 3.5.2 does not prevent the creation of duplicate subproblems.
Also the selection method for deciding which subproblem to analyze next is important. When analyzing a problem using the B&B algorithm, the user has two options. One is to start the algorithm and wait until it has evaluated all active nodes. In this case it is better to use a DFS approach because, as mentioned before, it requires a little less computer memory. The other is to start the algorithm and stop it at a prespecified time. In this case the current lowest upper bound (the best candidate solution) and the lowest lower bound (the best invalid solution), specify a range for the optimal solution. When this approach is used it might be better to start evaluation branches with the lowest costs so far instead of selecting the last one created. This increases the chance of the algorithm to find good solutions in a reasonable amount of time.
Since we are not interested in a range for the objective value but actual valid and good solution cycles which cannot be derived from a certain range, it is opted to create an algorithm that is able to evaluate all active nodes. The drawback of this approach is that it will limit the problem size (i.e. the number of asteroids being evaluated) that can be analyzed using the B&B algorithm. This is due to two reasons. The first is that it will take the HA significantly more time to solve the APs. The second is that an increase in problem size will results in an increase in

the amount of subproblems. This will become problematic when considering the fact that computer memory is limited.

3.6 Nearest Neighbor Heuristic

The Nearest Neighbor Heuristic (NNH), also known as the greedy algorithm, is an alternative to the B&B for solving a TSP. Since the algorithm is very basic, it is a faster method than the B&B. The quality of the result, however, depends greatly on the search space (defined by the cost function used to model the problem) and the starting position. It will be investigated if the NNH is a useful alternative to the B&B for solving the discrete part of the GTOC2 problem.
The NNH is a very straightforward method. A starting point is selected, and from there the edge or arc with the lowest cost is traversed to the next vertex. From there on to the next vertex with the lowest cost, and so on. To increase the robustness of this method, a multi-start approach can be chosen. This means that the NNH is not merely run from one starting point, but for all vertices in the graph. This approach is sometimes referred to as a multistart NNH.

As an example, the TSP from Figure 3.4 will be solved using the multistart NNH. The first step is to set the diagonal entries to infinity. Although their actual cost might be 0, this number is not allowed because when looking for the cheapest transfer 0 will always be the lowest, hence this vertex will always be chosen. Instead, it is desired that the arcs with a cost of 0 are not chosen at all and hence they are set to infinity. In this case, when looking for a minimum, these arcs will never be included.
For two starting points (A and B) the entire procedure will be shown. The results for the other three points are stated as well and left for the reader to verify.
In Figure 3.11 the NNH steps are highlighted and the order of the visited vertices is indicated by bold numbers. In this case point A is the starting point. The cost

		A	B	C	D	E
1	A	∞	132	217	164	58
3	B	132	∞	290	201	79
5	C	217	290	∞	113	303
4	D	164	201	113	∞	196
2	E	58	79	303	196	∞

Figure 3.11 NNH process for TSP example of Figure 3.4, starting from city A.

matrix shows that the cheapest transfer from point A is to point E with a cost of 58. Then from row E the nearest vertex is B with a cost of 79. From there on it is to D with a cost of 201, and C with a cost of 113. To complete the Hamiltonian cycle the link form C to A is added with a cost of 217. The total cost of this path is

668. Now considering B as a starting point, the cycle becomes B→E→A→D→C, with a total cost of 704. This cycle is shown in Figure 3.12 As mentioned, every

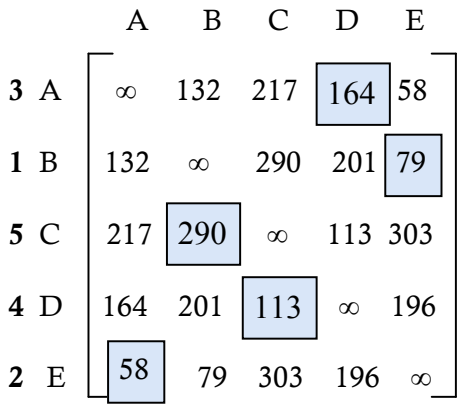

Figure 3.12 NNH process for TSP example of Figure 3.4, starting from city B.

city can be considered as a starting point. This method is known as the multistart NNH. The results for the multistart NNH are summarized in Figure 3.13.

Start	City 2	City 3	City 4	City 5	Cost
A	E	B	D	C	668
B	E	A	D	C	704
C	D	A	E	B	704
D	C	A	E	B	668
E	A	B	D	C	807

Figure 3.13 NNH results for TSP example of Figure 3.4.

Figure 3.13 shows that the optimal solution for the TSP is A→E→B→C→D→A. The solution is found twice, once starting from A and once starting from D. Interestingly, this result is the same as the optimal solution that was found when solving this problem using the B&B. In this particular example, the NNH is a good alternative for the B&B because the same solution is obtained with less effort. The reason why the NNH requires less effort is straightforward. The NNH only uses simple heuristics, whilst the B&B algorithm calls the HA several times. The latter is intrinsically a more complex method than the NNH and requires multiple matrix manipulations, making it computationally more expensive.

Chapter 4

Models for GTOC2

This chapter will present the models that will be used for analyzing the GTOC2 problem. First, the model for the discrete part of the problem, the asteroid selection and sequencing, will be described, followed by a description of the continuous model, that will be used for assessing phasing characteristics of asteroid sequences.

4.1 Discrete Model

Solving the asteroid sequencing problem for GTOC2 closely resembles the EGTSP problem: the asteroids are divided into four groups based on their physical properties and exactly one asteroid from each group needs to be visited. The problem will be stated in matrix form. Instead of the cities A, B, ... etc, the matrix columns and rows now describe asteroid 1, asteroid 2, ... etc. The entries represent the cost for traveling from asteroid i to asteroid j. The cost of traveling from one asteroid to another in the same group is set to infinity. At this point there are four issues left regarding the modeling of the GTOC2 problem with an EGTSP model:

- Calculating the cost of each individual transfer.
- Including Earth in the model.
- The size of the problem. The B&B algorithm cannot cope with the complete cost matrix.
- The complexity of solving an EGTSP.

The first two issues are related to the model. The last two issues are related to the method used to solve the problem. These four issues will be addressed in the next sections.

4.1.1 Cost Functions

The entries in the cost matrix represent the costs of all possible transfers. This section will present the functions used to calculate these transfer costs. The most important thing regarding the costs is that they need to be time independent. The reason for this is that the algorithm which will be used to solve the problem is not able to cope with changing values in the cost matrix. The constraint of time-independency implicates that phasing of one asteroid with respect to another

cannot be taken into account since this would require information about the position of the asteroid in its orbit and this position is not constant over time. To determine a transfer cost that is independent of time, the orbital elements can be used, because these elements are constant. The orbital plane of each asteroid and the shape of their orbits are constant.
Three cost functions will be analyzed: one based on energy, one based on ΔV, and one will be the cost function as used by ESA to select their asteroids during GTOC2.

Energy
The cost function will be the sum of the energy required to transfer from the orbital plane of the departure asteroid to the orbital plane of the target asteroid ($\Delta\mathcal{E}_{plane}$) and the difference in orbital energy between the orbits of the departing and target asteroid ($\Delta\mathcal{E}_{orbit}$).

The total orbital energy, the sum of the potential and kinetic energy, is given by the Vis-Viva relation [*Wakker*, 1997]:

$$\mathcal{E} = \frac{V^2}{2} - \frac{\mu}{r} = -\frac{\mu}{2a} \tag{4.1}$$

where $\mathcal{E}$ is the total orbital energy, μ is the gravitational parameter of the Sun, V is the velocity and a is the semi-major axis. The difference in total orbital energy between two asteroids then becomes [*Wakker*, 1997]:

$$\Delta\mathcal{E}_{orbit} = \left(\frac{-\mu}{2a_1}\right) - \left(\frac{-\mu}{2a_2}\right) = -\frac{\mu}{2}\left(\frac{a_2 - a_1}{a_1 a_2}\right) \tag{4.2}$$

The energy required to change the orbital plane is obtained by adding the ΔV required to change the inclination, i, and the right ascension of the ascending node, Ω. This ΔV is then translated into energy by using the relation between kinetic energy and the velocity of an object. The ΔV required to change the inclination of the orbit is given by:

$$\frac{\Delta V_i}{V_1} = 2\sin\left(\frac{1}{2}\Delta i\right) \tag{4.3}$$

and the ΔV required to change Ω is:

$$\frac{\Delta V_\Omega}{V_1} = 2\sin\left(i_1\right)\sin\left(\frac{1}{2}\Delta\Omega\right) \tag{4.4}$$

In these equations V_1 indicates the velocity of the body in the departure orbit. It is assumed that the plane change is done as efficiently as possible, meaning that the transfer is executed in the apocenter. Hence V_1 indicates the apocenter velocity in the departing orbit. This velocity is given by:

$$V_1 = \sqrt{\frac{\mu}{r_{a1}}(1 - e_1)} \tag{4.5}$$

Substituting this relation for V_1 in equations 4.3 and 4.4 gives:

$$\Delta V_i = 2\sqrt{\frac{\mu}{r_{a1}}(1 - e_1)}\sin\left(\frac{|i_2 - i_1|}{2}\right) \tag{4.6}$$

$$\Delta V_\Omega = 2\sqrt{\frac{\mu}{r_{a1}}(1-e_1)}\sin(i_1)\sin\left(\frac{|\Omega_2-\Omega_1|}{2}\right) \tag{4.7}$$

The sum of these ΔVs is the total ΔV required to change the orbital plane. Because the change in orbital energy is proportional to the change in velocity, a relation is required between velocity and energy. The simplest relation between velocity and energy is the kinetic energy law, hence this was used to convert the velocity into energy. Applying the ΔV at pericenter provides the largest increase in energy, because the velocity is highest at this point [1]. For this reason the ΔV was applied at perigee.

Whether the ΔV is added to the pericenter velocity or subtracted, depends on the semi-major axis of the departure and arrival orbit.
If $a_2 > a_1$:

$$\Delta\mathcal{E}_{plane} = \frac{1}{2}(V_{1,p}+\Delta V_{tot})^2 - \frac{1}{2}(V_{1,p})^2 \tag{4.8}$$

If $a_2 < a_1$:

$$\Delta\mathcal{E}_{plane} = \frac{1}{2}V_{1,p}^2 - \frac{1}{2}(V_{1,p}-\Delta V_{tot})^2 \tag{4.9}$$

where $\Delta V_{tot} = \Delta V_i + \Delta V_\Omega$ and $V_{1,p}$ is given by:

$$V_{1p} = \sqrt{\frac{\mu}{r_p}(1+e_1)} \tag{4.10}$$

The total energy required for each individual transfer is:

$$\Delta\mathcal{E}_{tot} = |\Delta\mathcal{E}_{plane}| + |\Delta\mathcal{E}_{orbit}| \tag{4.11}$$

Equation 4.11 is the cost function used to determine the entries in the cost matrix of the EGTSP problem. Since this cost function will give different results for transfers from A to B and from B to A this cost function is asymmetric.

ΔV
The cost function will determine the cost of a transfer based on the ΔV required to match the orbital elements, excluding the true anomaly, of the departure orbit with the arrival orbit. This means that a ΔV has to be determined for changing a, e, ω, i and Ω. First, the orbital planes are aligned, next the argument of perigee is matched and finally the semi-major axis and the eccentricity are matched.

The equations for i and Ω are given by equations 4.6 and 4.7 and repeated here.

$$\Delta V_i = 2\sqrt{\frac{\mu}{r_{a1}}(1-e_1)}\sin\left(\frac{|i_2-i_1|}{2}\right) \tag{4.12}$$

$$\Delta V_\Omega = 2\sqrt{\frac{\mu}{r_{a1}}(1-e_1)}\sin(i_1)\sin\left(\frac{|\Omega_2-\Omega_1|}{2}\right) \tag{4.13}$$

Next, the difference in the argument of pericenter is corrected for. The geometry is shown in Figure 4.1. The ΔV for this change is given by [*Sidi*, 2006]:

[1] It is, from an energy point of view, more efficient to increase a higher velocity instead of a lower velocity. For example, increasing a velocity of 2 km/s with 1 km/s results in $\frac{3^2}{2}-\frac{2^2}{2} = 2.5MJ/kg$, while increasing a velocity of 3 km/s by 1 km/s results in $\frac{4^2}{2}-\frac{3^2}{2} = 3.5MJ/kg$

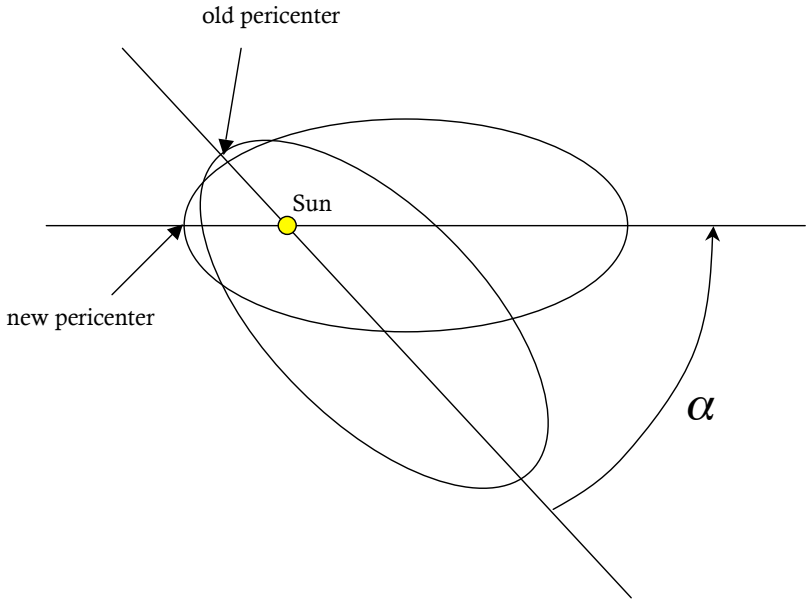

Figure 4.1 Geometry for changing the argument of pericenter. Based on [*Sidi*, 2006].

$$\Delta V_\omega = 2\sqrt{\frac{\mu}{a(1-e^2)}e\sin\left(\frac{\alpha}{2}\right)} \tag{4.14}$$

The ΔV required for the change of a and e is combined in one maneuver. The equations are obtained from [*Sidi*, 2006]. The geometry of this transfer is shown in Figure 4.2. The velocity at the apocenter is given, as before, by:

$$V_{a1} = \sqrt{\frac{\mu}{r_{a1}}(1-e_1)} \tag{4.15}$$

The subscript 1 and 2 indicate departure and arrival orbits repectively. The velocity in the arrival orbit at the location where the radius is equal to the apocenter distance of the departure orbit is:

$$V_2^2 = 2\mu\left(\frac{1}{a_1(1+e_1)} - \frac{1}{2a_2}\right) \tag{4.16}$$

The angle between the two vectors is:

$$\cos^2\beta = \frac{\mu a_2(1-e_2^2)}{V_2^2 a_1^2(1+e_1)^2} \tag{4.17}$$

The ΔV required for the orbit change related to a and e then becomes:

$$\Delta V_{ae} = \sqrt{(V_2\cos\beta - V_{a1})^2 + V_2^2\sin^2\beta} \tag{4.18}$$

To change a and e with this maneuver, the radius of apocenter of the departing orbit should be larger than the radius of pericenter of the arrival orbit and smaller than the radius of apocenter of the arrival orbit. If this is not the case, then, depending on the situation, the apocenter of the departure body is raised or lowered using a simple two-impulse transfer. The cost of this correction ΔV is added to the

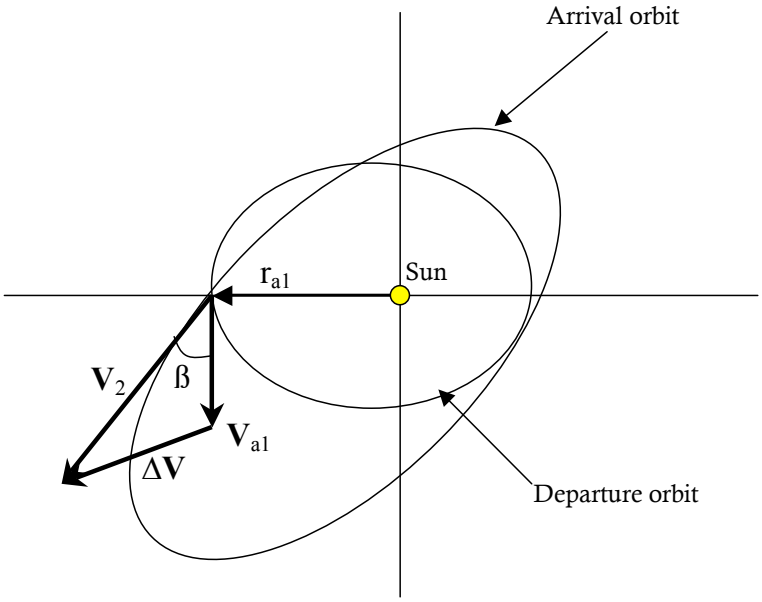

Figure 4.2 Change of a and e of a Keplerian orbit. Based on [*Sidi*, 2006].

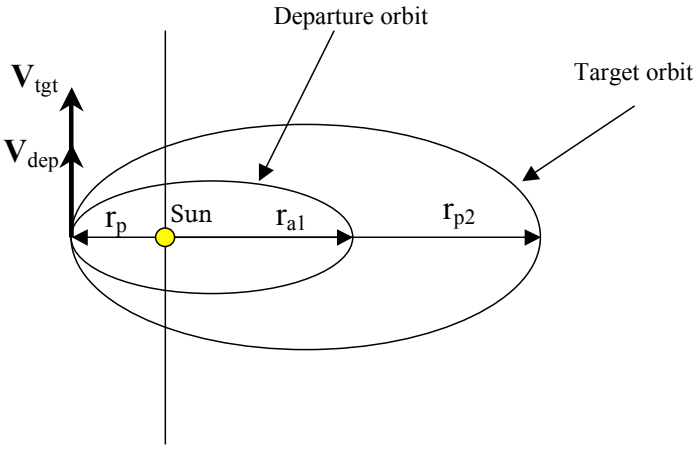

Figure 4.3 Raising the apocenter radius.

total cost of the transfer. If the apocenter of the departure body is lower than the perigee of the arrival body, the apocenter is raised by using a burn at pericenter (see Figure 4.3):

$$\Delta V_{cor} = V_{tar} - V_{dep} \tag{4.19}$$

where:

$$V_{dep} = \sqrt{2\left(\frac{\mu}{r_p} - \frac{\mu}{r_p + r_{a1}}\right)} \tag{4.20}$$

and

$$V_{tar} = \sqrt{2\left(\frac{\mu}{r_p} - \frac{\mu}{r_p + r_{p2}}\right)} \tag{4.21}$$

If the apocenter of the departure body is higher than the apogee of the arrival body, the apocenter is lowered by using a burn at pericenter (see Figure 4.4):

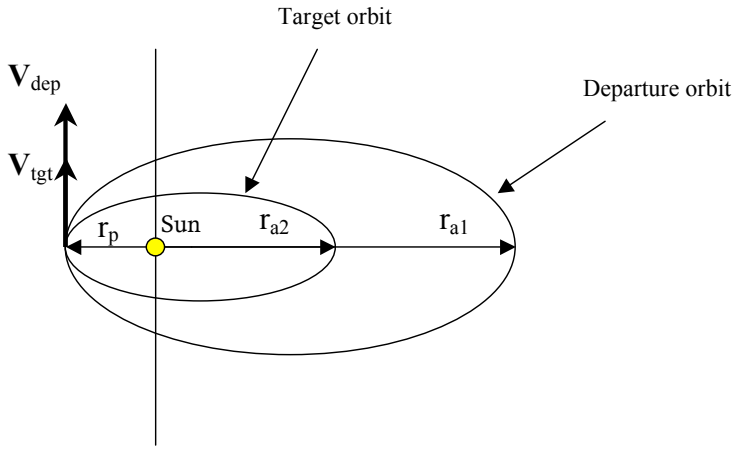

Figure 4.4 Lowering of the apocenter radius.

$$\Delta V_{cor} = V_{dep} - V_{tar} \tag{4.22}$$

where:

$$V_{tgt} = \sqrt{2\left(\frac{\mu}{r_p} - \frac{\mu}{r_p + r_{a2}}\right)} \tag{4.23}$$

and

$$V_{dep} = \sqrt{2\left(\frac{\mu}{r_p} - \frac{\mu}{r_p + r_{a1}}\right)} \tag{4.24}$$

After these correction maneuvers are done, the eccentricity of this intermediate orbit is also recalculated. This intermediate orbit is then used to evaluate the maneuver to change a and e.

The total ΔV cost required for each individual transfer is given by adding the different ΔVs for each correction of the orbital elements:

$$\Delta V_{tot} = \Delta V_i + \Delta V_\Omega + \Delta V_\omega + \Delta V_{ae} + \Delta V_{cor} \tag{4.25}$$

According to this cost function, the transfer costs from asteroid A to B will not be the same as from asteroid B to A, hence the cost function based on ΔV is asymmetric.

ESA Cost Function
The cost function used by ESA for the asteroid selection during the GTOC2 competition is based on the ΔV consumption of a high thrust transfer between two different orbits in two different planes. One impulse is given at the pericenter of the lower orbit to achieve an apocenter raise and one in the apocenter of the arrival orbit to achieve the pericenter raise and inclination change [*Izzo et al.*, 2007]:

$$\Delta V_{tot} = \Delta V_1 + \Delta V_2 \tag{4.26}$$

where

$$\Delta V_1 = \sqrt{\mu}\left(\sqrt{2/r_{p1} - 2/(r_{p1} + r_{a1})} - \sqrt{2/r_{p1} - 2/(r_{p1} + r_{a2})}\right) \tag{4.27}$$

and

$$\Delta V_2 = \sqrt{V_i^2 + V_f^2 - 2V_i V_f \cos i_{rel}} \tag{4.28}$$

where

$$V_i = \sqrt{\mu}\left(\sqrt{2/r_{a2} - 2/(r_{p1} + r_{a2})}\right) \tag{4.29}$$

and

$$V_f = \sqrt{\mu}\sqrt{2/r_{a2} - 1/a_2} \tag{4.30}$$

and

$$\cos i_{rel} = \cos i_1 \cos i_2 + \sin i_1 \sin i_2 \cos \Omega_1 \cos \Omega_2 + \sin i_1 \sin i_2 \sin \Omega_1 \sin \Omega_2 \tag{4.31}$$

Index 1 refers to the asteroid with the lowest apocenter of the pair in between which the transfer is considered. Note that the differences in Ω and ω are not corrected for, and thus will not be taken into account when selecting asteroids. Since every pair of asteroids is evaluated twice, but the asteroid with the lowest apocenter will always be the same, this cost function is symmetric.

4.1.2 Including Earth

The GTOC2 problem does not only concern transfers between asteroids, but also an initial leg from Earth to the first asteroid. In order to include Earth a fifth group (called group 0) is introduced. This fifth group contains Earth only. Adding the Earth to the problem means increasing the size of the EGTSP matrix with one row and one column. The entries in this row and column are calculated in the same way the transfers between asteroids are calculated. Adding Earth to the cost matrix introduces a new issue. If the EGTSP is solved in its current

format, the solution would be optimal for a trajectory that is returning to Earth (because the solutions of an EGTSP are cyclic). The optimal solution of this cycle is not the same as the optimal solution for a trajectory that is departing from Earth, visiting four asteroids without returning to Earth. To see this, realize that each individual link in a solution cycle is not independent. By choosing one link between asteroids you restrict certain other links from being included in the same link. Also, by choosing an optimal transfer from the fourth asteroid to Earth fixes the last (fourth) asteroid of the sequence, but maybe the optimal sequence that terminates before returning to Earth, ends at an asteroid other than the optimal one for returning to Earth.
To solve this issue, the costs for returning to Earth from all asteroids are set to zero. This means that the entire first column of the cost matrix is set to zero, except for the first element, which is infinity because it describes the transfer from Earth to Earth. In this way the cost for traveling up to the fourth asteroid will be optimized and the return to Earth will not be taken into account. After including the Earth and filling the cost matrix with the individual transfer costs, the format of the EGTSP problem model is as is shown in Figure 4.5. The entries in this model depend on the chosen cost function.

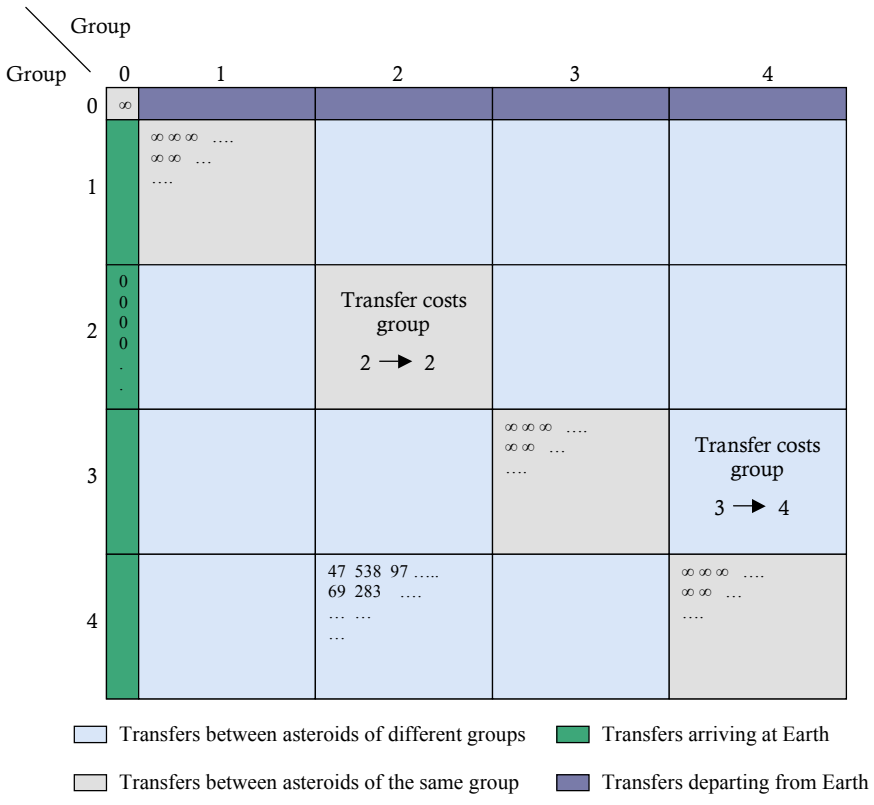

Figure 4.5 Cost Matrix of the EGTSP problem.

4.1.3 Reducing the Cost Matrix

In sections 4.1.1 and 4.1.2 the complete model of the discrete part of the GTOC2 problem is developed. The problem in its current form, a square matrix of 911×911, is hard to solve because of its large size. To reduce the size of the

cost matrix, the observation is made that the matrix can be divided in several blocks corresponding to the transfers between the 5 asteroid groups. These blocks are also shown in Figure 4.5. To reduce the size of the cost matrix the best four transfers from each block of the cost matrix are located and the corresponding asteroids are selected.
This method of selecting asteroids is very crude. There is, however, one reason to believe that it is a relatively good one. Observe the fact that there are 25 blocks in the cost matrix. From the diagonal blocks no transfers are selected, since in a valid EGTSP solution it is not allowed to have transfers within the same group. This leaves 21 blocks. Of those blocks 8 have group 0 as either its starting or arrival group. If the four best transfers of these groups are selected, this will always result in four selected asteroids, because each entry in these blocks represents the transfer to or from a unique asteroid (If you pick two entries from one of those eight blocks, the corresponding transfers will always concern two distinct asteroids and Earth). For the groups that do not have group 0 as either their departing or arrival group there are at most 8 asteroids selected, since each of the four best transfers require a starting and arrival asteroid. This could lead to a total of 8 times 4 plus 16 times 8 is 160 selected asteroids. It is, however, possible to have overlap in the selected asteroids. An asteroid that is located favorable with respect to several other asteroids might be selected more than once. This would reduce the total number of selected asteroids. It turns out that when selecting the best four transfers of each block a total of about 60 asteroids is obtained instead of the possible 160. This gives reason to believe that the selected asteroids are located favorably with respect to several other asteroids and the search space is reduced in an effective way.

To give an impression of the reduced search space defined by the various cost functions, a visualization of the reduced cost matrices is included in figures 4.6-4.8. The layout of the cost matrix has not changed, i.e. asteroids from group 1 are still identified by low numbers (upper and left part of the cost matrix), and asteroids from group 4 are identified with high numbers (lower and right part of the cost matrix). Note that the first column of all three cost matrices only contains 0 values (is dark blue). This is due to the fact that the return to Earth has been set to 0, as explained in Section 4.1.2.
Figure 4.6 presents the reduced cost matrix for the cost function based on ΔV. According to this cost function, most transfers are relatively good with the exception of a few asteroids, that have a lot of bad transfers and only a few with a low cost. Also the asteroids in the lower and right part are a little worse than the others. This indicates that these asteroids are relatively hard to reach or to depart from. Figure 4.7 presents the reduced cost matrix for the cost function based on energy. According to this cost function, the worst transfers a located in the lower part of the matrix, indicating that it is hard to depart from asteroids of group 4. Figure 4.7 presents the reduced cost matrix for the cost function implemented by ESA. Because the lower part and the right part of the cost matrix contains worse transfers, this cost function qualifies transfers to and from group 4, as significantly harder than the other transfers. Figure 4.7 clearly indicates that the cost matrix is symmetric. The only exception is the first row and column, because the transfers to Earth haven been manually set to 0.

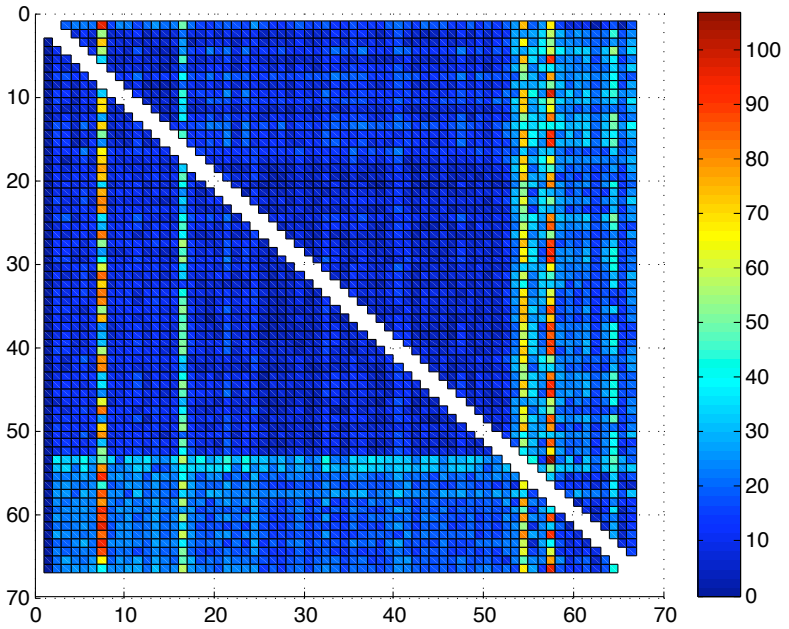

Figure 4.6 Reduced cost matrix EGTSP problem for the cost function based on ΔV.

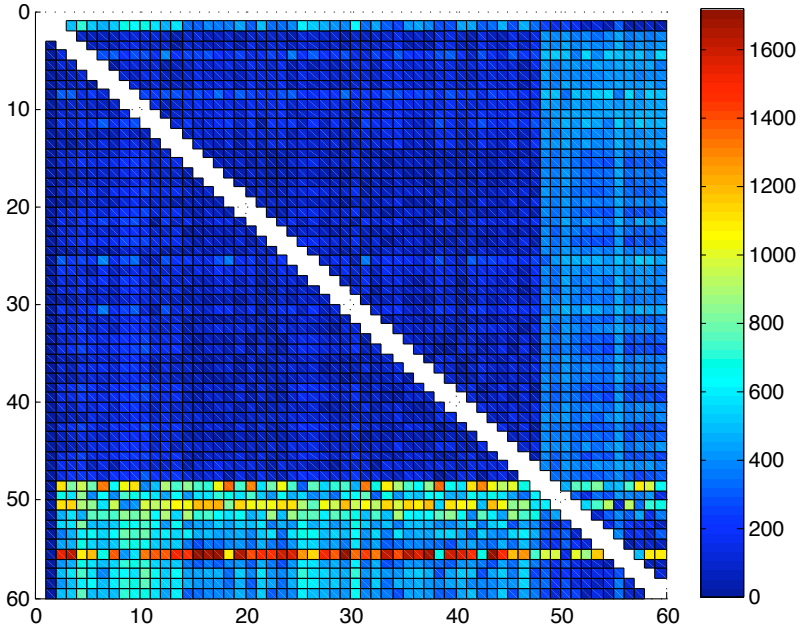

Figure 4.7 Reduced cost matrix EGTSP problem for the cost function based on energy.

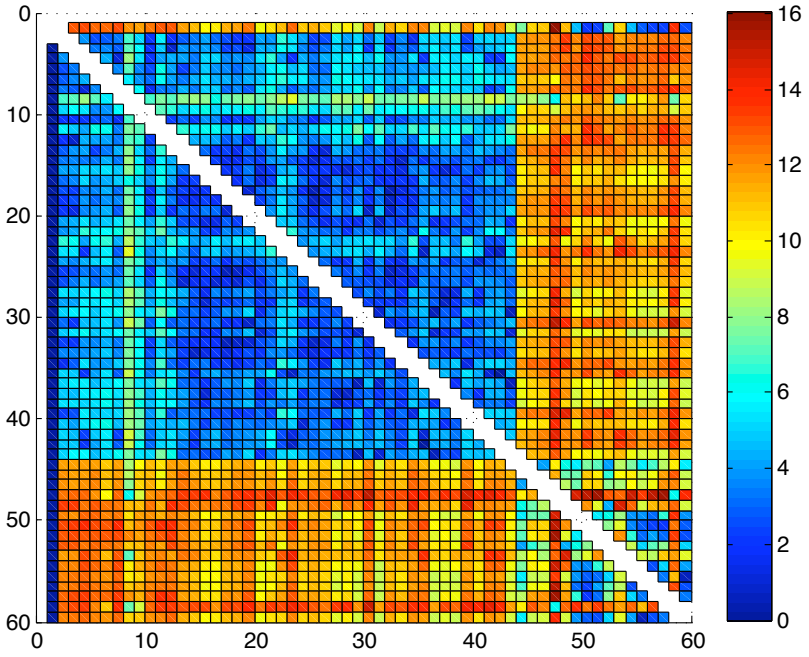

Figure 4.8 Reduced cost matrix EGTSP problem for the cost function based on ESA.

4.1.4 EGTSP to TSP Transformation

To solve the EGTSP it will be transformed into a TSP. This makes it possible to solve the problem with the B&B algorithm. The transformation will be presented here first, followed by an explanation of how to extract the EGTSP solution from the TSP solution. The transformation is detailed in [*Behzad and Modarres*, 2002]. For the mathematical proof of the validity of the transformation the reader is referred to this paper.

Transformation
The transformation requires three steps:

- Determine the number M, which is a random number larger than the sum of all non-infinite entries of the cost matrix.
- All nodes of each group are connected into a single cycle, a cluster path. The asteroid that succeeds asteroid V_i^r in the cycle is called $V_{i(s)}^r$, where r indicates the group and i indicates a specific asteroid within that group. In terms of the cost matrix this transformation is given by:

  $$c'(V_i^r, V_{i(s)}^r) = 0 \tag{4.32}$$

  By setting consecutive transfers to zero, the solution of the problem will always contain these cluster paths.
- The elements of the transformed cost matrix which are not included in the cluster path are given by:

  $$c'(V_i^r, V_j^t) = c(V_{i(s)}^r, V_j^t) + M \qquad r \neq t \tag{4.33}$$

  where t indicates another group different from r.

These transformations are visualized in Figure 4.9. An example for each type of cost matrix block is given in Figure 4.10 (in this example M is equal to 100). If these operations were to be performed on the matrix shown in Figure 3.5 the result would be as shown in Figure 4.11. In this specific example, M should be larger than 162, which is the sum of all entries.

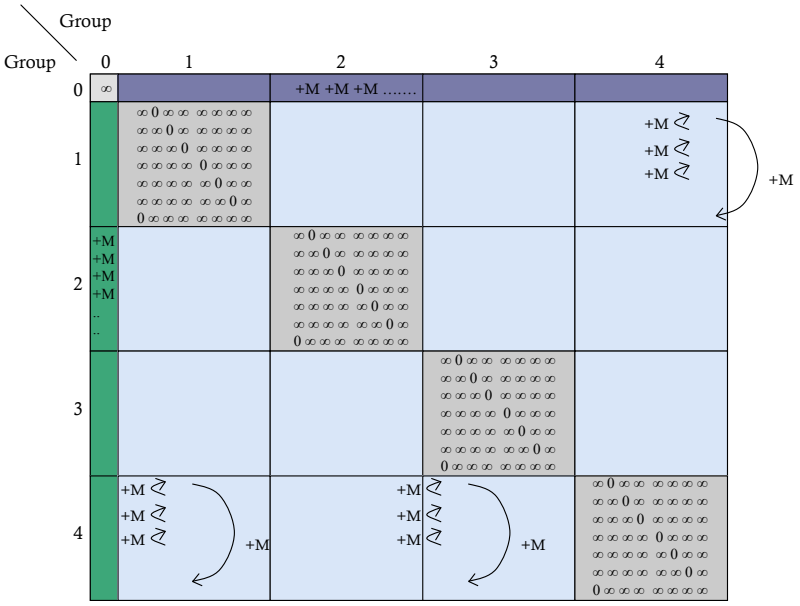

Figure 4.9 Transformation operations to transform EGTSP to TSP.

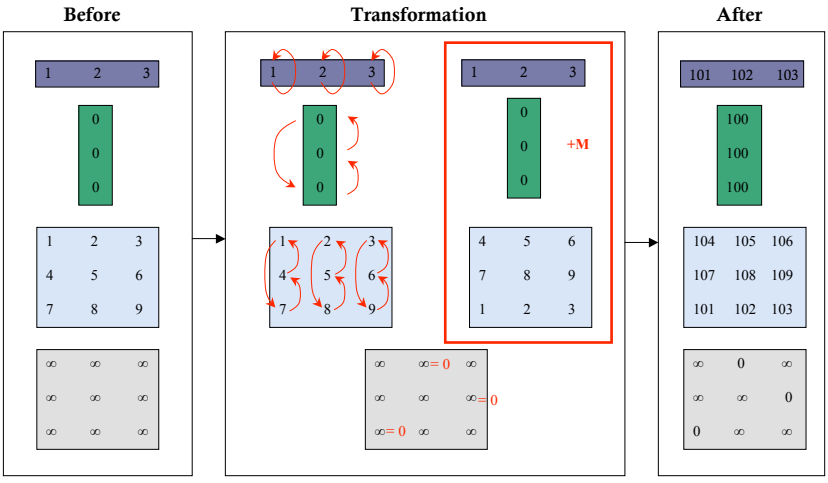

Figure 4.10 Example transformation per type of cost matrix block. On the left the block before the transformation is shown, on the right after the transformation is completed.

	A	B	C	D	E	F	G
A	∞	0	8+M	9+M	3+M	1+M	5+M
B	0	∞	5+M	7+M	4+M	6+M	2+M
C	2+M	1+M	∞	0	5+M	6+M	1+M
D	6+M	3+M	0	∞	4+M	2+M	4+M
E	8+M	4+M	6+M	5+M	∞	0	∞
F	4+M	7+M	9+M	7+M	∞	∞	0
G	9+M	7+M	9+M	3+M	0	∞	∞

Figure 4.11 Result of transformation from example GTSP of Figure 3.5 to TSP.

Solution Extraction

The solution cycle of the TSP can be transformed into a solution cycle of the corresponding EGTSP. The EGTSP cycle is constructed by finding all first accessed cities of every group in the TSP solution cycle. For example, the optimal solution of the example shown in Figure 4.11 is A→E→F→G→D→C→B→A, with a total cost of 523 [*Behzad and Modarres*, 2002]. The corresponding solution cycle of the EGTSP would then be E→D→B→E. An illustration of this EGTSP problem and solution is shown in Figure 4.12. An illustration of the associated TSP solution is shown in Figure 4.13. Note that, although it is the first element

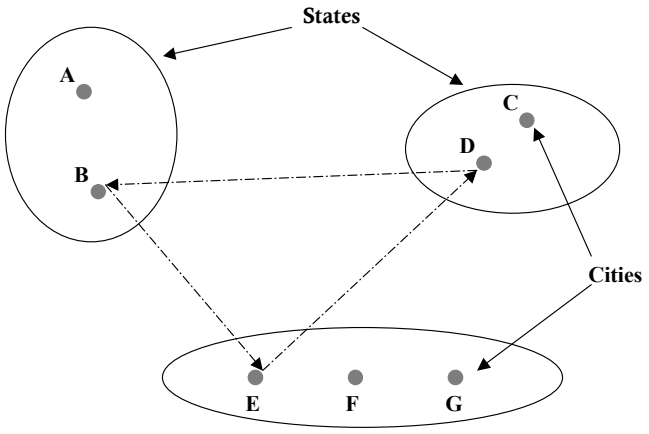

Figure 4.12 An illustration of the EGTSP and its optimal solution.

listed in the TSP solution, the first accessed element of the group consisting of city A and B is not A because city A is accessed by city B which is in the same group. To find the total cost of this EGTSP solution cycle the costs of the GTSP cycles are extracted from the untransformed EGTSP cost matrix. This would result in the addition of the cost for the transfers $E \rightarrow D$, $D \rightarrow B$ and $B \rightarrow E$, which is $3+1+3=7$. The connection between the cost of the TSP solution cycle and the EGTSP solution cycle is given by the relation:

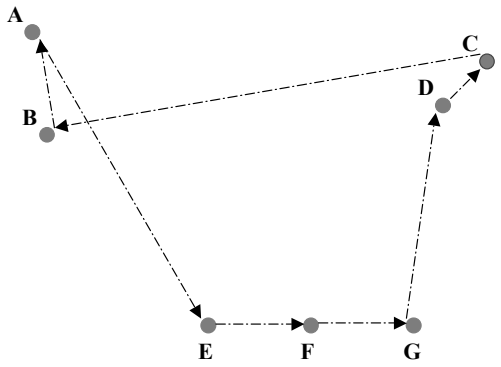

Figure 4.13 An illustration of the TSP solution associated with the EGTSP solution of Figure 4.12.

Cost TSP cycle = Cost EGTSP cycle + M × #groups

Checking this for the example above would give TSP cycle cost = 7+3M. Since M was set to 172, this would add up to 523 which is indeed equal the cost of the TSP solution cycle.

4.2 Continuous Model

Solving the discrete aspect of the GTOC2 problem results in candidate asteroid sequences. The sequences are expected to have favorable sequencing characteristics such that relatively little fuel is needed and transfer times will be short. To assess the validity of this expectation, a continuous orbit model is required. Because a large number of candidate trajectories have to be evaluated, a relatively fast method is required. Shape-based techniques are very suitable for these kinds of evaluations. In specific, the exponential sinusoid shape is chosen. This choice was the result of circumstances. Exponential sinusoids are well studied, also at the Delft University of Technology (see [*Paulino*, 2008]), and a tool implementing exponential sinusoids was under development at the Department of Aerospace Engineering in Delft at the time of this research. This tool was used as a basis and modified such that it is suitable for studying the GTOC2 problem. In this section, first the exponential sinusoid is introduced. Next the shape is applied to transfers between two points in space, and a fixed transfer time. In the last section this transfer is implemented for multileg transfers. This multileg model will be applied when analyzing asteroid sequences.

4.2.1 Exponential Sinusoids

The exponential sinusoid (exposin) method has been developed by Petropoulos and Longuski at Purdue University. This section is based on their work [*Petropoulos et al.*, 2004] as well as that of [*Paulino*, 2008]. The shape of the most general exposin trajectory is given by:

$$r = k_0 \exp\left[q\theta + k_1 sin(k_2\theta + \phi)\right] \tag{4.34}$$

where r gives the distance of the spacecraft. The constants k_0, k_1, k_2 and ϕ fix the shape of the exposin. k_2 is the winding parameter and describes roughly how many windings (revolutions) are made during the completion of the orbit. This is illustrated in Figure 4.14. k_1 is called the dynamic range parameter. It controls

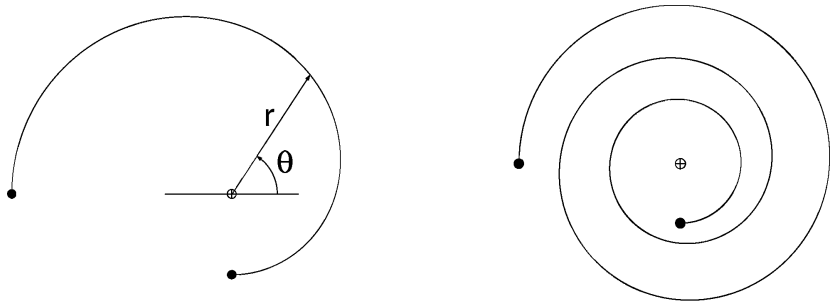

a) k_2 = 2/3 **b) k_2 = 2/11**

Figure 4.14 Influence of k_2 [*Petropoulos et al.*, 2004].

the ratio of apoapsis distance with respect to the periapsis distance. k_0 is a scaling parameter to give the orbit practical dimensions. ϕ controls the orientation of the exposin within its plane. The parameter q introduces flexibility in the exposin.
To further analyze the use of exposins, they are applied to the two-body equations of motion for a spacecraft in polar coordinates [*Petropoulos et al.*, 2004]:

$$\ddot{r} - r\dot{\theta}^2 + \frac{\mu}{r^2} = a \sin\alpha \tag{4.35}$$

$$\frac{1}{r}\frac{d}{dt}(r^2\dot{\theta}) = a\cos\alpha \tag{4.36}$$

where α is the trust angle and a is the magnitude of the thrust acceleration, see figure 4.15. Taking the first and second derivative of r as defined in eq 4.34:

$$\dot{r} = \dot{\theta}(q + k_1 k_2 c)r \tag{4.37}$$

$$\ddot{r} = \left(\ddot{\theta}(q + k_1 k_2 c) + \dot{\theta^2}(q + k_1 k_2 c)^2 - \dot{\theta}^2 k_1 k_2^2 s\right) r \tag{4.38}$$

where

$$s = \sin(k_2\theta + \phi) \tag{4.39}$$
$$c = \cos(k_2\theta + \phi) \tag{4.40}$$

Also the flight-path angle γ can be derived, see Figure 4.15:

$$\tan\gamma = \frac{dr/dt}{rd\theta/dt} = q + k_1 k_2 c \tag{4.41}$$

At this point the problem consists of five quations (4.34 - 4.38) and seven unknowns $(r, \dot{r}, \ddot{r}, \dot{\theta}, \ddot{\theta}, a, \alpha)$. Two more equations are needed to solve the system. From [*Paulino*, 2008], we have for $\dot{\theta}$, based on equations 4.35- 4.38:

$$\dot{\theta}^2 = \left(\frac{\mu}{r^3}\right)\frac{a_0\cos\alpha\tan\gamma - a_0\sin\alpha + 1}{\tan\gamma^2 + k_1 k_2^2 s + 1} \tag{4.42}$$

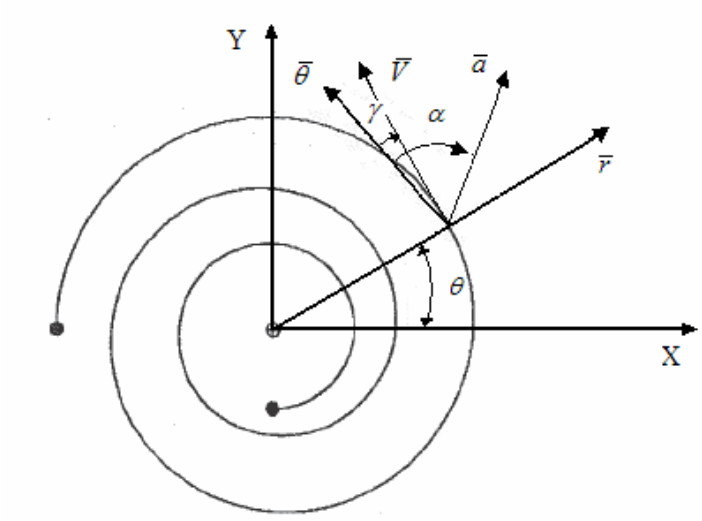

Figure 4.15 Parameters of exposin [*Paulino*, 2008].

where a_0 is the normalized thrust acceleration:

$$a_0 = \frac{F_{thrust}/M_{S/C}}{\mu/r^2} = \frac{a}{\mu/r^2} \tag{4.43}$$

with $\dot{\theta}$ known, it is possible to write down the tangential and radial velocity components:

$$V_r = \dot{r} = \dot{\theta}(q + k_1 k_2 c)r \tag{4.44}$$

$$V_\theta = r\dot{\theta} = r\sqrt{\left(\frac{\mu}{r^3}\right)\frac{a_0 \cos\alpha \tan\gamma - a_0 \sin\alpha + 1}{\tan\gamma^2 + k_1 k_2^2 s + 1}} \tag{4.45}$$

Note that to calculate $\dot{\theta}$, the position r needs to be known first. From $\dot{\theta}$ the velocity components can be obtained, which in turn are needed to calculate the required acceleration. This implies that, during the orbit model determination process, no bounds can be imposed on the acceleration a. From these two expressions it is possible to calculate the derivative of the thrust direction angle $\dot{\alpha}$ [*Paulino*, 2008]. The expressions for $\dot{\alpha}$ and $\dot{\theta}$ are coupled first-order differential equations. Therefore a numerical integration needs to be performed to obtain solutions for α and θ. These solutions are needed to calculate position, velocity and the time of flight (TOF). The TOF is found by integrating the inverse of $\dot{\theta}$:

$$TOF = \int_{\theta_0}^{\theta_f} \frac{dt}{d\theta} d\theta = \int_{\theta_0}^{\theta_f} \left[\left(\frac{\mu}{r^3}\right)\frac{a_0 \cos\alpha \tan\gamma - a_0 \sin\alpha + 1}{\tan\gamma^2 + k_1 k_2^2 s + 1}\right]^{-\frac{1}{2}} d\theta \tag{4.46}$$

Summarizing: for the case where the thrust angle and magnitude are free, the position, velocity, acceleration and TOF are known, provided that the expressions for $\dot{\alpha}$ and $\dot{\theta}$ are numerically integrated. This case can be reduced to a case where the thrust direction is limited to the directions tangential to the velocity vector in Figure 4.15. This would remove the need of numerical integration since one of the two variables is known and the other can be solved for analytically. Mathematically, for the thrust direction:

$$\alpha = \gamma + n\pi, \qquad with \quad n = 0, 1 \tag{4.47}$$

where n=0 represents the case where the thrust is along the velocity vector, and n=1 is the case where the thrust is against the velocity vector. In this case, due to simplifications in equation 4.42 the parameters $\dot{\theta}$ and a_0 are given by:

$$\dot{\theta}^2 = \left(\frac{\mu}{r^3}\right) \frac{1}{\tan\gamma^2 + k_1 k_2^2 s + 1} \tag{4.48}$$

$$a_0 = \frac{(-1)^n \tan\gamma}{2\cos\gamma} \left[\frac{1}{\tan^2\gamma k_1 k_2^2 s + 1} - \frac{k_2^2(1 - 2k_1 s)}{(\tan^2\gamma + k_1 k_2^2 s + 1)}\right] \tag{4.49}$$

The expression for the TOF can also be simplified to:

$$TOF = \int_{\theta_0}^{\theta_f} \sqrt{r^3(\tan^2\gamma + k_1 k_2^2 s + 1)/\mu} d\theta \tag{4.50}$$

The tangential thrust case provides a fast way of generating orbits since no numerical integration is necessary to obtain the thrust acceleration: it is given as a function of the shape parameters in equation 4.49. There are, however, some issues that need to be addressed:

1. As $k_1 k_2^2$ approaches unity from below, $\dot{\theta}$ and a_0 approach infinity at periapsis (where s = -1)
2. If $k_1 k_2^2 > 1$, $\dot{\theta}^2$ will be less than 0. In this region the exposin shape cannot be followed using tangential thrust only.

These two effects force the mission designer to restrict the range of values for $k_1 k_2^2$. This limitation on the allowable shapes given by the exposin has consequences for both the shape as well as the velocity profile. First, the effects on the shape are considered.
If k_1 is large then k_2 must be small. This means that if a large distance needs to be travelled (result of large k_1, meaning apoapsis is far away) then a large number of revolutions are required (small k_2). The other way around, if k_1 is small and k_2 is large, then only a short distance will be travelled with few, if any, revolutions. Both may not be the result the mission designer is after.
The influences on the velocity can best be evaluated by comparing the velocity on the exposin with the local circular velocity. In the previously described case with many revolutions, the velocity on the exposin will be quite similar to that of the local circular velocity, especially at periapsis and apoapsis. This means that launching from or rendezvous with a body in a circular orbit would be most effective at periapsis or apoapsis. In the case of a gravity assist, however, it is more effective in between periapsis and apoapsis, where the velocity differs more from the local circular velocity. In the few-revolutions case the velocity profile is significantly non-circular making this case well suited to use gravity-assists at bodies in a circular orbit. Also, for orbits with a high eccentricity, low hyperbolic excess velocities can only be achieved with the few-revolution case. High hyperbolic excess velocities can be achieved in both the few and many revolution case [*Petropoulos et al.*, 2004].

4.2.2 Low-thrust Lambert's Problem

The determination of an orbit, having a specified transfer time and connecting two position vectors, is called Lambert's Problem [*Battin*, 1999]. Lambert's problem can be solved both with high-thrust and with low-thrust trajectories. For

a discussion of the high-thrust variant see [*Gooding*, 1990]. In this section, a multi-revolution low-thrust approach to solve Lambert's problem is presented. It is based on the exponential sinusoid theory detailed in section 4.2.1. The goal is to find all the exposins defined by equation 4.34, that connect r_1 and r_2 separated by a transfer angle ψ in a given transfer time t, allowing for multiple revolutions. Four main steps are taken to solve the problem. First, a geometric class of solutions is identified, which fulfill the boundary constraints (meaning they pass through the desired departure and arrival point). Second, the class is evaluated on dynamic feasibility, meaning it is checked which solutions are feasible spacecraft trajectories. Third, the TOF is evaluated. Last, the corresponding relative velocities are to be obtained. This section is written based on the work presented in [*Izzo*, 2006] and the reader is referred to this paper for further details.

To find the class of exposins that passes through the departure point (P_1 at r_1) and the destination point (P_2 at r_2) the parameter k_2 is assumed to be fixed, see figure 4.16. Also the polar coordinate system is fixed such that $\theta_1 = 0$. The equation for the flight-path angle then becomes (using equation 4.41):

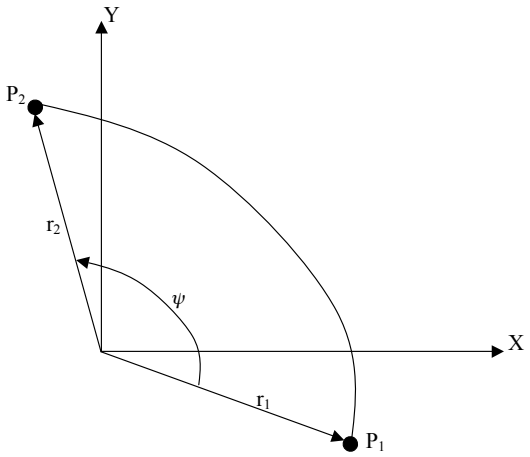

Figure 4.16 Exposin geometry.

$$\tan\gamma_1 = k_1 k_2 \cos\phi \tag{4.51}$$

From equation 4.34, at points 1 and 2 it holds that:

$$r_1 = k_0 \exp\left[k_1 sin(\phi)\right] \tag{4.52}$$
$$r_2 = k_0 \exp\left[k_1 sin(k_2\bar{\theta} + \phi)\right] \tag{4.53}$$

where $\bar{\theta} = \psi + 2\pi N$ and N = 1,2,..., account for the possibility of having more than one revolution. Note that q is set to 0. This means that only exact exposin shapes are considered.Next the sign of k_1 is determined by dividing the equations for r_1 and r_2 and taking the logarithm:

$$\frac{k_1}{|k_1|}\sqrt{k_1^2 - \frac{\tan^2\gamma_1}{k_2^2}} = \frac{\ln r_1/r_2 + (\tan\gamma_1/k_2)\sin k_2\bar{\theta}}{1 - \cos k_2\bar{\theta}} \tag{4.54}$$

The magnitude of k_1 is obtained from:

$$k_1^2 = \left(\frac{\ln r_1/r_2 + (\tan \gamma_1 / k_2) \sin k_2 \bar{\theta}}{1 - \cos k_2 \bar{\theta}} \right) + \frac{\tan^2 \gamma_1}{k_2^2} \tag{4.55}$$

For ϕ:

$$\phi = \arccos \left(\frac{\tan \gamma_1}{k_1 k_2} \right) \tag{4.56}$$

and k_0 is found from:

$$k_0 = \frac{r_1}{\exp(k_1 \sin \phi)} \tag{4.57}$$

At this point, given the geometry (r_1, r_2, transfer angle ψ and number of revolutions N) a class of exposins is determined that pass through P_1 and P_2 and are parameterized using the sole free parameter γ_1 (the flight-path angle at P_1).

The second step considers such a class of possible exposins and determines whether they are feasible spacecraft trajectories. As in section 4.2.1, tangential thrust is adopted, which introduces the condition $|k_1 k_2^2| < 1$. Substituting this condition in equation 4.55 and rewriting gives:

$$\tan \gamma_{1_{min,max}} = \frac{k_2}{2} \left[-\ln \frac{r_1}{r_2} \cot \frac{k_2 \bar{\theta}}{2} \pm \sqrt{\Delta} \right] \tag{4.58}$$

where:

$$\Delta = \frac{2(1 - \cos k_2 \bar{\theta})}{k_2^4} - \ln^2 \frac{r_1}{r_2} \tag{4.59}$$

These equations define an interval of feasible spacecraft trajectories.

The third step is to evaluate the TOF. In the high-thrust case, the TOF equation could be expressed analytically as a function of the parameters describing the feasible ellipses. This is not possible in the low-thrust case, where the TOF needs to be determined separately by numerically integrating equation 4.48 as shown in equation 4.50. The resulting time of flight curves can have different characteristics. They can be monotone increasing or monotone decreasing or have a bathtub-like shape. In [*Izzo*, 2006] monotonic increasing curves are analyzed for the specific problem geometry where $r_1 = 1$, $r_2 = 1.5$, $\psi = \pi/2$ and different values of N. Figure 4.17 shows these normalized TOF curves. In [*Paulino*, 2008] the bathtub shape is presented, as shown in Figure 4.18. The desired solution (for a specific TOF) can be found by applying a rootfinder method to obtain the intersection between the time of flight curves obtained from numerical integration, and a horizontal line indicating the desired value. If the TOF curves have a bathtub-like shape two possible values for γ_1 can be obtained. In this case both options are evaluated using the objective function, and the solution corresponding to the best objective value is selected for further analysis.

Although Lambert's problem is solved at this point a last step to obtain the corresponding terminal velocity vectors is useful. For example, one may want to know the difference between the arrival velocity of the spacecraft and the velocity

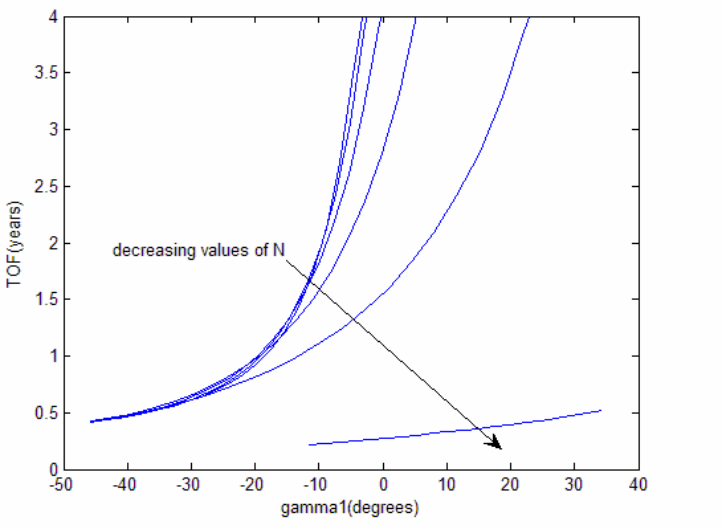

Figure 4.17 Normalized flight time curves for $r_1 = 1$. $r_2 = 1.5$ and $\psi = \pi/2$ for several values of N. [*Paulino*, 2008], after [*Izzo*, 2006].

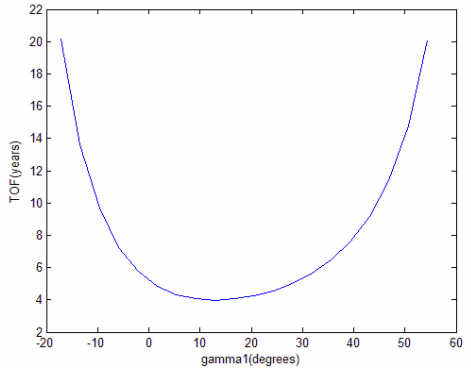

Figure 4.18 Time of flight curve for $r_1 = r_{Earth}$. $r_2 = r_{Mars}$ and $\psi = \pi/2$ and $N = 3$ [*Paulino*, 2008].

of the arrival body. In [*Izzo*, 2006] a relation between the initial and final flight path angles is presented:

$$\tan\gamma_2 = \tan\gamma_{1_min} + \tan\gamma_{1_max} - \tan\gamma_1 \tag{4.60}$$

with γ_2 and the other exposin parameters now fixed, the velocities can be computed from equations 4.44 and 4.45.

4.2.3 Patched Exposins

Section 4.2.2 described how to find an exposin between two position vectors in space for a fixed TOF. GTOC2, however, requires four successive transfers. Starting from Earth, four asteroids have to be visited, with a stay time of at least 90 days at the first three asteroids. If the positions of Earth and the asteroids, the TOF for each leg and the stay times at the asteroids are prescribed, the geometry of the problem can be described by 4 exposins, as is shown geometry is shown in Figure 4.19. The trajectory starts from Earth with an exposin arc. The engine

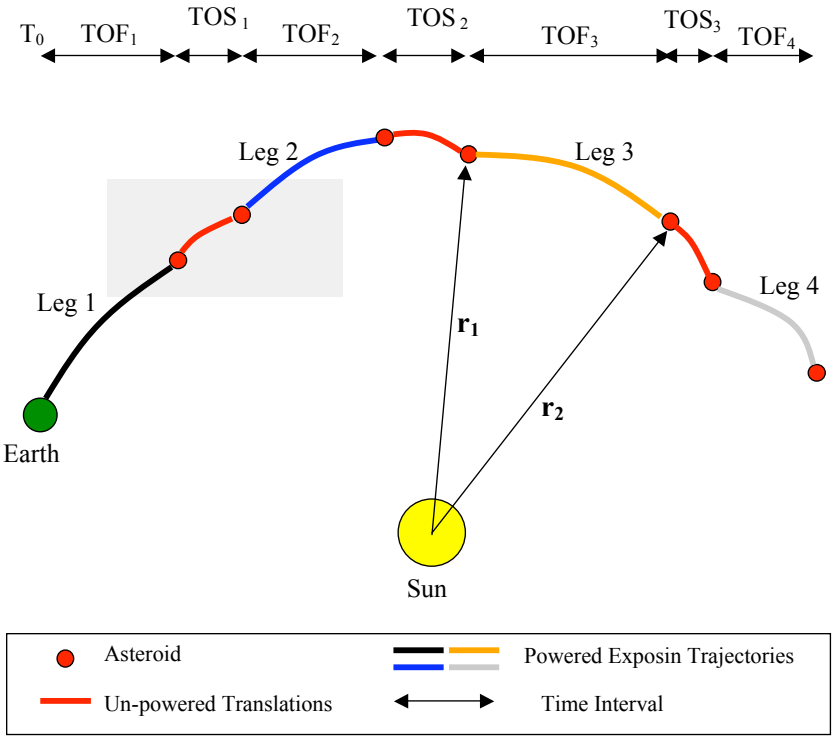

Figure 4.19 Continuous Model for Mulitleg Exposin Trajectories.

is used to fly along this exposin shape. Upon arrival at the asteroid the engine is assumed to be switched off and the spacecraft is translated along the trajectory of the asteroid for the duration of the prescribed stay time. Then the engine is switched on again and the next exposin shape is flown, etc. The model disregards any correction maneuvers to stay within the allowable position mismatch limit. To fully describe the geometry x, 16 parameters are required. A start date is required to fix the starting point of the mission (the location of Earth at a certain epoch). Each individual exposin requires three parameters. It needs a k_2 to describe a whole set of exposins parameterized by γ_1 (see section 4.2.1). A TOF is required in order to fix the positions of the relevant bodies. To select an exposin from the exposin set with a particular TOF, also the number of revolutions needs to be known, because there is no unique relation between TOF and N (see Figure 4.17). The last three elements are the stay times at the different asteroids. These stay times are introduced because GTOC2 requires a minimum stay time, not a fixed one. To implement this in the model an additional variable is required at the three asteroids where a stay time is required.

The total geometry is now described by:

$$\begin{aligned} x = [&T_0 \quad TOF_1 \quad k_{2(1)} \quad N_1 \quad TOS_2 \quad TOF_2 \quad k_{2(2)} \quad N_2 \ldots \\ &\ldots \quad TOS_3 \quad TOF_3 \quad k_{2(3)} \quad N_3 \quad TOS_4 \quad TOF_4 \quad k_{2(4)} \quad N_4] \end{aligned} \tag{4.61}$$

where T_0 indicates the mission departure date, TOF indicates the time of flight, $k_{2(i)}$ indicates the k_2 exposin parameter of the i-th leg, N the number of complete

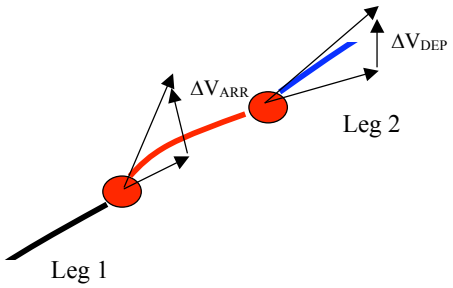

Figure 4.20 Arrival and departure ΔV. Magnification of shaded area in Figure 4.19.

revolutions and TOS indicates the time of stay at the first three asteroids. The subscripts indicate for which leg the parameter is valid.

Now that the variables that are required to determine the complete trajectory are identified, an objective function is required to assess the fitness of a solution in the form of x. The chosen objective function is a modification of the main GTOC2 objective, which is the maximization of the final mass over total mission duration. In particular, a penalty component is added to the GTOC2 objective to improve the performance of the various optimizers by steering them towards valid and/or promising parts of the solution space. The objective function is:

$$J = \frac{M_0 - (M_{fuel} + P_{tot})}{\sum_{i=1}^{nlegs}(TOF_i + TOS_i)} \tag{4.62}$$

where J is the objective value and M_0 indicates the departure mass of the spacecraft. M_{fuel} is the total fuel used in kilograms to fly the exposin trajectories. The used fuel mass is determined by integrating the fuel use along the exposins. P_{tot} is the added penalty component. It is constructed out of four different parts. The first part is a penalty for a mismatch in the departure velocity vector of the spacecraft flying along the exposin shaped trajectory and the velocity vector of the departure body (see Figure 4.20). The second part is a similar penalty for the arrival velocity. The third part is a penalty which becomes active in case the thrust limit of the engine is exceeded. The final part is a penalty applied when the total mission duration of 10 years is exceeded. Based on these four components the total penalty function becomes:

$$P_{tot} = \sum_{i=1}^{nlegs} P_{departure,i} + \sum_{i=1}^{nlegs} P_{arrival,i} + \sum_{i=1}^{nlegs} P_{thrust,i} + P_{mission\,duration} \tag{4.63}$$

To obtain a velocity penalty that can be combined properly with equation 4.62, the departure and arrival velocity mismatches, for each individual exposin, are converted to kg using Tsiolkovsky's basic rocket equation:

$$P_{departure,i} = M_0(1 - e^{-\frac{\Delta V_{dep}}{I_{sp} g_0}}) \tag{4.64}$$

$$P_{arrival,i} = M_0(1 - e^{-\frac{\Delta V_{arr}}{I_{sp} g_0}}) \tag{4.65}$$

Then, if the velocity mismatch, upon departure or arrival, was more than 1.2 km/s the mass is penalized even harder using a quadratic relation. The value of 1.2 was

determined empirically. This issue will be revisited when the additional tests are discussed in chapter 7.

$$P_{(departure,i \mid \Delta V > 1.2km/s)} = P^2_{departure} \tag{4.66}$$

$$P_{(arrival,i \mid \Delta V > 1.2km/s)} = P^2_{arrival} \tag{4.67}$$

There are two exceptions to this penalty. For the departure leg from Earth a penalty is applied when the initial velocity is larger than 3.5 km/s. This is because the GTOC2 assignment assumes this is the velocity with which the launch vehicle inserts the satellite into its orbit. The second exception occurs at the arrival asteroid. Here GTOC2 does not require a stay time or limit the arrival velocity, hence it is not implemented in the penalty function.
The thrust constraint violation penalty is determined while integrating the trajectory to obtain the fuel use. If the required acceleration on a specific integration segment is higher than the engine is capable of delivering (engine thrust for GTOC2 is limited to 0.1 N), the excess acceleration will be added tot the total excess acceleration so far. After the integration is completed, the total required excess acceleration, $a_{tot}(m/s^2)$, is scaled empirically, such that it becomes of the same order of magnitude as the other penalties. This scaled value is penalized as well, by using a quadratic relation.

$$P_{(thrust,i \mid thrust > 0.1N)} = (1000 * a_{tot})^2 \tag{4.68}$$

The mission duration penalty is implemented to make sure that the maximum mission duration as given by GTOC2 is not exceeded. This limit is 20 years, due to a design error, however, the penalty threshold was set to 10 years. This issue will be revisited in chapter 7. As with the thrust constraint violation penalty, the mission duration of the solutions ($TOF_{mission}$) that violate the constraint of 10 years are scaled and penalized using an empirical quadratic relation.

$$P_{(mission\ duration \mid TOF_{mission} > 10y)} = (50 * TOF_{mission})^2 \tag{4.69}$$

On top of these constraints, J is set to infinity when the mass of the total fuel used is more than M_0, because these orbits are physically impossible. Although the allowed fuel mass of GTOC2 is limited to 1000 kg of the initial mass of 1500 kg, it turns out no penalty is needed to steer the optimizer to an optimal solution under this limit. This indicates that the available mass is not a dominating constraint.
One thing should be noted about the described penalties. First, the penalties are applied to the absolute values and not to the amount with which a certain limit was exceeded. This results in a jump in the objective function, see Figure 4.21. This approach was chosen to stimulate the results to be within a certain desired region. Within this pit of reasonable solutions penalties are much lower relative to the main objective function (final mass over total mission duration). This causes the optimizer to place more value on the actual objective value instead of any of the constraint mismatches. Since the solutions within the pit are all relatively good, it is allowed to place more emphasis on the objective functions since the constraints are all either met or violated with an allowable tolerance.

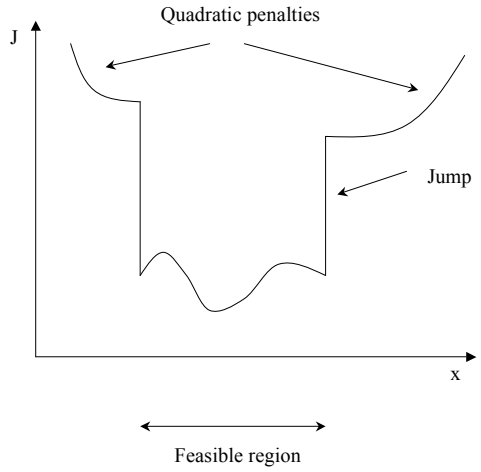

Figure 4.21 Visualization of jump in objective function due to applied penalties.

Chapter 5

Solution Methods for GTOC2

This chapter will present the methods that are used to find an optimal solution for the discrete and continuous part of the GTOC2 problem. The first section considers the discrete aspect. The second section discusses the continuous aspect.

5.1 Discrete Aspect

For solving the problem of asteroid selection and sequencing, two alternatives will be discussed. The first method is the B&B method as presented in section 3.5. A tool is developed that implements the B&B for solving the discrete aspect of the GTOC2 problem. The second method is the NNH as presented in section 3.6. Two issues regarding the implementation of the NNH will be discussed.

5.1.1 Branch- and Bound Algorithm

As mentioned in chapter 3, the models and methods in combinatorial analysis are related. This section will describe how these relations are used when solving the asteroid selection and sequencing problem of GTOC2. The goal is to solve the TSP problem as formulated in section 4.1.4. The result will be an Asteroid Selection Tool (AST). AST will be able to automatically generate the problem (create the cost matrix) from an ephemeris file and a cost function, solve this problem using a B&B algorithm, and extract the required solutions.

In figure 5.1 the flowchart describing the complete process is shown. As shown in figure 5.1 the process is divided into 5 parts. These five parts will be discussed here.

- **Input:** The input consists of two parts. The first is the ephemerides data. This data is provided with the GTOC2 assignment in a .txt file. The second is the cost function used to determine the entries of the cost matrix. The possible cost functions are detailed in section 4.1.1.
- **TSP formulation:** Formulating the TSP that will be passed to the B&B algorithm requires four steps. First, the ephemerides data is extracted from the input file and loaded into the program. Second, the cost function and the provided ephemerides data will be used to fill the entries of the cost matrix. At this point the problem is a square matrix with a dimension of 911 (910

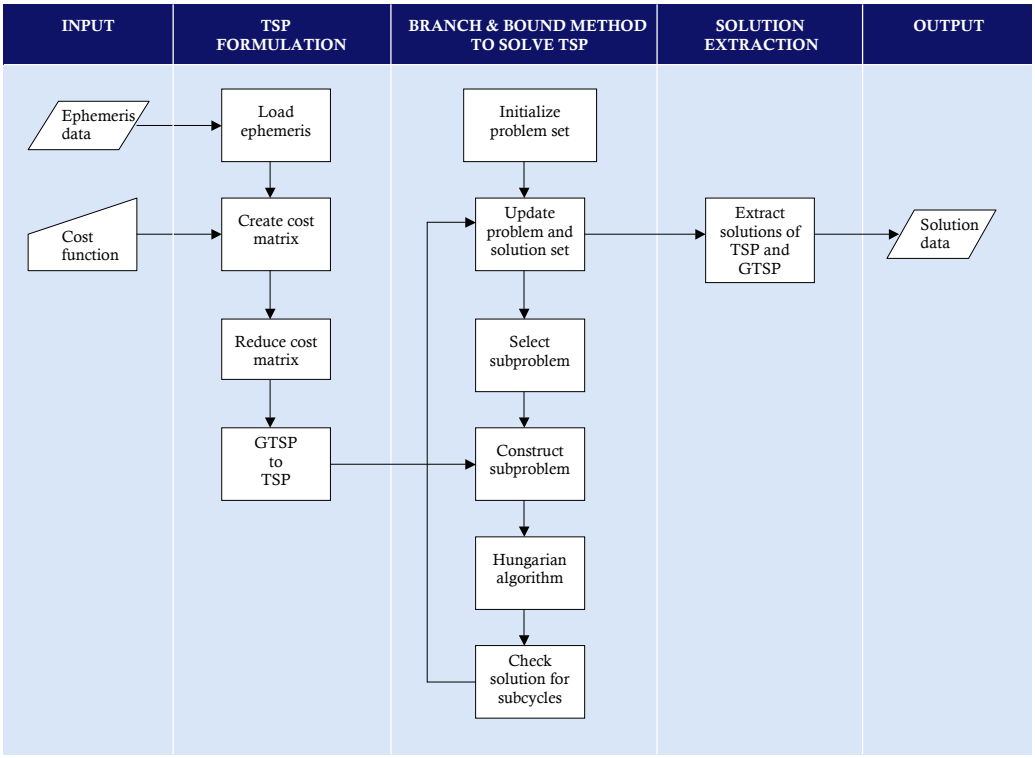

Figure 5.1 AST flowchart.

asteroids plus Earth), formulating an EGTSP. The third step is to reduce this cost matrix as explained in section 4.1.3. The fourth step is to apply the transformation detailed in section 4.1.4 to transform the EGTSP into a TSP.

- **B&B algorithm:** After the TSP is formulated, it is solved using the B&B algorithm detailed in section 3.5. The first subproblem is initialized by setting all constraints to zero. The first subproblem is equal to the TSP cost matrix. The HA (described in section 3.4) is used to solve the problem, and then the solution is checked for subcycles. Based on this outcome the problem set is updated. If subcycles are found, additional subproblems are created, whereas if a valid solution was found it is stored and no new subproblems are created. Duplicate subproblems are eliminated. The next subproblem is selected based on the DFS approach (section 3.5.1). The subproblem is constructed by obtaining all constraints from the subproblem object and implemented in the cost matrix by setting the constrained transfers to infinity. This process is repeated until all active problems have been analyzed.
- **Solution extraction:** During the B&B iterations every time (an improvement of) the solution is found, it is stored. The TSP solution is used to obtain the solution of the EGTSP as specified in section 4.1.4.
- **Output:** The output of the algorithm consists of a number of text files. In these separate files the following data is stored:
  - TSP solution cycles in terms of locations in the reduced cost matrix (length is equal to the size of the reduced cost matrix).
  - EGTSP solution sequence in terms of location in the reduced cost matrix. (length of sequence is equal to 5, one body of each group is selected).

- EGTSP solution sequence in terms of location in the original cost matrix (length of sequence is 5, size of cost matrix is 911).
- EGTSP solution sequence in terms of asteroid IDs (length of sequence is 5).
- EGTSP solution sequence in terms of group numbers corresponding to the asteroids in the solution sequence (length of sequence is 5).
- EGTSP solution cost per transfer (length of sequence is 4, because a sequence of 5 asteroids describes 4 transfers).
- EGTSP total solution costs (1 solution sequence has only 1 corresponding total cost).

5.1.2 Applying the Nearest Neighbor Heuristic

The TSP problem formulated in section 4.1.4 can be solved by the NNH as well. It is an alternative for the B&B method. The NNH algorithm has been discussed in section 3.6. This section will discuss two issues regarding the implementation of the NNH for solving the TSP problem at hand.

The first issue regarding the implementation of the NNH concerns the cost matrix transformation as discussed in section 4.1.4. When transforming the cost matrix the EGTSP problem is changed into a TSP problem. This was done to make it possible to solve the EGTSP using the B&B method. Such a transformation, however, is not required when solving the problem using the NNH algorithm. In order to make the NNH able to deal with the EGTSP, instead of a transformation, a simple mask is introduced. This mask is imposed on the cost matrix blocks corresponding to the groups of which an asteroid has already been selected, blocking the NNH from selecting another asteroid from that group. In this way, the NNH can find a solution to the EGTSP.
Although it has not been tested, it is believed that the NNH is able to solve the EGTSP by applying it to the transformed cost matrix without using the mask. The transformation, however, requires more computational effort than a simple statement prohibiting the NNH from selecting asteroids from a certain group. This becomes more important with increasing problem dimensions.

The second issue regarding the implementation of the NNH concerns the inclusion of Earth. Section 4.1.2 explains how Earth is included in the problem. Because the GTOC2 problem does not require the satellite to return to Earth, the transfer cost for all transfers returning to Earth were set to 0. In this way, the costs of the Hamiltonian cycles obtained by the B&B correctly represent the GTOC2 problem.
Setting the cost for the transfers returning to Earth to 0, however, imposes a problem when the TSP problem is being solved by the NNH. The NNH searches for the transfer with the lowest cost. Since returning to Earth from any asteroid has its cost set to 0, the NNH will always select Earth as its second body in its sequence. This is of course undesirable, and for this reason the return to Earth is not set to 0 when the NNH is used to solve the problem.
The drawback of not setting the return to Earth to 0 is the fact that the NNH is now optimizing for a GTOC2 problem including a return to Earth. This is however not the assignment. In order to solve this discrepancy, the obtained Hamiltonian cycles are not ranked according to their total cost, but to the cost of the first four transfers starting from Earth.

5.2 Solving the Continuous Aspect

This section will describe the procedure for solving the continuous part of the GTOC2 problem. The entire procedure is casted into a tool implemented in MATLAB. Parallel to this research, a tool for orbital analysis based on exposins was developed at the Faculty of Aerospace Engineering of the DUT. The tool originally served a purpose different from analyzing GTOC2, but modifications were made such that it became suitable for finding the optimal solution of a GTOC2-like mission scenario. The MATLAB optimization toolbox will be used extensively.

An overview of the entire procedure is given in figure 5.2. In the figure the

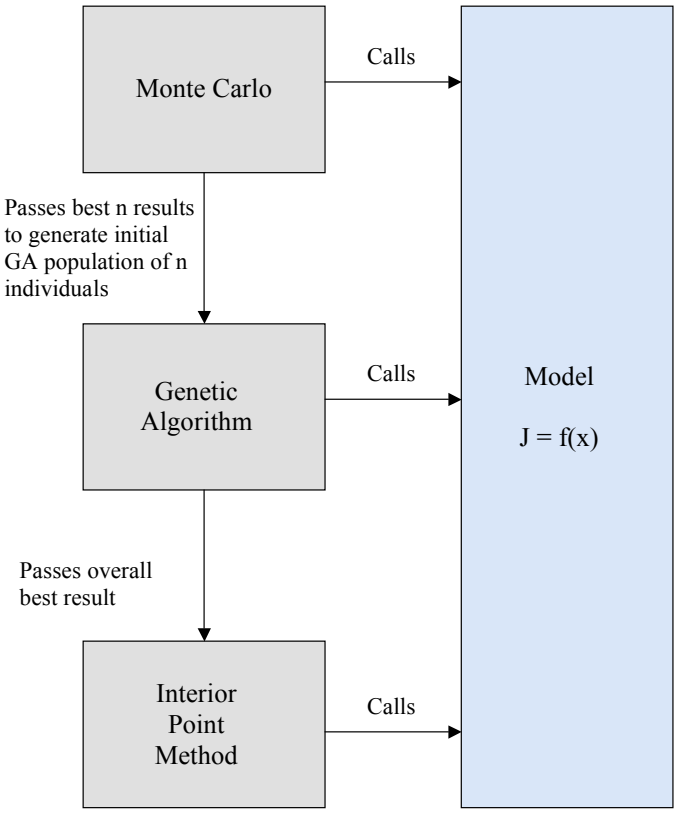

Figure 5.2 Overview of the solution procedure for the continuous aspect of GTOC2.

blue model block refers to the model as described in section 4.2.3. The grey blocks indicate methods used to find optimal solutions of the search space described by this model. Optimal solutions are maxima of J as described by equation 4.62. Since, however, the algorithms applied are searching for minima by default, the negative of equation 4.62 is taken during the computations. Three optimization methods are consecutively used to find the overall maximum, see Figure 5.2. First, the Monte Carlo method is applied, followed by a Genetic Algorithm search, and finally a local search method, the Interior Point Method, is applied. These three steps will be elaborated upon in the next sections.

5.2.1 Monte Carlo

The Monte Carlo (MC) method evaluates the search space at random points. The next iteration is independent of previous results. The main strength of these methods is the fact that they require only simple calculations. No information from the previous iteration is required to create new solutions. The MC methods evaluate the search space faster than, for example, the pure enumerative methods since they do not evaluate every option. The drawback is of course that there is no guarantee that the best solution is found because not the entire search space is evaluated. The rationale, however, for using the Monte Carlo method is to probe the search space for regions of feasible solutions and basins of attraction. These results will be passed on to the Genetic Algorithm. The number of results that will be passed on is equal to the size of the population used in the Genetic Algorithm. The number of iterations used was varied. Two values were evaluated: 50,000 and 100,000. These values were selected based on [*Pagano*, 2009], who has experience in applying the MC method on a search space consisting of more than 10 parameters.

5.2.2 Genetic Algorithm

The Genetic Algorithm (GA) is an enumerative optimization method that performs a structured search of the search space. The GA uses an evolving population to find the desired optimum. The individuals in this population each describe one single solution vector x, where x is given by equation 4.61. The added value of a GA over an MC method is that it uses information of previous iterations (previous populations) to direct the algorithm to more promising parts of the search space. The MATLAB optimization toolbox provides the implemented GA. The GA is a well-studied algorithm and has been applied extensively in the field of astrodynamics [*Myatt et al.*, 2003]. Therefore, only a description of the algorithm is provided in semicode format in figure 5.3. If needed, a good discourse on the GA can be found in [*Goldberg*, 1989]. The applied settings are as follows:

GA semi code

- Initialize population vectors uniformly over search space.
- Repeat
  - Evaluate objective function for all population members.
  - Select proportion of population with best objective values.
  - For each individual in selected set:
    - Select another individual in the set to me 'mated' with.
    - Produce two children through using crossover/mutation operator.
  - End
  - Replace the less fit members of the population with the newly generated children.
- Until convergence.

Figure 5.3 Semi code for Genetic Algorithm. Based on [*Myatt et al.*, 2003].

- **Population type:** There are two common options for describing individuals, the binary string representation and the real valued representation. The latter is used. In specific, a double vector describes one individual.

- **Population size:** The number of individuals of each generation has the largest impact on the performance of the algorithm. It is comparable to the amount of iterations of the MC method. Two different values for the population size were used, 300 and 500. If relevant, this setting will be specified.
- **Elitism:** Describes how many of the best individuals of each generation, counting from the top down, will survive and be part of the new generation. This value is set to 2.
- **Selection:** To determine which individuals in the current population will be parenting the next, a selection algorithm is used. he algorithm lays out a line in which each parent corresponds to a section of the line of length proportional to its scaled value. The algorithm moves along the line in steps of equal size. At each step, the algorithm allocates a parent from the section it lands on. Note that in this way, a parent can be selected more than once.
- **Crossover:** The part of the population remaining after the elite individuals have been transferred, is created by either crossover or mutation. The fraction of the new generation, excluding the elite individuals, that will be generated by crossover is 0.8. The remaining 20% will be generated by mutation. A random crossover function is used. This means that two individual from the current population will be selected (parent A and parent B) and a random binary vector is generated with the same length as the parents. For every position in this binary vector where the entry is 0, the value from parent A is selected. When the value in the binary vector is 1, the value from parent B is selected.
- **Mutation:** Mutation of individuals is applied to create a more diverse set of individuals. This helps to prevent the algorithm from getting stuck in local optima. As mentioned, 20% of the remaining fraction of the new population after elitism is created by mutation. The selection algorithm provides the mutation candidates. Each element of an individual has the same chance to mutate. This chance is 1%. If a certain element is selected for mutation, that element will be replaced by a random value within the range of that specific entry. The mutation function makes sure that the mutated individuals are within the bounds of the problem. Since the mutation rate is fairly low (1%), the part of the new population that is generated by mutation will be quite similar to their parents. This means that this 20% most likely contains relatively good individuals from the previous generation.
- **Migration:** Specifies the fraction of one subpopulation that will be transported to another subpopulation. This parameter is only of interest when multiple populations are used. Since only one population is used, this setting is irrelevant.

A visualization of the various parts of the new population is given in Figure 5.4. This figure gives an impression of which size of the new population is created by what part of the GA, and what the relative quality, in terms of objective value, of that part of the population is. The tuning of the various parameters is a very involved issue, and it is a study in itself to find the optimal combination of settings for the problem at hand. Because a lot of different combinations of the optimizer settings are possible and the evaluation of a single combination of settings takes a week, only two settings for the population size were evaluated. The population size was selected, because this parameter is the most influential when it comes to computational cost and quality of the solution. More on this in chapter 7.

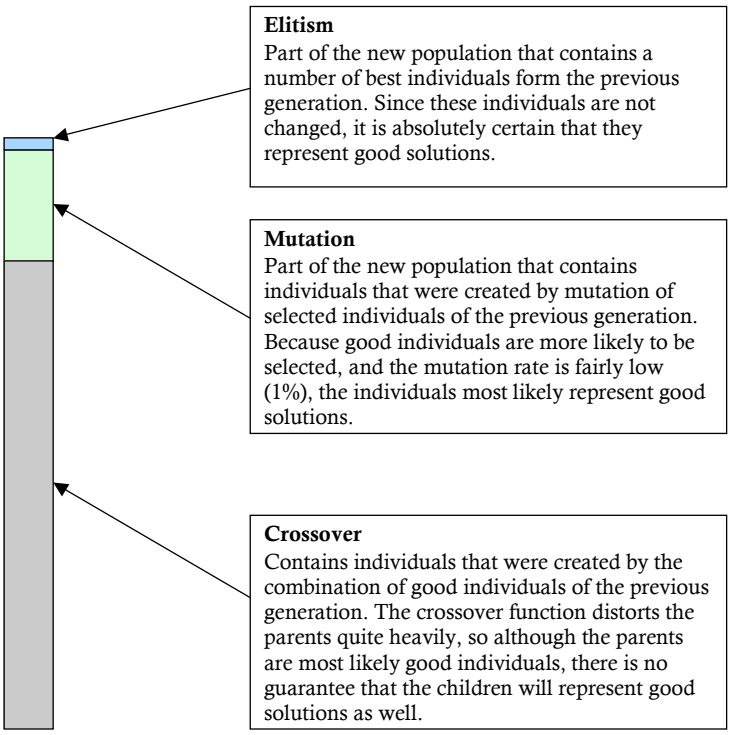

Figure 5.4 Visualization of new population as created by GA.

The individual with the best objective value is passed to the local optimizer.

5.2.3 Interior Point Method

The term Interior method is used as a common name for methods of penalty- and barrier type for nonlinear optimization. Interior Point (IP) methods belong to the class of analytical local optimization methods. They are used for solving bounded, constrained optimization problems. It is an iterative method starting from a user supplied initial point and making steps in the direction of a better solution, while steering away from bad solutions (by using the barrier) and complying with the constraints.
The IP method included in the fmincon function of the MATLAB optimization toolbox was used. This reason for choosing this method is because during the development the IP proved to be able to cope with the gaps in the search space (see appendix J), its ease of implementation and because it is readily available in a MATLAB toolbox.
Since the algorithm requires a background in optimal control theory and the IP method was used merely as a black box, only an outline of the method will be described in this section. For an introduction into optimal control theory the reader is referred to [*Visser*, 2000], [*Kirk*, 1998] or [*Gorter*, 2009]. An extensive discussion of the algorithm, including mathematical proof, is given in [*Byrd et al.*, 1998].

In short, the method consists of three steps. First, the optimization problem is transformed into a barrier problem. Second, the optimality conditions are iden-

tified. Third, the barrier problem is solved iteratively, using sequential quadratic programming, until the optimality conditions are satisfied and the original problem is solved within the desired accuracy. These steps will be outlined now.

The goal is to find a solution to the following minimization problem [1]:

$$\min_{\mathbf{x}} \ f(\mathbf{x}) \tag{5.1}$$

$$\text{subject to } \mathbf{g}(\mathbf{x}) \leq 0$$

where f is the objective function (equation 4.62), the equations $\mathbf{g}$ are real constraint functions, and $\mathbf{x}$ is given by 4.61. In order to help the algorithm to steer away from undesirable solutions, a barrier problem associated with equation 5.1 is defined:

$$\mathbf{z} = \begin{pmatrix} \mathbf{x} \\ \mathbf{s} \end{pmatrix}, \qquad \min_{\mathbf{x},\mathbf{s}} \ \phi(\mathbf{z}) = f(\mathbf{x}) - \mu \sum_{i=1}^{m} \ln s^{(i)} \tag{5.2}$$

$$\text{subject to } c(\mathbf{z}) = g(\mathbf{x}) + \mathbf{s} = 0$$

where μ is a barrier parameter and $\mathbf{s}$ is the vector of all slack variables. Both μ and $\mathbf{s}$ are (assumed to be) positive. From optimal control theory it is known that the optimal (minimum) solutions of equation 5.2 occur at the root of the gradient of the Lagrangian. The Lagrangian of equation 5.2 is:

$$L(\mathbf{x}, \mathbf{s}, \boldsymbol{\lambda}) = \phi(\mathbf{z}) + \boldsymbol{\lambda}^T c(\mathbf{z}) = f(\mathbf{x}) - \mu \sum_{i=1}^{m} \ln s^{(i)} + \boldsymbol{\lambda}^T (g(\mathbf{x}) + \mathbf{s}) \tag{5.3}$$

The conditions for optimality (zero gradient of the Lagrangian) then become:

$$\nabla_x L(\mathbf{x}, \mathbf{s}, \boldsymbol{\lambda}) = \nabla f(\mathbf{x}) + \mathbf{A}(\mathbf{x})\boldsymbol{\lambda} = 0 \tag{5.4}$$

$$\nabla_s L(\mathbf{x}, \mathbf{s}, \boldsymbol{\lambda}) = -\mu \mathbf{S}^{-1}\mathbf{e} + \boldsymbol{\lambda} = 0 \tag{5.5}$$

where

$$\mathbf{A}(\mathbf{x}) = (\nabla g^{(1)}(\mathbf{x}), \ldots, \nabla g^{(m)}(\mathbf{x})) \tag{5.6}$$

is the matrix of constraint gradients, and where

$$\mathbf{e} = \begin{pmatrix} 1 \\ \vdots \\ 1 \end{pmatrix}, \quad \mathbf{S} = \begin{pmatrix} s^{(1)} & & \\ & \ddots & \\ & & s^{(m)} \end{pmatrix} \tag{5.7}$$

The problem that is now completely described will be solved iteratively by making steps in the directions in which the objective value improves. These steps $\mathbf{d}$:

$$\mathbf{d} = \begin{pmatrix} d_x \\ d_s \end{pmatrix} \tag{5.8}$$

are obtained by approximately solving the quadratic problem:

$$\min_{\mathbf{d}} \nabla\phi(\mathbf{z})^T \mathbf{d} + \frac{1}{2}\mathbf{d}^T \mathbf{H} \mathbf{d} \tag{5.9}$$

[1] Note that minimization and maximization can be used interchangeably, without loss of generality. When maximization is required, the sign of the objective function need simply be reversed.

$$\text{subject to } \hat{\mathbf{A}}(\mathbf{z})^T\mathbf{d} + c(\mathbf{z}) = 0$$

where $\mathbf{H}$ is the Hessian of the Lagrangian of equation 5.2 with respect to $\mathbf{z}$ and where $\hat{\mathbf{A}}(\mathbf{z})$ is the Jacobian of c, given by:

$$\hat{\mathbf{A}}(\mathbf{z})^T = (\mathbf{A}(\mathbf{x})^T\ \mathbf{I}) \tag{5.10}$$

When the obtained value for $\mathbf{d}$ is deemed valid and helpful in progressing towards the optimum that step is made and the Lagrange multipliers λ are updated. Next, the barrier parameter μ is reduced and another approximate solution to equation 5.9 is obtained. This process is continued until equation 5.1 is solved to within the required accuracy.

Chapter 6

Validation

This chapter will present the validation results for both discrete methods as well as the continuous method. The discrete methods, AST and NNH, are tested with examples from literature. The validation of the continuous method is somewhat harder, since this model has not been used before in literature. The continuous method will be validated by applying it to a single leg Earth-Mars transfer instead. Results for this transfer, using exponential sinusoids, were obtained by [*Paulino*, 2008].

6.1 Discrete Method

In this section the ASt and NNH method will be tested using test problems from literature. First the AST will be evaluated, followed by the evaluation of the NNH.

6.1.1 AST

To validate the AST, two problems (one symmetric, one asymmetric) are passed to AST and the output is checked against the optimum found in literature. The problems are described by the cost matrices in figures 3.4 and 4.11. The core of AST (the B&B algorithm) is called to solve the problems. The input part of AST is deactivated because the problems already are in the TSP format and no cost function needs to be evaluated because the cost are already in the matrix. The output of AST has been modified such that it returns the solutions of the TSP only. The part of AST where the results of the GTSP are returned, as described in the output part of section 5.1.1, is deactivated. This part merely evaluates the TSP solution and determines the corresponding GTSP solution based on the GTSP-to-TSP transformation. The output of AST will give a sequence of numbers and the corresponding objective value J. The sequence of numbers correspond to the various nodes/cities. The output of the AST tool for both problems is included in appendix B.

The first validation problem is obtained from [*Winston*, 2004]. The (symmetric) cost matrix for this problem is given in figure 6.1. The optimal solution from literature is A→E→B→D→C→A, with a total cost of 668. The output of AST gives that the optimal solution is 0→4→1→3→2→0 (see appendix B), which is equivalent to A→E→B→D→C→A. The objective value is 668. Note that for the

	A	B	C	D	E
A	∞	132	217	164	58
B	132	∞	290	201	79
C	217	290	∞	113	303
D	164	201	113	∞	196
E	58	79	303	196	∞

Figure 6.1 Example of a Traveling Salesman Problem with 5 cities [*Winston*, 2004].

third iteration (process count equals 3), a candidate solution is found which equals the global optimum of 668. The corresponding cycle is 0→2→3→1→4→0, which is equivalent to A→C→D→B→E→A. Note that these solutions are the same, but they traverse the optimal Hamiltonian cycle in the opposite way.
The reason for the existence of both of these solutions is the fact that the cost matrix for this problem is symmetric: the cost to travel from city A to B is the same as from B to A. It logically follows that when one optimal solution is found in a symmetric matrix there exists another solution with the same cost but a reversed path through the cities.
The next question that arrises is how this affects the use of AST for symmetric matrices and for GTOC2. The answer is "not at all". For every valid cyclic solution found in a symmetric cost matrix it is known that there exists a complementary solution traversing the same nodes in the opposite direction. Finding one means having found the other one too.
One remaining question of lesser importance is whether or not both solutions are always found during the B&B process. The answer is "no". In Appendix B both solutions were obtained. If, however, the solution procedure from [*Winston*, 2004] is used, only one of the solutions is found. The difference in both procedures lies in the way in which the next subproblem to be evaluated is selected. If another choice is made another route to the optimal solution is found. That other route may not come across both solutions.
However, finding a sequence of asteroids for the GTOC2 problem is not a symmetric problem. The (optimal) orbit from asteroid A to B is always different from the (optimal) orbit from asteroid B to A. If, however, the problem is made time-independent as is done in this research, it is possible to choose a symmetric cost function. If, for example, the difference in orbital elements is chosen as a cost for a specific transfer (note: this cost function is not necessarily a good one), then the cost matrix will be symmetric. Most other choices for a cost function, however, will result in an asymmetric cost matrix. Based on these considerations and the validation results it can be stated that symmetry will not be an issue when using AST for asteroid sequencing, and the choice for the cost function is not restricted in any way.
It should be noted that the efficiency of the solution process for symmetric matrices is lower than that for asymmetric matrices, because the algorithm spends time to find duplicate solutions.

The second validation problem is obtained from [*Behzad and Modarres*, 2002]. The (assymetric) cost matrix is given in figure 6.2. The optimal solution from

	A	B	C	D	E	F	G
A	∞	0	8+M	9+M	3+M	1+M	5+M
B	0	∞	5+M	7+M	4+M	6+M	2+M
C	2+M	1+M	∞	0	5+M	6+M	1+M
D	6+M	3+M	0	∞	4+M	2+M	4+M
E	8+M	4+M	6+M	5+M	∞	0	∞
F	4+M	7+M	9+M	7+M	∞	∞	0
G	9+M	7+M	9+M	3+M	0	∞	∞

Figure 6.2 Result of transformation from example GTSP of figure 3.5 to TSP [*Behzad and Modarres*, 2002].

literature is A→E→F→G→D→C→B→A, with a total cost of 7+3M, where M is a number larger than the sum of all finite elements. In this validation the sum of all elements is 162 and M is randomly set to 172. This results in an optimal solution of $7 + 3 * 172 = 523$. Note that this example is the TSP equivalent of a GTSP problem with three groups as shown in figure 3.5. The output of AST gives that the optimal solution is 0→5→6→4→3→2→1→0 (see appendix B), which is equivalent to A→F→G→E→D→C→B→A. The objective value is 523. Note that the objective value is the same as what was found in literature, but the cycle is not. This means that two different optimal solutions to the TSP exist. The cycle as presented in literature is also found by the AST. Step 17 of the output (process count is 17) shows that a candidate solution is found for which the objective value is 523 and the corresponding solution is 0→4→5→6→3→2→1→0, or A→E→F→G→D→C→B→A. This is equal to the optimal solution in [*Behzad and Modarres*, 2002].

When the two solutions are translated into the GTSP solution (finding the first accessed city of each group), the following two sequences are obtained: E→D→B→E and F→D→B→F. If the costs for these sequences are checked using figure 3.5, it is found that both costs add up to 7. This indicates that the problem has no unique solution. An interesting fact to notice is that in [*Behzad and Modarres*, 2002] there is no mentioning of the transformation being able to deal with non-unique solutions.

The existence of non-unique solutions has an influence on the quality of the solutions as delivered by AST. AST returns every candidate solution it comes across. If it has the same objective value as the best solution found so far it will return it as well. If it comes across a valid solution (cyclic) but with an objective value higher than the current best, it will not be returned, and the branch will be disregarded for further analysis. In principle this is what is required for progressing towards an optimal solution and the B&B algorithm is supposed to operate in this way.

The disadvantage is, that at this point of solving the complete GTOC2 problem, it is not known if a sequence which is considered better by the AST is also better

when considering the continuous aspect of the problem (i.e. if the orbit through the asteroid sequence of one candidate solution is indeed better than the orbit through another asteroid sequence of another candidate solution). The result is that although the AST will find optimal solutions with the same objective value as the current best, it can also miss sequences which have a discrete value a little worse than the optimum, but which could result in good solutions from a continuous point of view.
The extent of the impact of this observation is based on chance. The algorithm might choose a path which finds a large number of these suboptimal solutions, but it can also miss a fair few of them. This is inherent to the algorithm and cannot be changed. The impact of this disadvantageous characteristic of the algorithm can be mitigated by allowing the B&B to choose its path randomly, and have it run several times. Unfortunately, the time available did not permit the testing of this setting.

Based on the above observations, it is concluded that the tool is able to work towards good candidate solutions. The quality of the overall result is based heavily on the combination of the quality of the objective function and the settings of the algorithm (e.g. deterministic path vs. random path).

6.1.2 NNH

To validate the performance of the NNH it will be tested on the problem given in Figure 3.5. This problem is the untransformed version of the problem given in Figure4.11, used to validate the AST. First this problem is solved by hand. The results are given in Figure 6.3.

City 1	City 2	City 3	Cost 1	Cost 2	Cost 3	Total cost
A	G	D	2	7	2	11
B	F	D	1	5	1	7
C	F	B	2	4	8	14
D	B	F	1	1	5	7
E	D	B	3	1	3	7
F	B	C	4	8	2	14
G	A	C	4	5	2	11

Figure 6.3 Manual solution of EGTSP problem of Figure 3.5.

The output of the NNH is given in Figure 6.4. The IDs 1 to 7 correspond with cities A to G. Comparing the result of figures 6.4 and 6.3 shows that the NNH produces the same results. The results also shows, like the AST validation results that this particular problem contains multiple optimal solutions.The optimal solutions are the same as the ones that were obtained by the AST (E→D→B→E and F→D→B→F). Note that the optimal result in Figure 6.3 obtained when starting at city B is the same optimal solution that was found when starting at city D. Based on these results it is concluded that the NNH performs correctly when solving the EGTSP.

```
Cost matrix is:

inf inf 5 7 4 6 2
inf inf 8 9 3 1 5
6 3 inf inf 4 2 2
2 1 inf inf 5 6 1
9 7 9 3 inf inf inf
8 4 6 5 inf inf inf
4 7 9 7 inf inf inf

IDs: 1-7-4
costs: 2-7-2
total cost:  11

IDs: 2-6-4
costs: 1-5-1
total cost:  7

IDs: 3-6-2
costs: 2-4-8
total cost:  14

IDs: 4-2-6
costs: 1-1-5
total cost:  7

IDs: 5-4-2
costs: 3-1-3
total cost:  7

IDs: 6-2-3
costs: 4-8-2
total cost:  14

IDs: 7-1-3
costs: 4-5-2
total cost:  11


IDs of best cycle: 2-6-4
transfer costs of best cycle: 1-5-1
total cost of best transfer:  7
```

Figure 6.4 NNH output for EGTSP problem of Figure 3.5.

6.2 Continuous Method

Due to the absence of tests performed in literature on the applied patched exposin model, it is impossible to validate the entire model. Instead, a well-studied single leg transfer for Earth to Mars will be used to validate the continuous method for one leg. A thorough study of exposins has been performed in [*Paulino*, 2008], and the results obtained for the EM transfer will be used for validation.
In [*Paulino*, 2008] a multi-objective approach was used. The used fuel mass and the total velocity mismatch at departure and arrival are minimized. In the continuous method a single-objective approach is used and additional terms are added in the form of penalties. To mimic the objective function used in [*Paulino*, 2008] the objective function of the continuous method was changed such that the used fuel mass is minimized and a penalty is added for velocity mismatches upon departure and arrival. Also the fact that a ΔV budget of 3.5 km/s is available during the GTOC 2 competition at Earth departure is disregarded.

Two tests were performed. An overview of the tests is given in figure 6.5. The two tests are used to mimic the objective function of [*Paulino*, 2008] as

Test ID	Transfer	Objective	Initial mass	Penalty
1	EM	Fuel Mass	486.3	Mass equiv.
2	EM	Fuel Mass	486.3	>0.5 Q

Figure 6.5 Overview of the validation tests for the continuous method.

well as possible. Both tests use the same settings: an MC of 50,000 iterations and a GA using 150 individuals and an initial spacecraft mass of 486.3 kg. The penalties, however, differ. Since there are no penalties included in the model used by [*Paulino*, 2008], no knowledge is available about the penalty settings. To solve this problem, two different penalty settings have been tested. The first test applies a penalty to the velocity mismatch by converting this to a mass, using Tsiolkovsky's law, as explained in section 4.2.3. The second test uses this conversion as well, but on top of that, if the velocity mismatch is larger than 0.5 km/s, the mass will be squared. This stronger penalty should make it easier for the GA to find solutions with a lower velocity mismatch. The results in [*Paulino*, 2008] were obtained by using an MC with 100,000 iterations. The continuous method will use an MC algorithm of 50,000 iterations followed by a GA algorithm of 150 individuals; the transfer was analyzed ten times using the continuous method. The results are summarized in Figure 6.6. In this figure six parameters are given. J is the objective value as given by Equation 4.62, J GTOC is the corresponding objective value as used during GTOC2. It is obtained by evaluating Equation 4.62 without the penalties. TOT DV indicates the total velocity mismatch in km/s, obtained by adding the departure velocity mismatch to the arrival velocity mismatch. T0 is the departure date given in MJD.

Test ID	J			Mass Used [kg]			TOF [year]		
	mean	std	best	mean	std	best	mean	std	best
1	70	0.5	69	44	9	33	1.07	0.36	0.75
2	71	1.8	70	48	4	47	1.05	0.11	1.07

	J GTOC			TOT DV			T0		
	mean	std	best	mean	std	best	mean	std	best
1	1477	416	1948	2.14	0.68	2.99	60038	3077	64395
2	1401	135	1361	1.89	0.30	1.89	59933	2366	58935

Figure 6.6 Results of the validation tests for the continuous method.

The results obtained by [*Paulino*, 2008] are presented in figure 6.7. When comparing the best results of the continuous method with the Pareto front in figure 6.7, it follows that the continuous method finds slightly better solutions. The reason for this difference is the fact that there is a slight difference in the implementation of the objective function as well as in the solution method. Because the continuous method uses a GA and [*Paulino*, 2008] does not, it follows that a GA is probably better in finding optimal exposin shapes than the MC. This topic will be returned to in the results chapter.
Based on these results, it is concluded that the exposins are implemented correctly.

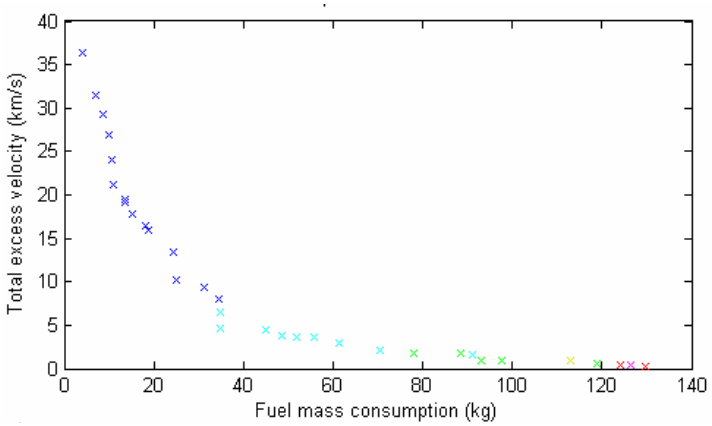

Figure 6.7 Results for the Earth-Mars transfer as presented in [*Paulino*, 2008].

Chapter 7

Results

This chapter will present the results of various analyses performed by both the discrete and the continuous methods.

7.1 Discrete Method

This section discusses the results of the discrete method. First, an analysis of the cost matrix reduction procedure, described in section 4.1.3, will be performed. This will give insight in the quality and efficiency of the reduction procedure. Second, the results of both the AST and the NNH are presented and compared. The output of both the AST and the NNH will be generated using the three different cost functions described in section 4.1.1. This will give an indication of the performance of both methods on a search space defined by any of the three cost functions that are relevant for solving the asteroid selection and sequencing problem.

7.1.1 Cost Matrix Reduction Results

In order to facilitate the analysis of the discrete aspect of GTOC2 by using the AST, the cost matrix is reduced. As discussed in section 4.1.3 a certain number of best transfers are selected from each cost matrix block and the corresponding asteroids are extracted and a new (reduced) cost matrix is constructed using only the selected asteroids. To assess the quality and efficiency of the reduction procedure, the asteroids selected by the reduction procedure are compared to the asteroids in the sequences obtained by all GTOC participants. Each GTOC2 participant found an asteroid sequence of four asteroids. Combining all asteroids in the solutions of all participants forms a set of relatively good asteroids. Comparing the asteroids that are left after the reduction procedure with this set of relatively good asteroids, and counting the number of matching asteroids provides a way to measure the quality of the reduction procedure: a high number of matching asteroids in a small (reduced) cost matrix is preferred over a low number of matching asteroids in a large (reduced) cost matrix. The number of selected best transfers can be varied and it is up to the mission designer to choose an appropriate number. The cost matrix is reduced using a varying number of best transfers, starting from 2 and ending at 7. In Figure 7.1 the results of these reduction procedures are summarized.

Best nr. of transfers	Delta V			Energy			ESA		
	Reduced cost matrix size	Nr. of matching asteroids	Ratio	Reduced cost matrix size	Nr. of matching asteroids	Ratio	Reduced cost matrix size	Nr. of matching asteroids	Ratio
2	30x30	5	0.167	25x25	4	0.160	28x28	3	0.107
3	47x47	8	0.170	46x46	6	0.130	42x42	8	0.190
4	63x63	12	0.190	60x60	7	0.117	60x60	10	0.167
5	74x74	13	0.176	73x73	8	0.110	75x75	10	0.133
6	87x87	15	0.172	89x89	11	0.124	90x90	12	0.133
7	89x89	15	0.169	104x104	12	0.115	102x102	12	0.118

Figure 7.1 Overview of cost matrix reduction results.

For each cost function, based on ΔV, energy or ESA, three items are listed. First, the size of the reduced cost matrix. This is a square matrix with a dimension equal to the number of selected asteroids. Second, the number of matching asteroids that correspond with any of the asteroids in all best sequences submitted by the GTOC2 participants. Third, the ratio between the number of selected asteroids and the reduced cost matrix dimension. As mentioned, a good cost function will provide a high number of matches but in a small reduced cost matrix size. Cost matrices with this characteristic represent efficient problems to solve, since they are small but contain a large number of good candidates. This translates into a high ratio of good asteroids with respect to the reduced cost matrix dimension.

From Figure 7.1 it can be concluded that the cost function based on ΔV has the highest ratio values and is therefore, at this point, preferable over the other two cost functions. Based on these results the number of best transfers is chosen to be 4 when creating the reduced cost matrix, because it gives a relatively good ratio value for all cost functions and also provides a high absolute number of good candidate asteroids. On top of this there is a practical reason. It turned out that the Hungarian Algorithm was able to solve matrices with a dimension of 60 in a relatively short amount of time (about 1s). A matrix with a larger dimension will require significantly more time to solve and therefore will make it unpractical to use it for solving subproblems of the B&B algorithm.

Comparing the asteroids selected by the reduction procedure with the asteroids in the sequences produced by the GTOC2 participants provides interesting results. Figures 7.2 -7.4 show all asteroid sequences as obtained by the GTOC2 participants. This was based on a reduction using the 4 best transfers from each cost matrix block. In these figures the first column specifies the rank of the sequence. The next five columns specifies the sequence itself, where the first body is always Earth, indicated by ID 1. The last column shows the corresponding group order. The asteroids that match with the asteroids selected by the reduction procedure are highlighted in blue. Figure 7.2 highlights the matching asteroids that were obtained using a cost function based on ΔV. Figure 7.3 highlights the asteroids that were obtained using a cost function based on energy. Figure 7.4 highlights the asteroids that were obtained using the cost function used by ESA.

Rank	GTOC ID 1	GTOC ID 2	GTOC ID 3	GTOC ID 4	GTOC ID 5	Group order
1	1	3258076	2000060	2000058	2002959	4321
2	1	3250293	2000149	2000569	2002483	4321
3	1	3170221	2000574	2000209	2011542	4321
4	1	3170221	2001990	2000240	2001754	4321
5	1	3017309	2000443	2000490	2001345	4321
6	1	3250293	2000027	2000110	2001038	4321
7	1	3288933	2001707	2000047	2014569	4231
8	1	3329255	2000232	2000807	2001754	4321
9	1	3170221	2000043	2000074	2002483	4321
10	1	3250293	2000149	2000224	2009661	4321
11	1	3343104	2000169	2000075	2000659	4321

Figure 7.2 Visualization of the matching asteroids with the GTOC2 results. The matching asteroids are highlighted in blue.

Rank	GTOC ID 1	GTOC ID 2	GTOC ID 3	GTOC ID 4	GTOC ID 5	Group order
1	1	3258076	2000060	2000058	2002959	4321
2	1	3250293	2000149	2000569	2002483	4321
3	1	3170221	2000574	2000209	2011542	4321
4	1	3170221	2001990	2000240	2001754	4321
5	1	3017309	2000443	2000490	2001345	4321
6	1	3250293	2000027	2000110	2001038	4321
7	1	3288933	2001707	2000047	2014569	4231
8	1	3329255	2000232	2000807	2001754	4321
9	1	3170221	2000043	2000074	2002483	4321
10	1	3250293	2000149	2000224	2009661	4321
11	1	3343104	2000169	2000075	2000659	4321

Figure 7.3 Visualization of the matching asteroids with the GTOC2 results. The matching asteroids are highlighted in blue.

Rank	GTOC ID 1	GTOC ID 2	GTOC ID 3	GTOC ID 4	GTOC ID 5	Group order
1	1	3258076	2000060	2000058	2002959	4321
2	1	3250293	2000149	2000569	2002483	4321
3	1	3170221	2000574	2000209	2011542	4321
4	1	3170221	2001990	2000240	2001754	4321
5	1	3017309	2000443	2000490	2001345	4321
6	1	3250293	2000027	2000110	2001038	4321
7	1	3288933	2001707	2000047	2014569	4231
8	1	3329255	2000232	2000807	2001754	4321
9	1	3170221	2000043	2000074	2002483	4321
10	1	3250293	2000149	2000224	2009661	4321
11	1	3343104	2000169	2000075	2000659	4321

Figure 7.4 Visualization of the matching asteroids with the GTOC2 results. The matching asteroids are highlighted in blue.

From figures 7.2 -7.4 an important observations can be made. All three cost functions identify good asteroids belonging to group 1 easily. For the other groups, however, this is not the case. Only one or two asteroids from groups 2, 3 and 4 are selected. This indicates that the quality of the cost functions might not be optimal. Some caution needs to be taken into account when drawing this conclusion. The participants most likely analyzed numerous asteroid sequences, but only the best one is presented in their results. It might be that other sequences that were considered promising, contain the asteroids that are selected by the reduction procedure here.

Another interesting observation is the high correlation between the selected asteroids using the three different cost functions. This is visualized in Figure 7.5. In this figure the asteroids that were selected by the reduction procedure, using the best four transfers, that matched with any of the asteroids selected by the GTOC2 participants is given. The green fields indicate asteroids that were selected by two of the cost functions. The blue fields indicate asteroids that were selected by all three cost functions. This high overlap in selected asteroids indicates that the cost functions, although based on different concepts and equations, are effectively not very different.

Selected Asteroid ID's		
DV	E	ESA
2000027	2000149	2000043
2000058	2001038	2000075
2000074	2001345	2001038
2000075	2001754	2001345
2000659	2009661	2001754
2001038	2011542	2002959
2001345	3170221	2009661
2002483		2011542
2002959		3017309
2009661		3170221
2011542		
3017309		

Figure 7.5 Overview of selected asteroid ID's.

When a statistic approach to the results is adopted, the impact of the reduction procedure and the various cost functions can be quantified. Out of the 910 asteroid candidates, 38 distinct good asteroids are selected by the participants, see Appendix A. This is a ratio of 0.042. The reduced cost matrices all have better ratios than 0.042, indicating that selection based on these cost functions does increase the efficiency of the solution process. It is also known, however, that promising candidates are discarded as well, since not all asteroids selected by the GTOC2 participants are present in the reduced cost matrices.
In appendix C more extensive results of the reduction procedure are included.

7.1.2 AST and NNH Results

The two presented discrete methods, the B&B (as implemented in AST) and the NNH method (as described in sections 5.1.1 and 3.6 respectively), are both applied to three different cost functions (detailed in section 4.1.1). The NNH is applied, for each cost function, to both the complete cost matrix as well as the reduced cost matrix. The best results are presented in Figure 7.6.

	Method	Cost matrix	Cost	GTOC ID 1	GTOC ID 2	GTOC ID 3	GTOC ID 4	GTOC ID 5	Group order
DV	NNH	reduced (63)	25.6	1	3064315	2000421	3297182	2011351	4321
	NNH	total (911)	21.3	1	9033382	2001830	2000206	2002959	4321
	AST	reduced (63)	22.9	1	3072273	2001621	2000206	2002959	4321
E	NNH	reduced (60)	465.9	1	3072273	2000197	3114017	2001621	4321
	NNH	total (911)	451.3	1	3250293	2000149	2000207	2011542	4321
	AST	reduced (60)	420.6	1	3167353	2000975	2000104	2011542	4321
ESA	NNH	reduced (60)	17.1	1	3170221	2000104	2000489	2011542	4321
	NNH	total (911)	15.0	1	3339082	2001055	2000163	2002959	4321
	AST	reduced (60)	16.0	1	3167353	2000075	2000642	2011542	4231

Figure 7.6 Best results of the B&B and the NNH for the three different cost functions based on ΔV (DV), energy (E) and the ESA cost function (ESA).

In figure 7.6, the first column indicates which method is used. There are two options: either the AST tool or the NNH. The second column indicates on which cost matrix the method was used and in between brackets the dimension of the cost matrix. There are two options. One is the complete cost matrix, the other is the reduced cost matrix. In this case the reduced cost matrix was created using the best 4 transfers from each matrix block, as argued in section 7.1.1. It should be noted that in practice the total cost matrix is constructed by AST as well, but that the core of the tool, the B&B procedure, is applied to the reduced matrix only. This is because the Hungarian Algorithm is unable to deal with the complete cost matrices. The reduction is performed by the AST as well. The third column shows the minimum total cost of the corresponding asteroid sequence as specified in columns four to eight [1] Note that the presented cost is not the cost of the complete Hamiltonian cycle but the cost of the transfers starting from Earth and ending at the fourth asteroid. The NNH is used to obtain Hamiltonian cycles for different starting points (any of the asteroids or Earth), but the quality of the solution is determined by the cost of the first four transfers starting from Earth. This is because this cost resembles the GTOC problem better. A complete Hamiltonian cycle would model a GTOC2 mission including a return to Earth. The GTOC2 problem, however, does not include the return to Earth.
Columns 4 to 8 contain the GTOC2 asteroid ID's (GTOC ID) of the visited asteroids, where columns 4 indicates the starting point (which is always Earth), column 5 indicates the asteroid that is visited first, column 6 the asteroid that is visited second, etcetera.
The last column states the group sequence of the asteroids in that particular sequence.

Based on the results presented in Figure 7.6 it can be concluded that the AST outperforms the NNH on the same search space for all three cost functions. An improvement of 10.5% for the cost function based on ΔV is obtained, an improvement of 9.7% for the energy cost function, and an improvement of 5.9% when using the ESA cost function. In case of the energy cost function, the AST even outperforms the NNH when the NNH is applied to the full set of asteroids. For the other two cost functions however, the NNH, when applied tot the total set of asteroids, finds a better result than the AST. Moreover, the NNH method produces this result much faster. The NNH took minutes to produce its results, while the

[1] remember that the cost of the transfer when analyzing the discrete aspect needs to be minimized, i.e., a cheap transfer is sought, but that the objective value for the continuous aspect needs to be maximized. Due to the nature of the cost functions, low objective values for the discrete aspect will most likely result in high objective values for the continuous aspect.

AST has been running for 3 weeks, after which this process was terminated by the user. The complete output of AST, however, was generated within a few hours, and from there on AST has only been evaluating the tree of options without further improvement of the objective value.
It should be noted that stopping the AST can have a disadvantageous effect on the quality of the solution. It is not known if the global optimum has been found. As mentioned in section 3.5.1, stopping the algorithm results in a range for the global optimum. If it was known beforehand that the algorithm would not be able to finish, the search strategy of the B&B would most likely have been changed from DFS to BFS. The fact that the algorithm was stopped does not mean its results are invalid, it does implicate that more good solutions might have been obtained if another search strategy was used. It is emphasized that this is merely a hypothesis.

The group order of the obtained sequences matches those of the GTOC2 participants. Both the NNH as well as the AST indicate that either 4-3-2-1 or 4-2-3-1 is a promising sequence of asteroid groups. This coincides with the results from the GTOC2 participants (see appendix A or C). Although results do not indicate that the cost function based on energy results in more asteroid sequences with group order of either 4-3-2-1 or 4-2-3-1, the explanation given in section 2.3 that this group order is preferable because of an efficient use of energy, is deemed plausible.

Figures 7.7-7.9 show the top ten results of the AST for the cost function based on ΔV, E and the cost function used by ESA respectively. These results confirm that good sequences have group sequences of either 0-4-3-2-1 or 0-4-2-3-1. When the results for the ESA cost function are scrutinized it is noted that a fair number of duplicate solutions exist. This is due to the symmetry of the cost function as described in sections 4.1.1 and 3.3. The symmetry reduces the efficiency of the solution process, since time is spent looking for duplicate solutions.

DV value [km/s]	GTOC ID 1	GTOC ID 2	GTOC ID 3	GTOC ID 4	GTOC ID 5	Group order
22.92	1	3072273	2001621	2000206	2002959	0 4 3 2 1
24.48	1	3170221	2012746	2000206	2002959	0 4 3 2 1
24.58	1	3072273	2001621	2000558	2001345	0 4 3 2 1
25.19	1	3170221	2012746	2000558	2001345	0 4 3 2 1
27.00	1	3170221	2012746	2000558	2004754	0 4 3 2 1
27.83	1	3170221	2012746	2000010	2005209	0 4 3 2 1
28.35	1	3170221	2000010	2000975	2011542	0 4 2 3 1
30.79	1	3170221	2012746	2011542	2000010	0 4 3 1 2
39.32	1	3170221	2011542	2000010	2000008	0 4 1 2 3
41.08	1	2002959	2000010	2000158	3297182	0 1 2 3 4

Figure 7.7 Top 10 AST results for the cost function based on ΔV: asteroid and group sequences.

E value [MJ/kg]	GTOC ID 1	GTOC ID 2	GTOC ID 3	GTOC ID 4	GTOC ID 5	Group order
421	1	3167353	2000975	2000104	2011542	0 4 3 2 1
438	1	3167353	2000975	2002407	2011542	0 4 3 2 1
454	1	3339082	2000016	2000245	2011542	0 4 2 3 1
456	1	3167353	2000104	2011542	2000642	0 4 2 1 3
465	1	3167353	2000975	2011542	2000121	0 4 3 1 2
474	1	3167353	2000104	2011542	2001087	0 4 2 1 3
479	1	3339082	2000016	2011542	2000642	0 4 2 1 3
497	1	3339082	2000016	2011542	2001087	0 4 2 1 3
513	1	3339082	2001621	2011542	2000121	0 4 3 1 2
521	1	3339082	2001621	2011542	2000334	0 4 3 1 2

Figure 7.8 Top 10 AST results for the cost function based on energy: asteroid and group sequences.

ESA value [km/s]	GTOC ID 1	GTOC ID 2	GTOC ID 3	GTOC ID 4	GTOC ID 5	Group order
15.98	1	3167353	2000075	2000642	2011542	0 4 2 3 1
15.98	1	3167353	2000075	2000642	2011542	0 4 2 3 1
16.32	1	3347493	2000075	2000642	2011542	0 4 2 3 1
16.56	1	3167353	2002407	2000642	2011542	0 4 2 3 1
16.56	1	3167353	2002407	2000642	2011542	0 4 2 3 1
16.75	1	3347493	2002407	2000642	2011542	0 4 2 3 1
16.84	1	3170221	2000937	2002407	2011542	0 4 3 2 1
16.87	1	3167353	2001047	2000021	2011542	0 4 3 2 1
16.93	1	3170221	2012746	2002407	2011542	0 4 3 2 1
17.11	1	3167353	2000075	2011542	2000642	0 4 2 1 3

Figure 7.9 Top 10 AST results for the cost function used by ESA: asteroid and group sequences.

Comparing the results of the AST for the ESA cost function with the results of the GTOC2 competition, included in appendix A, shows that the ESA asteroid sequence is not the same as the solution sequence found by AST. This is due to the fact that not all asteroids in the sequence obtained by ESA survived the reduction process of the cost matrix. Apparently, ESA used a stronger B&B algorithm than the one developed during this research.
More extensive AST results are presented in appendix D.

Figures 7.10-7.12 show the top ten results of the NNH, applied to the reduced cost matrix, for the cost function based on ΔV, E and the cost function used by ESA respectively. The results show that when a reduced cost matrix is analyzed, the best solution is found when starting from Earth. The next best sequence is significantly worse for all three cases. The reason why the best sequences start at Earth can be explained by considering that the NNH searches for a Hamiltonian cycle. The multistart algorithm constructs a cycle for every starting body by looking for the transfer with the lowest cost to a body in a group that has not been visited yet. At some point however the situation arises that all groups have been visited and the cycle needs to be closed by returning to the starting body. This last transfer is not a variable to be optimized, it is fixed by the final body obtained by the NNH and the starting body.

DV value [km/s]	GTOC ID 1	GTOC ID 2	GTOC ID 3	GTOC ID 4	GTOC ID 5	Group order
25.59	1	3064315	2000421	3297182	2011351	4321
28.02	2001723	2002223	2012746	1	3064315	23104
28.21	2000642	2000975	2012746	1	3064315	32104
28.44	2000975	2000642	2000010	1	3064315	23104
28.73	2000519	2000138	2000021	1	3064315	23104
29.05	2011542	2000642	2000010	1	3064315	23104
29.27	3072273	2000558	2000010	1	3064315	23104
29.47	3297182	2000642	2000010	1	3064315	23104
29.68	2005209	3072273	2000010	1	3064315	32104
29.68	2000558	3072273	2000010	1	3064315	32104

Figure 7.10 Top 10 NNH results when applied to the reduced cost matrix, for the cost function based on ΔV.

E value [MJ/kg]	GTOC ID 1	GTOC ID 2	GTOC ID 3	GTOC ID 4	GTOC ID 5	Group order
466	1	3072273	2000197	3114017	2001621	4321
542	2004063	2000245	2011542	2100004	1	43120
657	2003362	2000245	2011542	2100004	1	43120
707	2000149	2000196	2001621	2000346	1	42130
741	2000521	2001345	2011542	2004063	1	32140
756	2000413	1	2000521	2001345	2011542	40321
757	2000642	3350633	2011542	2004063	1	32140
760	3177176	1	2000521	2001345	2011542	40321
764	2000207	3114017	2001621	2000149	1	32140
768	2000489	2000121	2011542	2004063	1	23140

Figure 7.11 Top 10 NNH results when applied to the reduced cost matrix, for the cost function based on energy.

ESA value [km/s]	GTOC ID 1	GTOC ID 2	GTOC ID 3	GTOC ID 4	GTOC ID 5	Group order
17.10	1	3170221	2000104	2000489	2011542	4321
24.97	2000010	3072273	2000937	2001087	1	32140
25.08	2000121	3350633	2000937	2001087	1	32140
25.46	2000009	3017309	2000937	2001087	1	32140
25.63	2000104	2000489	2011542	2001087	1	32140
25.63	2001087	1	2000104	2000489	2011542	40321
25.79	3072273	2000010	2000937	2001087	1	23140
25.80	2001665	3017309	2000937	2001087	1	32140
25.82	3046844	3017309	2000937	2001087	1	32140
25.85	3350633	2000121	2009661	2001087	1	23140

Figure 7.12 Top 10 NNH results when applied to the reduced cost matrix, for the cost function used by ESA.

As previously mentioned, the quality of the sequence is not determined by the cost of the complete cycle but by the cost of the first four transfers starting from Earth. In practice this will mean that all sequences of four transfers starting from Earth, will contain that one transfer that is fixed, except when the NNH starts at Earth itself. When the NNH starts at Earth a Hamiltonian cycle is obtained of five transfers, of which the fifth transfer is the one which is not optimized. The quality, however, is determined by the first four transfers only, which are all optimized for. The fact that all transfers are optimized for instead of only three out of four, which is the case when starting at any of the asteroids, explains why the multistart NNH obtains its best result when starting at Earth. It also explains the jump in objective value present between the best solution and the other solution values for some cost functions.

When, however, the results for the complete asteroid set are considered it shows a smoother increase in objective value. Figures 7.13-7.15 show the top ten results of the NNH, applied to the complete cost matrix, for the cost function based on ΔV, E and the cost function used by ESA respectively. It can be seen that the difference in objective value between the first and second best sequence is smaller compared to the difference in figures 7.10-7.12.

DV value [km/s]	GTOC ID 1	GTOC ID 2	GTOC ID 3	GTOC ID 4	GTOC ID 5	Group order
21.28	1	3339082	2001830	2000206	2002959	4321
21.28	2001830	2000206	2002959	1	3339082	32104
22.91	2000851	2000206	2002959	1	3339082	32104
23.25	2000443	2000034	2002207	1	3339082	32104
23.45	2000534	2000206	2002959	1	3339082	32104
23.46	2000058	2000533	2002207	1	3339082	23104
23.63	2000673	2000206	2002959	1	3339082	32104
23.65	2000548	2000206	2002959	1	3339082	32104
24.06	2000182	2000206	2002959	1	3339082	32104
24.13	2001350	2000206	2002959	1	3339082	32104

Figure 7.13 Top 10 NNH results when applied to the reduced cost matrix, for the cost function based on ΔV.

E value [MJ/kg]	GTOC ID 1	GTOC ID 2	GTOC ID 3	GTOC ID 4	GTOC ID 5	Group order
451	1	3250293	2000149	2000207	2011542	4321
498	3064315	2001078	2000535	2100004	1	43210
532	3330538	2000230	2000156	3081550	1	43210
538	3102762	2001504	2000410	2100004	1	43210
541	3102787	2000453	2000207	2011542	1	43210
545	3250195	2001047	2000021	2002959	1	43210
562	3017060	2001717	2000224	2011542	1	43210
565	3046648	2000115	2000054	3046844	1	43210
569	3266035	2000487	2000559	2100004	1	43210
570	3092347	2000161	2001500	2011542	1	42310

Figure 7.14 Top 10 NNH results when applied to the reduced cost matrix, for the cost function based on energy.

ESA value [km/s]	GTOC ID 1	GTOC ID 2	GTOC ID 3	GTOC ID 4	GTOC ID 5	Group order
15.03	1	3339082	2001055	2000163	2002959	4321
21.05	2003362	2100004	2000413	2000532	1	41230
21.25	2096590	2100004	2000413	2000532	1	41230
21.92	3063789	2100004	2000413	2000532	1	41230
22.62	3309858	2100004	2000413	2000532	1	41230
22.69	3031176	2100004	2000413	2000532	1	41230
22.75	3297356	2100004	2000413	2000532	1	41230
22.76	3092339	3046844	2000036	2000328	1	41230
22.83	2066400	2100004	2000413	2000532	1	41230
22.93	3328632	2100004	2000413	2000532	1	41230

Figure 7.15 Top 10 NNH results when applied to the reduced cost matrix, for the cost function used by ESA.

It also shows that there is a large number of promising sequences found in the total set which are not present in the reduced set because they were filtered when reducing the cost matrix. This indicates that the reduction procedure is discarding good candidates.

In general, it can be stated that a multi-start NNH adds relatively little to the quality of the result, since the best result can be obtained by a single start NNH from Earth. The multistart NNH is useful, however, for generating multiple candidate asteroid sequences, when it is applied to the complete cost matrix.
More extensive multistart NNH results are presented in appendix E.

The biggest remaining question is what an AST-like method would find when able to deal with the complete asteroid set. The NNH and AST results for the reduced cost matrix indicates that solutions invisible to the NNH are present and improvements of several percent points are to be expected. Moreover, the results for the cost function based on energy in Figure 7.1 show that the AST, when applied to the reduced set, finds a better solution than the NNH that was applied to the complete asteroid set. This proves that, for the cost function based on energy, the NNH method, when applied to the complete asteroid set, will be unable to find the optimal solution.
These results indicate that a more powerful B&B method might improve the results obtained by the NNH, when both are applied to the complete asteroid set. A number of issues might be addressed when attempting to improve the quality of the B&B. First, the rule that is used for selecting which node/subproblem to evaluate next can be changed. As mentioned, in this research a DFS rule is applied, but the other two rules presented in section 3.5, BFS or random, can be used as well. Second, the rule according to which the subproblems are created can be changed. In this research the shortest subcycle was selected for branching. Alternatively, the longest subcycle can be selected, or a subcycle at random, or maybe even all subcycles. Third, an initial upper bound for the BB can be created by evaluating the problem first with NNH. This initial upper limit will prevent that the B&B will pursue solutions of which it is known they are not optimal. Last, the efficiency of the code can be increased.

7.2 Continuous Method

This section will present the results obtained for the continuous model for a number of tests. First, an overview of the performed tests will be given, as well as the

settings with which the test were performed. A total of 17 tests will be performed. The first two tests will consider sequences selected from the GTOC participants, with different optimizer settings. Based on these test results, a performance assessment of the continuous model and method, detailed in section 5.2, can be made. The next three tests will evaluate the top 8 sequences obtained by the AST, using the three different cost functions presented in section 4.1.1. The following three tests evaluate the top 8 sequences obtained by applying the NNH to the *complete* cost matrix, using the three different cost functions. The test results of the sequences obtained by the AST and NNH make it possible to give an indication of the quality of the applied methods and cost functions. After assessing the quality of the continuous model and method and evaluating the various methods and cost functions, a number of additional tests will be performed to further investigate the characteristics of the GTOC2 problem.
The settings for the various optimizers will be determined based on the results for the sequences obtained by the GTOC participants. The lower and upper bounds (LB and UB) used on x (equation 4.61) to evaluate the sequences are shown in Figure 7.16. The bounds on TOF, k_2, N and TOS are applied for every exposin leg.

Parameter	Unit	LB	UB
T0	MJD	57023.5	64693.5
TOF	days	1	2000
k2	-	0.01	1
N	-	0	1
TOS	days	90	150

Figure 7.16 Bounds used to evaluate GTOC2 results.

Each asteroid sequence will be evaluated 20 times using the continuous method. This is done because the continuous method is not a deterministic process. By running it several times, a more reliable result is obtained, and the robustness of the method can be determined by evaluating the standard deviation of the results of the 20 runs.
For every sequence, the results for nine different parameters will be given. The first row contains the values for the objective value J [-], the corresponding GTOC objective value J GTOC [-] (which is J without penalties) and the total velocity mismatch DV TOT [km/s], of the best solution of the 20 runs, at three different points in the solution process. They will be given after the MC has finished, after the GA has finished, and finally after completing the IP method, which is the end of the solution process.
The last two rows in each figure shows the results for the objective value (J), the mass use in kg, the total time of flight in years (TOF), the corresponding GTOC2 objective value (J GTOC), the sum of the velocity mismatches upon arrival and departure at the first three asteroids and, if applicable, at Earth (TOT DV), and finaly the launch date in MJD (T0) for the best results after the IP method, and with that the continuous method, has finished. For these parameters the mean and standard deviation of the results produced by the 20 runs is presented as well. For each test, more extensive results will be presented in the appendices.

7.2.1 Continuous Results for the GTOC2 Sequences

In order to assess the performance of the continuous method described in Section 5.2, it is applied to the sequences obtained by the GTOC2 participants. The se-

quences that are evaluated are those of the winner (number 1) and of the numbers 3, 7, 9, 10 and 11. These were selected because of the spread in their objective values. The objective values and corresponding asteroid sequences of the selected participants are shown in Appendix A. The spread in the objective values makes it possible to determine with what accuracy the continuous method is able to differentiate between relatively good and relatively bad sequences. If the method described in Section 5.2 is perfect, then it will rank the sequences of the various participants in the same order as they are ranked in the GTOC2 results of Appendix A.

The sequences were evaluated with two different sets of settings for the optimizers. One set used relatively weak settings with an MC using 50,000 iterations and a GA using a population size of 300 individuals. The other set used stronger settings with an MC using 100,000 iterations and a GA using 500 individuals. The best results out of these 20 runs for the weak optimizer settings are shown in Figure 7.17 and for the strong settings in Figure 7.18.

	Monte Carlo			Genetic Algorithm			Interior Point Method		
Rank	J	J GTOC	TOT DV	J	J GTOC	TOT DV	J	J GTOC	TOT DV
1	-10068	86	18.13	-3013	106	10.93	-3000	105	10.85
3	-9661	86	18.13	-2735	105	10.38	-2714	104	10.45
7	-12463	88	22.35	-4449	57	13.32	-4443	57	13.30
9	-8247	101	16.35	-2140	103	9.58	-2114	103	9.50
10	-7098	80	14.57	-2291	114	9.56	-2240	115	9.49
11	-10919	93	19.26	-5107	95	12.76	-5012	94	12.77

	J			Mass Used [kg]			TOF [year]		
	mean	std	best	mean	std	best	mean	std	best
1	-5595	1728	-3000	676	130	529	9.63	0.36	9.25
3	-4592	1260	-2714	490	75	477	9.78	0.32	9.82
7	-7943	2442	-4443	744	207	926	9.73	0.34	10.00
9	-4112	1922	-2114	534	123	469	9.73	0.62	10.00
10	-4464	1127	-2240	551	116	353	9.76	0.37	10.00
11	-7034	1731	-5012	730	101	670	9.53	0.44	8.79

	J GTOC			TOT DV [km/s]			T0 [MJD]		
	mean	std	best	mean	std	best	mean	std	best
1	86	13	105	14.25	2.11	10.85	57974	1652.6	57343
3	103	10	104	13.46	1.61	10.45	61998	1650.3	63592
7	78	21	57	16.87	2.48	13.30	59169	2511.1	57474
9	100	18	103	12.47	2.47	9.50	61703	2551.6	64173
10	97	10	115	12.84	1.61	9.49	62073	2505.5	64145
11	81	12	94	15.19	1.89	12.77	62711	507.39	62402

Figure 7.17 Results of analysis of GTOC2 candidates with an MC of 50,000 iterations and a GA of 300 individuals (weak settings).

The final objective values J, obtained after the IP method has finished, for each of the selected GTOC participants (first column of the Interior Point results of Figures 7.17 and 7.18) are represented graphically in Figure 7.19. Based on Figures 7.17, 7.18, 7.19 a number of observations can be made.

When looking at the objective values J, produced after the IP method has finished, for the various GTOC2 participants in an absolute sense, it becomes clear that all objective values J are negative and one or two orders of magnitude larger than the J GTOC results. Since the J value is constructed from the GTOC2 objective value (J GTOC) and the penalties, this implies that the penalties still form a significant part of the objective value.
A second observation regarding the J values is that the standard deviation is very large. This indicates that the algorithm is finding very different optimum values for each of the 20 runs, i.e., the algorithm is not robust. This might be increased by using more MC iterations or a larger GA population. This comes at the cost

Rank	Monte Carlo			Genetic Algorithm			Interior Point Method		
	J	J GTOC	TOT DV	J	J GTOC	TOT DV	J	J GTOC	TOT DV
1	-9211	98	19.25	-2436	109	9.64	-2407	107	9.54
3	-8266	101	18.309	-2438	107	10.01	-2406	106	9.96
7	-10903	84	20.16	-3197	61	11.30	-2971	61	11.18
9	-4326	98	12.914	-1958	106	9.93	-1934	108	9.51
10	-7251	98	16.112	-2835	109	11.09	-2832	109	11.07
11	-10808	94	19.299	-4708	77	12.59	-4434	76	12.52

	J			Mass Used [kg]			TOF [year]		
	mean	std	best	mean	std	best	mean	std	best
1	-4808	1413	-2407	554	99	508	9.37	0.48	9.23
3	-3742	781	-2406	495	52	472	9.90	0.15	9.66
7	-6066	2005	-2971	724	193	924	9.80	0.28	9.51
9	-2873	722	-1934	508	87	440	9.77	0.29	9.82
10	-4663	1153	-2832	558	125	406	9.76	0.32	10.00
11	-6001	939	-4434	750	90	776	9.58	0.43	9.49

	J GTOC			TOT DV [km/s]			T0 [MJD]		
	mean	std	best	mean	std	best	mean	std	best
1	102	15	107	13.25	1.93	9.54	57681	832	57024
3	102	6	106	12.48	1.16	9.96	62270	1518	63592
7	79	19	61	14.83	2.07	11.18	58060	1870	57651
9	102	10	108	10.97	1.08	9.51	62438	2578	64155
10	96	12	109	13.12	1.58	11.07	61312	2682	64123
11	78	11	76	14.17	1.02	12.52	62508	390	62579

Figure 7.18 Results of analysis of GTOC2 candidates with a MC of 100,000 iterations and a GA of 500 individuals (strong settings).

Figure 7.19 Visualization of results after local optimization for both the weak and the strong settings of the MC and GA algorithms.

of an increased computation time.

When looking at the objective values J for the various GTOC2 contestants in a relative sense, most notably in figure 7.19, it shows that they are not decreasing overall with decreasing GTOC2 rank. The goal is to optimize J, thus the winner is expected to have a higher objective value than the number 3, whereas this number 3 is expected to have a higher objective value than number 7, etcetera. This is, however, not the case for every consecutive rank, see Figure 7.19. For the weak settings the objective values show a strong fluctuation. There is hardly a decreasing trend in the data. For the strong settings, however, all values are between approximately -2000 and -3000 with the exception of rank 11. Rank 11 has a value that is relatively bad in comparison with the other ranks. This leads us to believe that the continuous method can distinguish between relatively good and relatively bad sequences, where relatively good means GTOC2 objective values of 50 or higher and relatively bad is between 0 and 50. A sequence with a J value of

over -3000 is considered good, and a sequence with a J value of less than -3000 is considered bad.

The J GTOC values obtained by the continuous method are all larger than the objective values obtained by the GTOC2 participants, except for rank 7 (compare results in figures 7.18 and A.1). It is expected that the J GTOC values of the continuous method are larger than the GTOC2 value because constraint mismatches are present. In general, it is easier to solve an unconstrained problem instead of a constrained problem, and therefore higher objective values are expected when constraint mismatches are allowed. Although constraint mismatches are undesirable and it is attempted to minimize them, they are still present in the solution. So if the GTOC2 results (without constraint violations) are compared to the results of Figures 7.17 and 7.18 (with constraint violations) then the results of the latter are expected to be better. Physically this can be interpreted by comparing the case with and without mismatch in arrival velocity. In order for the spacecraft to match the velocity of the asteroid it will need to maneuver (use propellant mass and time) to get into an orbit that better matches the asteroid's orbit. Since both time and mass are used while maneuvering, which both affect the objective value negatively, the orbit that arrives at the asteroid without constraint violation will have a worse objective value compared to the orbit with arrival velocity mismatches.

Figures 7.17 and 7.18 show that for the best results, the fuel mass used is always lower than the prescribed limit of 1000 kg and the total time of flight is always shorter than the prescribed limit of 20 years.
The results for the time of flight also reveal an error in the settings for the time of flight penalty. A quadratic penalty was applied when the total time of flight of the mission exceeded 10 years. The allowed mission duration for GTOC2, however, is 20 years. This means that a penalty inside the problem bounds is applied. The results show that all mission durations are near the penalty threshold of 10 years, indicating that the penalty has a significant influence on the results. Comparing the results for the total time of flight obtained by the continuous method in figures 7.17 and 7.18 with the results obtained by the GTOC2 participants in appendix A, however, shows that the time of flight penalty does steer the optimizer in the right direction. The solutions of the top 8 ranks of the GTOC2 participants all have a time of flight of about 10 years. The applied penalty thus steers the solution method towards an optimal region in the search space for the sequences obtained by the GTOC2 participants. When evaluating other sequences this might not be the case. It should be noticed that for absolute certainty of the effect of this setting, all tests have to be redone using a penalty threshold of 20 years.
Another remark has to be made regarding this error. Although the penalty was applied for erroneous reasons, preliminary output obtained during the development of the continuous method showed that if no penalty is applied, the total time of flights obtained during the 20 runs for the winner sequences would range from roughly 12 years to 21 years, but with J GTOC values half as good as compared to when the 10+ penalty is applied to the time of flight. If at the time these results were compared to the results obtained by the GTOC2 participants, it was most likely opted to implement a penalty on the time of flight or to drastically increase the strength of the optimizers. In the end, applying the erroneous penalty unknowingly resulted in reducing the computational time, since less strong optimizer settings are required. The results in Figure 7.18 do indicate that the applied quadratic penalty might be a little too severe. Considering the mean and standard

deviations shows that the solutions are clustered just under the 10 years, whilst the solutions of the GTOC2 participants are just over 10 years.
The GTOC results show a correlation between good solutions and a time of flight of about 10 years. The implemented exposin model uses a continuous thrust arc and hence increasing the time of flight will most likely have a detrimental effect on the objective function, since both the time of flight and the mass consumption are increased. A more accurate model where, for example, multiple thrust and coast arcs are implemented, should not use this penalty with a threshold of 10 years. Considering the limited accuracy of the applied exposin model and the fact that the results are near an optimal region in the search space supports the conclusion that the erroneous settings do not make the results presented in this chapter invalid. The effect of this penalty setting will be revisited by one of the additional tests performed at the the end of this chapter.

	Departure DV				Arrival DV			
Rank	leg 1	leg 2	leg 3	leg 4	leg 1	leg 2	leg 3	leg 4
1	3.09	2.04	0.71	1.18	2.97	1.38	1.25	2.10
3	2.35	2.40	1.20	1.97	0.40	1.20	2.79	4.33
7	3.42	2.07	2.05	1.70	2.06	1.18	2.11	1.75
9	2.03	0.98	1.62	2.70	1.19	0.92	2.11	3.16
10	1.91	1.19	3.14	1.17	1.17	1.43	3.09	4.02
11	3.35	1.13	1.52	2.45	4.06	1.56	1.79	3.09

Figure 7.20 Departure and arrival velocity mismatches of best solutions obtained using an MC with 100,000 iterations and a GA with 500 individuals.

Figure 7.18 shows that the total constraint mismatch in terms of velocity is on average about 10 km/s, but with each individual sequence this value can vary about 30%. This total ΔV is the summation of three arrival and three or four departure velocity mismatches. Remember that the departure velocity at Earth is not taken into account when lower than 3.5 km/s and that the arrival velocity at the final asteroid is also excluded by the GTOC2 assignment. This means that at each departure and arrival, on average, about 1.7 km/s velocity mismatch is found. This is a serious constraint violation, since the GTOC2 assignment only allows for 1 m/s of velocity mismatch.
Figure 7.20 presents the departure and arrival velocity mismatches for every individual leg. These results show that the departure ΔV at Earth is always lower than the constraint of 3.5 km/s for all ranks except rank 11. The arrival ΔV at asteroid 4 is bad in a large number of cases, relative to the arrival velocities at the other asteroids. This is as expected since no rendezvous, but only a flyby with the last asteroid is required, and therefor no penalty was applied to the arrival velocity at the last asteroid.
These results indicate that the exposins are far from accurate enough for the purpose of finding valid GTOC2 solutions. This indicates that a strong local optimizer in combination with a more accurate model is required.

In order to make a clear comparison of the mission time lines obtained by the continuous method and the GTOC2 participants, both results are summarized in Figure 7.21. Comparing these numbers reveals that the continuous method does not find the same (optimal) mission timelines. This indicates that, in its current form, the continuous method is not suitable for search space reduction with the goal of minimizing the search space for more accurate methods (i.e., it cannot provide the input for more accurate methods).

R	J GTOC		T0		TOS 1		TOS 2		TOS 3	
	Part.	C.M.	Part.	C.M.	Part.	C.M.	Part.	C.M.	Part.	C.M.
1	99	107	59870	57024	90	90	90	149	105	149
3	87	106	57372	63592	102	103	102	91	90	90
7	82	61	62201	57651	90	113	90	149	90	90
9	75	108	57561	64155	119	129	90	131	90	150
10	57	109	58448	64123	94	147	222	140	90	130
11	28	76	58246	62579	90	136	90	94	90	150

	TOF 1		TOF 2		TOF 3		TOF 4	
	Part.	C.M.	Part.	C.M.	Part.	C.M.	Part.	C.M.
1	413	189	1606	920	578	1348	459	527
3	253	539	1636	515	447	1369	712	820
7	253	707	1900	950	860	1026	660	436
9	426	461	1521	867	1218	992	739	857
10	304	275	1980	567	943	642	943	1752
11	879	602	2516	623	731	636	2615	1223

Figure 7.21 Comparison of mission timelines between results of GTOC2 participants and the results of the Continuous Method (C.M.) using an MC with 100,000 iterations and a GA with 500 individuals.

To check the performance outside of the range of the winners, one sequence of which it is known to be bad beforehand (large inclination differences between subsequent asteroids) was tested as well. The tested sequence is (GTOC2 ID numbers): 1→2000944→2000024→2000584→3293923. After the GA was finished it found an objective value J, of -51344. This shows that the continuous method will detect a (very) bad sequence. This bad sequence, however, should already have been filtered out by the AST. In case the AST method would produce this (or any other) bad sequence, the continuous method will detect and discard it. Based on this result, it is concluded that the continuous method is at least able to confirm the B&B results.

Rank	N 1	N 2	N 3	N 4
1	0.40	0.25	0.75	0.44
3	0.88	0.49	0.03	0.25
7	0.71	0.71	0.95	0.02
9	0.92	0.81	0.27	0.37
10	0.46	0.25	0.48	0.37
11	0.65	0.53	0.39	0.26

Figure 7.22 Number of revolutions of best solutions obtained using an MC with 100,000 iterations and a GA with 500 individuals.

Figure 7.22 presents the number of revolutions N for the best solutions obtained by the strong optimizer settings. This figure shows that all numbers are between 0 and 1. The model, however, only accepts integer values. The number 0 indicates a transfer angle between 0 and 2π, the number 1 indicates a transfer angle between 2π and 4π. The reason why these numbers are no integers is because the GA creates a double value for every model parameter (every variable). When determining the value for N the double value will be rounded to either 0 or 1.

A first observation regarding the applied methods is the fact that the MC finds a finite value in all cases. It is known that some exposin shapes are impossible to fly, so there will be gaps in the solution space. This is confirmed in appendix J where the search space is partially visualized. Because the MC finds finite values it can be stated that it is successful in identifying feasible solution regions, which was the reason for including the MC in the analysis.

A second important observation regarding the applied methods is that the biggest improvement in the objective value is achieved by the GA, and hardly any by the local optimizer (see Figures 7.17 and 7.18). This indicates that the search space contains smooth regions of (local) optimal values. It does not exclude, however, the presence of very narrow optimal regions that are very hard to find by a GA. The partial visualization of the search space in appendix J shows that narrow feasible regions do exist. It is, however, unknown if the GA is looking into these regions or if they contain local optima or not.

Additional observations can be made when scrutinizing the results in figures 7.17 and 7.18. In most cases, the stronger optimizer settings find better values for the mean and lower standard deviation of the results. This means that the robustness of the optimizer is better for the stronger settings than for the weaker settings, indicating that strong optimizer settings are required to analyze the objective function under consideration. Also, the results of the strong optimizer settings match the expectations better. It finds a somewhat stronger decreasing trend in the objective values than in the results obtained with the weak optimizer settings (Figure 7.19).
Taking a closer look at the mean and standard deviation values indicates that there is a wide spread in all parameters. This could indicate the presence of a large number of local minima. It also implies that, although the GA is significantly improving the objective value, it is not robust enough for the task at hand and even stronger optimizer settings should be considered. One thing to keep in mind, however, is that the landscape of the search space is shaped by the objective function. As shown in Appendix J, the search space is determined to a large extent by the penalty values. Since the quality of the results of a particular method are only as accurate as its model, it is emphasized that before changing the optimizer settings, first the model needs to be scrutinized and improved.

The trajectories and corresponding acceleration profile of the best and worst continuous result for GTOC2 result (ranks 9 and 11 resp.) are included in Figures 7.23 - 7.26. There figures show two reasons why the orbit obtained of rank 9 is better than the orbit belonging to rank 11.
Comparing figures 7.23 and 7.26 shows that the trajectory of the worst orbit terminates at an asteroid which located farther from the Sun than the trajectory of the best result. Flying further away will require both time and fuel, which both has an adverse effect on the objective value.
The second reason why the trajectory of rank 9 is better than the trajectory of rank 11 is a lower constraint violation for the allowed thrust acceleration. The acceleration profiles in figures 7.24 and 7.26 indicate constraint violations in the second leg of the trajectory for rank 9 and in the first and second leg of the trajectory for rank 11. Also this constraint violation for rank 11 is much larger (peak at $8.0e^{-4}m/s^2$ instead of $2.5e^{-4}m/s^2$).
Combining these results with the fact that the objective value is 14 points higher for the better trajectory and that the velocity mismatch is also 3 km/s larger for the worst trajectory (see figures 7.17 and 7.18) shows that indeed the continuous method is able to differentiate between good and bad results.

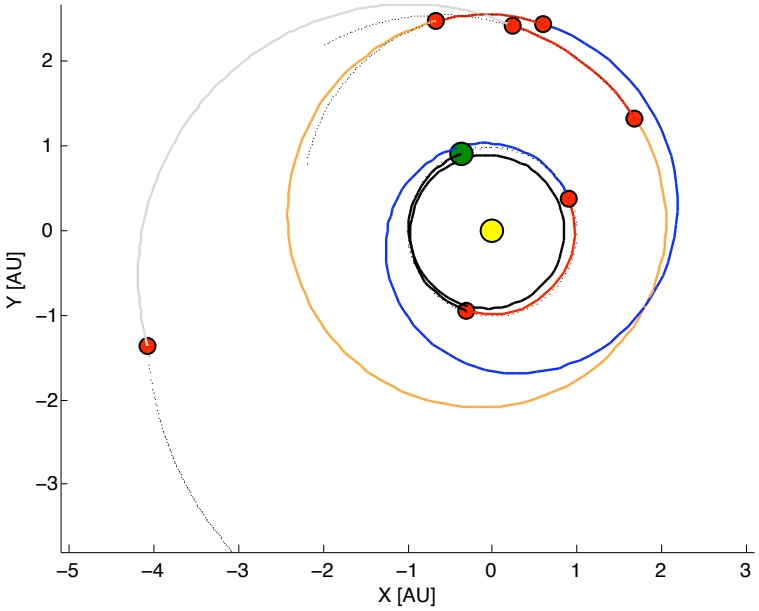

Figure 7.23 Orbit of best continuous result for sequences obtained by the GTOC2 participants. GTOC rank = 9, J = -1934, J GTOC = 108. Trajectory is plotted according to the definitions in figure 4.19.

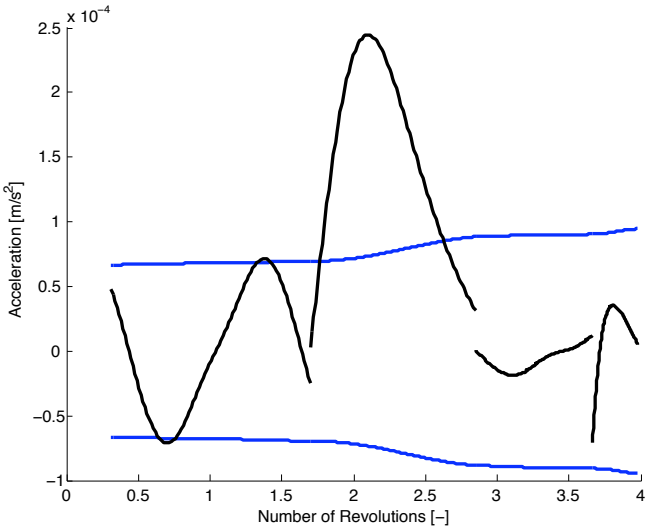

Figure 7.24 Allowed and required acceleration of best continuous result for sequences obtained by the GTOC2 participants. GTOC rank = 9, J = -1934, J GTOC = 108. The blue line indicates the acceleration limit, the black line the required acceleration for flying the trajectory shown in figure 7.23.

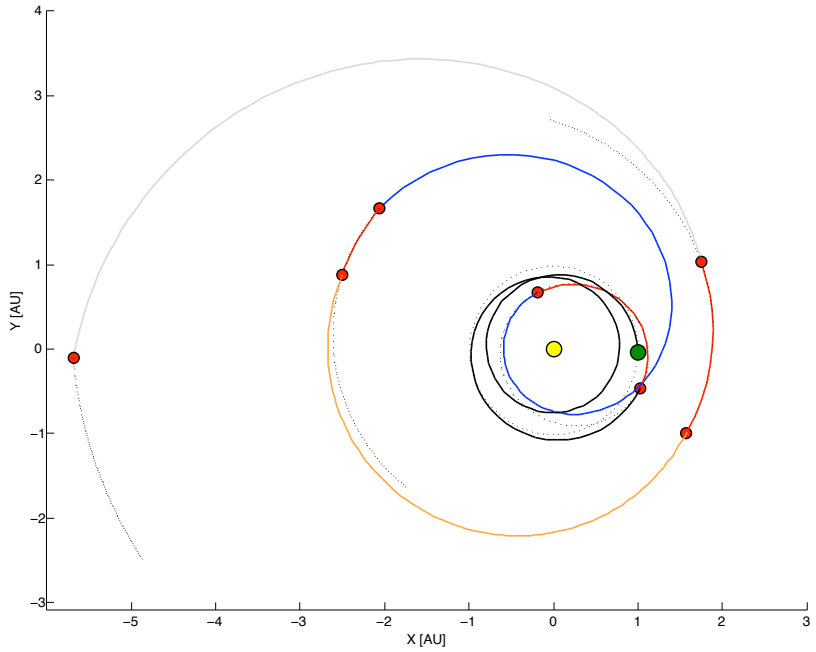

Figure 7.25 Orbit of worst continuous result for sequences obtained by the GTOC2 participants. GTOC rank = 11, J = -5012, J GTOC = 94. Trajectory is plotted according to the definitions in figure 4.19.

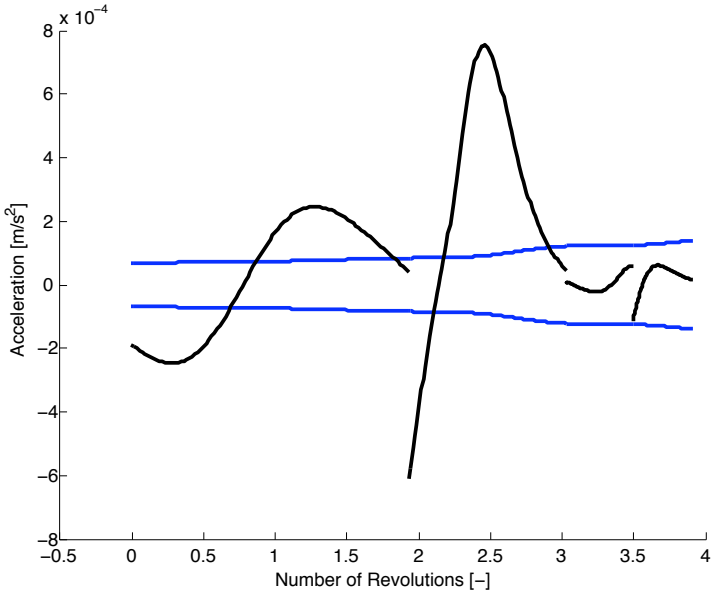

Figure 7.26 Allowed and required acceleration of worst continuous result for sequences obtained by the GTOC2 participants. GTOC rank = 11, J = -5012, J GTOC = 94. The blue line indicates the acceleration limit, the black line the required acceleration for flying the trajectory shown in figure 7.26.

Based on the observations stated so far, two consequences regarding the implementation of the continuous method as a tool for assessing the phasing behavior of asteroid sequences are identified. The relatively large contribution of the penalty to the objective value and the magnitude of the velocity mismatches at the asteroids implies that no accurate analysis of the phasing characteristics with respect

to the GTOC objective value can be made. The results do show, however, that when implementing the strong optimizer settings, the continuous method can be used to roughly divide the quality of the sequences obtained by the AST and NNH in three categories: relatively good, relatively bad, and near unfeasible. When feasible solutions are found they will most likely fulfill the constraints for mass use, mission duration and departure velocity. Sequences that are near unfeasible, might demonstrate constraint violations for these parameters.

One drawback needs to be mentioned regarding the use of the GTOC2 results as a benchmark. The GTOC2 participants may not have performed a perfect global search of the total search space or in performing an accurate local optimization. This introduces some uncertainty when comparing the results of other asteroid sequences with the results for the sequences of the GTOC2 participants. It might, for example, be the case that the asteroid sequence obtained by the participant of rank 10 contains a better continuous solution in its search space than the one handed in by the contestants. The results of the participant do however provide a lower bound for the obtainable objective value. To assess if the search space indeed contains alternative optimal solutions requires a very thorough search of the entire search space, using more powerful methods and more accurate models, such that all constraint violations are removed. This is, however, outside the scope of this report, and is identified as a recommendation.

7.2.2 Continuous Results for the AST Output

This section summarizes the results of the continuous method for the three sets of asteroid sequences obtained by the AST, using the three cost functions described in section 4.1.1 (each set of sequences corresponds to one cost function). The top 8 asteroid sequences, obtained using a cost function based on ΔV, are shown in Figure 7.27. The solutions are ranked according to their cost in terms of velocity given in km/s (DV value). The top 8 asteroid sequences, obtained using a cost function based on energy, are shown in Figure 7.28. The solutions are ranked according to their costs in terms of energy given in MJ/kg (E value). The top 8 asteroid sequences, obtained by the AST, when using the ESA cost function, are shown in Figure 7.29. The solutions are ranked according to their cost in terms of velocity given in km/s (ESA value). More extensive results are included in Appendix G.

DV Value [km/s]	Monte Carlo			Genetic Algorithm			Interior Point Method		
	J	J GTOC	TOT DV	J	J GTOC	TOT DV	J	J GTOC	TOT DV
22.9	-4685	82	12.96	-2067	92	9.23	-2067	92	9.23
24.5	-10278	99	19.12	-2850	83	11.13	-2835	82	11.11
24.6	-6634	103	15.11	-2771	101	11.08	-2654	102	10.96
25.2	-6000	90	14.18	-3366	92	11.26	-3366	92	11.26
27.0	-7366	101	17.23	-2566	99	10.57	-2564	99	10.60
27.8	-5407	100	15.15	-1871	98	8.77	-1871	98	8.77
28.4	-5068	110	14.34	-2862	114	10.96	-2820	114	10.90
30.8	-6008	94	15.41	-1706	101	9.15	-1706	101	9.15

	J			Mass Used [kg]			TOF [year]		
	mean	std	best	mean	std	best	mean	std	best
22.9	-2650	790	-2067	639	33	621	9.27	0.55	9.51
24.5	-5703	1591	-2835	636	108	703	9.67	0.35	9.71
24.6	-4105	1074	-2654	529	62	489	9.85	0.18	9.94
25.2	-5255	1153	-3366	592	52	615	9.87	0.22	9.60
27.0	-3963	1158	-2564	516	56	521	9.93	0.13	9.92
27.8	-3311	1519	-1871	473	53	520	9.84	0.29	10.00
28.4	-4422	1050	-2820	495	96	439	9.64	0.32	9.31
30.8	-3450	1540	-1706	535	104	489	9.94	0.12	10.00

	J GTOC			TOT DV [km/s]			T0 [MJD]		
	mean	std	best	mean	std	best	mean	std	best
22.9	93	7	92	10.03	1.44	9.23	59992	617	59659
24.5	90	12	82	14.44	1.97	11.11	60294	1710	61564
24.6	99	7	102	12.85	1.43	10.96	61519	459	61650
25.2	92	6	92	13.51	1.37	11.26	60939	1168	61207
27.0	99	6	99	12.26	1.43	10.60	62401	1938	63586
27.8	104	8	98	11.24	2.08	8.77	60754	1068	60874
28.4	105	11	114	13.05	1.39	10.90	58625	1080	59559
30.8	97	11	101	11.62	1.98	9.15	60427	1103	60133

Figure 7.27 Results of continuous method for the best sequences selected by AST using a cost function based on ΔV.

E Value [MJ/kg]	Monte Carlo			Genetic Algorithm			Interior Point Method		
	J	J GTOC	TOT DV	J	J GTOC	TOT DV	J	J GTOC	TOT DV
420	-1371	107	7.67	-181	104	5.55	-181	104	5.54
437	-7090	82	15.56	-2057	84	9.17	-1785	83	9.20
454	-9627	93	20.06	-5127	98	14.43	-5125	98	14.43
456	-6648	113	15.83	-2490	109	10.46	-2490	109	10.45
465	-11161	79	22.22	-4578	87	13.94	-4530	88	13.84
473	-7321	83	15.76	-2176	84	8.91	-2174	84	8.96
479	-4771	97	13.84	-1624	108	9.10	-1623	108	9.06
496	-8180	53	17.31	-4541	67	12.69	-4536	67	12.62

	J			Mass Used [kg]			TOF [year]		
	mean	std	best	mean	std	best	mean	std	best
420	-1217	556	-181	490	49	465	9.28	0.50	9.92
437	-3156	984	-1785	631	111	669	9.89	0.11	10.00
454	-7950	1613	-5125	643	208	517	9.95	0.19	10.00
456	-3663	829	-2490	476	92	414	9.80	0.16	10.00
465	-7347	2541	-4530	710	103	625	9.93	0.18	10.00
473	-5089	2089	-2174	694	121	664	9.83	0.22	10.00
479	-2966	902	-1623	443	32	417	9.87	0.19	10.00
496	-6306	738	-4536	675	170	839	9.83	0.17	9.90

	J GTOC			TOT DV [km/s]			T0 [MJD]		
	mean	std	best	mean	std	best	mean	std	best
420	109	7	104	7.68	1.18	5.54	64340	197	64065
437	88	11	83	11.44	1.47	9.20	60093	2848	58072
454	86	21	98	16.86	1.51	14.43	62490	2411	64690
456	104	10	109	12.30	1.32	10.45	62729	2003	63319
465	80	10	88	16.58	2.18	13.84	61097	853	60985
473	82	12	84	14.71	5.61	8.96	58627	1062	58036
479	107	4	108	10.37	1.21	9.06	62999	266	63177
496	84	18	67	15.09	1.18	12.62	62059	1593	63233

Figure 7.28 Results of continuous method for the best sequences selected by AST using a cost function based on Energy.

ESA Value [km/s]	Monte Carlo			Genetic Algorithm			Interior Point Method		
	J	J GTOC	TOT DV	J	J GTOC	TOT DV	J	J GTOC	TOT DV
15.98	-8875	74	18.55	-2926	88	10.05	-2882	88	10.05
16.32	-12709	92	22.96	-2565	72	9.90	-2557	73	9.92
16.56	-4538	117	12.92	-1983	105	8.87	-1983	105	8.87
16.75	-6564	109	14.95	-2772	100	11.17	-2758	100	11.16
16.84	-4522	89	12.52	-1984	104	10.01	-1981	104	10.01
16.87	-7874	109	18.21	-1877	76	9.04	-1857	77	9.00
16.93	-3438	104	10.42	-958	87	7.76	-934	87	7.65
17.11	-5883	68	14.37	-4020	98	13.14	-4018	98	13.14

	J			Mass Used [kg]			TOF [year]		
	mean	std	best	mean	std	best	mean	std	best
15.98	-4339	989	-2882	603	140	619	9.91	0.13	10.00
16.32	-7459	2577	-2557	679	88	774	9.87	0.24	10.00
16.56	-2638	411	-1983	479	79	482	9.66	0.33	9.66
16.75	-3625	652	-2758	570	116	525	9.76	0.25	9.77
16.84	-3024	928	-1981	498	82	473	9.85	0.22	9.87
16.87	-4575	1220	-1857	600	111	750	9.64	0.40	9.80
16.93	-1795	669	-934	479	172	644	9.64	0.58	9.83
17.11	-5989	1681	-4018	610	159	522	9.86	0.19	10.00

	J GTOC			TOT DV [km/s]			T0 [MJD]		
	mean	std	best	mean	std	best	mean	std	best
15.98	91	15	88	12.47	1.47	10.05	62894	481	62797
16.32	83	9	73	17.02	4.53	9.92	62464	1170	62415
16.56	106	8	105	11.11	3.51	8.87	62816	294	62610
16.75	95	12	100	12.90	3.95	11.16	62833	240	63002
16.84	102	9	104	11.01	1.50	10.01	60039	3007	63975
16.87	93	11	77	13.16	1.68	9.00	63135	1268	63471
16.93	106	20	87	9.93	4.17	7.65	62744	1443	59911
17.11	90	17	98	14.61	1.92	13.14	62812	555	62156

Figure 7.29 Results of continuous method for the best sequences selected by AST using a cost function based on ESA.

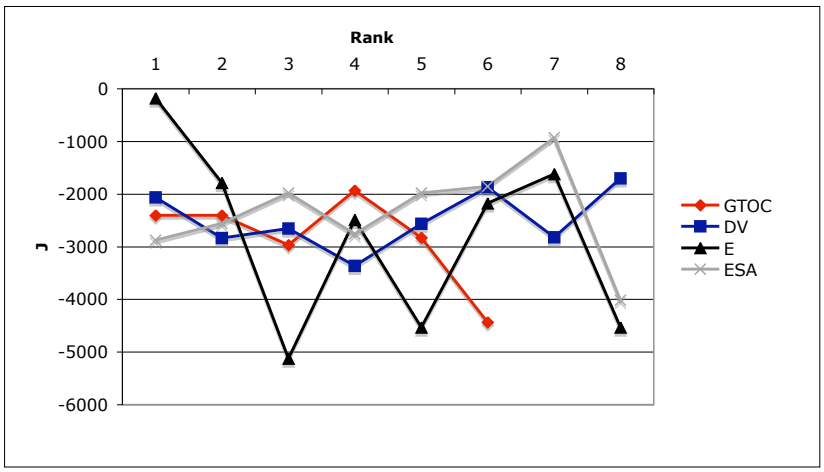

Figure 7.30 Visualization of the results of the continuous method, for the asteroid sequences obtained by the AST using three different cost functions. The GTOC2 results are added for comparison.

Observations can be made based on the presented results. Some of these observations are similar to the observations for the GTOC2 sequences: from figures 7.27, 7.28 and 7.29 it follows that all J values are negative and one or two orders larger in magnitude than the J GTOC values. From appendix G it follows that mass and mission duration constraints are met. The ΔV constraints upon departure and arrival are not met, except for the departure at Earth where less than the allowed 3.5 km/s is used by all best solutions. For all cost functions, again the GA provided the largest increase in quality.

Especially the relative results of the various cost functions are of interest. Relative to each other as well as relative to the results for the sequences of the GTOC2 participants. To facilitate the comparison of the continuous results for the three different cost functions, the results are presented graphically in Figure 7.30. The results for the sequences obtained by the GTOC2 participants are also included in the graph for a comparison of the order of magnitude of the results. Note that the rank on the horizontal axis refers to the rank as determined by the AST. The GTOC results are *ordered* according to the GTOC2 ranking, but the actual GTOC2 rank differs from the one on the x-axis in Figure 7.30.
The first interesting observation is that none of the three objective functions show a decreasing trend. Apparently there is no strong downward trend in the sequence quality for the best eight solutions of each cost function. It also indicates that the discrete model alone is not enough to differentiate between the quality of two relatively good sequences.
The graph for the cost function based on ΔV shows that all results are in the range of good objective values starting from -3000. When comparing with the results of the GTOC2 participants, it follows that the sequences obtained by the AST, using a cost function based on ΔV, provides sequences which are likely to have good GTOC2 objective values when subjected to more accurate analysis.
The graph for the cost function based on energy shows a strong fluctuation in the objective value. Some results are better than the results for the GTOC2 sequences, and some are significantly worse. Using again the GTOC results as a benchmark, it follows that the sequences obtained by the AST, using a cost function based on energy, probably include bad sequences when they are subjected to more accurate analysis. On top of that, appendix G shows that most of the best solutions run into the time of flight penalty of 10 years. This indicates that the solution method tries to find solutions with a longer time of flight. As argued when discussing the continuous results for the sequences obtained by the GTOC participants, searching past the 10 year threshold most likely does not lead to better J GTOC values. This indicates that the sequences obtained with the AST, using a cost function based on energy, are most likely worse than sequences obtained using another combination of discrete method and cost function.
The graph for the cost function used by ESA shows results similar to the results obtained by the cost function based on ΔV, except for the last two ranks. Although the ESA cost function outperforms the other two cost functions for most ranks, the differences are not significant enough, considering the accuracy of the continuous method, to state that the ESA cost function is better. It can be stated, however, that the cost function based on ΔV, when applied to a reduced cost matrix, is a viable alternative for the cost function used by ESA.

The trajectory with the highest J value (the best result) in Figure 7.30 was obtained using the AST in combination with the energy cost function, and had

an E value of 420 MJ/kg (see Figure 7.28). The corresponding trajectory and acceleration profile is shown in figures 7.31 and 7.32 respectively.

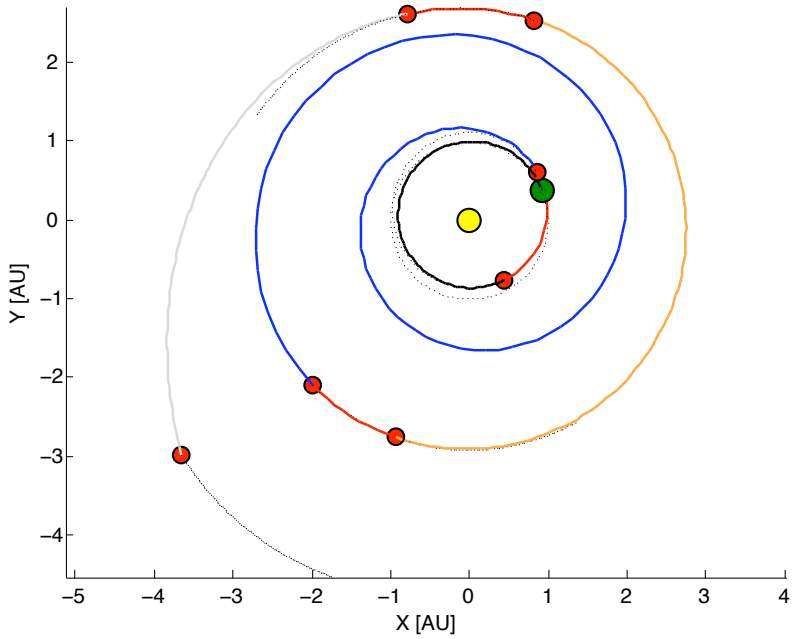

Figure 7.31 Orbit of best continuous result for sequences obtained by the AST. E value = 420, J = -181, J GTOC = 104. Trajectory is plotted according to the definitions in figure 4.19.

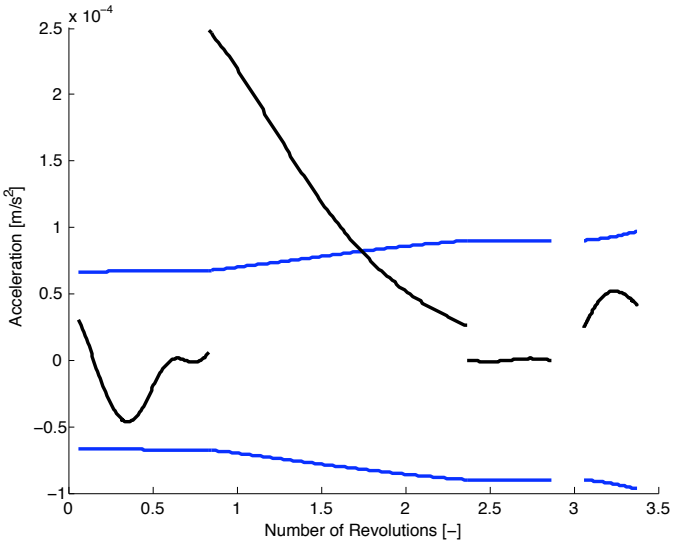

Figure 7.32 Allowed and required acceleration of best continuous result for sequences obtained by the AST. E value = 420, J = -181, J GTOC = 104. The blue line indicates the acceleration limit, the black line the required acceleration for flying the trajectory shown in figure 7.31.

The trajectory with the lowest J value (the worst result) in Figure 7.30 was obtained using the AST in combination with the energy cost function, and had an E value of 454 MJ/kg (see Figure 7.28). The corresponding trajectory and acceleration profile is given in figures 7.33 and 7.34 respectively.

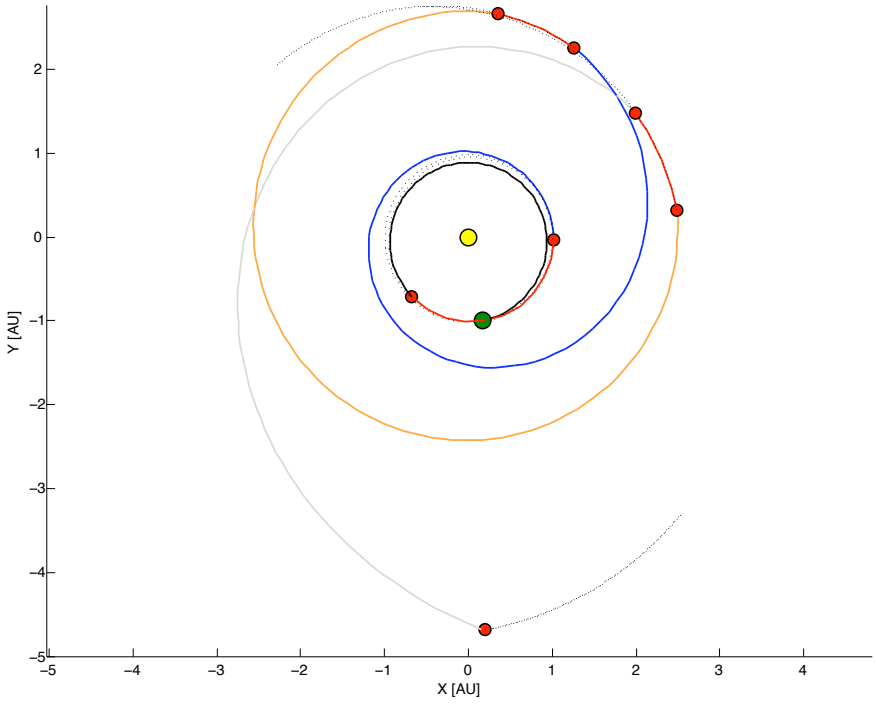

Figure 7.33 Orbit of worst continuous result for sequences obtained by the AST. E value = 454, J = -5125, J GTOC = 98. Trajectory is plotted according to the definitions in figure 4.19.

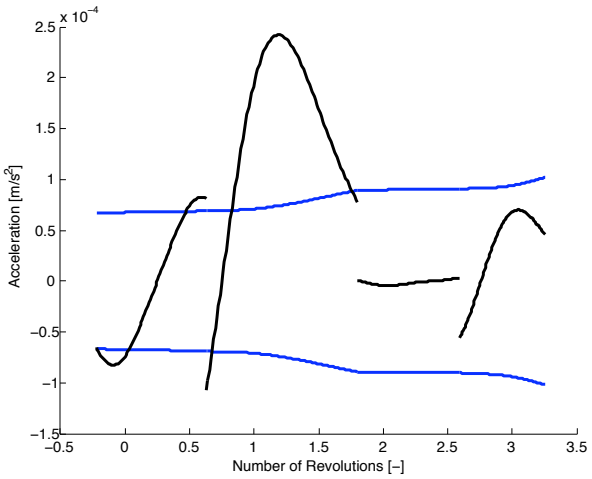

Figure 7.34 Allowed and required acceleration of worst continuous result for sequences obtained by the AST. E value = 454, J = -5125, J GTOC = 98. The blue line indicates the acceleration limit, the black line the required acceleration for flying the trajectory shown in figure 7.33.

The best result is a reasonable approximation for a low-thrust trajectory. The reason why this trajectory is better than the others is the far lower total velocity mismatch. Figure 7.28 shows, however, that the velocity constraint violation is still of the order of several km/s. Figure 7.33 shows that especially the departure of the last leg is problematic. It has a large angle with respect to the departure orbit. This results in high constraint violations and therefore a bad J value. These results indicate, again, that a good objective value indeed represents a good trajectory, and a bad objective value does represent a bad solution.
A second observation can be made regarding the acceleration profiles. If the profiles in figures 7.24, **??**, 7.32 and 7.34 are compared, it follows that each solution has acceleration constraint violations for the second leg. This indicates that the second leg is the hardest to fly with the tangential thrust assumption and the allowed thrust acceleration.

7.2.3 Continuous Results for the NNH output

This section summarizes the results of the continuous method for the three sets of asteroid sequences obtained by applying the NNH to the *complete* cost matrix, using the three cost functions described in section 4.1.1. The results for the asteroid sequences obtained by the NNH, using a cost function based on ΔV, are shown in Figure 7.35. The results for the asteroid sequences obtained by the NNH using a cost function based on energy are shown in Figure 7.36. The results for the asteroid sequences obtained by the NNH, using the ESA cost function, are shown in Figure 7.37. Extensive results are included in appendix H. A graphical representation of the results is given in figures 7.38 and 7.39.

DV Value [km/s]	Monte Carlo			Genetic Algorithm			Interior Point Method		
	J	J GTOC	TOT DV	J	J GTOC	TOT DV	J	J GTOC	TOT DV
21.28	-3614	108	12.12	-1278	104	8.84	-1260	104	8.93
21.28	-4778	93	13.23	-1424	113	9.08	-1391	113	9.15
22.91	-3801	109	12.46	-1508	108	9.24	-1482	107	9.24
23.25	-5173	121	13.35	-1767	114	8.45	-1757	115	8.43
23.45	-8845	85	18.53	-2722	100	11.37	-2710	100	11.27
23.46	-8100	95	18.41	-2481	100	10.10	-2372	102	10.29
23.63	-9212	70	18.81	-4475	75	13.24	-4360	73	13.07
23.65	-5772	66	14.66	-1842	61	9.69	-1803	62	9.54

	J			Mass Used [kg]			TOF [year]		
	mean	std	best	mean	std	best	mean	std	best
21.28	-2422	1137	-1260	452	47	464	9.87	0.19	9.95
21.28	-2448	956	-1391	508	151	368	9.89	0.14	10.00
22.91	-2421	333	-1482	478	43	425	9.37	0.41	10.00
23.25	-3097	917	-1757	486	131	393	9.84	0.19	9.64
23.45	-3869	662	-2710	537	89	503	9.69	0.37	9.99
23.46	-4509	1270	-2372	557	135	490	9.84	0.20	9.95
23.63	-6304	2524	-4360	778	126	781	9.74	0.20	9.80
23.65	-3381	1704	-1803	732	165	883	9.76	0.30	10.00

	J GTOC			TOT DV [km/s]			T0 [MJD]		
	mean	std	best	mean	std	best	mean	std	best
21.28	106	5	104	10.18	1.66	8.93	62015	1140	61493
21.28	100	15	113	10.29	1.27	9.15	61307	1407	61627
22.91	109	5	107	10.15	0.36	9.24	61756	165	61495
23.25	103	13	115	10.82	1.32	8.43	61732	2081	63211
23.45	100	10	100	12.44	0.77	11.27	60423	1797	61458
23.46	96	14	102	13.24	1.78	10.29	60183	1086	59777
23.63	74	13	73	15.30	2.50	13.07	61512	1313	61682
23.65	79	17	62	11.58	2.25	9.54	61697	855	61483

Figure 7.35 Results of continuous method for the best sequences selected by NNH using a cost function based on ΔV.

E Value [MJ/kg]	Monte Carlo			Genetic Algorithm			Interior Point Method		
	J	J GTOC	TOT DV	J	J GTOC	TOT DV	J	J GTOC	TOT DV
451	-4655	103	13.37	-1621	94	8.69	-1594	93	8.63
497	-8052	78	16.52	-3518	94	11.81	-3251	89	10.84
531	-10797	97	16.75	-4352	107	11.74	-4335	107	11.73
537	-4686	85	12.73	-1572	85	8.52	-1562	85	8.47
540	-8734	119	17.79	-2378	96	10.10	-2342	104	10.05
545	-11659	68	20.74	-6009	78	13.91	-5736	84	14.91
562	-7814	109	15.51	-2309	104	8.78	-2249	95	9.27
565	-15870	90	24.58	-5620	52	13.65	-5392	52	13.81

	J			Mass Used [kg]			TOF [year]		
	mean	std	best	mean	std	best	mean	std	best
451	-2750	1076	-1594	699	119	567	9.80	0.19	10.00
497	-5325	1239	-3251	706	211	666	9.34	0.70	9.36
531	-6638	2051	-4335	677	134	536	9.70	0.37	9.01
537	-3717	1729	-1562	676	105	664	9.67	0.34	9.86
540	-4097	1386	-2342	614	98	467	9.83	0.29	9.91
545	-9089	3210	-5736	728	115	667	9.77	0.33	9.91
562	-4114	1534	-2249	680	119	583	9.69	0.30	9.62
565	-11013	2977	-5392	846	130	999	9.81	0.26	9.68

	J GTOC			TOT DV [km/s]			T0 [MJD]		
	mean	std	best	mean	std	best	mean	std	best
451	82	12	93	10.26	1.36	8.63	59389	2375	64691
497	86	25	89	14.06	4.91	10.84	58662	635	58249
531	85	16	107	14.78	2.71	11.73	62170	945	62632
537	85	12	85	11.54	2.27	8.47	58740	1301	58496
540	90	10	104	12.81	4.10	10.05	60426	1936	60396
545	79	12	84	16.87	2.63	14.91	62007	1608	62305
562	85	14	95	11.69	2.10	9.27	63142	2048	64388
565	67	13	52	19.87	2.91	13.81	62339	1952	61062

Figure 7.36 Results of continuous method for the best sequences selected by NNH using a cost function based on Energy.

ESA Value [km/s]	Monte Carlo			Genetic Algorithm			Interior Point Method		
	J	J GTOC	TOT DV	J	J GTOC	TOT DV	J	J GTOC	TOT DV
15.03	-4681	120	12.76	-1992	107	9.59	-1989	107	9.60
21.05	-47110	78	46.04	-29425	81	34.18	-29027	83	34.88
21.25	-27788	54	34.42	-14908	68	22.80	-14832	68	23.30
21.92	-34053	59	36.30	-22831	60	28.59	-22822	58	28.67
22.62	-45434	55	44.13	-20127	66	28.61	-20125	66	28.58
22.69	-35865	84	39.14	-20981	58	28.58	-20980	58	28.58
22.75	-44416	31	42.72	-31174	46	35.87	-29783	37	33.67
22.76	-62317	49	49.34	-43741	43	42.29	-43706	43	42.33

	J			Mass Used [kg]			TOF [year]		
	mean	std	best	mean	std	best	mean	std	best
15.03	-2777	789	-1989	519	76	455	9.68	0.35	9.77
21.05	-37553	5388	-29027	807	191	702	9.85	0.21	9.56
21.25	-22586	5191	-14832	902	142	823	9.83	0.19	10.00
21.92	-29299	4272	-22822	900	138	944	9.80	0.24	9.65
22.62	-30166	7676	-20125	946	121	841	9.82	0.21	9.98
22.69	-31452	7981	-20980	937	168	917	10.00	0.48	10.00
22.75	-39658	7126	-29783	1157	143	1128	10.28	1.16	10.00
22.76	-57519	5679	-43706	1044	146	1069	13.25	2.49	10.00

	J GTOC			TOT DV [km/s]			T0 [MJD]		
	mean	std	best	mean	std	best	mean	std	best
15.03	102	10	107	11.09	1.61	9.60	63420	515	63718
21.05	70	19	83	39.57	3.30	34.88	60419	1341	59446
21.25	61	14	68	28.74	4.31	23.30	61268	1283	62813
21.92	61	14	58	34.05	3.55	28.67	60877	1448	61128
22.62	56	12	66	34.80	4.59	28.58	61483	1684	62874
22.69	56	16	58	35.06	5.47	28.58	61259	1545	62808
22.75	34	14	37	36.59	4.71	33.67	60401	1644	59216
22.76	36	17	43	41.61	6.20	42.33	59037	1299	59995

Figure 7.37 Results of continuous method for the best sequences selected by NNH using a cost function based on ESA. GTOC2 results are added for comparison.

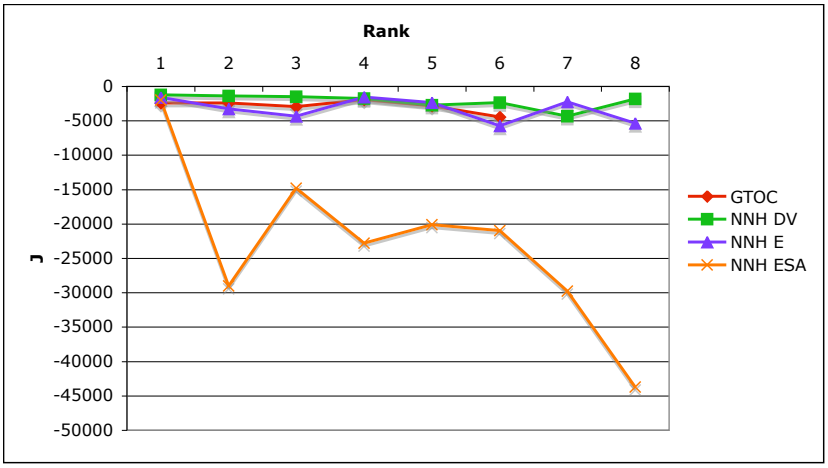

Figure 7.38 Visualization of the results of the continuous method, for the asteroid sequences obtained with the NNH and three different cost functions. GTOC2 results are added for comparison.

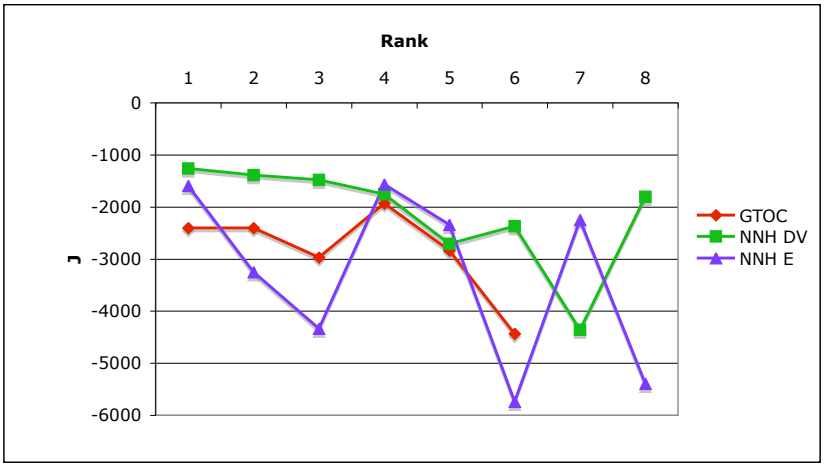

Figure 7.39 Figure 7.38 excluding the results for the ESA cost function. GTOC2 results are added for comparison.

The most surprising result is observed in figures 7.37 and 7.38. These figures show that only the first rank of the results obtained using the NNH and the cost function implemented by ESA has a solution of the same order as the other sequences. The sequences belonging to the other ranks all perform significantly worse. Figure 7.40 shows a top view of the orbit of the sequence with the lowest J value, obtained with the NNH using the ESA cost function, and had an ESA value of 22.76. A side view of this orbit is shown in Figure 7.41. Figure 7.42 gives the acceleration profile.

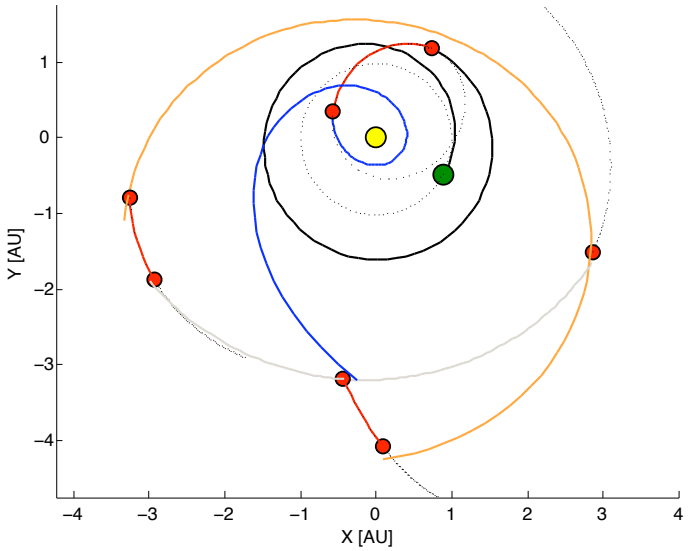

Figure 7.40 Orbit of continuous result for worst sequence obtained by the erroneous combination of the NNH with the symmetric ESA cost function. ESA value = 22.76 , J = -43706, J GTOC = 43. Trajectory is plotted according to the definitions in figure 4.19.

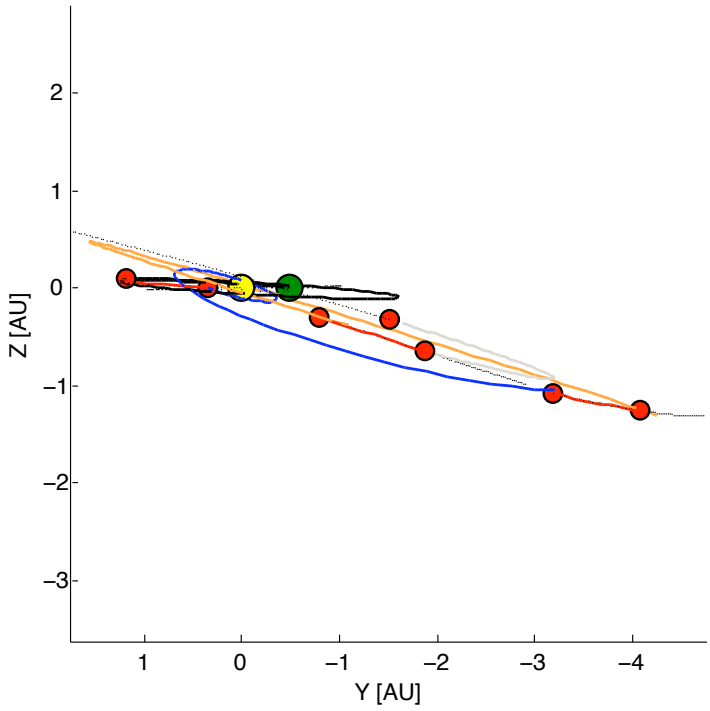

Figure 7.41 Side view of orbit of continuous result for worst sequence obtained by the erroneous combination of the NNH with the symmetric ESA cost function. ESA value = 22.76 , J = -43706, J GTOC = 43. Trajectory is plotted according to the definitions in figure 4.19.

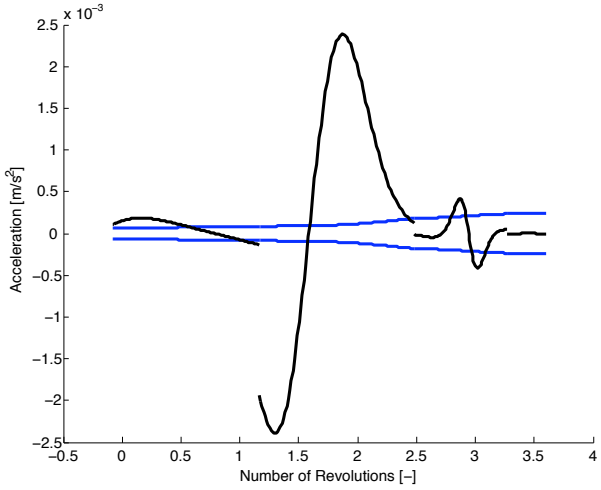

Figure 7.42 Allowed and required acceleration for worst sequence obtained by the erroneous combination of the NNH with the symmetric ESA cost function. ESA value = 22.76 , J = -43706, J GTOC = 43.The blue line indicates the acceleration limit, the black line the required acceleration for flying the trajectory shown in figure 7.40.

Figures 7.40 - 7.42 show that large departure and arrival angles between the trajectory of the spacecraft and the relevant bodies are present. On top of this large inclination changes are present and a very large acceleration constraint violation (note that the y-axis changed one order of magnitude from -4 to -3, with respect to the acceleration profiles presented so far). These three factors combined result in a very low J value. This behavior is not seen in the other NNH results or in the results generated by the AST, using the ESA cost function. This indicates that the bad objective values in figures 7.37 and 7.38 are the result of a combination of the NNH algorithm with the ESA cost function.
One possible explanation is the following. The ESA cost function is symmetric, resulting in a diagonally symmetric cost matrix. The cost function is based on a transfer from the asteroid with the lowest apocenter to the asteroid with the highest apocenter. This means that the cost function gives representative values for transfers from a lower group to a higher group (higher in terms of group number), since asteroids in a lower group have a shorter apocenter distance than asteroids in a higher group. Returning to the symmetric cost matrix, this implies that the part above the diagonal contains numbers that are representative for the transfer, but the values in the part below the diagonal are not representative for the transfer cost. A good value for a transfer below the diagonal might represent a transfer that is not efficient in real life.
The problem now is that the NNH searches for the lowest transfer cost in a particular row from left to right and it only updates the best value, if a value *lower* than the current best is found, and not when a *similar* value is found. Due to the fact that the cost matrix is symmetric and the algorithm starts searching form left to right it will always find transfers in the lower left part of the cost matrix, since the lowest value above the diagonal will at best be equal to the lowest value below the diagonal. This was the part, however, that contained bad approximations for the transfer costs. This means that the NNH, in combination with the ESA cost function, will most likely give bad results. The AST has no problems in dealing with the symmetry of the cost matrix, since it does not search the cost matrix from left tot right but finds combinations of transfers from anywhere in the cost

matrix. The NNH gives good results for the other cost functions since they are not symmetric. The reason why the first rank does give a good solution, is because the NNH starts at Earth. If the NNH starts searching from Earth in the cost matrix (Earth is the upper most left entry) then it will be searching in the part above the diagonal and hence will find a better solution.
One way to solve this problem is to update the NNH, such that it starts each search above the diagonal of the cost matrix. In this way it will only search the part of the cost matrix with entries that are an accurate approximation of the transfer cost for that particular transfer.
Another explanation is found in the fact that the evaluated sequences are quite similar. A large number of the asteroids they contain are the same and even in a similar order (see Figure E.5). It might be a question of mere chance that the NNH found a bad sequence. This latter argument is deemed less plausible since the eighth sequence selected for analysis is completely different from the others, but produces bad results as well.
It is emphasized that the presented explanations are merely hypothetical. Additional research has to be done in order to confirm this theory. The results do confirm that the continuous method is able to detect unfeasible options.

Figure 7.39 shows the results of the continuous method for the ΔV and energy cost function, and the GTOC solutions for comparison purposes. The results for the ESA cost function have been omitted to be able to rescale the graph to a size similar to that of Figure 7.30. For both the cost functions a stronger downward trend is detected in the NNH results than in the AST results. The behavior is, however, very volatile. Especially for the energy cost function, as was the case for the AST energy results. Nevertheless, both cost functions are able to produce results that are relatively good (i.e. solutions that have an objective value of over -3000). The results for the ΔV cost function are less volatile and consistently good. Only the seventh rank produces a bad result. In general, it can be stated that the behavior of the NNH result for the ΔV and energy cost functions are consistent with the results obtained by the AST. In an absolute sense, for the cost function based on ΔV, the results for the top 4 ranks of the NNH are generally better than the AST results.

Both trajectories and acceleration profiles of the trajectory with the highest and lowest J value of the NNH results have been included in figures 7.43 -7.46. The best trajectory in Figure 7.39 has been obtained using the NNH in combination with the cost function based on ΔV and had a DV value of 21.28 km/s. The worst trajectory in Figure 7.39 has been obtained using the NNH in combination with the cost function based on energy and had an E value of 545 MJ/kg.

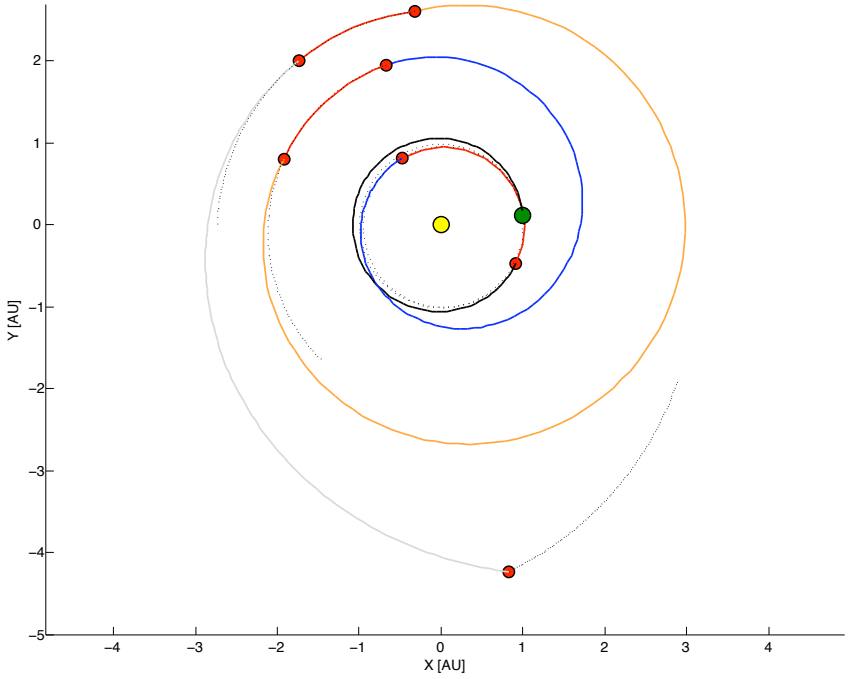

Figure 7.43 Orbit of best continuous result for sequences obtained by the NNH. DV value = 21.28, J = -1260, J GTOC = 104.

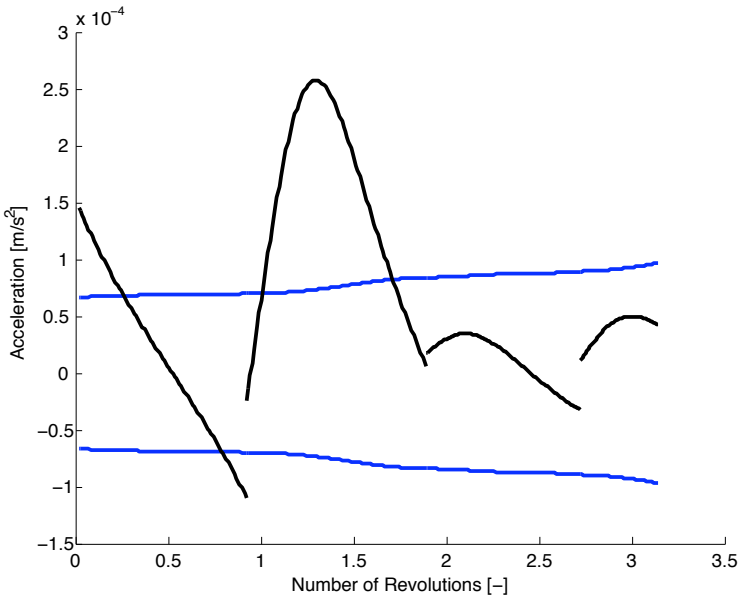

Figure 7.44 Allowed and required acceleration of best continuous result for sequences obtained by the NNH. DV value = 21.28, J = -1260, J GTOC = 104.

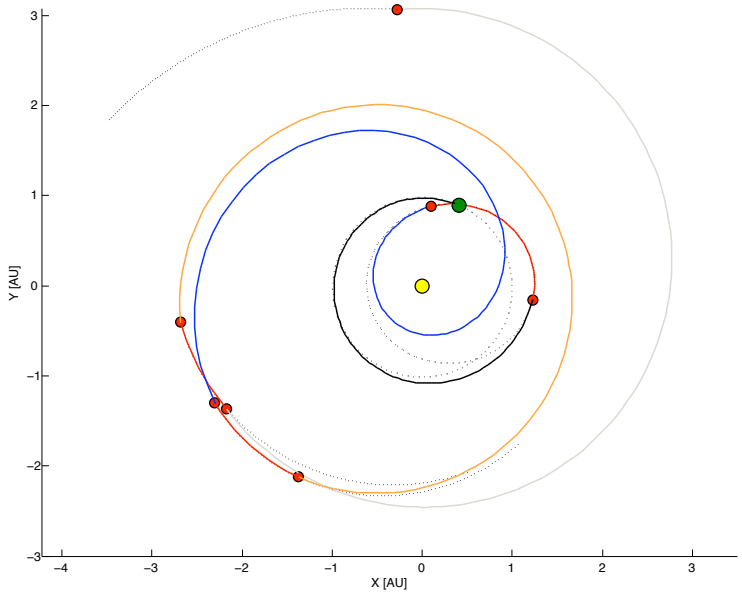

Figure 7.45 Orbit of worst continuous result for sequences obtained by the NNH. E value = 545, J = -5736, J GTOC = 84.

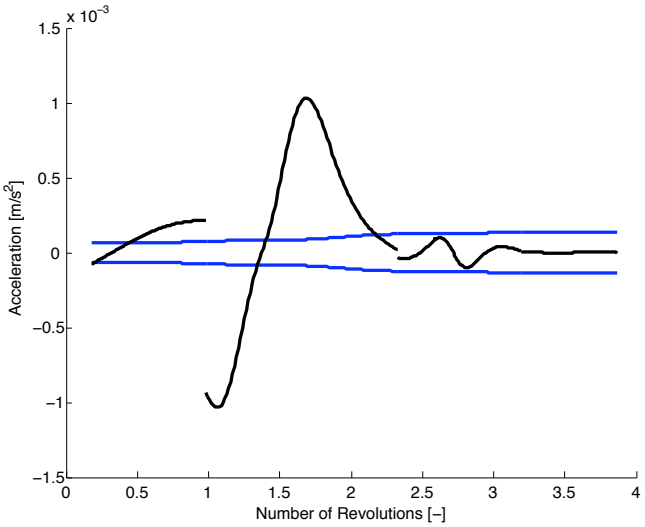

Figure 7.46 Allowed and required acceleration of worst continuous result for sequences obtained by the NNH. E value = 545, J = -5736, J GTOC = 84.

The trajectory in figure 7.43 appears to be a reasonable approximation of a low-thrust trajectory, but, as with the best solution obtained with the AST, velocity constraint violations of several km/s are present in this orbit. Also the acceleration limit is exceeded.
The main reason why the trajectory of Figure 7.45 is an suboptimal trajectory is the fact that it contains a very high total velocity mismatch (14.91 km/s). On top of that Figure 7.46 shows that the trajectory contains a very large transgression of the acceleration limit in the second leg (note that the scale of the y-axis has changed from an order of magnitude of -4 to -3).

Combining these results, it can be stated that the NNH, when applied to the

complete cost matrix, is a useful alternative for the AST as long as no symmetric cost function is used. Again it holds that, like for the other continuous results, concrete statements regarding the quality of any method can only be made after a solution is found that matches all the problem constraints.

7.2.4 Additional Tests for Continuous Method

In order to get more insight into the GTOC2 problem and the applied models and methods, a number of additional tests are performed. First, single leg transfers will be submitted to several tests, followed by two tests on the sequences selected by the GTOC2 participants. Lastly, the influence of the previously mentioned error in the total TOF will be investigated. The sequences selected by the NNH, using a cost function based on energy, are used for this test because these results were hindered the most by the penalty setting.

Tests for single leg transfers
An overview of the performed tests on a single leg transfer is shown in Figure 7.47. The first five tests are performed to analyze the influence of the penalty settings. An Earth-Asteroid transfer (EA) is taken as a test case, where the target asteroid is the first asteroid in the sequence of the GTOC2 winner (GTOC2 asteroid ID: 3258076). The original GTOC2 cost function is implemented and the spacecraft mass is set to the GTOC2 initial spacecraft mass of 1500 kg. GTOC2 also provides an initial velocity of up to 3.5 km/s if needed, thus no penalty will be applied to a ΔV smaller than 3.5 km/s at Earth departure.

Test ID	Transfer	Objective	Initial mass	Penalty	Other
1	EA	Mf/TOF	1500	>0.5 L	
2	EA	Mf/TOF	1500	Mass equiv.	
3	EA	Mf/TOF	1500	>0.5 Q	
4	EA	Mf/TOF	1500	>1.2 L	
5	EA	Mf/TOF	1500	>1.2 Q	
6	EA	Mf/TOF	1500	>0.5 L	Inclination set to 0
7	EA	Mf	1500	>0.5 L	
8	EM	Mf/TOF	1500	>0.5 L	

Figure 7.47 Overview of additional tests for a single leg transfer.

The first test is the reference test. The linear penalty is set to 50 times the mass equivalent for a velocity mismatch of over 0.5 km/s. The second test applies a penalty function similar to the one used for the first validation test and the third test uses a penalty function similar to the second validation test as described in section 6.2. In addition, three other tests with varying penalty settings were performed. The fourth test is used to check the influence of the threshold value above which the penalty is applied. For this test the threshold value has been shifted from 0.5 to 1.2 km/s. The fifth test was performed because of the results of the first four tests. The results suggest that a quadratic penalty applied at a threshold of 1.2 km/s might provide better results. The fifth test will check if this is correct. The sixth test is performed to check the influence of the inclination difference between the transfer bodies. In this test the inclination for both the departure and arrival body is set to 0. The seventh test checks the influence of the objective function. Instead of testing the GTOC2 objective function, the same objective function used for validation (mass minimization) was used, with the exception that the applied penalty is linear instead of mass equivalent or quadratic. The last test is performed to determine if there is a difference between transfers to planets and to asteroids.

The same optimizer settings used for the validation tests were applied. An overview of the test results is given in Figure 7.48. The mean, standard deviation and best result of the 10 runs is given for the objective value J, the corresponding GTOC2 objective value, the mass consumption, the total time of flight, the total velocity mismatch (sum of excess departure velocity and excess arrival velocity) and the launch date.

Test ID	J			Mass Used [kg]			TOF [year]		
	mean	std	best	mean	std	best	mean	std	best
1	-1070	39.2	-1028	546	22	571	5.11	0.36	5.54
2	14085	746.4	14991	11	9	2	0.05	0.00	0.05
3	-1642	785.5	-643	250	211	138	2.80	1.68	1.56
4	-875	551.2	693	516	131	142	4.92	1.19	1.56
5	-1180	1084	769	167	181	143	1.66	0.41	1.54
6	-574	1063.2	2429	328	236	45	3.31	2.01	0.43
7	-954	418.9	-579	246	209	93	1.92	1.23	0.73
8	1190	0.4	1191	120	1	120	0.86	0.00	0.86

	J GTOC			TOT DV			T0		
	mean	std	best	mean	std	best	mean	std	best
1	188	19	168	6.70	0.10	6.82	59816	2259	63361
2	27538	1796	30025	21.35	1.52	22.58	62864	192	62954
3	609	307	874	5.33	1.08	4.23	62187	2277	63898
4	247	218	868	6.52	0.72	4.48	59724	2577	56974
5	870	365	882	6.78	6.09	4.55	61237	2493	63553
6	761	975	3367	5.29	1.46	3.76	61848	2042	62893
7	981	663	1932	7.70	1.73	6.29	61834	1879	62073
8	1608	5	1607	2.62	0.03	2.62	58940	1	58941

Figure 7.48 Results of additional tests for a single leg transfer.

Comparing the 1st test with the 2nd shows that a mass equivalent penalty is not strong enough to find solutions with good departure and arrival ΔV's. The reason why the function values are good for the 1st test is that although the velocity mismatches are high, the increase in the quality of the objective value achieved by mismatching the departure and arrival velocities is more than sufficient to compensate for the penalty imposed by the velocity mismatches. This is undesirable behavior, since a good J GTOC value is worthless if it also has huge constraint violations. Fortunately, other tests show that when a stronger penalty is applied, this behavior is prevented because extremely high objective values have become unfeasible when the orbit also has to fulfill the velocity constraints. Note that the validation tests did not have this problem. This is due to the fact that the transfer time was not part of the objective. Only mass needed to be minimized, which this does not require high velocity mismatches at departure or arrival in order to accommodate a fast transfer.
Comparing the first result with the third result shows that a quadratic penalty achieves a lower velocity mismatch than a linear penalty. Also the best objective value J obtained by using a quadratic penalty is better than the best solution obtained when using a linear function. When the mean and standard deviation of the results is scrutinized it shows that the objective function with a quadratic penalty has a mean which is worse than the mean of the objective function with a linear penalty. Also the standard deviation is larger. This is an interesting result since it shows that when using a quadratic penalty, the complexity of the search space is increased and the optimizers have more trouble identifying the best solution. Put in a different way, in order to increase the contrast between good and bad solutions, the complexity of the search space has to be increased. This also means that a more powerful solution method is required. This is confirmed when

the search spaces for the mass equivalent and the quadratic penalty are visualized. Appendix J includes the results of such visualizations.
Comparing the test result of the 4th test with the result of the first, shows that loosening the threshold value for the penalty also leads to better results for the objective values, J and J GTOC and for the velocity mismatch. This result is not as expected. By lowering the penalty threshold, the optimizer will shift its focus from low velocity mismatches to good J GTOC objective values (i.e. less emphasis on the penalty part and more emphasis on the actual objective part of equation 4.62). It is expected that better objective values are found at the cost of larger constraint violations, i.e., larger velocity mismatches. The mean and standard deviations of test 1 and 4 show that the better result for the total velocity mismatch of test 4 is an outlier. This indicates that it is already hard for the exposin to stay within the threshold for the velocity mismatch of 1.2 km/s, and almost impossible to find solutions with a mismatch lower than 0.5 km/s. These tests reveal a limiting factor of the exposins. Improvements might be obtained by increasing the optimizer strength. The drawback of this approach is that more computational effort is required.
Comparing test 1 with test 5 shows that a quadratic penalty after a threshold of 1.2 km/s provides better results compared to a linear penalty applied after 0.5 km/s. Since test 4 already demonstrated that a penalty applied at a threshold of 1.2 km/s already provides better objective values than one applied at a threshold of 0.5, it is more interesting to compare the results of test 5 with test 4. This shows if using a quadratic penalty (which, as already demonstrated, makes the search space more complex/irregular) has a beneficial effect. When looking at the objective values J and J GTOC, Figure 7.48 shows that the quadratic penalty finds slightly better values. It does find these better values at the expense of a slightly higher velocity mismatch. There appears to be some sort of Pareto optimality relation between the results of test 4 and 5. Because the difference in J is relatively large compared to the differences in J GTOC, mass used, TOF and TOT DV, it is believed that the quadratic penalty also results in trajectories that better match the thrust limit constraint. This makes the quadratic penalty preferable over the linear penalty. Comparing the standard deviations of test 4 and 5 also show an increase in irregularity of the search space when applying the quadratic penalty, which was concluded before by comparing the first and third test. Also, the departure dates are completely different for test 4 and 5. This indicates that the two trajectories are very different, and not just a slight deviation form one another, that could have been explained by the accuracy of the algorithm.
The combination of the results of tests one to four supports the choice for using a quadratic penalty applied after a threshold value of 1.2 km/s for the analysis of the patched exposin model.

Comparing the results for tests 1 and 5 shows that the inclination difference between the arrival and departure body is significant. This is to be expected, since the velocity mismatch in the third dimension is eliminated. This makes it easier to find better solutions. In reality however this mismatch in the third dimension has to be compensated for as well, for example, by thrusting in directions other than tangent to the trajectory. This reduces the thrust available for the in plane maneuvering, and hence will affect the phasing results. This makes it necessary to implement the third dimension, since the influence on the results is quite significant. It is deemed unwise to approximate phasing behavior by a 2D model.

The 7th test optimizes for the fuel use only, instead of optimizing for a low fuel use and a fast transfer. The J value for the transfer considering both fuel use and time of flight, is worse than for the transfer that only considers the minimization of fuel use. This is expected because the the minimization of mass use and flight time are two conflicting objectives. The fuel use for test 1 is also larger than for test 8. This is also according to expectations because it requires more fuel to fly faster. The time of flight, however, is not lower for test 1 than for test 7, even though it was part of the objective function. This is an unexpected result. Also the J GTOC value is higher for test 7 than for test 1. This should be the other way around, because in test 1 the J GTOC value is optimized for. An explanation for these strange results might be found in the fact that the total velocity mismatch is quite large. This means that the obtained exposins give a relatively bad approximation of a low-thrust transfer trajectory. Also the velocity budget available at departure might influence the results such that they become harder to interpret. Additional tests should be performed to be able to make a statement about the influence of the objective function.
Test 8 is performed to analyze the difference between a planet-planet transfer and a planet-asteroid transfer. For the planet-planet case an Earth-Mars transfer is used. It is expected that a planet-planet transfer will provide better results, since planetary orbits are more similar to each other than asteroid orbits are. Comparing the results of test one and seven shows that this is indeed the case. A much better objective value is found, with a far lower velocity mismatch and an extremely low standard deviation. This indicates that the optimizer finds almost the exact same solution with every run, and therefore it can be concluded that the planet-asteroid transfer is indeed more complicated than a planet-planet transfer. Of course, this result is only based on only one comparison and additional tests, with different asteroids and planets, need to be performed in order to make a more definite statement about the difficulty of Earth-asteroid and Earth-planet transfers. The results of this test are in concordance with the expectations.

Tests for multileg transfers
Two tests on the asteroid sequences selected by the GTOC2 participants and one on the sequences obtained by the NNH using a cost function based on energy will be performed. The first test will try to improve the performance of the continuous method by creating a pit in the penalty function where no penalties are applied. The second test tries to identify the most stringent constraint, by allowing the local optimizer to search outside the problem bounds. The third test is used to assess the influence of the erroneous penalty setting for the total time of flight. The model, method and optimizer settings used for testing are the same as those used for obtaining the continuous results of sections 7.2.1 - 7.2.3.

The goal of the continuous method is to assess the phasing characteristic of a certain sequence, in order to determine if that sequence possibly has a good J GTOC value. The continuous method, however, is not able to meet the GTOC2 constraints. A hypothesis is now formed, that if a velocity mismatch is allowed and within this band of allowable velocity mismatches only the original GTOC objective is analyzed, it might be possible to get the desired result when used on the selected sequences submitted by the GTOC2 participants. The desired results in this case is that the continuous method ranks the sequences of the GTOC2 participants according to their GTOC2 rank, meaning that it ranks the sequence of the winner as the best one, the sequence of the second place as second best

and so on. To create the pit, the penalty is set to zero when the total velocity mismatch is smaller than 14 km/s, the time of flight is lower than 10 years and the objective value is higher than -5500. A summary of the results of this penalty function with a 'penalty pit' is shown in Figure 7.49. More extensive results are included in appendix I.

Rank	Monte Carlo			Genetic Algorithm			Interior Point Method		
	J	J GTOC	TOT DV	J	J GTOC	TOT DV	J	J GTOC	TOT DV
1	-8943	92	17.17	137	137	10.54	142	142	11.09
3	-8313	99	16.76	121	121	13.05	121	121	13.06
7	-6721	50	15.64	-3018	46	11.02	-3008	46	11.01
9	-5850	96	14.66	228	228	11.22	228	228	11.24
10	-5479	97	15.19	115	115	13.40	117	117	12.62
11	-6352	99	15.86	110	110	13.45	110	110	13.45

	J			Mass Used [kg]			TOF [year]		
	mean	std	best	mean	std	best	mean	std	best
1	-3837	2730	142	601	166	402	9.36	0.68	7.75
3	-2874	2350	121	502	67	420	9.76	0.29	8.92
7	-4908	1386	-3008	876	133	1043	9.69	0.35	9.90
9	-127	1156	228	460	104	293	8.65	1.63	5.30
10	-3090	2783	117	543	106	476	9.70	0.41	8.75
11	-3062	2407	110	498	108	408	9.61	0.36	9.90

	J GTOC			TOT DV [km/s]			T0 [MJD]		
	mean	std	best	mean	std	best	mean	std	best
1	97	23	142	13.53	1.58	11.09	58001	1679	57368
3	103	9	121	13.08	1.08	13.06	62074	1778	63730
7	64	13	46	13.97	2.52	11.01	58205	1374	57816
9	128	45	228	12.05	0.85	11.24	60882	2979	57031
10	99	13	117	13.32	1.25	12.62	62308	2225	64021
11	104	10	110	13.41	0.77	13.45	63107	2091	64030

Figure 7.49 Results of additional tests when a pit in the penalty is created.

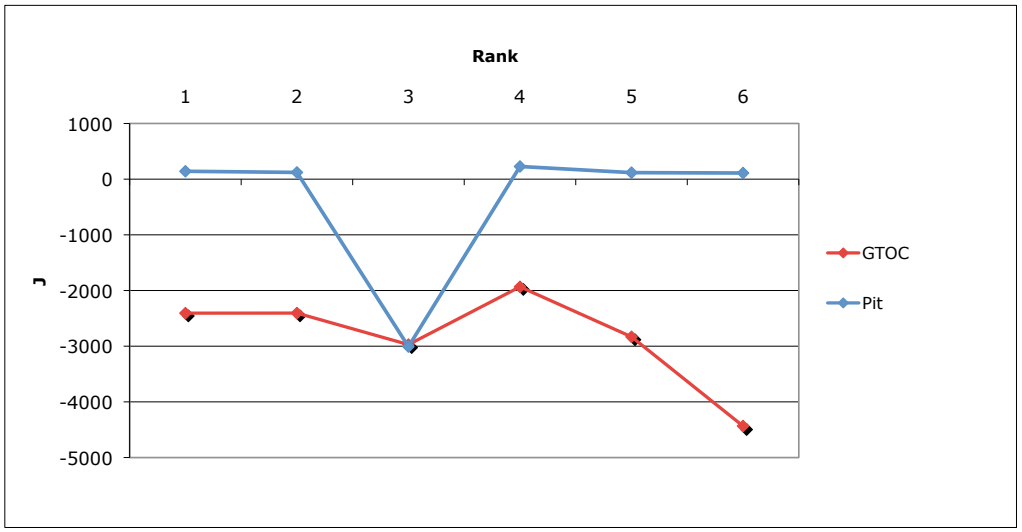

Figure 7.50 Visualization of the results of the continuous method when a pit in the penalty is created. The GTOC2 results are added for comparison.

From figures 7.49 and 7.50 it becomes clear that the continuous method with a 'pit' in its penalty function does not rank the sequences of the GTOC2 participants according to their GTOC2 ranks. In fact, when comparing the results in figure 7.49 with Figure 7.18, it becomes clear that the exact opposite of the desired result is achieved. Allowing a certain velocity mismatch facilitates a faster transfer, reducing the total time of flight and increasing the J GTOC objective value, whilst increasing the amount of velocity mismatch. This is according to expectations,

but the problem is that the continuous method still does not rank the asteroid sequences according to their GTOC2 ranks. So allowing for constraint violations does not increase the performance of the continuous method. A second observation is that for the third rank (corresponding to GTOC rank 7) no solution within the pit is obtained. This could indicate that the optimizer is not strong enough to find the pit. For the other sequences, however, the optimizer did find the pit. Considering this, a more likely explanation is that it is relatively hard to find a good solution using exposins for this asteroid sequence. Based on the presented results the hypothesis of finding better results when allowing for certain velocity mismatches is dismissed.

An additional test is performed where the Interior Point method is allowed to search outside the problem bounds. This test gives information about the influence of the bounds on the difficulty of finding good results. It is also a check if some of the bounds that are not specified by GTOC2 are set correctly (for example, the upper limit on the stay time of 150 days). The results of this test are shown in Figure 7.51. Extensive results are included in Appendix I.

	Monte Carlo			Genetic Algorithm			Interior Point Method		
Rank	J	J GTOC	TOT DV	J	J GTOC	TOT DV	J	J GTOC	TOT DV
1	-8219	92	17.25	-2455	115	10.07	-2066	110	9.79
3	-6775	113	15.59	-2955	109	10.59	-1850	106	9.55
7	-10562	83	20.12	-3532	56	11.81	-2276	56	10.20
9	-6960	99	16.46	-1619	119	8.23	-803	108	8.17
10	-7968	85	17.99	-2901	108	10.91	-2096	112	10.26
11	-10425	86	18.25	-5366	84	13.39	-4389	66	12.57

	J			Mass Used [kg]			TOF [year]		
	mean	std	best	mean	std	best	mean	std	best
1	-4771	1391	-2066	644	132	527	9.67	0.48	8.83
3	-4068	1344	-1850	517	67	478	9.95	0.10	9.68
7	-5558	1901	-2276	779	192	955	9.88	0.22	9.67
9	-2610	994	-803	507	105	433	9.91	0.21	9.92
10	-4243	1069	-2096	570	132	382	9.77	0.34	10.00
11	-6075	1423	-4389	826	247	840	9.85	0.37	10.00

	J GTOC			TOT DV [km/s]			T0 [MJD]		
	mean	std	best	mean	std	best	mean	std	best
1	89	15	110	13.42	1.90	9.79	57781	858	57150
3	99	7	106	12.76	1.66	9.55	61731	1705	62313
7	73	19	56	14.35	2.34	10.20	58870	2410	57625
9	100	12	108	10.55	1.51	8.17	61236	2917	57002
10	95	13	112	12.58	1.32	10.26	61868	2612	64098
11	69	25	66	15.96	6.45	12.57	62789	603	62341

Figure 7.51 Results of additional tests when IP method is allowed to search outside the problem bounds.

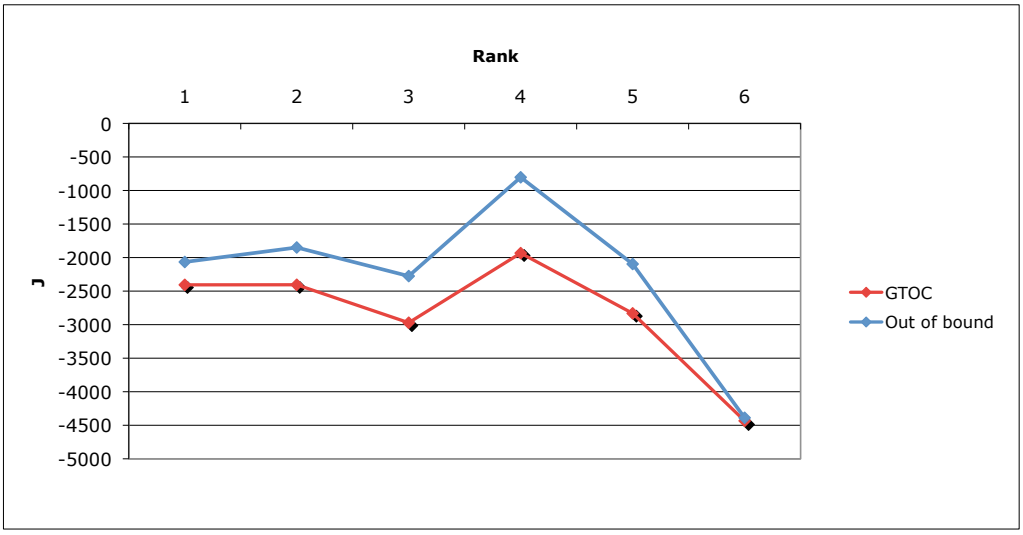

Figure 7.52 Visualization of the results of the continuous method when it is allowed to search outside the problem bounds. The GTOC2 results are added for comparison.

When comparing the J values in Figure 7.51 with the J values for the GTOC sequences in Figure 7.18, it follows that, when allowed to search outside the problem bounds, the IP method will return better J values. The corresponding J GTOC values and total velocity mismatch has changed relatively little, whilst the mission timeline has been changed significantly. Figure 7.53 shows the departure date (T0), the TOF for all four legs and the TOS at the first three asteroids.

The mission departure date has changed a few months for most sequences. The

Rank	T0		TOS 1		TOS 2		TOS3	
	GTOC2	Test	GTOC2	Test	GTOC2	Test	GTOC2	Test
1	57024	57150	90	82	149	81	149	111
3	63592	62313	103	120	91	288	90	-219
7	57651	57625	113	85	149	144	90	60
9	64155	57002	129	81	131	-1	150	139
10	64123	64098	147	91	140	135	130	144
11	62579	62341	136	91	94	98	150	77

	TOF 1		TOF 2		TOF 3		TOF 4	
	GTOC2	Test	GTOC2	Test	GTOC2	Test	GTOC2	Test
1	189	407	920	1295	1348	755	527	495
3	539	252	515	1043	1369	1135	820	918
7	707	713	950	1068	1026	1014	436	447
9	461	263	867	728	992	295	857	2120
10	275	361	567	491	642	948	1752	1483
11	602	264	623	670	636	1096	1223	1358

Figure 7.53 Comparison of the mission timeline obtained by the continuous method for the GTOC results (left columns) and the test case where the IP is allowed to search out of the bounds.

time of flights and stay times at the first three asteroids have changed considerably. Stay times (far) beyond the bounds are found. Some stay times even have become negative, indicating that a good solution would have to depart from that asteroid before it even gets there. From these results it follows that the stay time is a relatively hard constraint. The upper bound of 150 days is user defined and should be relaxed.

The last test is performed to investigate the influence of the erroneous penalty setting for the total time of flight. The threshold after which the penalty is applied is changed from 10 years to 20 years. The test was performed using the asteroid

sequences obtained by the AST, using a cost function based on energy. This set of asteroid sequences was selected because most of its solutions ran into the threshold of 10 years. A summary of the test results is included in Figure 7.54. More extensive results are included in appendix I. The J values are plotted in figure 7.55.

E Value [MJ/kg]	Monte Carlo			Genetic Algorithm			Interior Point Method		
	J	J GTOC	TOT DV	J	J GTOC	TOT DV	J	J GTOC	TOT DV
420	-924	79	6.76	-188	28	6.38	-188	28	6.32
437	-2317	87	10.51	-404	42	6.13	-402	42	6.41
454	-2079	63	11.53	-336	45	7.19	-336	45	7.19
456	-2027	60	10.34	-543	42	6.67	-507	42	6.92
465	-2636	54	13.05	-732	52	7.88	-732	52	7.88
473	-1361	56	9.57	-343	58	6.64	-313	43	6.64
479	-1850	67	10.57	-681	65	8.35	-657	65	8.46
496	-1960	51	10.93	-761	37	7.40	-761	37	7.40

	J			Mass Used [kg]			TOF [year]		
	mean	std	best	mean	std	best	mean	std	best
420	-412	230	-188	624	158	998	16.11	1.46	18.17
437	-837	408	-402	655	90	770	15.61	1.78	17.18
454	-784	317	-336	554	90	665	16.32	0.87	18.52
456	-1031	353	-507	695	135	829	16.10	1.78	16.10
465	-1127	255	-732	691	165	716	16.83	1.47	15.04
473	-676	252	-313	642	130	733	17.03	1.20	17.72
479	-899	135	-657	512	60	531	15.56	1.16	14.82
496	-1106	253	-761	706	116	808	17.49	1.46	18.62

	J GTOC			TOT DV [km/s]			T0 [MJD]		
	mean	std	best	mean	std	best	mean	std	best
420	55	13	28	7.03	0.90	6.32	63292	950	63184
437	55	12	42	8.10	1.37	6.41	60967	1605	61360
454	58	8	45	8.23	0.96	7.19	62931	2046	62048
456	51	12	42	8.76	1.28	6.92	60144	3095	58214
465	49	11	52	9.30	0.77	7.88	63342	1551	63334
473	51	10	43	8.96	4.98	6.64	58359	1933	57674
479	64	6	65	8.42	0.50	8.46	62141	215	62145
496	46	8	37	9.19	1.07	7.40	60299	2575	62574

Figure 7.54 Results of additional tests when the penalty threshold for the mission duration is changed from 10 to 20 years.

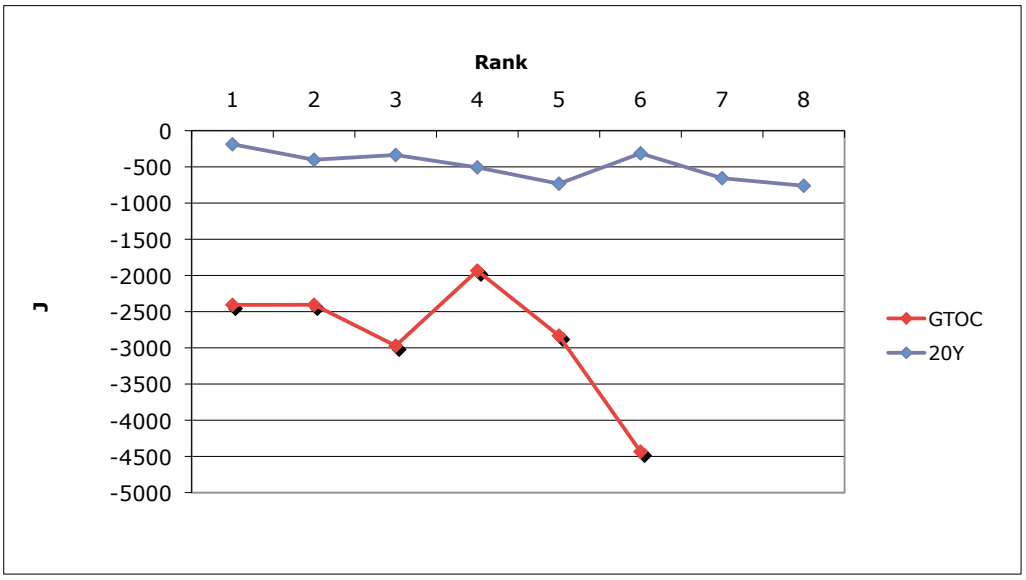

Figure 7.55 Visualization of the results of the continuous method when the penalty threshold for the total TOF is set to 20 years. The GTOC2 results are added for comparison.

Comparing the results for the penalty threshold of 20 years, shown in Figure 7.54 (and appendix I), with the results for the penalty threshold of 10 years, shown

in Figure 7.28 (and appendix G), leads to an interesting result.
The objective values for the threshold setting of 20 years are significantly better than the results obtained when the threshold is set to 10 years. This improvement is due to the fact the total velocity mismatch is lower. This leads to lower penalty values, and hence better J values. The fact that the velocity mismatch is lower, can, in its turn, be explained by the increase in the time of flight for each leg (compare Figure 7.54 with Figure 7.18). If more time is available to fly the mission, the spacecraft could complete another revolution around the Sun. This is confirmed by the trajectory and acceleration profile plotted in figures 7.56 and 7.57 respectively. Note that 6 revolutions are completed instead of about 4, as

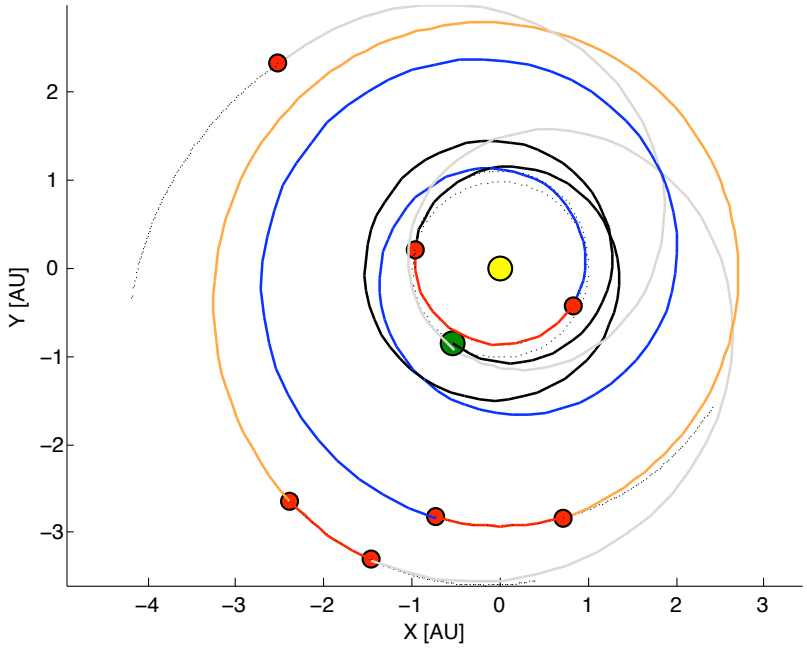

Figure 7.56 Orbit of best continuous result for the sequences obtained by the NNH using ESA cost function and a time of flight penalty threshold of 20 years. E value = 420, J = -188, J GTOC = 28.

was the case for the asteroid sequences evaluated with a TOF penalty threshold at 10 years. By completing more revolutions around the Sun, the arrival angle will decrease and the spacecraft has more time to accelerate towards a velocity similar to that of the target asteroid. Both factors decrease the velocity mismatch upon arrival at the target body. This decrease in (total) velocity mismatch, however, comes at the expense of the J GTOC value. As mentioned before, increasing the time of flight has a detrimental effect on the mass use. Both the increase of the time of flight and increase in mass consumption are directly affecting the J GTOC value negatively. This is confirmed by the results. The J GTOC values in Figure 7.54 are about half the J GTOC values in Figure 7.28. This indicates that without the penalty threshold for the total time of flight set to 10 years, the continuous method is not able to obtain J GTOC values matching or surpassing the values obtained by the GTOC2 participants (as previously explained, higher J GTOC values are to be expected when constraint violations are present).
Moreover, Monte Carlo results obtained with the threshold set to 20 years (Figure 7.54) prove the presence of better J GTOC values in the search space, but that

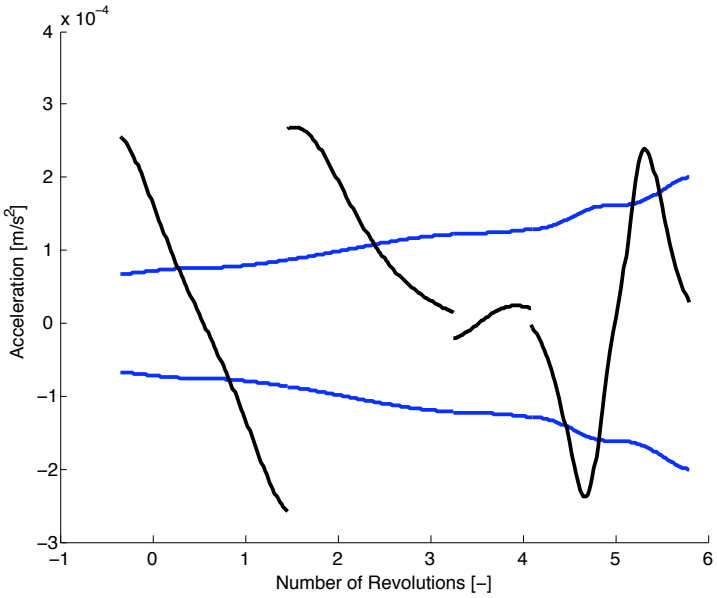

Figure 7.57 Allowed and required acceleration of best continuous result for the sequences obtained by the NNH using ESA cost function and a time of flight penalty threshold of 20 years. E value = 420, J = -188, J GTOC = 28.

the GA and IP method discard those solutions. These solutions also have J values similar to those obtained by the IP method with the threshold set to 10 years (Figure 7.28). The reason for the GA and IP method to discard the solutions is that these orbits have a higher (total) velocity mismatch.

The conclusion that can be drawn on these results is that the continuous method prefers to match the velocity constraints over finding a good J GTOC value. Although this is desirable (a good solution is worthless if it has high constraint violations), it also demonstrates that the exposin is not a suitable model for exact phasing assessment. Good solutions, analyzed with the continuous method, will contain velocity mismatches, and due to the current penalty settings the corresponding J value is not an accurate indication of the phasing quality of such a sequence.

Regarding the erroneous penalty setting, it turns out that the setting is actually beneficial in terms of finding trajectories with J GTOC values similar to those obtained by the GTOC2 participants. It would, however, require foreknowledge about the optimal solution to set the penalty threshold to this value. This disqualifies the continuous method to be used as a phasing assessment tool.

Chapter 8

Conclusions and Recommendations

This chapter will present conclusions based on the results of the research presented in this report. An answer to the main research question will be formulated and recommendations for future research will be given.

8.1 Conclusions

Conclusions based on research results

1. *The cost function based on a ΔV budget that matches the orbital elements of the departure asteroid with the orbital elements of the target asteroid, reduces the asteroid set most efficiently in terms selecting asteroids that were selected by the GTOC2 participants too.*
   Because the reduction procedure selected asteroids that match those selected by the participants, it is believed that the reduction procedure, combined with any of the cost functions, is able to indicate whether or not a certain transfer is promising or not. The results in figure 7.1 show that, overall, for the cost function based on ΔV, the reduced cost matrix contains the most asteroids that are also present in one of the asteroid sequences obtained by the GTOC2 participants with respect to the dimension of the reduced cost matrix. There is, however, still room for improvement. All three cost functions are able to select good asteroids from group 1. Unfortunately, only a limited number of asteroids from group 2, 3 or 4 are selected that match those selected by the GTOC2 participants (see appendix C). This is most likely due to the fact that no phasing characteristics are taken into account during the reduction procedure. There is a high overlap in the asteroids selected with the different cost functions, indicating that the three cost functions are effectively not very different.
2. *The Branch and Bound algorithm outperforms the Nearest Neighbor Heuristic on the same search space, irrespective of the cost function used.*
   The results in figure 7.6 show that the B&B algorithm used by the AST finds a better result than the NNH for all three cost functions. Improvements of 5%-10% are obtained by the B&B. This improvement comes at the cost of a much longer computation time (hours instead of minutes). The results indicate that selecting the asteroid which is closest as seen from the current position is

not the best approach for constructing a multiple leg asteroid mission, because solutions exist that are not visible to this approach.

3. *The NNH, when applied to the complete search space, is a viable alternative to the AST, which can only be applied to the reduced cost matrix.*
   The results in figure 7.6 show that, for the cost function based on ΔV, and the cost function used by ESA, when the NNH is applied to the complete cost matrix it will find better results. The AST cannot be applied to the complete search space because it takes too long to solve the subproblems created during the B&B procedure. This makes the NNH applied to the complete cost matrix an useful alternative to the B&B (as implemented in the AST) applied to the reduced cost matrix.

4. *Improving the B&B, such that it is able to deal with the complete asteroid set, will most likely result in better sequences.*
   Combining the fact that the B&B finds better results on the same search space, and the fact that the NNH showed that the complete cost matrix contains better results than the reduced search space indicates that improvements can be made by applying a stronger B&B to the complete search space. For the cost function based on energy, the AST, when applied to the reduced cost matrix, already outperforms the NNH applied to the complete cost matrix. This proves that the NNH is not finding all the optimal solutions even though it is applied to the complete set of asteroids.

5. *The most promising sequence of asteroid groups is either 4-3-2-1 or 4-2-3-1.*
   Both the AST and NNH results in figure 7.6 show that the best solutions have a group order of 4-3-2-1 or 4-2-3-1. When considering not only the best sequences obtained by each method, but also other good solutions these methods found (see appendices D and E), it follows that other good sequences have this group order too. An explanation is found when considering the orbital energies of the various asteroid groups. Selecting asteroids sequentially from groups 4, 3, 2, and 1 or 4, 2, 3 and 1, will most likely demonstrate a pattern of increasing orbital energy, due to the positioning of the groups in the solar system. A pattern of increasing orbital energy is desirable from a propulsion point of view. It eliminates the need of lowering the orbital energy by using the engine, only to regain that energy when a transfer to an orbit with higher orbital energy is desired. The result regarding the group order is an improvement considering past research on GTOC2 at the Mission Analysis Department of the DUT Aerospace Engineering Faculty. The group order was only an assumption based on the GTOC2 results in the research performed in [*Evertsz*, 2008].

6. *The NNH cannot be used in combination with a symmetric cost function.*
   The continuous results for the sequences obtained by the NNH using the ESA cost function show that this combination is inadequate for identifying candidate asteroid sequences. It is believed that this is due to the combination of the algorithm search pattern and the symmetry of the cost function. The symmetry of the cost function causes the values beneath the diagonal of the cost matrix to be inaccurate approximations of the transfer cost. The NNH algorithm searches the cost matrix from left to right, meaning that it will start in this region with inaccurate cost approximations. Because of the symmetry of the cost matrix, and the fact that the NNH only updates its solution when it finds a better solution, but not when it finds a similar solution, the NNH is stuck in this region of inaccurate approximations. This problem might be solved by

updating the NNH such that it starts each search above the diagonal of the cost matrix. This has, however, not been tested in this research.

7. *The best NNH results are obtained when starting from Earth.*
   The results in appendix E show that for all cost functions the lowest cost for the complete sequence was obtained when starting form Earth. The reason for this is that when starting from Earth, non of the transfers is fixed because the Hamiltonian cycle needs to be closed. If the goal is to find the single best asteroid sequence, a single start NNH starting from Earth is sufficient. If the goal, however, is to find several promising candidate sequences for further analysis, then a multi start NNH can be used, provided that a asymmetric cost function is used.

8. *The continuous method, in its current form, can be used for confirmation and increase in accuracy of the results of the AST and NNH, but it cannot be used to give an accurate assessment of the phasing characteristics of a certain asteroid sequence.*
   The continuous results in figure 7.19 for the asteroid sequences of the GTOC2 participants show that the continuous method is able to distinct between relatively good and relatively bad sequences in terms of favorable asteroid orbit characteristics for transfer trajectories. Results obtained during the development of the method as well as results obtained for the sequences found by the NNH in combination with the ESA cost function (figure 7.38), show that the continuous method can detect practically unfeasible sequences as well.
   Because an exposin model is used, the results inherently take the phasing of the asteroid sequence into account as well. The extensive results included in appendices F to I, however, show that a velocity mismatch of the order of several km/s is obtained. Also, when comparing the obtained mission timelines with the timelines obtained by the GTOC participants (see figure 7.21) it follows that the continuous method finds completely different results. In addition, when the penalty threshold for the total time of flight was loosened from 10 to 20 years, the continuous method was not able to find solutions with GTOC objective values resembling those obtained by the GTOC2 participants. The order of magnitude of the velocity mismatch, the fact that obtained mission timelines do not resemble those obtained by the participants and the fact that a penalty inside the search space is required to find good GTOC objective values, indicates that the continuous method, in its current state, cannot be used for accurate phasing analysis or for providing bounds on the search space for more accurate methods.
   The performance of the continuous method could not be increased by creating a pit in the penalty function. Results in figure 7.49 show that the quality of the solutions decreases whilst the continuous method was not able to rank the sequences of the GTOC2 participants according to the GTOC2 results. Setting the inclination of the bodies in the sequence being evaluated to 0 does improve the objective value, it is, however, not believed that this is an adequate method for evaluating phasing characteristics, because it eliminates an important aspect of the transfer. Plane changes are amongst the most expensive maneuvers and neglecting these costs results in an inaccurate assessment of the transfer.

9. *The best combination of models and methods described in this report for finding good asteroid seqeunces consistently is the combination of the NNH and the cost function based on ΔV.*
   The results of the continuous method for the sequences found by the AST and

NNH (Figures 7.30, 7.38 and 7.39) show that the combination of the NNH and a cost function based on ΔV provide good asteroids sequences consistently. Of the top 8 sequences only one sequence was qualified as relatively bad, all other solutions were good and in all instances outperformed the continuous results for the sequences of the GTOC2 participants. The sequences obtained by the AST using the cost function based on ΔV resulted in sequences that are comparable in quality to the GTOC2 sequences. The AST, in combination with the cost function based on energy found the overall best solution. For generating a large number of good sequences, however, this combination is not adequate, since relatively bad sequences were found repeatedly. Again, it is believed that an B&B algorithm that is able to cope with the complete cost matrix will provide the overall best results.
The cost function based on ΔV is a viable alternative to the cost function used by ESA. It not only provides comparable results on a reduced search space, but it is also possible to analyze the cost function by using a low fidelity method like the NNH. Overall, it is believed that the obtained sequences that have an objective value comparable to or better than the GTOC2 sequences are good alternatives for the GTOC2 sequences after a solution is obtained that matches all the constraints.

10. *Part of the reason why the GTOC2 problem is hard to solve is the fact that the assignment involves asteroids instead of, for example, planets.*
Another reason why the GTOC2 problem is a relatively complicated orbital analysis problem is because it has to rendezvous with asteroids instead of, for example, planets. Asteroid orbits are generally more exotically shaped than planetary orbits, which are nearly circular. To transfer between two very different orbits, as is the case for transfers between asteroid orbits, is much harder than to transfer between two concentric circular orbits, which planetary orbits approximately are. The exposin shape has difficulties to find trajectories that depart and arrive parallel to these exotic orbits, hence the velocity mismatches will be larger when trajectories between asteroids are analyzed opposed to when trajectories between planets analyzed.

11. *Penalties are required to eliminate unfeasible parts of the search space.*
Figure J.1 in Appendix J shows that the optimum solution moves from unrealistically low transfer times to more realistic time of flights. This is due to the fact that the GTOC2 objective is a function of the time of flight. Without applying penalties the most optimal transfer, according to the objective function, is almost a straight line from the starting body to the target body. Such a trajectory is unfeasible since it requires too much thrust and has huge velocity mismatches upon departure and arrival. Applying penalties on the departure and arrival velocity mismatches eliminates the existence of these unrealistic trajectories. The fact that the mass equivalent penalties allow the existence of unrealistic trajectories, indicates that the mass equivalent penalty is not strong enough. This is confirmed by the results of test 2, included in figure 7.48.

12. *Applying (stronger) penalties increases the contrast in the search space.*
In appendix J a partial visualization of the search space for two different penalty settings is shown. The images show that by applying penalties, the search space is contorted such that undesirable solutions have a worse objective value than they would have if only the objective function itself, without penalties, was evaluated. This increase in irregularity of the landscape of the search space makes it easier for the optimizers to identify good solutions. The drawback

is that also local minima tend to stand out more, which makes the landscape more treacherous for an optimizer to search. The chance that an optimizer gets stuck in a local optimum increases.

13. *Part of the difficulty of solving the GTOC2 assignment is the narrow timeframe in which participants have to provide a solution.*
This conclusion is not based on results presented in the report, but on the experience of the author. During the presented research, relatively simple tools were designed to solve the GTOC2 problem. Developing these tools already required several months. An overall observation of this research is that simple tools are not able to cope with the GTOC2 problem. Developing more advanced tools for orbital analysis requires time. Because only one month is available for generating solutions for the GTOC2 problem, developing these tools is not an option.

14. *The second leg is the hardest to fly with the available thrust.*
The acceleration profiles in the results chapter all show constraint violations for the second leg, indicating that the transfer departing from group 4 to group 2 or 3 is the most difficult transfer to complete using a low-thrust engine.

Answering the research question
The goal of the research presented in this report is to find an answer to the following research question:

What is the best way to handle the GTOC2 problem in order to find the optimal solution with the least amount of computational effort?

To answer this question the GTOC2 assignment was divided in 3 parts. The first part concerned the generation of promising asteroid sequences, the second part concerned a phasing assessment of the generated sequences, and the third part focused on finding the actual trajectory that matches the assignment constraints. Due to time constraints, only the first two parts were investigated in this report. Therefore, only a partial answer to the main research question can be formulated. In order to provide a complete answer to this question additional research needs to be conducted. Starting points for this research are provided in the recommendations. The answer consists of four parts:

- *Of the models and methods analyzed in this report, a cost function based on the velocity budget required to match all orbit elements of the departure orbit to the arrival orbit in combination with an NNH search algorithm provides the most promising asteroid sequences for the GTOC2 competition with the least amount of computational effort.*
This is mainly due to the fact that the NNH requires a low computational cost such that it can deal with the complete asteroid set, opposed to the B&B which can only handle reduced asteroid sets.
- *Results indicate that a B&B algorithm that is able to cope with the complete asteroid set will most likely provide better solutions at the expense of an increased computational effort.*
A straightforward B&B algorithm is not able to cope with the complete asteroid set. Applying a simple B&B algorithm to a subset of the asteroids provides results that are competitive to the NNH , but requires more computational effort. The B&B algorithm, however, outperforms the NNH on the same search

space. This indicates that developing a more advanced B&B algorithm that is able to cope with the complete asteroid set, will provide a significant increase in the quality of the results obtained by the NNH.

- *A model based on exponential sinusoids, in the form presented in this report, is not able to perform an accurate phasing assessment of an asteroid sequence.*
  An orbit model based on exponential sinusoids can be used to check if the sequences obtained by a NNH or B&B algorithm are indeed promising, but it is not able, in its current form, to give an accurate phasing assessment of the asteroid sequence or to provide bounds for more accurate methods.
- *An more accurate orbit model and stronger optimizer than the ones implemented in this research are required to match the GTOC2 constraints. Matching these constraints will require a large amount of computational effort.*
  Matching the velocity constraints proved to be one of the most dominating parts of the assignment. Although the exposin model developed in this report was intended to perform a preliminary phasing assessment (analyze the second part of the GTOC assignment), and not intended to provide an orbit that is matching all GTOC2 constraints (which is the third part of the GTOC assignment), it did show that the exposin model was far from accurate enough to perform such a task. In order to increase this accuracy a stronger and more accurate method is required. These kinds of methods require, by definition, a lot of computational effort.

8.2 Recommendations

The conclusions can be translated into an advise on how to tackle the GTOC2 problem. This section provide a list of recommended developments and a few practical tips for solving the GTOC2 problem.

- The implementation of a B&B algorithm or any other TSP solver able to cope with the TSP problem covering the complete asteroid set is believed to provide significant improvement in the quality of the asteroid sequences. Developing such a B&B algorithm is not straight forward and the use of of-the-shelf software should be considered. The most powerful TSP solver currently available is the Concorde solver [*Cook*, 2009]. This solver is able to cope with several thousands of vertices and might be too powerful for the GTOC2 problem, i.e., it might require more computational effort or implement an algorithm that is more advanced than strictly necessary, therefor alternatives should be investigated.
  A second aspect regarding the TSP solver that is interesting to investigate is the Time Dependent TSP or TDTSP. Because this research focused on finding the most simple algorithms that require the lowest amount of computational effort to solve the GTOC2 problem and the algorithms to solve the TDTSP generally are more complex, these algorithms have not been investigated. Implementing a time dependent model had both an advantage and a disadvantage. The advantage is that the obtained sequences most likely have better phasing characteristics. The disadvantage is that these algorithms require more computational effort and that no information is obtained about search space bounds that are required when implementing a more accurate model. Also it should be investigated if the transformation from the EGTSP to the TSP is still valid

when a time dependent model is used.
Another aspect that should be investigated further is the quality of the answer produced by the B&B algorithm. Due to a lack of time it has not been investigated if the B&B algorithm has found the global optimum when it is finished. The validation results did show that the B&B algorithm is able to find the global optimum for small problems.

- Alternative cost functions for asteroid selection should be investigated, based on, for example, angular momentum. Asteroid selection based on angular momentum has been performed by [*Heiligers*, 2008] for an asteroid sample return mission. This study, however, only applied heuristics and not a more sophisticated method like a B&B method.
- It should be attempted to develop a more accurate continuous model. Since the accuracy of the continuous method is limited by the accuracy of the exponential sinusoid, alternative models should be investigated. Alternative analytical models are inverse polynomials [*Wall and Conway*, 2009] or pseudospectral methods [*Vogeleer*, 2008], although the latter has trouble dealing with multiple revolutions.
  Introducing coast arcs should be investigated. A model that includes coast arcs should be able to align better with the departure and arrival orbits.
  Numerical models should also be considered because of their accuracy. This accuracy, however, comes at a higher computational cost. Current research at the Delft Aerospace Engineering Department suggests that the unified state model might reduce the computational cost (or increase the accuracy) of numerical based methods significantly [*Vittaldev*, 2010]. In the end this research will boil down to a trade off between the speed of shape based models and the accuracy of the numerical models. The added value of an accurate continuous method is not only a more reliable phasing assessment, but the results can also be used for the definition of the bounds for a very accurate method that is able to deal with the rigorous GTOC2 constraints.
- Search space reduction methods like, for example, the boxing principle described in [*Myatt et al.*, 2003] should be considered. Reducing the search space results in a more effective search. A method for assessing phasing characteristics, could benefit form this approach.
- Instead of using a separate discrete and continuous approach, a hybrid method should be analyzed. A nice starting point for this research is provided in [*Ross and D'Souza*, 2005]. This work introduces a pseudospectral knotting method for solving a problem consisting of both discrete and continuous variables. In this case the discrete variables are used for the asteroid selection and the continuous variables are used for trajectory modeling.
- The most important recommendation concerns the implementation of a strong (local) optimizer, in combination with a more accurate model, to be able to match the tough GTOC2 constraints. Only when the sequences are evaluated by such a method, accurate statements regarding the quality of the obtained sequences and overall solution method can be made. A tool that fulfills these requirements might, for example, be HQP developed by Rüdiger Franke. For further details about HQP see [*Franke*, 1998], or [*Gorter*, 2009]. ESA ESTEC is looking into the use of HQP for space mission analysis applications as well. At the time of writing, HQP has been successfully compiled, but no results obtained by HQP are available yet.

- It is recommended not to participate in the GTOC competition until a decent software toolbox is available. The time available to generate a solution for GTOC2 (one month) is too short to develop the required tools.
- To conclude, a practical recommendation regarding the handling of the GTOC2 problem in a master thesis framework is given. Solving the GTOC2 problem is, generally speaking, not a one-man project. A large number of specialized tools and a large dose of experience with those tools specifically, and in orbital mechanics generally, is required to successfully solve the GTOC2 problem. On top of that, solving GTOC2 requires knowledge about numerous topics, like mathematics, optimal control theory, numerical analysis and optimization. It is not realistic to expect expertise in all fields at a master thesis level. Therefore, if it is desired to solve the problem within a master thesis framework, it is advised to split the GTOC2 problem. A three-way division could, for example, be similar to the one made in this report:
  - 1. Asteroid selection and sequencing (discrete aspect)
  - 2. Phasing analysis (continuous aspect)
  - 3. Local optimization for elimination of constraint violations (implement HQP)

  A two-way division could, for example, be:
  - 1. Asteroids selection, sequencing and phasing analysis (hybrid approach)
  - 2. Local optimization for elimination of constraint violations (implement HQP)

Bibliography

Battin, R. H. (1999), *An Introduction to the Mathematics and Methods of Astrodynamics, Revised Edition*, AIAA, AIAA Education Series, ISBN 1-56347-342-9.

Behzad, A, and M Modarres (2002), A New Efficient Transformation of Generalized Traveling Salesman Problem into Traveling Salesman Problem, `http://www.ee.ucla.edu/~abehzad/ICSE02.pdf`, Last accessed: 19-09-2009.

Bondy, J.A., and U.S.R. Murty (2009), Graph theory with applications, `http://www.ecp6.jussieu.fr/pageperso/bondy/books/gtwa/gtwa.html`, Last accessed: 10-12-2009.

Byrd, R.H., J.C. Gilbert, and J. Nocedal (1998), A trust region method based on interior point techniques for nonlinear programming, *Mathematical Programming Servey A 89: 149-185 (2000)*, Published online October 18, 2000. Springerlink.

Cook, W. (2009), Concorde solver for tsp problems, `http://www.tsp.gatech.edu/concorde.html`, Last accessed: 16-01-2010.

ESA (2005), Gtoc site, `http://www.esa.int/gsp/ACT/mad/op/GTOC/index.htm`, Last accessed: 03-02-2010.

Evertsz, C. (2008), *GTOC2: Multiple asteroid rendezvous*, Master Thesis, Delft University of Technology, Department of Aerospace Engineering.

Franke, Rüdiger (1998), *Integrierte dynamische Modellierung und Optimierung von Systemen mit saisonaler Wrmespeicherung*, VDI Verlag GmbH, PhD thesis. Written in German.

Froushani, M A, and R M Yusuff (2009), Development of an Innovative Algorithm for the Traveling Salesman Problem (TSP), *European Journal of Scientific Research*, ISSN 1450-216X Vol. 29 No. 3 (2009), pp.349-359.

Goldberg, D.E. (1989), *Genetic Algorithms in Search, Optimization & Machine Learning*, Addison-Wesley Longman Publishing Co., ISBN 978-0201157673.

Gooding, R.H. (1990), A procedure for the solution of lambert's orbital boundary-value problem, Royal Aerospace Establishment, Farnborough, England.

Gorter, H. (2009), *Analysis of models and methods for solving multiple leg low-thrust trajectory problems*, Literature Survey, Delft University of Technology, Department of Aerospace Engineering.

Hartmann, A.K., and M. Weigt (2009), Phase transitions in combinatorial optimization problems, `http://arxiv.org/pdf/cond-mat/0602129`, Last accessed: 10-12-2009.

Heiligers, J. (2008), *Trajectory optimization for an asteroid/comet sample return mission*, Master Thesis, Delft University of Technology, Department of Aerospace Engineering.

Izzo, D. (2006), Lambert's problem for exponential sinusoids, *Journal of Guidance, Control, and Dynamics*, Vol. 29, No. 5, September-October 2006.

Izzo, D., T. Vinko, C. Bombardelli, S. Brendelberger, and S. Centuori (2007), Automated asteroid selection for a 'grand tour' mission, *57th International Astronautical Congress*, Paper IAC-07-C1.7.07.

Kirk, D.E. (1998), *Optimal Control Theory. An Introduction*, Dover Publications, Inc., ISBN 0-486-43484-2.

Lawler, E.L., and D.E. Wood (1966), Branch-and-bound methods: A survey, University of Michigan.

Munkres, J (1957), Algortihms for the assignment and transportation problems, *Journal by the Society for industrial and applied mathematics*, Vol 5. No. 1, March, 1957.

Myatt, D.R., V.M. Becerra, S.J. Nasuto, S.J. Bishop, and D. Izzo (2003), Advanced global optimisation for mission analysis and design, *Ariadna 03/4101*, Combined effort of ESA ACT and University of Reading.

NASA (2006), Gtoc2 press release, `http://www.nasa.gov/vision/universe/solarsystem/asteroidf-20070404.html`, Last accessed: 03-02-2010.

Pagano, A. (2009), Private communication.

Paulino, T. (2008), *Analytical representations for low-thrust trajectories*, Master Thesis, Delft University of technology, Department of Aerospace Engineering.

Petropoulos, A.E. (2006), Problem description for the 2nd global trajectory optimization competition, *Assignment handout*.

Petropoulos, A.E. (2007), Final rankings and brief descriptions of the returned solutions and methods used for the 2nd global trajectory optimisation competition.

Petropoulos, A.E., J.M. Longuski, and N.X. Vinh (2004), Shape-based algorithm for automated design of low-thrust, gravity-assist trajectories, *Journal of Spacecraft and Rockets*, Vol. 41, No. 5, September-October 2004.

Pilgrim, B (2009), Munkres' Assignment Algorithm, `http://csclab.murraystate.edu/bob.pilgrim/445/munkres.html`, Last accessed: 19-09-2009.

Ross, I.M., and C.N. D'Souza (2005), Hybrid optimal control framework for mission planning, *Journal of Guidance, Control, and Dynamics*, Vol. 28, No. 4, July-August 2005.

Sidi, M.J. (2006), *Spacecraft Dynamics & Control*, Cambridge University Press, ISBN-13: 978-0-521-55072-7.

Visser, H.G. (2000), *Aircraft Performance Optimization - Part 1*, Delft University of Technology, Department of Aerospace Engineering, Lecture notes ae4-212.

Vittaldev, V. (2010), Private communication.

Vogeleer, B (2008), *Automatic and fast generation of sub optimal low thrust trajectories using a pseudo-spectral method*, Master Thesis, Delft University of Technology, Department of Aerospace Engineering.

Wakker, K.F. (1997), *Astrodynamics I*, Delft University of Technology, Department of Aerospace Engineering, Lecture notes ae4-873 (partly in Dutch).

Wall, B.J., and B.A. Conway (2009), Shape-based approach to low-thrust rendezvous trajectory design, *Journal of Guidance, Control, and Dynamics*, Vol. 32, No. 1, January-February 2009.

Winston, W.J. (2004), *Operations Research, Applications and Algorithms*, Duxbury, fourth edition, ISBN: 0-534-42362-0.

Appendix A

GTOC2 Results

This appendix contains the results of the GTOC 2 competition as presented in [*Petropoulos*, 2007].

Rank	Team		J (kg/yr)
1	4:	Politecnico di Torino	98.64
2	13:	Moscow Aviation Institute, and Khrunichev State Research and Production Space Center	87.93
3	10:	Advanced Concepts Team, ESA	87.05
4	15:	Centre National d'Etudes Spatiales (CNES)	85.43
5	1:	GMV Aerospace and Defence	85.28
6	2:	German Aerospace Center (DLR)	84.48
7	9:	Politecnico di Milano	82.48
8	19:	Alcatel Alenia Space	76.37
9	14:	Moscow State University	75.08
10	7:	Tsinghua University	56.87
11	18:	Carnegie Mellon University, J.J. Arrieta-Camacho	27.94
–	17:	University of Glasgow, *et al.*	73.87[a]
–	21:	Technical University of Delft and Dutch Space	15.95[b]
–	23:	Facultes Universitaires Notre-Dame de la Paix (FUNDP)	–[c]
–	26:	University of Maribor, Bostjan Eferl	–[d]

[a] Significant position and velocity violations at the asteroids and Earth

[b] Significant position and velocity violations at the asteroids and Earth, and flight time limit violation

[c] Only one leg computed (Earth to Group 4)

[d] Only a proposed method described, no solution computed

Figure A.1 Overview of GTOC results: rankings with corresponding objective values.

Rank	Team	$v_{\infty L}$ (km/s)	TOF (yrs)	m_f (kg)	Asteroid sequence (SPKID) and group numbers
1	4	3.50	9.106	898.2	3258076 (4) 2000060 (3) 2000058 (2) 2002959 (1)
2	13	3.50	10.394	913.9	3250293 (4) 2000149 (3) 2000569 (2) 2002483 (1)
3	10	2.58	9.523	829.0	3170221 (4) 2000574 (3) 2000209 (2) 2011542 (1)
4	15	2.45	9.777	835.2	3170221 (4) 2001990 (3) 2000240 (2) 2001754 (1)
5	1	2.18	10.096	861.0	3017309 (4) 2000443 (3) 2000490 (2) 2001345 (1)
6	2	3.23	10.170	859.1	3250293 (4) 2000027 (3) 2000110 (2) 2001038 (1)
7	9	3.50	10.796	890.5	3288933 (4) 2001707 (3) 2000047 (2) 2014569 (1)
8	19	3.50	10.816	826.1	3329255 (4) 2000232 (2) 2000807 (3) 2001754 (1)
9	14	2.46	11.509	864.1	3170221 (4) 2000043 (3) 2000074 (2) 2002483 (1)
10	7	3.50	12.941	735.9	3250293 (4) 2000149 (3) 2000224 (2) 2009661 (1)
11	18	3.50	19.195	536.3	3343104 (4) 2000169 (3) 2000075 (2) 2000659 (1)
–	17	–	12.991	959.6	3250293 (4) 2000443 (3) 2000058 (2) 2002959 (1)
–	21	–	32.25	514.3	3170221 (4) 2001314 (3) 2000395 (2) 2002483 (1)
–	23	–	–	–	3177202 (4)

Figure A.2 Overview of GTOC results: departure velocity ($v_\infty L$), Time of flight (TOF), final mass(m_f) and asteroid sequences.

Rank	Team	Earth launch, and asteroid arrival and departure dates (MJD)						
1	4	59870	60283	60373	61979	62069	62647	62737	63196
2	13	62866	63028	63118	64907	64997	65712	65802	66662
3	10	57372	57747	57849	59485	59587	60034	60139	60851
4	15	59574	60104	60194	61749	61839	62306	62396	63145
5	1	61073	61258	61348	63178	63268	64011	64101	64761
6	2	58021	58379	58469	60236	60326	60872	60963	61735
7	9	62201	62454	62544	64444	64534	65394	65484	66144
8	19	59418	59610	59700	61603	61693	62288	62378	63369
9	14	57561	57987	58106	59627	59717	60935	61025	61764
10	7	58448	58752	58846	60826	61048	61991	62232	63175
11	18	58246	59125	59215	61731	61821	62552	62642	65257
–	17	58460	58794	58884	60623	60714	62303	62393	63204
–	21	57755	58659	58749	61861	62190	64925	65200	69534
–	23	57052	59226						

Figure A.3 Overview of GTOC results: departure and arrival dates.

Appendix B

Validation Results for AST

This appendix includes the output as generated by the B&B algorithm for the problems shown in figures 3.4 and 4.11. The obtained solution paths for each subproblem are represented by numbers, and each number corresponds to a city (i.e. where 0 indicates city A, 1 indicates B, etc...). First, the output for the problem of figure 3.4 is given.

The following pages include the output of the B&B algorithm for the problem in figure 4.11.

Appendix C

Extensive Cost Matrix Reduction Results

In this appendix the results of the cost matrix reduction procedure as described in section 4.1.3 are presented. For each of the three cost functions a figure is included. The figure states the results for the matrix dimension, the number of matching asteroids with those selected by the GTOC2 participants and all the matching asteroid IDs, for a varying number of best transfers selected form the complete cost matrix.

Cost function based on DV						
Nr. of best transfers	2	3	4	5	6	7
Size reduced cost matrix	30x30	47x47	63x63	74x74	87x87	98x98
Nr. of matching asterids	5	8	12	13	15	15
Matching asteroid Ids	2001038	2000074	2000027	2000027	2000027	2000027
	2001345	2001038	2000058	2000058	2000058	2000058
	2002483	2001345	2000074	2000074	2000074	2000074
	2009661	2002483	2000075	2000075	2000075	2000075
	3017309	2002959	2000659	2000110	2000110	2000110
		2009661	2001038	2000659	2000149	2000149
		2011542	2001345	2001038	2000659	2000659
		3017309	2002483	2001345	2001038	2001038
			2002959	2002483	2001345	2001345
			2009661	2002959	2001754	2001754
			2011542	2009661	2002483	2002483
			3017309	2011542	2002959	2002959
				3017309	2009661	2009661
					2011542	2011542
					3017309	3017309

Figure C.1 Reduction results for the cost function based on ΔV.

Cost function based on Energy						
Nr. of best transfers	2	3	4	5	6	7
Size reduced cost matrix	25x25	46x46	60x60	73x73	89x89	104x104
Nr. of matching asterids	4	6	7	8	11	12
Matching asteroid Ids	2000149	2000149	2000149	2000149	2000027	2000027
	2001345	2001038	2001038	2000232	2000075	2000075
	2009661	2001345	2001345	2001038	2000149	2000149
	2011542	2009661	2001754	2001345	2000232	2000232
		2011542	2009661	2001754	2001038	2001038
		3170221	2011542	2009661	2001345	2001345
			3170221	2011542	2001754	2001754
				3170221	2009661	2002959
					2011542	2009661
					3170221	2011542
					3258076	3170221
						3258076

Figure C.2 Reduction results for the cost function based on energy.

Cost function based on ESA						
Nr. of best transfers	2	3	4	5	6	7
Size reduced cost matrix	28x28	42x42	60x60	75x75	90x90	102x102
Nr. of matching asterids	3	8	10	10	12	12
Matching asteroid Ids	2001754	2000075	2000043	2000043	2000043	2000043
	2009661	2001345	2000075	2000075	2000074	2000074
	2011542	2001754	2001038	2001038	2000075	2000075
		2002959	2001345	2001345	2001038	2001038
		2009661	2001754	2001754	2001345	2001345
		2011542	2002959	2002959	2001754	2001754
		3017309	2009661	2009661	2002483	2002483
		3170221	2011542	2011542	2002959	2002959
			3017309	3017309	2009661	2009661
			3170221	3170221	2011542	2011542
					3017309	3017309
					3170221	3170221

Figure C.3 Reduction results for the cost function as implemented by ESA during the GTOC2 competition.

Appendix D

Extensive AST Results

This appendix contains the results as produced by AST for the different cost functions presented in section 4.1.1. The first cost function is based on the ΔV required to transfer from the orbit of the departing asteroid to the orbit of the arrival asteroid. The second cost function is based on the energy required to transfer from the orbit of the departure asteroid to the orbit of the arrival asteroid. The last cost function is the same as was used by ESA during GTOC2. Some comments regarding the results should be made.

For all cost functions two tables have been included. The first table contains the sequence cost as obtained by the AST, the asteroid sequence in GTOC2 ID numbers and the corresponding group order. The second table states the individual transfer costs.

D.1 Cost Function Based on ΔV

Cost	GTOC ID 1	GTOC ID 2	GTOC ID 3	GTOC ID 4	GTOC ID 5	Group order
22.92	1	3072273	2001621	2000206	2002959	0 4 3 2 1
24.48	1	3170221	2012746	2000206	2002959	0 4 3 2 1
24.58	1	3072273	2001621	2000558	2001345	0 4 3 2 1
25.19	1	3170221	2012746	2000558	2001345	0 4 3 2 1
27.00	1	3170221	2012746	2000558	2004754	0 4 3 2 1
27.83	1	3170221	2012746	2000010	2005209	0 4 3 2 1
28.35	1	3170221	2000010	2000975	2011542	0 4 2 3 1
30.79	1	3170221	2012746	2011542	2000010	0 4 3 1 2
39.32	1	3170221	2011542	2000010	2000008	0 4 1 2 3
41.08	1	2002959	2000010	2000158	3297182	0 1 2 3 4
41.38	1	2002959	2000010	2000208	3297182	0 1 2 3 4
44.04	1	2002959	2000010	2000158	2002062	0 1 2 3 4
45.78	1	2002959	2000010	2000208	2002062	0 1 2 3 4
48.16	1	2002959	2000010	2000824	2002062	0 1 2 3 4
48.89	1	2002959	2000010	2001532	2002062	0 1 2 3 4
49.05	1	2002959	2000010	2002411	2002062	0 1 2 3 4
49.60	1	2000010	2005209	2000158	2002062	0 2 1 3 4
49.72	1	2000010	2005209	2001532	2002062	0 2 1 3 4
50.18	1	2000010	2004754	2000824	2002062	0 2 1 3 4
50.34	1	2000010	2000158	2011351	2002062	0 2 3 1 4
50.41	1	2000010	2011351	2000378	2002062	0 2 1 3 4
50.59	1	2000534	2000010	2011351	2002062	0 3 2 1 4
51.50	1	2000010	2011351	2000824	2002062	0 2 1 3 4
51.69	1	2001621	2000010	2011351	2002062	0 3 2 1 4
51.82	1	2000010	2000975	2011542	2002062	0 2 3 1 4
54.43	1	2000010	2011542	2001532	2002062	0 2 1 3 4
55.99	1	2000010	2011542	2002411	2002062	0 2 1 3 4
59.04	1	2011542	2000010	2002411	2002062	0 1 2 3 4
60.93	1	2000010	2011542	2012746	2002062	0 2 1 3 4
61.22	1	2000008	2000010	2011542	2002062	0 3 2 1 4
64.14	1	2011542	2000010	2000008	2002062	0 1 2 3 4
65.42	1	2002062	2000040	2000010	2011542	0 4 3 2 1
65.49	1	2002062	2000534	2000010	2011542	0 4 3 2 1
67.39	1	2002062	2002411	2011542	2000010	0 4 3 1 2
68.23	1	2002062	2000008	2000010	2011542	0 4 3 2 1
69.92	1	2002062	2000008	2011542	2000010	0 4 3 1 2

Figure D.1 B&B results for the cost function based on ΔV: asteroid and group sequences.

Cost	Cost Transfer 1	Cost Transfer 2	Cost Transfer 3	Cost Transfer 4
22.92	3.34	11.06	3.64	4.88
24.48	3.28	9.95	6.37	4.88
24.58	3.34	11.06	5.85	4.33
25.19	3.28	9.95	7.63	4.33
27.00	3.28	9.95	7.63	6.14
27.83	3.28	9.95	7.52	7.08
28.35	3.28	16.83	3.92	4.32
30.79	3.28	9.95	9.98	7.58
39.32	3.28	20.96	7.58	7.50
41.08	16.52	5.13	3.58	15.85
41.38	16.52	5.13	3.38	16.35
44.04	16.52	5.13	3.58	18.82
45.78	16.52	5.13	3.38	20.75
48.16	16.52	5.13	8.96	17.55
48.89	16.52	5.13	4.65	22.59
49.05	16.52	5.13	9.26	18.13
49.60	15.31	7.08	8.41	18.82
49.72	15.31	7.08	4.76	22.59
50.18	15.31	8.10	9.22	17.55
50.34	15.31	3.58	8.00	23.45
50.41	15.31	8.12	6.84	20.14
50.59	14.13	4.90	8.12	23.45
51.50	15.31	8.12	10.52	17.55
51.69	12.75	7.37	8.12	23.45
51.82	15.31	3.92	4.32	28.27
54.43	15.31	11.71	4.82	22.59
55.99	15.31	11.71	10.84	18.13
59.04	24.07	7.58	9.26	18.13
60.93	15.31	11.71	10.10	23.81
61.22	12.57	8.68	11.71	28.27
64.14	24.07	7.58	7.50	24.99
65.42	25.48	20.83	7.40	11.71
65.49	25.48	23.41	4.90	11.71
67.39	25.48	22.18	12.16	7.58
68.23	25.48	22.37	8.68	11.71
69.92	25.48	22.37	14.50	7.58

Figure D.2 B&B results for the cost function based on ΔV: costs per transfer.

D.2 Cost Function Based on Energy

Cost	GTOC ID 1	GTOC ID 2	GTOC ID 3	GTOC ID 4	GTOC ID 5	Group order
420.6	1	3167353	2000975	2000104	2011542	0 4 3 2 1
437.8	1	3167353	2000975	2002407	2011542	0 4 3 2 1
454.3	1	3339082	2000016	2000245	2011542	0 4 2 3 1
456.2	1	3167353	2000104	2011542	2000642	0 4 2 1 3
465.0	1	3167353	2000975	2011542	2000121	0 4 3 1 2
473.5	1	3167353	2000104	2011542	2001087	0 4 2 1 3
479.3	1	3339082	2000016	2011542	2000642	0 4 2 1 3
496.5	1	3339082	2000016	2011542	2001087	0 4 2 1 3
512.7	1	3339082	2001621	2011542	2000121	0 4 3 1 2
521.2	1	3339082	2001621	2011542	2000334	0 4 3 1 2
522.7	1	3339082	2001621	2011542	2000566	0 4 3 1 2
537.6	1	3339082	2000016	2011542	2001723	0 4 2 1 3
544.1	1	3339082	2000016	2011542	2000028	0 4 2 1 3
630.8	1	3350633	2000021	2011542	2000642	0 4 2 1 3
645.3	1	3350633	2000104	2011542	2000642	0 4 2 1 3
648.1	1	3350633	2000021	2011542	2001087	0 4 2 1 3
662.5	1	3350633	2000104	2011542	2001087	0 4 2 1 3
669.7	1	3350633	2000566	2011542	2001087	0 4 2 1 3
689.2	1	3350633	2000021	2011542	2001723	0 4 2 1 3
695.7	1	3350633	2000021	2011542	2000028	0 4 2 1 3
710.1	1	3350633	2000104	2011542	2000028	0 4 2 1 3
717.3	1	3350633	2000566	2011542	2000028	0 4 2 1 3
744.3	1	3350633	2000016	2011542	2000028	0 4 2 1 3
810.2	1	2000149	2000104	2011542	2002062	0 3 2 1 4
815.2	1	2000149	2002407	2011542	2002062	0 3 2 1 4
828.2	1	2000149	2000016	2011542	2002062	0 3 2 1 4
829.8	1	2000296	2000104	2011542	2002062	0 3 2 1 4
835.2	1	2000975	2000104	2011542	2002062	0 3 2 1 4
844.9	1	2000975	2011542	2000413	2002062	0 3 1 2 4
852.4	1	2000975	2002407	2011542	2002062	0 3 2 1 4
857.2	1	2001621	2000016	2011542	2002062	0 3 2 1 4
890.9	1	2000104	2011542	2001723	2002062	0 2 1 3 4
891.3	1	2000104	2011542	2000028	2002062	0 2 1 3 4
893.6	1	2002407	2011542	2000028	2002062	0 2 1 3 4
902.5	1	2000016	2011542	2000028	2002062	0 2 1 3 4
995.1	1	2002062	2000413	2011542	2000028	0 4 2 1 3
1060.0	1	2002062	2000521	2011542	2000028	0 4 2 1 3
1066.0	1	2002062	2000776	2011542	2000028	0 4 2 1 3
1179.0	1	2002062	2000028	2011542	2002407	0 4 3 1 2
1206.0	1	2002062	2000028	2011542	2000016	0 4 3 1 2

Figure D.3 B&B results for the cost function based on energy: asteroid and group sequences.

Cost	Cost Transfer 1	Cost Transfer 2	Cost Transfer 3	Cost Transfer 4
420.60	53.33	294.20	17.94	55.15
437.80	53.33	294.20	18.72	71.59
454.30	38.30	312.00	44.35	59.72
456.20	53.33	311.70	55.15	36.06
465.00	53.33	294.20	74.38	43.14
473.50	53.33	311.70	55.15	53.30
479.30	38.30	312.00	92.94	36.06
496.50	38.30	312.00	92.94	53.30
512.70	38.30	270.60	160.70	43.14
521.20	38.30	270.60	160.70	51.61
522.70	38.30	270.60	160.70	53.08
537.60	38.30	312.00	92.94	94.37
544.10	38.30	312.00	92.94	10.90
630.80	125.90	352.20	116.70	36.06
645.30	125.90	428.20	55.15	36.06
648.10	125.90	352.20	116.70	53.30
662.50	125.90	428.20	55.15	53.30
669.70	125.90	437.50	53.05	53.30
689.20	125.90	352.20	116.70	94.37
695.70	125.90	352.20	116.70	100.90
710.10	125.90	428.20	55.15	100.90
717.30	125.90	437.50	53.05	100.90
744.30	125.90	424.60	92.94	100.90
810.20	244.10	88.68	55.15	422.30
815.20	244.10	77.15	71.59	422.30
828.20	244.10	68.82	92.94	422.30
829.80	270.70	81.71	55.15	422.30
835.20	339.90	17.94	55.15	422.30
844.90	339.90	74.38	133.20	297.50
852.40	339.90	18.72	71.59	422.30
857.20	282.30	59.66	92.94	422.30
890.90	359.30	55.15	94.37	382.10
891.30	359.30	55.15	100.90	375.90
893.60	345.10	71.59	100.90	375.90
902.50	332.70	92.94	100.90	375.90
995.10	261.70	315.40	317.10	100.90
1060.00	261.70	548.60	148.30	100.90
1066.00	261.70	476.10	227.70	100.90
1179.00	261.70	677.50	168.50	71.18
1206.00	261.70	677.50	168.50	98.20

Figure D.4 B&B results for the cost function based on energy: costs per transfer.

D.3 Cost Function According to ESA Approach

Cost	GTOC ID 1	GTOC ID 2	GTOC ID 3	GTOC ID 4	GTOC ID 5	Group order
15.98	1	3167353	2000075	2000642	2011542	0 4 2 3 1
15.98	1	3167353	2000075	2000642	2011542	0 4 2 3 1
16.32	1	3347493	2000075	2000642	2011542	0 4 2 3 1
16.56	1	3167353	2002407	2000642	2011542	0 4 2 3 1
16.56	1	3167353	2002407	2000642	2011542	0 4 2 3 1
16.75	1	3347493	2002407	2000642	2011542	0 4 2 3 1
16.84	1	3170221	2000937	2002407	2011542	0 4 3 2 1
16.87	1	3167353	2001047	2000021	2011542	0 4 3 2 1
16.93	1	3170221	2012746	2002407	2011542	0 4 3 2 1
17.11	1	3167353	2000075	2011542	2000642	0 4 2 1 3
17.11	1	3167353	2000075	2011542	2000642	0 4 2 1 3
17.44	1	3167353	2011542	2000245	2000086	0 4 1 3 2
17.48	1	3167353	2002407	2011542	2000642	0 4 2 1 3
17.48	1	3167353	2002407	2011542	2000642	0 4 2 1 3
17.66	1	3347493	2002407	2011542	2000642	0 4 2 1 3
18.21	1	3167353	2002407	2011542	2001087	0 4 2 1 3
18.21	1	3167353	2002407	2011542	2001087	0 4 2 1 3
18.40	1	3347493	2002407	2011542	2001087	0 4 2 1 3
18.56	1	3167353	2011542	2000642	2000010	0 4 1 3 2
18.68	1	3167353	2000010	2011542	2000642	0 4 2 1 3
18.69	1	3170221	2000010	2011542	2000642	0 4 2 1 3
18.69	1	3170221	2000010	2011542	2000642	0 4 2 1 3
18.74	1	3347493	2000010	2011542	2000642	0 4 2 1 3
19.30	1	3167353	2001047	2011542	2000010	0 4 3 1 2
19.41	1	3167353	2001087	2011542	2000010	0 4 3 1 2
19.42	1	3167353	2000010	2011542	2001087	0 4 2 1 3
19.42	1	3167353	2000010	2011542	2001087	0 4 2 1 3
19.43	1	3170221	2000010	2011542	2001087	0 4 2 1 3
19.48	1	3347493	2000010	2011542	2001087	0 4 2 1 3
19.58	1	3170221	2012746	2011542	2000010	0 4 3 1 2
19.89	1	3347493	2012746	2011542	2000010	0 4 3 1 2
19.93	1	3167353	2000008	2011542	2000010	0 4 3 1 2
20.15	1	3347493	2000008	2011542	2000010	0 4 3 1 2
25.58	1	2003362	2000008	2011542	2000010	0 4 3 1 2

Figure D.5 B&B results for the cost function based on ESA: asteroid and group sequences.

Cost	Cost Transfer 1	Cost Transfer 2	Cost Transfer 3	Cost Transfer 4
15.98	2.40	9.88	2.03	1.66
15.98	2.40	9.88	2.03	1.66
16.32	2.56	10.06	2.03	1.66
16.56	2.40	10.75	1.75	1.66
16.56	2.40	10.75	1.75	1.66
16.75	2.56	10.77	1.75	1.66
16.84	2.31	9.03	2.83	2.67
16.87	2.40	9.14	1.20	4.14
16.93	2.31	9.12	2.83	2.67
17.11	2.40	9.88	3.17	1.66
17.11	2.40	9.88	3.17	1.66
17.44	2.40	12.21	2.26	0.57
17.48	2.40	10.75	2.67	1.66
17.48	2.40	10.75	2.67	1.66
17.66	2.56	10.77	2.67	1.66
18.21	2.40	10.75	2.67	2.40
18.21	2.40	10.75	2.67	2.40
18.40	2.56	10.77	2.67	2.40
18.56	2.40	12.21	1.66	2.29
18.68	2.40	11.65	2.97	1.66
18.69	2.31	11.75	2.97	1.66
18.69	2.31	11.75	2.97	1.66
18.74	2.56	11.55	2.97	1.66
19.30	2.40	9.14	4.79	2.97
19.41	2.40	11.64	2.40	2.97
19.42	2.40	11.65	2.97	2.40
19.42	2.40	11.65	2.97	2.40
19.43	2.31	11.75	2.97	2.40
19.48	2.56	11.55	2.97	2.40
19.58	2.31	9.12	5.18	2.97
19.89	2.56	9.18	5.18	2.97
19.93	2.40	9.26	5.31	2.97
20.15	2.56	9.32	5.31	2.97
25.58	7.77	9.54	5.31	2.97

Figure D.6 B&B results for the cost function based on ESA: costs per transfer.

Appendix E

Extensive NNH Results

This appendix contains the results of the NNH algorithm for each of the three cost functions discussed in section 4.1.1. For each cost function two tables are included. The first presents the best 30 NNH sequences with corresponding costs (excluding the return to Earth) when the NNH is applied to the reduced cost matrix. The second table presents the best 30 NNH sequences with corresponding costs when the NNH is applied to the total cost matrix describing complete set of asteroids. Note that round off errors might be present.

E.1 Cost Function Based on ΔV

Cost	GTOC ID 1	GTOC ID 2	GTOC ID 3	GTOC ID 4	GTOC ID 5	Group order
25.59	1	3064315	2000421	3297182	2011351	4321
28.02	2001723	2002223	2012746	1	3064315	23104
28.21	2000642	2000975	2012746	1	3064315	32104
28.44	2000975	2000642	2000010	1	3064315	23104
28.73	2000519	2000138	2000021	1	3064315	23104
29.05	2011542	2000642	2000010	1	3064315	23104
29.27	3072273	2000558	2000010	1	3064315	23104
29.47	3297182	2000642	2000010	1	3064315	23104
29.68	2005209	3072273	2000010	1	3064315	32104
29.68	2000558	3072273	2000010	1	3064315	32104
30.48	2002483	2000138	2000021	1	3064315	23104
32.34	2000107	2000558	2000010	1	3064315	23104
32.91	2000137	2000138	2000021	1	3064315	23104
33.16	2000334	2000138	2000021	1	3064315	23104
33.61	2000024	2002959	2012746	1	3064315	32104
34.01	2002959	2000024	2012746	1	3064315	23104
34.46	2000010	2000558	3072273	1	3064315	13204
37.27	2002223	2001723	2009661	3064315	1	32140
37.27	3064315	1	2002223	2001723	2009661	40321
37.71	2001047	2011542	2000642	1	3064315	12304
37.91	2004754	2000107	2000558	1	3064315	12304
37.92	2000195	2000138	2000021	1	3064315	23104
38.59	3114017	1	2002223	2001723	2009661	40321
38.76	2000429	2001723	2009661	3064315	1	32140
38.79	2000535	2001723	2009661	3064315	1	32140
39.06	3005821	2001038	2000107	1	3064315	31204
39.24	2012746	3046844	2005209	3114017	1	12340
39.82	2001345	2004754	2000558	1	3064315	21304
39.87	2000021	3046844	2005209	3114017	1	12340
40.19	2000138	2000519	2000208	3064315	1	32140

Figure E.1 NNH results when applied to the reduced cost matrix, for the cost function based on ΔV: asteroid sequences.

Cost	GTOC ID 1	GTOC ID 2	GTOC ID 3	GTOC ID 4	GTOC ID 5	Group order
21.28	1	3339082	2001830	2000206	2002959	4321
21.28	2001830	2000206	2002959	1	3339082	32104
22.91	2000851	2000206	2002959	1	3339082	32104
23.25	2000443	2000034	2002207	1	3339082	32104
23.45	2000534	2000206	2002959	1	3339082	32104
23.46	2000058	2000533	2002207	1	3339082	23104
23.63	2000673	2000206	2002959	1	3339082	32104
23.65	2000548	2000206	2002959	1	3339082	32104
24.06	2000182	2000206	2002959	1	3339082	32104
24.13	2001350	2000206	2002959	1	3339082	32104
24.29	2000540	2000034	2002207	1	3339082	32104
24.43	2001245	2000206	2002959	1	3339082	32104
24.44	2000124	2000058	2002207	1	3339082	32104
24.70	2000215	2000206	2002959	1	3339082	32104
25.10	2000163	2001052	2002959	1	3339082	23104
25.10	2000962	2000206	2002959	1	3339082	32104
25.13	2000462	2000206	2002959	1	3339082	32104
25.36	2000189	2000168	2002207	1	3339082	32104
25.37	2000027	2000206	2002959	1	3339082	32104
25.47	2001336	2000206	2002959	1	3339082	32104
25.49	2000034	2000032	2002207	1	3339082	23104
25.52	2000811	2000206	2002959	1	3339082	32104
25.78	2000005	2000058	2002207	1	3339082	32104
25.96	2000060	2000206	2002959	1	3339082	32104
26.02	2000755	2000533	2002207	1	3339082	23104
26.02	2002357	2000334	2000811	1	3339082	12304
26.02	2000872	2000533	2002207	1	3339082	23104
26.07	2001636	2000206	2002959	1	3339082	32104
26.38	2000103	2000206	2002959	1	3339082	32104
26.49	2000169	2000224	2002959	1	3339082	32104

Figure E.2 NNH results when applied to the total asteroid set, for the cost function based on ΔV: transfer costs.

E.2 Cost Function Based on Energy

Cost	GTOC ID 1	GTOC ID 2	GTOC ID 3	GTOC ID 4	GTOC ID 5	Group order
465.89	1	3072273	2000197	3114017	2001621	4321
541.92	2004063	2000245	2011542	2100004	1	43120
656.82	2003362	2000245	2011542	2100004	1	43120
707.20	2000149	2000196	2001621	2000346	1	42130
740.93	2000521	2001345	2011542	2004063	1	32140
756.06	2000413	1	2000521	2001345	2011542	40321
757.16	2000642	3350633	2011542	2004063	1	32140
759.97	3177176	1	2000521	2001345	2011542	40321
764.39	2000207	3114017	2001621	2000149	1	32140
768.17	2000489	2000121	2011542	2004063	1	23140
778.94	3114017	2000121	2011542	2004063	1	23140
779.85	2000135	2000489	2011542	2004063	1	32140
780.71	2002207	1	2000521	2001345	2011542	40321
781.13	2000334	2000642	2011542	2004063	1	23140
781.15	2000111	1	2000521	2001345	2011542	40321
784.72	3167353	2000642	2011542	2004063	1	23140
786.34	2001345	2000121	2011542	2004063	1	23140
789.24	2000296	1	2000521	2001345	2011542	40321
790.04	2001723	2000016	2000558	2000296	1	21340
790.53	2000776	2000566	2000016	2000296	1	23140
790.72	2068347	1	2000521	2001345	2011542	40321
792.05	2000121	2000489	2011542	2004063	1	32140
793.98	2000197	3114017	2001621	2000149	1	32140
795.12	3072273	1	2000521	2001345	2011542	40321
795.66	3350633	2000642	2011542	2004063	1	23140
815.19	2001087	2001345	2011542	2004063	1	32140
820.86	3339082	2000975	2001038	3177176	1	23140
821.62	2002062	2000021	2001087	2001345	1	41320
832.43	2000086	2001754	2000206	2000111	1	32140
842.26	3072196	2000975	2001038	3177176	1	23140

Figure E.3 NNH results when applied to the reduced cost matrix, for the cost function based on energy: asteroid sequences.

Cost	GTOC ID 1	GTOC ID 2	GTOC ID 3	GTOC ID 4	GTOC ID 5	Group order
451.28	1	3250293	2000149	2000207	2011542	4321
497.92	3064315	2001078	2000535	2100004	1	43210
531.50	3330538	2000230	2000156	3081550	1	43210
537.54	3102762	2001504	2000410	2100004	1	43210
540.83	3102787	2000453	2000207	2011542	1	43210
545.49	3250195	2001047	2000021	2002959	1	43210
562.07	3017060	2001717	2000224	2011542	1	43210
565.01	3046648	2000115	2000054	3046844	1	43210
569.45	3266035	2000487	2000559	2100004	1	43210
570.15	3092347	2000161	2001500	2011542	1	42310
571.82	3072196	2000134	2000101	2014569	1	42310
576.17	3057545	2000963	2000481	2100004	1	43210
577.93	3176187	2000574	2000224	2011542	1	43210
578.80	3297182	2000341	2000207	2011542	1	43210
584.62	3285073	2000115	2000054	3046844	1	43210
587.32	3005972	2000963	2000481	2100004	1	43210
593.58	3092114	2000516	2000174	3046844	1	42310
594.61	3137844	2001500	2000161	2011542	1	43210
596.02	3180192	2000345	2000080	2003134	1	42310
597.81	3154520	2000230	2000156	3081550	1	43210
603.17	2005590	2000216	2000968	2006984	1	42310
606.72	3177197	2001418	2000224	2011542	1	43210
615.54	3092390	2001500	2000161	2011542	1	43210
620.04	3182187	2001504	2000410	2100004	1	43210
620.66	3249980	2000516	2000174	3046844	1	42310
620.98	3257077	2000258	2000393	2006984	1	43210
623.21	3005821	2000200	2000123	2003134	1	42310
624.42	3092245	2000565	2000712	3081550	1	43210
624.78	3297356	2000674	2000022	2100004	1	43210
625.63	3010201	2000897	2000405	3081550	1	43210

Figure E.4 NNH results when applied to the total asteroid set, for the cost function based on energy: transfer costs.

E.3 Cost Function According to ESA Approach

Cost	GTOC ID 1	GTOC ID 2	GTOC ID 3	GTOC ID 4	GTOC ID 5	Group order
17.10	1	3170221	2000104	2000489	2011542	4321
24.97	2000010	3072273	2000937	2001087	1	32140
25.08	2000121	3350633	2000937	2001087	1	32140
25.46	2000009	3017309	2000937	2001087	1	32140
25.63	2000104	2000489	2011542	2001087	1	32140
25.63	2001087	1	2000104	2000489	2011542	40321
25.79	3072273	2000010	2000937	2001087	1	23140
25.80	2001665	3017309	2000937	2001087	1	32140
25.82	3046844	3017309	2000937	2001087	1	32140
25.85	3350633	2000121	2009661	2001087	1	23140
25.94	2000075	2001038	2000937	2001087	1	32140
25.98	2105140	3017309	2000937	2001087	1	32140
25.99	2000228	2000086	3102787	2000135	1	42310
26.03	3167353	2000121	2009661	2001087	1	23140
26.03	2001362	1	2000104	2000489	2011542	40321
26.07	2000043	1	2000104	2000489	2011542	40321
26.08	2001723	2000121	2009661	2001087	1	23140
26.10	3017309	2105140	2000937	2001087	1	23140
26.12	3005964	1	2000104	2000489	2011542	40321
26.18	3092324	1	2000104	2000489	2011542	40321
26.19	2000937	2001723	2000121	2001087	1	12340
26.21	3184475	2002959	2009661	2001087	1	32140
26.22	3347493	1	2000104	2000489	2011542	40321
26.26	2000498	2001345	3169278	2001087	1	32140
26.26	2000196	2000121	2009661	2001087	1	23140
26.26	3064315	2001345	3169278	2001087	1	32140
26.29	2001754	2000121	2009661	2001087	1	23140
26.34	2003362	2000021	3167353	2000121	1	41230
26.44	2000016	2000489	2011542	2001087	1	32140
26.47	3092377	2000489	2011542	2001087	1	32140

Figure E.5 NNH results when applied to the reduced cost matrix, for the cost function based on ESA: asteroid sequences.

Cost	GTOC ID 1	GTOC ID 2	GTOC ID 3	GTOC ID 4	GTOC ID 5	Group order
15.03	1	3339082	2001055	2000163	2002959	4321
21.05	2003362	2100004	2000413	2000532	1	41230
21.25	2096590	2100004	2000413	2000532	1	41230
21.92	3063789	2100004	2000413	2000532	1	41230
22.62	3309858	2100004	2000413	2000532	1	41230
22.69	3031176	2100004	2000413	2000532	1	41230
22.75	3297356	2100004	2000413	2000532	1	41230
22.76	3092339	3046844	2000036	2000328	1	41230
22.83	2066400	2100004	2000413	2000532	1	41230
22.93	3328632	2100004	2000413	2000532	1	41230
22.95	3092156	3046844	2000036	2000328	1	41230
23.01	2086450	2100004	2000413	2000532	1	41230
23.18	3307228	2100004	2000413	2000532	1	41230
23.23	3102744	2100004	2000413	2000532	1	41230
23.35	2000198	2000405	3081550	3182186	1	32140
23.36	2068347	3079876	2000132	2000686	1	41230
23.45	3063058	2100004	2000413	2000532	1	41230
23.46	3092380	2100004	2000413	2000532	1	41230
23.52	3170202	2100004	2000413	2000532	1	41230
23.53	2003753	2100004	2000413	2000532	1	41230
23.57	2000550	2000405	3081550	3182186	1	32140
23.62	3153508	2100004	2000413	2000532	1	41230
23.62	2088213	2100004	2000413	2000532	1	41230
23.62	2002062	2100004	2000413	2000532	1	41230
23.79	3012397	3046844	2000036	2000328	1	41230
23.87	3350632	3046844	2000036	2000328	1	41230
23.99	2000584	2000405	3081550	3182186	1	32140
24.07	2000712	2000397	3081550	3182186	1	23140
24.13	2000405	2000550	3081550	3182186	1	23140
24.20	3249980	3046844	2000036	2000328	1	41230

Figure E.6 NNH results when applied to the total asteroid set, for the cost function based on ESA: transfer costs.

Appendix F

Extensive Results of Continuous Method for Best Asteroid Sequences of Selected GTOC2 Participants

This appendix presents the extensive results obtained by the continuous method for the selected sequences found by the GTOC2 participants, using two different optimizer settings. The selected ranks, 1, 3, 7, 9, 10 and 11 have each been run 20 times. The figures summarize the mean, standard deviation and best value of those 20 runs after the Interior Point method has finished for a number of parameters. For each optimizer setting three figures have been included. The first figure shows the results for the objective value (J), the mass use in kg, the total time of flight in years (TOF), the corresponding GTOC2 objective value (J GTOC), the sum of the velocity mismatches upon arrival and departure at the first three asteroids and, if applicable, at Earth (TOT DV), and finaly the launch date in MJD (T0). The second figure shows the k_2 and N values for each leg. The third figure specifies the flight times for each leg, the stay times at the first three asteroids and specifies all velocity mismatches upon departure and arrival individually.

F.1 Weak Optimizer Settings

Results obtained using a Monte Carlo with 50,000 initial guesses and a Genetic Algorithm with 300 individuals.

R	J			Mass Used [kg]			TOF [year]		
	mean	std	best	mean	std	best	mean	std	best
1	-5595	1728	-3000	676	130	529	9.63	0.36	9.25
3	-4592	1260	-2714	490	75	477	9.78	0.32	9.82
7	-7943	2442	-4443	744	207	926	9.73	0.34	10.00
9	-4112	1922	-2114	534	123	469	9.73	0.62	10.00
10	-4464	1127	-2240	551	116	353	9.76	0.37	10.00
11	-7034	1731	-5012	730	101	670	9.53	0.44	8.79

	J GTOC			TOT DV			T0		
	mean	std	best	mean	std	best	mean	std	best
1	86	13	105	14.25	2.11	10.85	57974	1653	57343
3	103	10	104	13.46	1.61	10.45	61998	1650	63592
7	78	21	57	16.87	2.48	13.30	59169	2511	57474
9	100	18	103	12.47	2.47	9.50	61703	2552	64173
10	97	10	115	12.84	1.61	9.49	62073	2506	64145
11	81	12	94	15.19	1.89	12.77	62711	507	62402

Figure F.1 J, mass used, Time of flight, J GTOC, TOT DV, and launch date for sequences found by GTOC participants, obtained with weak optimizer settings.

R	k2 leg 1			k2 leg 2			k2 leg 3			k2 leg 4		
	mean	std	best	mean	std	best	mean	std	best	mean	std	best
1	0.44	0.18	0.64	0.35	0.22	0.06	0.71	0.15	0.56	0.35	0.29	0.18
3	0.64	0.28	0.45	0.30	0.19	0.19	0.46	0.40	0.24	0.89	0.22	0.98
7	0.53	0.29	0.31	0.41	0.23	0.02	0.55	0.25	0.70	0.73	0.29	0.51
9	0.70	0.23	0.73	0.35	0.12	0.33	0.56	0.27	0.82	0.64	0.40	0.96
10	0.77	0.17	0.97	0.36	0.14	0.58	0.72	0.25	0.79	0.43	0.31	0.77
11	0.60	0.23	0.98	0.43	0.14	0.28	0.75	0.27	0.97	0.66	0.25	0.52

	N 1			N 2			N 3			N 4		
	mean	std	best	mean	std	best	mean	std	best	mean	std	best
1	0.67	0.19	0.28	0.50	0.27	0.58	0.34	0.14	0.31	0.32	0.14	0.35
3	0.63	0.26	0.66	0.48	0.33	0.12	0.34	0.12	0.17	0.32	0.13	0.40
7	0.62	0.21	0.73	0.53	0.30	1.00	0.53	0.24	0.54	0.39	0.14	0.29
9	0.55	0.32	0.54	0.55	0.25	0.63	0.33	0.22	0.26	0.38	0.17	0.13
10	0.53	0.24	0.39	0.74	0.23	0.29	0.29	0.15	0.40	0.40	0.27	0.36
11	0.63	0.20	0.49	0.54	0.25	0.92	0.26	0.16	0.18	0.32	0.16	0.35

Figure F.2 k_2 and N values of all four legs for sequences found by GTOC participants, obtained with weak optimizer settings.

R	Departure DV 1			Departure DV 2			Departure DV 3			Departure DV 4		
	mean	std	best	mean	std	best	mean	std	best	mean	std	best
1	3.20	0.49	3.40	2.54	0.96	1.60	2.00	1.15	1.65	2.45	0.75	2.05
3	2.19	0.65	2.40	2.75	0.84	2.85	2.45	1.01	1.20	2.26	0.67	1.70
7	3.26	0.70	3.49	3.30	1.30	2.82	3.04	1.38	1.81	3.16	1.73	1.13
9	2.01	0.79	2.37	1.55	0.74	0.77	2.62	1.35	1.55	2.80	0.76	2.72
10	1.93	0.77	2.52	1.43	0.42	1.24	2.71	0.84	0.91	3.49	1.40	1.20
11	3.14	0.92	2.30	2.73	1.25	4.06	1.42	1.05	1.14	2.53	0.87	1.82

	Arrival DV 1			Arrival DV 2			Arrival DV 3			Arrival DV 4		
	mean	std	best	mean	std	best	mean	std	best	mean	std	best
1	3.37	0.72	2.52	2.53	1.20	2.12	1.36	0.75	0.91	2.12	1.89	0.97
3	1.31	0.68	0.51	2.29	0.89	1.20	2.40	0.85	2.99	5.13	1.42	3.86
7	2.74	0.46	2.59	2.49	0.85	1.58	2.03	1.28	3.37	3.39	1.99	1.50
9	1.42	0.54	1.34	1.90	1.00	1.05	2.18	1.06	2.08	4.11	1.77	2.95
10	1.29	0.66	0.76	1.43	0.75	1.98	2.48	0.90	3.41	4.94	1.88	3.75
11	4.50	0.80	3.64	1.96	1.00	1.20	1.89	0.83	0.91	4.41	2.04	6.22

	Time of Flight 1			Time of Flight 2			Time of Flight 3			Time of Flight 4		
	mean	std	best	mean	std	best	mean	std	best	mean	std	best
1	643	335	216	784	314	1283	944	138	872	798	203	692
3	431	159	537	659	192	449	1150	228	1351	967	251	911
7	436	156	331	701	228	1151	1123	362	1236	940	397	576
9	387	137	411	862	291	877	960	257	964	985	245	972
10	363	133	280	767	175	467	774	311	898	1297	420	1692
11	508	286	195	780	248	797	655	258	1047	1177	325	848

	Stay Time 1			Stay Time 2			Stay Time 3		
	mean	std	best	mean	std	best	mean	std	best
1	121	24	90	108	18	130	118	24	95
3	114	22	102	131	22	145	119	23	90
7	120	24	121	120	25	113	114	21	124
9	117	19	146	118	20	146	125	20	137
10	119	19	130	125	19	95	119	23	90
11	127	19	137	123	22	98	112	19	91

Figure F.3 Velocity mismatches, flight times and stay times of all four legs for sequences found by GTOC participants, obtained with weak optimizer settings.

F.2 Strong Optimizer Settings

Results obtained using a Monte Carlo with 100,000 initial guesses and a Genetic Algorithm with 500 individuals.

R	J			Mass Used [kg]			TOF [year]		
	mean	std	best	mean	std	best	mean	std	best
1	-4808	1413	-2407	554	99	508	9.37	0.48	9.23
3	-3742	781	-2406	495	52	472	9.90	0.15	9.66
7	-6066	2005	-2971	724	193	924	9.80	0.28	9.51
9	-2873	722	-1934	508	87	440	9.77	0.29	9.82
10	-4663	1153	-2832	558	125	406	9.76	0.32	10.00
11	-6001	939	-4434	750	90	776	9.58	0.43	9.49

	J GTOC			TOT DV			T0		
	mean	std	best	mean	std	best	mean	std	best
1	102	15	107	13.25	1.93	9.54	57681	832	57024
3	102	6	106	12.48	1.16	9.96	62270	1518	63592
7	79	19	61	14.83	2.07	11.18	58060	1870	57651
9	102	10	108	10.97	1.08	9.51	62438	2578	64155
10	96	12	109	13.12	1.58	11.07	61312	2682	64123
11	78	11	76	14.17	1.02	12.52	62508	390	62579

Figure F.4 J, mass used, Time of flight, J GTOC, TOT DV, and launch date for sequences found by GTOC participants, obtained with strong optimizer settings.

R	k2 leg 1			k2 leg 2			k2 leg 3			k2 leg 4		
	mean	std	best	mean	std	best	mean	std	best	mean	std	best
1	0.55	0.21	0.73	0.26	0.19	0.20	0.70	0.21	0.83	0.36	0.35	0.02
3	0.69	0.28	0.51	0.28	0.18	0.37	0.45	0.38	0.18	0.92	0.12	0.99
7	0.39	0.24	0.14	0.40	0.16	0.36	0.65	0.25	0.61	0.65	0.30	0.33
9	0.69	0.21	0.83	0.33	0.13	0.38	0.55	0.27	0.83	0.77	0.32	0.97
10	0.62	0.31	0.80	0.36	0.14	0.54	0.70	0.26	0.91	0.46	0.29	0.63
11	0.42	0.22	0.40	0.39	0.19	0.51	0.81	0.23	0.99	0.69	0.21	0.77

	N 1			N 2			N 3			N 4		
	mean	std	best	mean	std	best	mean	std	best	mean	std	best
1	0.60	0.21	0.40	0.55	0.22	0.25	0.36	0.16	0.75	0.31	0.18	0.44
3	0.47	0.25	0.88	0.57	0.30	0.49	0.30	0.16	0.03	0.34	0.12	0.25
7	0.67	0.17	0.71	0.50	0.28	0.71	0.51	0.34	0.95	0.24	0.14	0.02
9	0.53	0.28	0.92	0.67	0.24	0.81	0.33	0.19	0.27	0.36	0.16	0.37
10	0.45	0.23	0.46	0.67	0.19	0.25	0.38	0.19	0.48	0.47	0.24	0.37
11	0.73	0.15	0.65	0.71	0.21	0.53	0.34	0.13	0.39	0.24	0.14	0.26

Figure F.5 k_2 and N values of all four legs for sequences found by GTOC participants, obtained with weak optimizer settings.

R	Departure DV 1			Departure DV 2			Departure DV 3			Departure DV 4		
	mean	std	best	mean	std	best	mean	std	best	mean	std	best
1	2.84	0.55	3.09	2.72	1.04	2.04	1.69	0.72	0.71	1.92	0.71	1.18
3	2.17	0.53	2.35	2.47	0.67	2.40	1.99	0.68	1.20	2.20	0.39	1.97
7	3.45	0.35	3.42	2.97	1.09	2.07	2.52	1.08	2.05	2.49	1.43	1.70
9	2.12	0.49	2.03	1.27	0.39	0.98	2.07	0.80	1.62	2.74	0.76	2.70
10	1.65	0.96	1.91	1.52	0.78	1.19	2.59	0.52	3.14	1.44	0.52	1.17
11	3.20	0.52	3.35	2.45	1.30	1.13	1.22	0.41	1.52	2.29	0.95	2.45

	Arrival DV 1			Arrival DV 2			Arrival DV 3			Arrival DV 4		
	mean	std	best	mean	std	best	mean	std	best	mean	std	best
1	3.05	0.60	2.97	2.30	0.99	1.38	1.58	0.89	1.25	2.06	0.93	2.10
3	1.34	0.60	0.40	2.22	0.91	1.20	2.26	0.82	2.79	4.48	0.96	4.33
7	2.65	0.52	2.06	2.32	1.07	1.18	1.82	1.06	2.11	2.56	1.56	1.75
9	1.48	0.50	1.19	1.50	0.59	0.92	1.92	0.64	2.11	3.44	1.41	3.16
10	1.44	0.52	1.17	1.52	0.77	1.43	2.28	0.72	3.09	4.95	1.83	4.02
11	4.29	0.42	4.06	1.75	0.58	1.56	2.10	0.68	1.79	4.18	1.60	3.09

	Time of Flight 1			Time of Flight 2			Time of Flight 3			Time of Flight 4		
	mean	std	best	mean	std	best	mean	std	best	mean	std	best
1	466	257	189	881	296	920	870	171	1348	854	353	527
3	351	129	539	740	245	515	1256	177	1369	920	198	820
7	466	198	707	799	181	950	1184	239	1026	787	354	436
9	387	152	461	933	196	867	875	235	992	1003	322	857
10	371	168	275	780	174	567	755	324	642	1298	375	1752
11	554	227	602	829	265	623	604	217	636	1170	291	1223

	Stay Time 1			Stay Time 2			Stay Time 3		
	mean	std	best	mean	std	best	mean	std	best
1	117	22	90	114	23	149	122	24	149
3	123	19	103	120	24	91	106	19	90
7	116	20	113	112	23	149	117	28	90
9	121	20	129	124	23	131	124	26	150
10	124	22	147	122	19	140	115	24	130
11	118	21	136	115	23	94	111	22	150

Figure F.6 Velocity mismatches, flight times and stay times of all four legs for sequences found by GTOC participants, obtained with weak optimizer settings.

Appendix G

Extensive Results of Continuous Method for Best Asteroid Sequences Obtained by AST

This appendix contains the results of the continuous method of the sequences obtained by AST for each of the three cost functions. Each sequences has been analyzed 20 times using the continuous method. The figures summarize the mean, standard deviation and best value of those 20 runs after the Interior Point method has finished for a number of parameters. For each cost function three figures have been included. The first figure shows the results for the objective value (J), the mass use in kg, the total time of flight in years (TOF), the corresponding GTOC 2 objective value (J GTOC), the sum of the velocity mismatches upon arrival and departure at the first three asteroids and, if applicable, at Earth (TOT DV), and finaly the launch date in MJD (T0). The second figure shows the k_2 and N values for each leg. The third figure specifies the flight times for each leg, the stay times at the first three asteroids and specifies all velocity mismatches upon departure and arrival individually.

G.1 Cost Function Based on ΔV

DV Value	J			Mass Used [kg]			TOF [year]		
	mean	std	best	mean	std	best	mean	std	best
22.9	-2650	790	-2067	639	33	621	9.27	0.55	9.51
24.5	-5703	1591	-2835	636	108	703	9.67	0.35	9.71
24.6	-4105	1074	-2654	529	62	489	9.85	0.18	9.94
25.2	-5255	1153	-3366	592	52	615	9.87	0.22	9.60
27.0	-3963	1158	-2564	516	56	521	9.93	0.13	9.92
27.8	-3311	1519	-1871	473	53	520	9.84	0.29	10.00
28.4	-4422	1050	-2820	495	96	439	9.64	0.32	9.31
30.8	-3450	1540	-1706	535	104	489	9.94	0.12	10.00

	J GTOC			TOT DV [km/s]			T0 [MJD]		
	mean	std	best	mean	std	best	mean	std	best
22.9	93	7	92	10.03	1.44	9.23	59992	617	59659
24.5	90	12	82	14.44	1.97	11.11	60294	1710	61564
24.6	99	7	102	12.85	1.43	10.96	61519	459	61650
25.2	92	6	92	13.51	1.37	11.26	60939	1168	61207
27.0	99	6	99	12.26	1.43	10.60	62401	1938	63586
27.8	104	8	98	11.24	2.08	8.77	60754	1068	60874
28.4	105	11	114	13.05	1.39	10.90	58625	1080	59559
30.8	97	11	101	11.62	1.98	9.15	60427	1103	60133

Figure G.1 J, mass used, Time of flight, J GTOC, TOT DV, and launch date for sequences found by the AST, using a cost function based on ΔV.

DV Value	k2 leg 1			k2 leg 2			k2 leg 3			k2 leg 4		
	mean	std	best	mean	std	best	mean	std	best	mean	std	best
22.9	0.62	0.34	0.44	0.29	0.11	0.19	0.61	0.16	0.57	0.64	0.16	0.70
24.5	0.56	0.28	0.84	0.40	0.16	0.47	0.49	0.23	0.45	0.50	0.26	0.08
24.6	0.70	0.31	0.44	0.38	0.20	0.40	0.55	0.15	0.60	0.63	0.33	0.86
25.2	0.84	0.16	0.97	0.33	0.13	0.44	0.35	0.27	0.65	0.38	0.29	0.39
27.0	0.72	0.21	0.57	0.29	0.09	0.24	0.31	0.34	0.02	0.07	0.03	0.12
27.8	0.82	0.20	0.80	0.26	0.22	0.05	0.46	0.36	0.20	0.07	0.05	0.04
28.4	0.63	0.38	0.90	0.37	0.11	0.36	0.95	0.04	0.91	0.53	0.33	0.26
30.8	0.77	0.27	0.02	0.22	0.14	0.21	0.63	0.11	0.68	0.31	0.31	0.26

	N 1			N 2			N 3			N 4		
	mean	std	best	mean	std	best	mean	std	best	mean	std	best
22.9	0.54	0.23	0.78	0.73	0.18	0.78	0.30	0.19	0.15	0.76	0.21	0.67
24.5	0.55	0.29	0.36	0.62	0.31	0.87	0.52	0.29	0.97	0.41	0.29	0.24
24.6	0.44	0.29	0.42	0.63	0.19	0.59	0.74	0.28	0.87	0.24	0.13	0.19
25.2	0.36	0.20	0.08	0.61	0.22	0.51	0.49	0.32	0.87	0.47	0.28	0.12
27.0	0.54	0.29	0.71	0.57	0.24	0.95	0.27	0.21	0.41	0.31	0.20	0.29
27.8	0.33	0.26	0.45	0.60	0.27	0.92	0.26	0.15	0.07	0.30	0.14	0.41
28.4	0.46	0.28	0.14	0.64	0.20	0.78	0.29	0.14	0.19	0.54	0.26	0.49
30.8	0.41	0.19	0.22	0.55	0.26	0.09	0.27	0.13	0.25	0.35	0.16	0.18

Figure G.2 k_2 and N values of all four legs for sequences found by the AST, using a cost function based on ΔV.

DV Value	Departure DV 1			Departure DV 2			Departure DV 3			Departure DV 4		
	mean	std	best	mean	std	best	mean	std	best	mean	std	best
22.9	2.49	0.53	2.23	1.19	0.63	1.12	1.80	0.46	1.75	2.51	0.64	2.44
24.5	2.00	0.60	2.58	1.66	0.65	1.79	3.09	1.39	2.34	2.99	1.37	1.84
24.6	2.10	0.63	2.71	2.49	0.80	1.95	2.93	0.73	2.15	2.03	0.89	2.25
25.2	2.45	0.64	2.35	1.63	0.83	1.56	3.18	0.73	3.03	3.50	2.00	1.36
27.0	2.41	0.46	2.33	1.19	0.37	1.16	2.86	0.78	2.58	2.90	1.15	2.14
27.8	2.28	0.31	2.43	1.47	0.98	0.53	1.58	0.70	0.95	3.02	0.95	2.85
28.4	2.17	0.53	3.04	1.75	0.54	1.20	3.30	0.55	2.71	2.73	0.71	2.11
30.8	2.28	0.53	2.83	1.08	0.53	1.02	2.41	0.71	2.03	2.57	1.01	1.56

	Arrival DV 1			Arrival DV 2			Arrival DV 3			Arrival DV 4		
	mean	std	best	mean	std	best	mean	std	best	mean	std	best
22.9	1.13	0.63	0.48	1.10	0.46	1.06	2.29	0.50	2.37	4.20	1.38	3.95
24.5	1.25	0.67	1.16	2.56	0.84	2.36	2.89	0.61	1.61	5.90	2.31	8.77
24.6	1.41	0.66	1.18	2.10	0.68	2.05	1.89	0.52	1.37	2.14	1.22	1.48
25.2	1.41	0.61	1.08	1.59	1.18	0.95	2.20	0.79	3.27	4.81	2.40	3.73
27.0	1.52	0.65	1.47	1.30	0.46	1.28	2.48	0.98	1.97	5.71	0.84	5.40
27.8	1.24	0.49	1.06	1.88	0.81	1.26	2.05	0.58	2.11	4.69	0.99	4.69
28.4	1.11	0.47	1.02	2.50	0.65	2.37	1.66	0.42	1.48	4.50	2.28	6.81
30.8	1.48	0.78	0.84	1.37	0.61	1.20	2.71	0.51	2.51	8.67	1.83	6.70

	Time of Flight 1			Time of Flight 2			Time of Flight 3			Time of Flight 4		
	mean	std	best	mean	std	best	mean	std	best	mean	std	best
22.9	394.1	148	628	827	150	745	617.8	248	542	1218	226	1209
24.5	356.3	130	271	739.6	166	1021	1091	210	1247	1010	245	657.8
24.6	315.2	133	242	824.2	203	952	1320	210	1408	780	257	703.5
25.2	290.6	120	243	802.6	242	1341	967.9	360	1102	1165	529	458.1
27.0	338.9	140	376	756	177	647	903.4	328	1079	1271	348	1200
27.8	281.1	66.9	248	858.6	204	1022	662.3	273	566	1449	305	1498
28.4	318.1	152	116	975.4	183	1081	800.9	313	1089	1102	342	816.3
30.8	295.6	132	214	599.5	128	544	1016	221	926	1378	290	1658

	Stay Time 1			Stay Time 2			Stay Time 3		
	mean	std	best	mean	std	best	mean	std	best
22.9	120	20	123	115	20	138	95	13	90
24.5	121	21	148	105	23	90	107	18	111
24.6	126	20	134	123	25	96	110	22	96
25.2	118	20	107	123	21	107	139	14	147
27.0	104	17	90	126	18	100	127	22	131
27.8	120	18	102	108	18	101	116	19	115
28.4	125	19	102	94	4	94	104	16	102
30.8	108	17	91	99	13	90	132	21	129

Figure G.3 Velocity mismatches, flight times and stay times of all four legs for sequences found by the AST, using a cost function based on ΔV.

G.2 Cost Function Based on Energy

E Value	J			Mass Used [kg]			TOF [year]		
	mean	std	best	mean	std	best	mean	std	best
420	-1217	556	-181	490	49	465	9.28	0.50	9.92
437	-3156	984	-1785	631	111	669	9.89	0.11	10.00
454	-7950	1613	-5125	643	208	517	9.95	0.19	10.00
456	-3663	829	-2490	476	92	414	9.80	0.16	10.00
465	-7347	2541	-4530	710	103	625	9.93	0.18	10.00
473	-5089	2089	-2174	694	121	664	9.83	0.22	10.00
479	-2966	902	-1623	443	32	417	9.87	0.19	10.00
496	-6306	738	-4536	675	170	839	9.83	0.17	9.90

	J GTOC			TOT DV [km/s]			T0 [MJD]		
	mean	std	best	mean	std	best	mean	std	best
420	109	7	104	7.68	1.18	5.54	64340	197	64065
437	88	11	83	11.44	1.47	9.20	60093	2848	58072
454	86	21	98	16.86	1.51	14.43	62490	2411	64690
456	104	10	109	12.30	1.32	10.45	62729	2003	63319
465	80	10	88	16.58	2.18	13.84	61097	853	60985
473	82	12	84	14.71	5.61	8.96	58627	1062	58036
479	107	4	108	10.37	1.21	9.06	62999	266	63177
496	84	18	67	15.09	1.18	12.62	62059	1593	63233

Figure G.4 J, mass used, Time of flight, J GTOC, TOT DV, and launch date for sequences found by the AST, using a cost function based on Energy.

E Value	k2 leg 1			k2 leg 2			k2 leg 3			k2 leg 4		
	mean	std	best	mean	std	best	mean	std	best	mean	std	best
420	0.74	0.24	0.91	0.25	0.14	0.15	0.94	0.06	1.00	0.15	0.13	0.04
437	0.61	0.33	0.68	0.36	0.08	0.36	0.71	0.23	0.63	0.44	0.41	0.40
454	0.68	0.19	0.77	0.34	0.13	0.29	0.86	0.16	0.90	0.18	0.23	0.06
456	0.69	0.31	0.85	0.29	0.16	0.30	0.58	0.35	0.70	0.20	0.25	0.10
465	0.58	0.26	0.81	0.39	0.12	0.52	0.94	0.06	0.88	0.63	0.13	0.56
473	0.51	0.25	0.42	0.44	0.06	0.48	0.88	0.13	0.93	0.56	0.21	0.60
479	0.83	0.22	0.87	0.31	0.12	0.41	0.92	0.06	0.95	0.49	0.34	0.21
496	0.63	0.28	0.99	0.32	0.10	0.42	0.92	0.13	0.99	0.66	0.30	0.79

	N 1			N 2			N 3			N 4		
	mean	std	best	mean	std	best	mean	std	best	mean	std	best
420	0.37	0.22	0.24	0.74	0.16	0.88	0.28	0.10	0.06	0.26	0.15	0.06
437	0.47	0.24	0.22	0.67	0.20	0.18	0.49	0.29	0.69	0.34	0.13	0.43
454	0.47	0.31	0.20	0.56	0.27	0.74	0.43	0.32	0.07	0.28	0.19	0.05
456	0.37	0.27	0.15	0.64	0.25	0.53	0.29	0.16	0.25	0.25	0.15	0.06
465	0.34	0.25	0.28	0.63	0.28	0.25	0.31	0.13	0.30	0.72	0.22	0.73
473	0.42	0.21	0.32	0.57	0.25	0.65	0.28	0.19	0.30	0.56	0.29	0.97
479	0.37	0.29	0.37	0.72	0.18	0.60	0.20	0.13	0.30	0.31	0.13	0.19
496	0.51	0.28	0.17	0.67	0.27	0.74	0.29	0.21	0.09	0.31	0.19	0.37

Figure G.5 k_2 and N values of all four legs for sequences found by the AST, using a cost function based on Energy.

E Value	Departure DV 1			Departure DV 2			Departure DV 3			Departure DV 4		
	mean	std	best	mean	std	best	mean	std	best	mean	std	best
420	2.40	0.71	2.38	1.71	0.53	1.15	0.72	0.52	0.24	1.49	0.17	1.35
437	2.50	0.58	3.48	1.37	0.67	1.18	2.46	0.79	1.36	1.84	0.98	0.98
454	1.97	0.75	1.85	1.75	0.59	1.47	3.90	1.53	2.43	4.08	1.49	3.95
456	2.67	0.74	2.57	1.56	0.75	0.92	2.29	0.71	1.80	2.24	0.45	1.68
465	2.38	1.10	2.28	2.12	0.57	2.37	3.55	1.24	2.53	3.05	1.18	2.79
473	3.43	2.45	3.47	1.67	0.83	1.57	2.27	1.71	0.79	2.51	1.15	2.74
479	0.84	0.53	1.07	1.30	0.19	1.28	3.04	1.24	1.55	1.05	0.44	1.17
496	1.50	0.72	2.15	1.61	0.55	1.29	4.16	0.55	4.01	2.63	0.81	2.37

	Arrival DV 1			Arrival DV 2			Arrival DV 3			Arrival DV 4		
	mean	std	best	mean	std	best	mean	std	best	mean	std	best
420	1.55	0.46	1.01	1.27	0.51	0.88	0.95	0.16	0.92	4.76	0.22	4.94
437	1.63	0.38	1.01	2.07	0.65	2.78	2.08	0.62	1.88	2.48	0.93	1.56
454	1.59	0.84	1.19	2.31	1.01	2.29	3.23	1.12	3.10	6.09	2.31	7.97
456	1.61	0.49	1.17	1.93	0.57	1.86	2.65	0.27	3.03	1.79	1.32	1.13
465	1.87	0.43	1.55	2.31	1.15	1.69	3.58	1.03	2.90	5.20	2.38	3.67
473	2.19	2.50	1.16	2.59	1.35	0.24	2.97	0.59	2.46	5.29	2.23	6.54
479	1.05	0.32	1.11	1.53	1.07	1.07	2.41	0.71	2.89	1.09	0.56	0.74
496	1.13	0.27	1.41	2.47	1.57	0.92	3.10	0.91	2.62	5.89	3.49	8.99

	Time of Flight 1			Time of Flight 2			Time of Flight 3			Time of Flight 4		
	mean	std	best	mean	std	best	mean	std	best	mean	std	best
420	279	124	255	1348	281	1481	676	281	859	730	67	664
437	398	180	393	965	100	803	1122	206	1294	770	265	770
454	340	123	278	775	123	776	1137	135	1166	1033	227	1095
456	328	141	247	966	175	1149	1335	220	1484	630	319	438
465	337	112	254	832	164	749	881	192	1043	1250	217	1275
473	435	129	360	832	170	988	890	346	854	1105	246	1129
479	318	170	97	996	166	906	1484	335	1826	455	243	468
496	389	185	70	848	119	1102	1119	227	988	889	341	1054

	Stay Time 1			Stay Time 2			Stay Time 3		
	mean	std	best	mean	std	best	mean	std	best
420	124	20	90	113	18	127	119	18	146
437	127	18	150	104	18	149	127	22	94
454	127	18	140	112	23	91	109	22	107
456	120	22	97	107	20	125	95	9	112
465	109	22	91	111	20	136	104	18	105
473	114	19	99	109	22	121	106	18	101
479	116	18	127	117	23	122	119	24	107
496	117	19	114	117	24	142	113	23	147

Figure G.6 Velocity mismatches, flight times and stay times of all four legs for sequences found by the AST, using a cost function based on Energy.

G.3 Cost Function According to ESA Approach

ESA Value	J			Mass Used [kg]			TOF [year]		
	mean	std	best	mean	std	best	mean	std	best
15.98	-4339	989	-2882	603	140	619	9.91	0.13	10.00
16.32	-7459	2577	-2557	679	88	774	9.87	0.24	10.00
16.56	-2638	411	-1983	479	79	482	9.66	0.33	9.66
16.75	-3625	652	-2758	570	116	525	9.76	0.25	9.77
16.84	-3024	928	-1981	498	82	473	9.85	0.22	9.87
16.87	-4575	1220	-1857	600	111	749.6	9.64	0.40	9.80
16.93	-1795	669	-934	479	172	644	9.64	0.58	9.83
17.11	-5989	1681	-4018	610	159	522	9.86	0.19	10.00

	J GTOC			TOT DV [km/s]			T0 [MJD]		
	mean	std	best	mean	std	best	mean	std	best
15.98	91	15	88	12.47	1.47	10.05	62894	481	62797
16.32	83	9	73	17.02	4.53	9.92	62464	1170	62415
16.56	106	8	105	11.11	3.51	8.87	62816	294	62610
16.75	95	12	100	12.90	3.95	11.16	62833	240	63002
16.84	102	9	104	11.01	1.50	10.01	60039	3007	63975
16.87	93	11	77	13.16	1.68	9.00	63135	1268	63471
16.93	106	20	87	9.93	4.17	7.65	62744	1443	59911
17.11	90	17	98	14.61	1.92	13.14	62812	555	62156

Figure G.7 J, mass used, Time of flight, J GTOC, TOT DV, and launch date for sequences found by the AST, using the cost function implemented by ESA.

ESA Value	k2 leg 1			k2 leg 2			k2 leg 3			k2 leg 4		
	mean	std	best	mean	std	best	mean	std	best	mean	std	best
15.98	0.70	0.30	0.99	0.42	0.19	0.55	0.67	0.13	0.75	0.61	0.38	0.93
16.32	0.59	0.27	0.49	0.43	0.15	0.56	0.61	0.26	0.75	0.60	0.31	0.70
16.56	0.67	0.27	0.69	0.29	0.17	0.48	0.38	0.23	0.56	0.85	0.23	0.85
16.75	0.51	0.26	0.85	0.26	0.17	0.02	0.41	0.19	0.55	0.83	0.21	0.99
16.84	0.70	0.31	0.54	0.30	0.21	0.47	0.74	0.31	0.52	0.77	0.30	0.99
16.87	0.63	0.33	0.91	0.34	0.16	0.22	0.64	0.39	0.91	0.15	0.13	0.11
16.93	0.63	0.26	0.96	0.19	0.19	0.15	0.91	0.21	1.00	0.82	0.23	0.45
17.11	0.73	0.27	0.98	0.17	0.16	0.06	0.67	0.21	0.78	0.66	0.37	0.06

	N 1			N 2			N 3			N 4		
	mean	std	best	mean	std	best	mean	std	best	mean	std	best
15.98	0.45	0.23	0.26	0.50	0.31	0.50	0.69	0.24	0.76	0.26	0.16	0.15
16.32	0.54	0.28	0.50	0.62	0.26	0.54	0.48	0.24	0.76	0.32	0.18	0.20
16.56	0.53	0.28	0.93	0.70	0.19	0.80	0.31	0.16	0.43	0.30	0.14	0.14
16.75	0.67	0.21	0.84	0.57	0.24	0.91	0.32	0.14	0.25	0.26	0.15	0.30
16.84	0.52	0.27	0.79	0.54	0.25	0.57	0.44	0.24	0.36	0.29	0.12	0.25
16.87	0.47	0.25	0.23	0.57	0.21	0.52	0.36	0.16	0.29	0.56	0.22	0.54
16.93	0.63	0.28	0.19	0.65	0.29	0.88	0.31	0.19	0.45	0.29	0.19	0.61
17.11	0.47	0.29	0.22	0.59	0.30	0.82	0.34	0.18	0.39	0.28	0.15	0.28

Figure G.8 k_2 and N values of all four legs for sequences found by the AST, using the cost function implemented by ESA.

ESA Value	Departure DV 1			Departure DV 2			Departure DV 3			Departure DV 4		
	mean	std	best	mean	std	best	mean	std	best	mean	std	best
15.98	2.49	0.78	3.14	2.43	1.04	2.64	2.01	1.20	0.81	1.11	0.75	0.68
16.32	3.26	1.22	3.27	3.81	1.06	2.02	2.62	1.41	0.98	1.78	1.58	0.56
16.56	2.75	1.62	2.36	1.92	0.56	1.00	2.24	0.40	2.50	0.86	0.52	0.65
16.75	3.07	1.74	2.98	2.64	0.73	2.17	2.38	0.42	2.69	0.81	0.44	1.19
16.84	2.21	0.50	2.13	1.70	0.77	2.03	2.40	0.80	1.82	1.76	0.72	1.90
16.87	2.58	1.12	3.49	2.50	0.84	1.01	2.02	0.98	2.11	2.86	0.94	1.45
16.93	2.95	1.89	1.93	1.14	0.44	1.17	1.99	0.42	2.18	1.57	0.49	0.43
17.11	2.49	0.61	1.71	2.63	1.04	2.57	3.21	1.05	1.92	1.31	1.21	1.42

	Arrival DV 1			Arrival DV 2			Arrival DV 3			Arrival DV 4		
	mean	std	best	mean	std	best	mean	std	best	mean	std	best
15.98	1.68	0.56	0.94	3.49	0.93	3.57	1.74	0.96	1.40	2.39	1.85	1.84
16.32	2.66	2.04	2.02	3.55	0.78	2.89	2.39	1.37	1.45	3.40	2.44	4.02
16.56	2.06	2.50	1.20	2.36	0.60	2.88	1.42	0.44	0.65	2.47	1.65	3.17
16.75	2.74	2.61	1.52	2.74	0.39	2.39	1.29	0.31	1.20	2.20	1.22	0.61
16.84	1.39	0.67	1.18	2.04	0.85	1.89	1.72	0.68	1.20	2.54	0.84	3.11
16.87	1.62	0.56	1.38	2.34	0.78	1.36	1.75	0.43	1.69	5.63	1.89	2.07
16.93	1.52	2.08	1.20	1.54	0.60	1.18	1.80	0.30	1.51	4.20	1.47	6.47
17.11	1.91	0.73	2.36	3.10	1.43	2.24	2.45	0.93	2.62	3.30	2.06	8.15

	Time of Flight 1			Time of Flight 2			Time of Flight 3			Time of Flight 4		
	mean	std	best	mean	std	best	mean	std	best	mean	std	best
15.98	337	150	228	865	260	800	1514	225	1329	542	164	860
16.32	404	196	535	987	334	1015	1267	342	1230	586	363	497
16.56	379	156	478	999	188	966	1089	407	1313	708	289	396
16.75	420	119	432	933	182	834	1077	448	1555	780	385	422
16.84	328	154	419	713	203	966	1086	253	745	1109	262	1163
16.87	369	147	283	765	209	744	770	257	461	1270	353	1783
16.93	423	145	248	709	151	691	840	147	794	1215	293	1509
17.11	316	160	135	698	216	839	1589	211	1603	652	258	737

	Stay Time 1			Stay Time 2			Stay Time 3		
	mean	std	best	mean	std	best	mean	std	best
15.98	117	22	150	119	25	148	127	20	138
16.32	116	24	133	117	24	127	128	19	117
16.56	113	24	111	104	18	122	137	16	143
16.75	111	19	103	104	17	90	139	16	130
16.84	119	21	97	128	17	99	128	17	99
16.87	118	20	128	116	25	90	113	24	91
16.93	113	21	121	103	17	96	118	23	133
17.11	116	20	91	108	23	133	122	24	115

Figure G.9 Velocity mismatches, flight times and stay times of all four legs for sequences found by the AST, using the cost function implemented by ESA.

Appendix H

Extensive Results of Continuous Method for Best Asteroid Sequences Obtained by NNH

This appendix contains the results of the continuous method of the sequences obtained by the NNH for each of the three cost functions. Each sequences has been analyzed 20 times using the continuous method. The figures summarize the mean, standard deviation and best value of those 20 runs after the Interior Point method has finished for a number of parameters. For each cost function three figures have been included. The first figure shows the results for the objective value (J), the mass use in kg, the total time of flight in years (TOF), the corresponding GTOC2 objective value (J GTOC), the sum of the velocity mismatches upon arrival and departure at the first three asteroids and, if applicable, at Earth (TOT DV), and finaly the launch date in MJD (T0). The second figure shows the k_2 and N values for each leg. The third figure specifies the flight times for each leg, the stay times at the first three asteroids and specifies all velocity mismatches upon departure and arrival individually.

H.1 Cost Function Based on ΔV

DV Value	J			Mass Used [kg]			TOF [year]		
	mean	std	best	mean	std	best	mean	std	best
21.28	-2422	1137	-1260	452	47	464	9.87	0.19	9.95
21.28	-2448	956	-1391	508	151	368	9.89	0.14	10.00
22.91	-2421	333	-1482	478	43	425	9.37	0.41	10.00
23.25	-3097	917	-1757	486	131	393	9.84	0.19	9.64
23.45	-3869	662	-2710	537	89	503	9.69	0.37	9.99
23.46	-4509	1270	-2372	557	135	490	9.84	0.20	9.95
23.63	-6304	2524	-4360	778	126	781	9.74	0.20	9.80
23.65	-3381	1704	-1803	732	165	883	9.76	0.30	10.00

	J GTOC			TOT DV [km/s]			T0 [MJD]		
	mean	std	best	mean	std	best	mean	std	best
21.28	106	5	104	10.18	1.66	8.93	62015	1140	61493
21.28	100	15	113	10.29	1.27	9.15	61307	1407	61627
22.91	109	5	107	10.15	0.36	9.24	61756	165	61495
23.25	103	13	115	10.82	1.32	8.43	61732	2081	63211
23.45	100	10	100	12.44	0.77	11.27	60423	1797	61458
23.46	96	14	102	13.24	1.78	10.29	60183	1086	59777
23.63	74	13	73	15.30	2.50	13.07	61512	1313	61682
23.65	79	17	62	11.58	2.25	9.54	61697	855	61483

Figure H.1 J, mass used, Time of flight, J GTOC, TOT DV, and launch date for sequences found by the NNH, using a cost function based on ΔV.

DV Value	k2 leg 1			k2 leg 2			k2 leg 3			k2 leg 4		
	mean	std	best	mean	std	best	mean	std	best	mean	std	best
21.28	0.50	0.34	0.04	0.43	0.13	0.52	0.78	0.13	0.71	0.23	0.20	0.14
21.28	0.57	0.29	0.99	0.46	0.10	0.56	0.80	0.11	0.78	0.17	0.17	0.60
22.91	0.57	0.30	0.59	0.30	0.13	0.60	0.74	0.09	0.88	0.39	0.27	0.03
23.25	0.73	0.30	0.89	0.44	0.15	0.57	0.85	0.13	0.82	0.13	0.11	0.03
23.45	0.60	0.23	0.49	0.43	0.08	0.40	0.91	0.11	0.82	0.39	0.33	0.03
23.46	0.73	0.17	0.91	0.35	0.14	0.30	0.89	0.12	0.95	0.16	0.14	0.08
23.63	0.68	0.35	0.97	0.38	0.13	0.30	0.65	0.09	0.65	0.56	0.35	0.69
23.65	0.70	0.22	0.38	0.31	0.14	0.18	0.63	0.15	0.62	0.31	0.28	0.05

	N 1			N 2			N 3			N 4		
	mean	std	best	mean	std	best	mean	std	best	mean	std	best
21.28	0.51	0.25	0.25	0.51	0.25	0.12	0.30	0.13	0.36	0.25	0.15	0.42
21.28	0.43	0.28	0.13	0.54	0.26	0.25	0.32	0.24	0.37	0.25	0.18	0.36
22.91	0.60	0.29	0.93	0.67	0.27	0.13	0.27	0.17	0.31	0.26	0.16	0.07
23.25	0.46	0.21	0.23	0.53	0.31	0.14	0.34	0.21	0.07	0.19	0.12	0.21
23.45	0.50	0.29	0.17	0.53	0.26	0.82	0.35	0.31	0.97	0.30	0.11	0.17
23.46	0.63	0.30	0.34	0.61	0.31	0.79	0.27	0.19	0.00	0.28	0.14	0.45
23.63	0.35	0.21	0.21	0.59	0.24	0.73	0.74	0.16	0.65	0.26	0.14	0.10
23.65	0.50	0.30	0.30	0.58	0.28	0.62	0.60	0.29	0.94	0.27	0.18	0.03

Figure H.2 k_2 and N values of all four legs for sequences found by the NNH, using a cost function based on ΔV.

DV Value	Departure DV 1			Departure DV 2			Departure DV 3			Departure DV 4		
	mean	std	best	mean	std	best	mean	std	best	mean	std	best
21.28	1.54	0.87	1.95	1.46	0.41	1.20	1.54	0.59	1.19	1.82	1.22	1.07
21.28	1.93	0.54	2.18	1.50	0.49	1.50	2.01	0.77	1.19	1.56	0.76	1.19
22.91	1.47	0.78	2.43	1.34	0.34	2.02	1.34	0.21	1.52	1.62	0.35	1.19
23.25	1.38	0.63	1.67	1.84	0.37	2.05	2.02	0.92	1.01	3.01	1.11	2.08
23.45	1.95	0.76	1.79	2.26	0.48	2.34	2.05	0.35	2.01	2.27	0.76	2.44
23.46	2.16	0.80	3.15	2.19	0.83	1.20	2.41	0.98	1.55	3.03	1.05	2.61
23.63	2.16	0.98	2.29	2.27	0.78	1.80	2.46	0.52	2.23	2.99	1.49	1.70
23.65	2.08	0.45	1.77	2.11	0.75	2.23	1.65	0.83	1.10	1.87	1.00	1.10

	Arrival DV 1			Arrival DV 2			Arrival DV 3			Arrival DV 4		
	mean	std	best	mean	std	best	mean	std	best	mean	std	best
21.28	1.24	0.17	1.20	1.76	0.62	1.65	2.36	0.70	2.62	8.21	1.35	8.42
21.28	1.29	0.33	1.19	1.79	0.51	1.93	2.15	0.56	2.15	7.56	1.58	5.96
22.91	1.13	0.33	1.15	1.83	0.33	2.19	2.88	0.62	1.16	7.50	1.11	7.85
23.25	1.21	0.51	1.22	1.77	0.83	1.67	0.97	0.35	0.40	4.93	1.48	4.80
23.45	1.27	0.42	1.20	2.12	0.75	1.11	2.47	0.69	2.16	6.65	1.56	8.94
23.46	1.56	0.52	1.81	2.23	1.00	1.23	1.82	0.49	1.89	6.06	0.87	6.86
23.63	1.72	1.04	1.13	2.79	0.92	2.26	6.95	1.81	6.07	6.95	1.81	6.07
23.65	1.31	0.48	1.18	2.16	0.62	1.63	2.47	0.76	2.30	7.84	1.23	8.33

	Time of Flight 1			Time of Flight 2			Time of Flight 3			Time of Flight 4		
	mean	std	best	mean	std	best	mean	std	best	mean	std	best
21.28	395	101	364	710	165	631	1174	245	1371	971	198	832
21.28	391	109	304	691	127	572	1090	192	1288	1106	272	1157
22.91	423	100	431	696	88	591	1165	78	976	822	188	1337
23.25	358	178	88	772	195	629	793	338	1121	1324	396	1336
23.45	449	141	375	805	146	1007	1153	213	1399	818	154	597
23.46	440	143	387	850	163	1009	971	308	1208	993	284	730
23.63	347	142	327	841	166	999	1247	213	1073	800	244	862
23.65	375	77	364	714	206	625	1285	267	1441	859	194	877

	Stay Time 1			Stay Time 2			Stay Time 3		
	mean	std	best	mean	std	best	mean	std	best
21.28	117	21	147	110	23	144	130	21	144
21.28	103	15	92	105	16	90	127	22	148
22.91	115	19	101	97	11	95	103	20	121
23.25	117	19	122	107	18	115	123	23	109
23.45	111	21	90	102	19	91	101	17	90
23.46	113	21	119	104	15	90	124	20	90
23.63	113	22	121	105	15	90	104	16	106
23.65	113	18	127	114	19	93	105	15	125

Figure H.3 Velocity mismatches, flight times and stay times of all four legs for sequences found by the NNH, using a cost function based on ΔV.

H.2 Cost Function Based on Energy

E Value	J			Mass Used [kg]			TOF [year]		
	mean	std	best	mean	std	best	mean	std	best
451	-2750	1076	-1594	699	119	567	9.80	0.19	10.00
497	-5325	1239	-3251	706	211	666	9.34	0.70	9.36
531	-6638	2051	-4335	677	134	536	9.70	0.37	9.01
537	-3717	1729	-1562	676	105	664	9.67	0.34	9.86
540	-4097	1386	-2342	614	98	467	9.83	0.29	9.91
545	-9089	3210	-5736	728	115	667	9.77	0.33	9.91
562	-4114	1534	-2249	680	119	583	9.69	0.30	9.62
565	-11013	2977	-5392	846	130	999	9.81	0.26	9.68

	J GTOC			TOT DV [km/s]			T0 [MJD]		
	mean	std	best	mean	std	best	mean	std	best
451	82	12	93	10.26	1.36	8.63	59389	2375	64691
497	86	25	89	14.06	4.91	10.84	58662	635	58249
531	85	16	107	14.78	2.71	11.73	62170	945	62632
537	85	12	85	11.54	2.27	8.47	58740	1301	58496
540	90	10	104	12.81	4.10	10.05	60426	1936	60396
545	79	12	84	16.87	2.63	14.91	62007	1608	62305
562	85	14	95	11.69	2.10	9.27	63142	2048	64388
565	67	13	52	19.87	2.91	13.81	62339	1952	61062

Figure H.4 J, mass used, Time of flight, J GTOC, TOT DV, and launch date for sequences found by the NNH, using a cost function based on Energy.

E Value	k2 leg 1			k2 leg 2			k2 leg 3			k2 leg 4		
	mean	std	best	mean	std	best	mean	std	best	mean	std	best
451	0.45	0.33	0.19	0.36	0.14	0.33	0.69	0.08	0.78	0.27	0.25	0.04
497	0.49	0.25	0.52	0.39	0.17	0.42	0.70	0.29	0.61	0.54	0.38	0.93
531	0.49	0.21	0.32	0.34	0.16	0.19	0.54	0.24	0.53	0.25	0.22	0.07
537	0.79	0.24	0.94	0.29	0.16	0.22	0.52	0.22	0.62	0.51	0.18	0.61
540	0.49	0.28	0.56	0.36	0.17	0.55	0.79	0.25	0.12	0.39	0.33	0.77
545	0.50	0.30	0.89	0.39	0.17	0.50	0.81	0.28	0.99	0.75	0.34	0.99
562	0.46	0.19	0.49	0.36	0.13	0.50	0.47	0.37	0.27	0.64	0.24	0.60
565	0.55	0.24	0.74	0.32	0.13	0.39	0.82	0.23	0.95	0.32	0.25	0.18

	N 1			N 2			N 3			N 4		
	mean	std	best	mean	std	best	mean	std	best	mean	std	best
451	0.57	0.25	0.16	0.66	0.23	0.85	0.73	0.20	0.10	0.26	0.15	0.45
497	0.56	0.18	0.68	0.65	0.24	0.59	0.35	0.25	0.14	0.38	0.20	0.09
531	0.69	0.20	0.63	0.51	0.22	0.36	0.30	0.23	0.35	0.27	0.17	0.37
537	0.40	0.25	0.14	0.60	0.26	0.58	0.38	0.19	0.46	0.59	0.29	0.85
540	0.68	0.19	0.85	0.64	0.27	0.46	0.33	0.23	0.01	0.38	0.16	0.28
545	0.45	0.23	0.19	0.48	0.33	0.20	0.42	0.28	0.22	0.28	0.14	0.24
562	0.58	0.28	0.77	0.67	0.23	0.58	0.30	0.14	0.17	0.28	0.18	0.19
565	0.64	0.25	0.78	0.68	0.27	0.58	0.34	0.19	0.78	0.54	0.25	0.75

Figure H.5 k_2 and N values of all four legs for sequences found by the NNH, using a cost function based on Energy.

E Value	Departure DV 1			Departure DV 2			Departure DV 3			Departure DV 4		
	mean	std	best	mean	std	best	mean	std	best	mean	std	best
451	2.29	1.24	3.37	1.38	0.49	1.34	2.50	0.81	2.36	2.04	1.03	1.50
497	3.59	0.79	3.48	2.45	2.58	0.47	1.52	0.55	1.11	2.68	0.76	2.86
531	3.58	0.56	3.50	1.75	0.87	1.18	1.77	1.22	1.19	2.59	0.85	2.58
537	3.56	0.42	3.50	2.01	1.00	1.33	1.42	0.55	1.62	1.47	0.70	0.72
540	3.85	1.45	3.50	1.79	0.66	1.10	1.73	0.87	1.78	2.24	1.12	1.81
545	4.01	1.20	3.50	2.04	0.92	1.67	1.57	0.70	2.54	2.82	1.51	1.98
562	3.41	0.19	3.49	1.93	1.02	1.19	1.09	0.58	1.67	2.00	1.20	0.92
565	3.76	1.43	3.46	2.34	1.04	1.18	3.11	1.61	2.97	3.35	1.54	1.78

	Arrival DV 1			Arrival DV 2			Arrival DV 3			Arrival DV 4		
	mean	std	best	mean	std	best	mean	std	best	mean	std	best
451	1.33	0.53	1.45	1.10	0.36	1.20	1.85	0.62	0.79	3.93	2.74	5.88
497	3.58	0.72	2.94	2.27	2.18	2.29	1.37	0.85	1.17	15.59	2.80	14.32
531	4.46	0.53	4.51	1.63	0.68	0.67	2.37	1.26	1.61	6.54	1.49	6.95
537	3.02	0.69	2.23	1.78	0.87	1.13	1.74	0.75	1.44	11.87	4.69	9.27
540	3.49	2.00	2.38	1.73	0.66	2.25	1.39	0.60	0.72	4.77	2.49	4.99
545	5.14	1.03	3.99	2.16	1.18	1.48	2.55	0.96	3.25	5.02	2.14	2.59
562	3.84	0.74	3.40	1.56	0.61	1.26	1.27	0.64	0.83	2.99	1.98	1.16
565	4.45	1.07	3.79	3.04	1.03	1.01	3.05	1.38	3.09	20.78	9.33	26.08

	Time of Flight 1			Time of Flight 2			Time of Flight 3			Time of Flight 4		
	mean	std	best	mean	std	best	mean	std	best	mean	std	best
451	455	168	242	818	214	856	1029	152	864	947	287	1360
497	429	216	403	863	233	855	1056	299	828	715	310	1022
531	474	185	297	782	218	774	1072	202	982	876	112	950
537	229	142	157	725	151	777	1163	260	1037	1060	290	1279
540	511	127	688	760	196	459	797	266	810	1178	337	1323
545	460	274	373	827	267	1049	836	223	759	1084	326	1073
562	543	180	517	722	139	577	412	237	113	1507	392	1988
565	467	119	546	781	273	582	951	410	1378	1020	488	701

	Stay Time 1			Stay Time 2			Stay Time 3		
	mean	std	best	mean	std	best	mean	std	best
451	116	23	90	109	17	104	105	17	137
497	127	20	129	114	19	90	109	18	90
531	107	18	103	112	21	92	118	22	90
537	115	22	97	118	16	106	123	19	149
540	118	20	118	112	21	90	114	23	133
545	127	21	150	118	17	116	115	21	102
562	119	22	108	121	21	93	115	24	119
565	124	21	97	119	22	121	121	23	110

Figure H.6 Velocity mismatches, flight times and stay times of all four legs for sequences found by the NNH, using a cost function based on Energy.

H.3 Cost Function According to ESA Approach

ESA Value	J			Mass Used [kg]			TOF [year]		
	mean	std	best	mean	std	best	mean	std	best
15.03	-2777	789	-1989	519	76	455	9.68	0.35	9.77
21.05	-37553	5388	-29027	807	191	702	9.85	0.21	9.56
21.25	-22586	5191	-14832	902	142	823	9.83	0.19	10.00
21.92	-29299	4272	-22822	900	138	944	9.80	0.24	9.65
22.62	-30166	7676	-20125	946	121	841	9.82	0.21	9.98
22.69	-31452	7981	-20980	937	168	917	10.00	0.48	10.00
22.75	-39658	7126	-29783	1157	143	1128	10.28	1.16	10.00
22.76	-57519	5679	-43706	1044	146	1069	13.25	2.49	10.00

	J GTOC			TOT DV [km/s]			T0 [MJD]		
	mean	std	best	mean	std	best	mean	std	best
15.03	102	10	107	11.09	1.61	9.60	63420	515	63718
21.05	70	19	83	39.57	3.30	34.88	60419	1341	59446
21.25	61	14	68	28.74	4.31	23.30	61268	1283	62813
21.92	61	14	58	34.05	3.55	28.67	60877	1448	61128
22.62	56	12	66	34.80	4.59	28.58	61483	1684	62874
22.69	56	16	58	35.06	5.47	28.58	61259	1545	62808
22.75	34	14	37	36.59	4.71	33.67	60401	1644	59216
22.76	36	17	43	41.61	6.20	42.33	59037	1299	59995

Figure H.7 J, mass used, Time of flight, J GTOC, TOT DV, and launch date for sequences found by the NNH, using the cost function implemented by ESA.

ESA Value	k2 leg 1			k2 leg 2			k2 leg 3			k2 leg 4		
	mean	std	best	mean	std	best	mean	std	best	mean	std	best
15.03	0.77	0.29	0.94	0.24	0.15	0.31	0.27	0.32	0.10	0.23	0.21	0.78
21.05	0.61	0.26	0.56	0.29	0.22	0.01	0.95	0.07	1.00	0.74	0.36	1.00
21.25	0.48	0.23	0.73	0.31	0.17	0.39	0.90	0.14	0.98	0.70	0.35	0.05
21.92	0.61	0.31	0.29	0.41	0.11	0.48	0.92	0.10	0.93	0.67	0.37	0.64
22.62	0.67	0.23	0.86	0.47	0.08	0.43	0.91	0.12	0.98	0.68	0.35	0.24
22.69	0.70	0.22	0.64	0.46	0.06	0.47	0.88	0.20	0.99	0.70	0.36	0.48
22.75	0.64	0.23	0.51	0.42	0.18	0.46	0.85	0.17	0.80	0.70	0.34	0.89
22.76	0.48	0.31	0.49	0.25	0.18	0.26	0.36	0.34	0.99	0.77	0.28	0.90

	N 1			N 2			N 3			N 4		
	mean	std	best	mean	std	best	mean	std	best	mean	std	best
15.03	0.39	0.23	0.39	0.48	0.27	0.17	0.30	0.20	0.08	0.33	0.17	0.08
21.05	0.71	0.28	0.82	0.38	0.22	0.18	0.27	0.15	0.16	0.29	0.15	0.15
21.25	0.61	0.28	0.42	0.61	0.29	0.90	0.34	0.20	0.22	0.30	0.14	0.37
21.92	0.56	0.26	0.62	0.55	0.26	0.90	0.28	0.18	0.31	0.33	0.21	0.34
22.62	0.40	0.27	0.03	0.72	0.21	0.62	0.28	0.17	0.39	0.28	0.15	0.28
22.69	0.45	0.27	0.24	0.61	0.28	0.85	0.41	0.23	0.15	0.30	0.15	0.37
22.75	0.54	0.30	0.83	0.67	0.17	0.58	0.35	0.27	0.45	0.36	0.16	0.17
22.76	0.53	0.26	0.59	0.43	0.24	0.70	0.59	0.32	0.08	0.32	0.15	0.37

Figure H.8 k_2 and N values of all four legs for sequences found by the NNH, using the cost function implemented by ESA.

ESA Value	Departure DV 1			Departure DV 2			Departure DV 3			Departure DV 4		
	mean	std	best	mean	std	best	mean	std	best	mean	std	best
15.03	1.37	0.89	0.66	1.94	0.73	1.44	1.84	0.34	1.50	2.48	0.33	2.76
21.05	6.16	1.65	5.53	9.35	1.93	7.15	5.51	0.83	5.13	3.51	1.63	4.14
21.25	4.92	1.79	3.50	2.32	1.30	1.19	5.29	0.60	5.61	2.56	1.78	1.12
21.92	6.47	1.67	4.73	4.49	1.16	3.53	5.40	1.04	4.77	3.08	1.75	0.94
22.62	4.07	1.86	3.49	6.31	0.97	5.76	5.38	0.79	6.34	2.98	1.47	2.05
22.69	5.84	2.18	3.50	6.97	2.60	5.53	6.05	1.06	6.15	3.00	1.94	1.19
22.75	7.89	1.51	7.16	4.83	2.62	2.94	5.44	0.80	5.26	3.31	1.96	2.00
22.76	4.81	2.29	3.36	8.11	2.71	10.86	7.95	1.32	11.26	2.28	1.39	3.83

	Arrival DV 1			Arrival DV 2			Arrival DV 3			Arrival DV 4		
	mean	std	best	mean	std	best	mean	std	best	mean	std	best
15.03	1.50	1.07	1.18	1.62	0.69	1.10	1.66	0.32	1.62	4.21	1.37	1.90
21.05	6.60	1.68	6.43	7.73	2.06	6.22	4.21	0.67	3.78	5.53	2.49	6.38
21.25	6.32	1.23	6.79	6.63	1.87	4.88	4.14	0.95	3.71	7.51	3.54	9.19
21.92	7.00	1.78	6.88	6.62	1.74	6.46	4.48	0.76	4.86	6.55	2.95	10.21
22.62	7.95	0.93	7.21	7.04	3.18	3.72	4.40	1.11	3.50	5.93	2.50	7.80
22.69	7.21	1.04	7.82	5.52	1.39	4.32	3.96	0.71	3.56	6.82	3.03	9.18
22.75	7.92	0.98	8.50	6.34	1.57	5.63	4.36	0.87	5.68	6.89	2.34	9.11
22.76	8.43	4.03	6.68	8.90	0.92	7.14	4.48	2.73	2.55	3.68	1.89	2.64

	Time of Flight 1			Time of Flight 2			Time of Flight 3			Time of Flight 4		
	mean	std	best	mean	std	best	mean	std	best	mean	std	best
15.03	283	152	302	624	170	515	960	213	1031	1316	284	1388
21.05	391	236	304	956	284	1071	1067	351	1226	811	270	523
21.25	448	197	275	834	241	750	1130	397	1225	793	256	988
21.92	385	175	397	1032	332	1087	971	409	1208	817	198	435
22.62	387	199	279	813	227	611	1174	287	1426	839	278	926
22.69	400	152	330	815	297	672	1297	297	1338	770	180	980
22.75	385	163	492	1076	404	1487	1082	445	584	860	363	696
22.76	644	373	767	1431	428	498	1716	309	1260	690	374	707

	Stay Time 1			Stay Time 2			Stay Time 3		
	mean	std	best	mean	std	best	mean	std	best
15.03	124	21	150	112	20	90	116	20	90
21.05	117	19	124	128	22	150	126	22	94
21.25	126	22	140	132	22	150	130	19	124
21.92	120	24	149	124	21	102	133	21	146
22.62	121	19	110	126	21	149	127	23	145
22.69	116	21	94	135	22	139	120	21	101
22.75	108	15	105	123	22	150	123	23	137
22.76	122	25	120	121	21	150	117	22	150

Figure H.9 Velocity mismatches, flight times and stay times of all four legs for sequences found by the NNH, using the cost function implemented by ESA.

Appendix I

Extensive Results of Continuous Method for Additional Tests

This appendix contains the results of the continuous method for the sequences obtained by GTOC participants for three additional tests. The first test investigates the implementation of a pit in the penalty function. The second test investigates what happens if the IP method is allowed to search outside the problem bounds. The third test investigates an alternative setting for the total mission duration penalty of 20 years instead of 10 years. Each sequences has been analyzed 20 times using the continuous method. The figures summarize the mean, standard deviation and best value of those 20 runs after the Interior Point method has finished for a number of parameters. For each cost function three figures have been included. The first figure shows the results for the objective value (J), the mass use in kg, the total time of flight in years (TOF), the corresponding GTOC2 objective value (J GTOC), the sum of the velocity mismatches upon arrival and departure at the first three asteroids and, if applicable, at Earth (TOT DV), and finaly the launch date in MJD (T0). The second figure shows the k_2 and N values for each leg. The third figure specifies the flight times for each leg, the stay times at the first three asteroids and specifies all velocity mismatches upon departure and arrival individually.

I.1 Including a pit in the objective function.

R	J			Mass Used [kg]			TOF [year]		
	mean	std	best	mean	std	best	mean	std	best
1	-3837	2730	142	601	166	402	9.36	0.68	7.75
3	-2874	2350	121	502	67	420	9.76	0.29	8.92
7	-4908	1386	-3008	876	133	1043	9.69	0.35	9.90
9	-127	1156	228	460	104	293	8.65	1.63	5.30
10	-3090	2783	117	543	106	476	9.70	0.41	8.75
11	-3062	2407	110	498	108	408	9.61	0.36	9.90

	J GTOC			TOT DV [km/s]			T0 [MJD]		
	mean	std	best	mean	std	best	mean	std	best
1	97	23	142	13.53	1.58	11.09	58001	1679	57368
3	103	9	121	13.08	1.08	13.06	62074	1778	63730
7	64	13	46	13.97	2.52	11.01	58205	1374	57816
9	128	45	228	12.05	0.85	11.24	60882	2979	57031
10	99	13	117	13.32	1.25	12.62	62308	2225	64021
11	104	10	110	13.41	0.77	13.45	63107	2091	64030

Figure I.1 J, mass used, Time of flight, J GTOC, TOT DV, and launch date for sequences obtained by GTOC2 participants, when a pit is implemented in the penalty function.

R	k2 leg 1			k2 leg 2			k2 leg 3			k2 leg 4		
	mean	std	best	mean	std	best	mean	std	best	mean	std	best
1	0.55	0.24	0.81	0.37	0.23	0.13	0.69	0.13	0.80	0.52	0.32	0.82
3	0.84	0.15	0.80	0.25	0.16	0.33	0.49	0.31	0.61	0.89	0.21	1.00
7	0.35	0.23	0.47	0.37	0.11	0.40	0.58	0.18	0.58	0.48	0.25	0.52
9	0.80	0.21	0.97	0.39	0.11	0.40	0.71	0.23	0.71	0.65	0.31	0.73
10	0.73	0.22	0.74	0.37	0.11	0.50	0.64	0.27	0.65	0.50	0.34	0.38
11	0.67	0.30	0.82	0.41	0.16	0.35	0.59	0.27	0.96	0.68	0.26	0.73

	N 1			N 2			N 3			N 4		
	mean	std	best	mean	std	best	mean	std	best	mean	std	best
1	0.66	0.20	0.39	0.59	0.31	0.66	0.28	0.16	0.34	0.31	0.13	0.26
3	0.47	0.32	0.79	0.49	0.25	0.16	0.31	0.13	0.36	0.31	0.16	0.24
7	0.73	0.16	0.71	0.60	0.32	0.84	0.72	0.24	0.85	0.27	0.16	0.12
9	0.54	0.24	0.49	0.63	0.22	0.72	0.31	0.24	0.10	0.29	0.19	0.24
10	0.46	0.23	0.51	0.71	0.24	0.52	0.29	0.20	0.48	0.40	0.25	0.48
11	0.51	0.28	0.32	0.54	0.26	0.63	0.34	0.14	0.49	0.29	0.13	0.24

Figure I.2 k_2 and N values of all four legs for sequences obtained by GTOC2 participants, when a pit is implemented in the penalty function.

R	Departure DV 1			Departure DV 2			Departure DV 3			Departure DV 4		
	mean	std	best	mean	std	best	mean	std	best	mean	std	best
1	2.97	0.63	2.90	2.65	1.16	2.12	1.88	0.64	2.18	2.06	0.88	0.60
3	2.05	0.67	0.94	2.71	0.56	3.44	2.18	1.12	0.77	1.80	0.35	2.45
7	3.42	0.94	3.50	2.43	1.06	1.17	2.34	0.90	2.26	2.16	1.00	1.76
9	2.01	0.72	2.74	1.47	0.61	0.94	2.63	1.34	2.32	2.67	0.87	2.52
10	1.49	1.01	1.38	1.65	0.44	1.51	2.45	0.83	2.33	4.23	1.23	4.75
11	1.14	0.86	0.55	1.68	0.53	2.18	2.26	0.60	2.41	3.96	1.34	2.01

	Arrival DV 1			Arrival DV 2			Arrival DV 3			Arrival DV 4		
	mean	std	best	mean	std	best	mean	std	best	mean	std	best
1	3.09	0.62	3.23	2.51	0.69	2.09	1.29	0.52	0.89	2.47	1.65	3.12
3	1.76	0.67	2.16	2.21	1.15	0.95	2.42	1.08	3.29	4.19	1.11	5.69
7	2.84	0.95	2.49	1.77	0.84	1.31	2.26	1.11	2.01	2.77	2.00	1.63
9	1.65	0.76	1.12	1.49	0.81	2.67	2.13	1.19	1.68	3.74	1.61	1.12
10	1.45	0.49	1.16	1.42	0.63	1.22	2.13	0.82	1.65	4.65	1.23	6.39
11	1.80	0.70	2.34	1.64	0.49	1.04	2.08	0.94	3.47	4.60	1.43	4.61

	Time of Flight 1			Time of Flight 2			Time of Flight 3			Time of Flight 4		
	mean	std	best	mean	std	best	mean	std	best	mean	std	best
1	506	217	199	862	271	1288	948	193	745	769	314	308
3	312	116	370	639	209	434	1223	205	1410	1050	199	714
7	538	207	527	865	347	1097	1130	216	966	651	298	736
9	319	112	257	821	206	590	790	306	338	903	300	480
10	326	166	409	727	116	586	924	267	1093	1215	401	789
11	382	164	321	681	146	773	963	248	682	1150	359	1520

	Stay Time 1			Stay Time 2			Stay Time 3		
	mean	std	best	mean	std	best	mean	std	best
1	116	21	94	108	19	99	112	20	99
3	113	18	106	116	22	106	113	21	117
7	118	22	96	125	21	95	112	19	100
9	109	13	91	111	20	90	106	19	90
10	123	22	93	112	18	105	115	20	120
11	115	22	105	112	23	91	107	19	124

Figure I.3 Velocity mismatches, flight times and stay times of all four legs for sequences obtained by GTOC2 participants, when a pit is implemented in the penalty function.

I.2 Allowing the IP Method to Search Outside the Problem Bounds.

R	J			Mass Used [kg]			TOF [year]		
	mean	std	best	mean	std	best	mean	std	best
1	-4771	1391	-2066	644	132	527	9.67	0.48	8.83
3	-4068	1344	-1850	517	67	478	9.95	0.10	9.68
7	-5558	1901	-2276	779	192	955	9.88	0.22	9.67
9	-2610	994	-803	507	105	433	9.91	0.21	9.92
10	-4243	1069	-2096	570	132	382	9.77	0.34	10.00
11	-6075	1423	-4389	826	247	840	9.85	0.37	10.00

	J GTOC			TOT DV [km/s]			T0 [MJD]		
	mean	std	best	mean	std	best	mean	std	best
1	89	15	110	13.42	1.90	9.79	57781	858	57150
3	99	7	106	12.76	1.66	9.55	61731	1705	62313
7	73	19	56	14.35	2.34	10.20	58870	2410	57625
9	100	12	108	10.55	1.51	8.17	61236	2917	57002
10	95	13	112	12.58	1.32	10.26	61868	2612	64098
11	69	25	66	15.96	6.45	12.57	62789	603	62341

Figure I.4 J, mass used, Time of flight, J GTOC, TOT DV, and launch date for sequences obtained by GTOC2 participants, when the IP is allowed to search outside the problem bounds.

R	k2 leg 1			k2 leg 2			k2 leg 3			k2 leg 4		
	mean	std	best	mean	std	best	mean	std	best	mean	std	best
1	0.55	0.17	0.57	0.26	0.18	0.04	0.62	0.21	0.70	0.38	0.27	0.52
3	0.82	0.27	1.14	0.31	0.14	0.35	0.62	0.40	1.01	0.82	0.24	0.21
7	0.45	0.27	0.35	0.39	0.19	0.40	0.51	0.34	0.58	0.68	0.31	0.36
9	0.82	0.32	1.17	0.34	0.12	0.14	0.60	0.44	0.08	0.64	0.40	0.82
10	0.69	0.28	0.90	0.38	0.11	0.57	0.67	0.33	0.49	0.44	0.31	0.86
11	0.60	0.30	1.14	0.51	0.20	0.39	0.83	0.34	0.91	0.72	0.22	0.71

	N 1			N 2			N 3			N 4		
	mean	std	best	mean	std	best	mean	std	best	mean	std	best
1	0.71	0.18	0.56	0.63	0.28	0.67	0.31	0.17	0.49	0.34	0.26	0.50
3	0.52	0.37	0.22	0.49	0.38	1.47	0.30	0.13	0.29	0.30	0.17	0.08
7	0.74	0.18	0.50	0.55	0.35	0.87	0.61	0.25	0.92	0.40	0.15	0.49
9	0.48	0.30	0.09	0.76	0.37	1.46	0.36	0.16	0.16	0.34	0.27	0.50
10	0.46	0.22	1.02	0.66	0.35	0.08	0.25	0.18	0.03	0.43	0.38	0.02
11	0.69	0.35	0.06	0.59	0.28	0.53	0.30	0.14	0.36	0.33	0.27	0.26

Figure I.5 k_2 and N values of all four legs for sequences obtained by GTOC2 participants, when the IP is allowed to search outside the problem bounds.

R	Departure DV 1			Departure DV 2			Departure DV 3			Departure DV 4		
	mean	std	best	mean	std	best	mean	std	best	mean	std	best
1	3.18	0.52	3.29	2.60	1.10	1.20	1.79	0.60	1.42	2.10	0.72	1.20
3	2.44	0.61	2.61	2.43	0.72	1.47	2.38	1.19	1.20	1.92	0.47	1.33
7	3.32	0.30	3.42	2.69	1.27	1.20	2.61	0.87	2.23	2.70	1.63	1.82
9	2.32	0.36	2.12	1.25	0.27	1.17	2.49	0.93	2.13	2.15	0.68	1.20
10	2.31	0.93	2.58	1.51	0.40	1.20	2.65	0.59	1.77	3.69	1.34	2.15
11	3.44	0.72	2.28	3.09	3.60	1.20	1.52	1.02	1.20	2.07	0.79	1.35

	Arrival DV 1			Arrival DV 2			Arrival DV 3			Arrival DV 4		
	mean	std	best	mean	std	best	mean	std	best	mean	std	best
1	2.94	0.48	2.67	2.43	0.88	2.10	1.51	0.79	1.20	1.91	0.88	2.21
3	1.41	0.73	1.20	2.70	1.05	2.33	1.93	0.65	2.01	3.94	1.65	6.77
7	2.49	0.47	2.07	2.30	0.99	1.20	1.55	0.75	1.69	2.65	1.39	1.72
9	1.21	0.52	1.15	1.58	0.59	1.32	1.86	0.73	1.20	3.37	1.68	1.02
10	1.22	0.39	1.18	1.35	0.37	1.79	2.15	0.73	2.17	4.93	1.46	4.09
11	4.16	0.56	4.21	3.09	3.05	2.36	1.78	0.77	2.26	3.35	1.61	3.30

	Time of Flight 1			Time of Flight 2			Time of Flight 3			Time of Flight 4		
	mean	std	best	mean	std	best	mean	std	best	mean	std	best
1	446	207	407	884	275	1295	831	131	755	1054	490	495
3	338	107	252	648	160	1043	1174	247	1135	1122	241	918
7	565	226	713	754	177	1068	1038	270	1014	925	422	447
9	344	139	263	884	192	728	823	242	295	1223	392	2120
10	330	117	361	800	171	491	849	301	948	1256	379	1483
11	489	219	264	745	274	670	600	249	1096	1416	364	1358

	Stay Time 1			Stay Time 2			Stay Time 3		
	mean	std	best	mean	std	best	mean	std	best
1	104	30	82	103	28	81	112	30	111
3	122	34	120	138	48	288	93	79	-219
7	112	28	85	106	31	144	108	34	60
9	126	35	81	112	41	-1	106	46	139
10	118	26	91	105	51	135	110	44	144
11	130	30	91	115	23	98	106	31	77

Figure I.6 Velocity mismatches, flight times and stay times of all four legs for sequences obtained by GTOC2 participants, when the IP is allowed to search outside the problem bounds.

I.3 Changing the Threshold for the Total Time of Flight Penalty.

E Value	J			Mass Used [kg]			TOF [year]		
	mean	std	best	mean	std	best	mean	std	best
420	-412	230	-188	624	158	998	16.11	1.46	18.17
437	-837	408	-402	655	90	770	15.61	1.78	17.18
454	-784	317	-336	554	90	665	16.32	0.87	18.52
456	-1031	353	-507	695	135	829	16.10	1.78	16.10
465	-1127	255	-732	691	165	716	16.83	1.47	15.04
473	-676	252	-313	642	130	733	17.03	1.20	17.72
479	-899	135	-657	512	60	531	15.56	1.16	14.82
496	-1106	253	-761	706	116	808	17.49	1.46	18.62

	J GTOC			TOT DV [km/s]			T0 [MJD]		
	mean	std	best	mean	std	best	mean	std	best
420	55	13	28	7.03	0.90	6.32	63292	950	63184
437	55	12	42	8.10	1.37	6.41	60967	1605	61360
454	58	8	45	8.23	0.96	7.19	62931	2046	62048
456	51	12	42	8.76	1.28	6.92	60144	3095	58214
465	49	11	52	9.30	0.77	7.88	63342	1551	63334
473	51	10	43	8.96	4.98	6.64	58359	1933	57674
479	64	6	65	8.42	0.50	8.46	62141	215	62145
496	46	8	37	9.19	1.07	7.40	60299	2575	62574

Figure I.7 J, mass used, Time of flight, J GTOC, TOT DV, and launch date for sequences obtained by the NNH, using a cost function based on energy, when the penalty threshold for the total time of flight is shifted from 10 to 20 years.

E Value	k2 leg 1			k2 leg 2			k2 leg 3			k2 leg 4		
	mean	std	best	mean	std	best	mean	std	best	mean	std	best
420	0.65	0.24	0.34	0.26	0.11	0.18	0.69	0.27	0.49	0.56	0.37	0.55
437	0.56	0.27	0.36	0.30	0.14	0.21	0.52	0.17	0.53	0.51	0.35	0.87
454	0.58	0.29	0.35	0.33	0.09	0.21	0.55	0.38	0.89	0.70	0.14	0.75
456	0.47	0.28	0.70	0.28	0.15	0.47	0.89	0.14	0.86	0.37	0.36	0.63
465	0.60	0.25	0.69	0.28	0.13	0.35	0.70	0.27	0.02	0.63	0.25	0.54
473	0.48	0.24	0.34	0.40	0.14	0.48	0.74	0.13	0.85	0.84	0.12	0.86
479	0.47	0.27	0.29	0.17	0.03	0.18	0.91	0.07	0.83	0.58	0.42	0.09
496	0.55	0.27	0.98	0.31	0.10	0.40	0.59	0.24	0.34	0.67	0.26	0.98

	N 1			N 2			N 3			N 4		
	mean	std	best	mean	std	best	mean	std	best	mean	std	best
420	0.63	0.29	0.91	0.74	0.16	0.51	0.34	0.22	0.48	0.30	0.24	0.57
437	0.63	0.28	0.65	0.69	0.19	0.74	0.81	0.13	0.71	0.31	0.21	0.12
454	0.60	0.20	0.62	0.70	0.13	0.79	0.72	0.22	0.87	0.30	0.22	0.92
456	0.68	0.19	0.68	0.71	0.16	0.60	0.38	0.22	0.16	0.54	0.25	0.58
465	0.65	0.23	0.91	0.75	0.12	0.80	0.35	0.20	0.60	0.47	0.30	0.45
473	0.65	0.25	0.54	0.78	0.21	0.78	0.26	0.13	0.33	0.23	0.14	0.18
479	0.77	0.16	0.98	0.77	0.15	0.80	0.25	0.18	0.00	0.30	0.12	0.48
496	0.76	0.14	0.93	0.75	0.16	0.57	0.38	0.27	0.75	0.48	0.33	0.26

Figure I.8 k_2 and N values of all four legs for sequences obtained by the NNH, using a cost function based on energy, when the penalty threshold for the total time of flight is shifted from 10 to 20 years.

E Value	Departure DV 1			Departure DV 2			Departure DV 3			Departure DV 4		
	mean	std	best	mean	std	best	mean	std	best	mean	std	best
420	2.65	0.60	2.92	1.09	0.35	0.98	1.02	0.53	1.56	1.59	0.34	0.93
437	2.69	0.68	2.94	1.35	0.61	1.07	0.99	0.19	0.70	1.60	0.37	1.47
454	0.95	0.42	0.45	1.18	0.24	0.79	1.94	0.59	1.67	1.22	0.30	1.13
456	2.75	0.65	2.97	1.33	0.38	1.21	1.66	0.90	1.68	1.25	0.54	0.67
465	2.68	0.66	2.68	1.20	0.34	0.87	2.18	0.55	2.53	1.57	0.39	1.20
473	3.19	2.54	3.18	1.40	0.24	1.20	1.60	0.25	1.58	0.83	0.29	0.92
479	1.16	0.47	0.91	0.91	0.32	1.20	1.48	0.35	1.20	1.36	0.25	1.05
496	1.29	0.76	0.86	1.17	0.31	1.27	2.07	0.63	1.90	1.00	0.62	0.76

	Arrival DV 1			Arrival DV 2			Arrival DV 3			Arrival DV 4		
	mean	std	best	mean	std	best	mean	std	best	mean	std	best
420	1.26	0.33	1.07	0.93	0.38	0.60	1.15	0.13	1.18	3.60	1.60	2.75
437	1.43	0.50	1.15	0.88	0.51	0.29	1.85	0.25	1.73	2.59	0.34	2.74
454	0.98	0.23	1.05	1.09	0.42	1.11	1.84	0.61	1.44	2.61	1.02	3.51
456	1.54	0.51	1.20	1.26	0.49	1.30	1.74	0.62	0.85	3.53	2.11	7.53
465	1.26	0.43	1.00	1.12	0.53	0.92	1.97	0.54	1.36	4.59	1.85	7.08
473	2.04	2.71	0.70	1.38	0.66	1.28	1.21	0.28	0.97	2.60	0.91	1.89
479	0.93	0.21	1.12	1.03	0.20	1.12	2.70	0.21	2.77	1.04	0.49	1.61
496	1.20	0.36	0.77	1.13	0.42	0.39	2.61	0.34	2.31	2.97	0.93	3.88

	Time of Flight 1			Time of Flight 2			Time of Flight 3			Time of Flight 4		
	mean	std	best	mean	std	best	mean	std	best	mean	std	best
420	604	308	1024	1622	272	1692	1396	282	1527	1905	181	1969
437	625	285	1057	1455	324	1815	1713	128	1708	1556	339	1349
454	1626	267	1931	1626	267	1931	1861	166	1880	1652	177	1946
456	647	353	564	1477	247	1390	1570	334	1746	1832	177	1861
465	584	286	477	1606	331	1264	1905	112	1938	1682	228	1416
473	620	221	1128	1588	265	1342	1758	151	1672	1876	129	1997
479	558	170	483	1399	153	1335	1928	62	1998	1437	423	1303
496	751	198	683	1566	289	1683	1953	46	2000	1756	189	1990

	Stay Time 1			Stay Time 2			Stay Time 3		
	mean	std	best	mean	std	best	mean	std	best
420	122	20	139	123	23	149	111	23	137
437	120	22	150	121	22	98	113	21	100
454	116	16	93	124	18	126	118	27	103
456	118	23	93	118	26	90	118	23	137
465	121	19	130	134	18	136	114	25	132
473	116	21	96	122	26	90	140	8	148
479	118	20	99	118	19	90	124	23	106
496	121	22	149	113	22	146	127	25	150

Figure I.9 Velocity mismatches, flight times and stay times of all four legs ffor sequences obtained by the NNH, using a cost function based on energy, when the penalty threshold for the total time of flight is shifted from 10 to 20 years.

Appendix J

Continuous Search Space Visualization

In this appendix a limited search space visualization of a single leg and the winning GTOC2 sequence will be presented. The visualizations are obtained by performing a grid search. The goal of visualizing the search space is to provide some feeling for the complexity of the search space and to support various discussions in this report. Since only a small part of the total search space will be visualized, the results in this appendix provide a lower limit for the search space complexity. The search space of the single leg transfer consists of four parameters, while the search space of the GTOC2 sequence consists of 16 transfers. Performing a grid search on a 16-dimensional search space with a useful accuracy requires a huge amount of time, and therefore only two variables are selected for analyses. The selected variables are the mission start date, T0, and the time of flight to the first asteroid, TOF. The two parameters will be visualized for both the single leg and the multiple leg transfer. For the single leg transfer the search space for two different penalty settings will be presented. The variables that are not subjected to a grid search are fixed. The variables for the single leg transfer that are being fixed are k_2 and N. The parameters are set to the values corresponding to the best objective value found by the grid search. Since it is not possible to perform a grid search for all sixteen variables for the multi leg transfer, the fourteen variables other than T0 and TOF in the solution vector (equation 4.61) will be set to the variables corresponding to the best objective value found by the continuous method.

Visualization of Search Space of a Single Leg Mission

First, a part of the search space for a single leg transfer from Earth to the first asteroid of the winning GTOC2 sequence will be visualized. The search spaces of the objective function with mass equivalent penalties and with a quadratic penalty of velocity mismatches over 0.5 km/s are presented. Three different views of the same search space are shown in figures J.1 to J.3. On the left side of figures J.1 to J.3 the search space with a mass equivalent penalty in the objective function is shown. On the right side the search space for the mass equivalent penalty with the added quadratic penalty is shown. The search space visualized on the left side of figures J.1 to J.3 is the search space corresponding to the second test in figures 7.47 and 7.48, the search space visualized on the right side shows the search space for test 3. The figures show two things. The first observation is

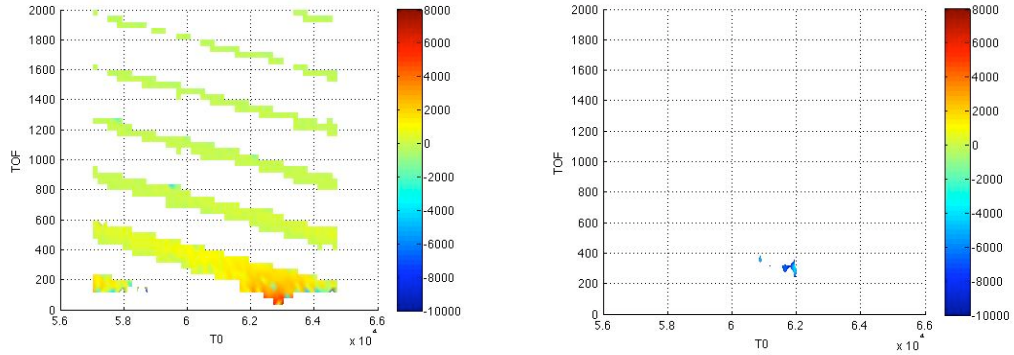

Figure J.1 Comparison of search space with mass equivalent penalty (left) and with an added quadratic penalty (right) for T0 vs. TOF.

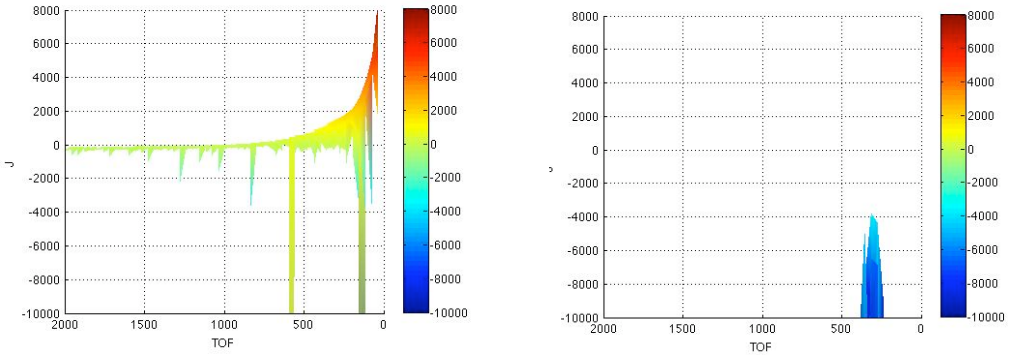

Figure J.2 Comparison of search space with mass equivalent penalty (left) and with an added quadratic penalty (right) for J vs. TOF.

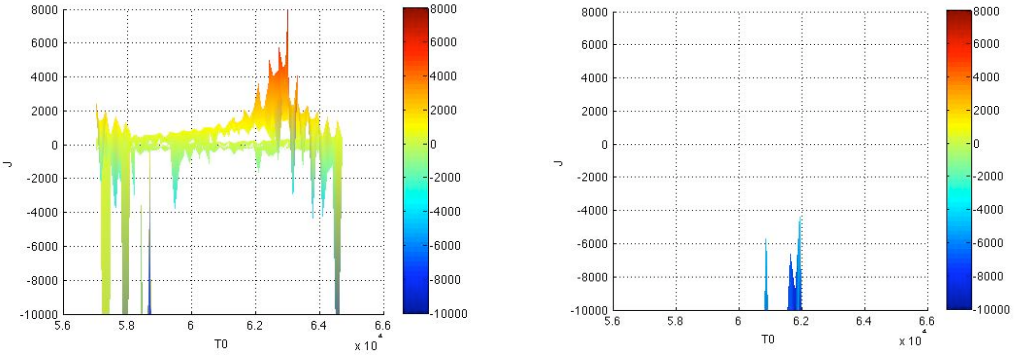

Figure J.3 Comparison of search space with mass equivalent penalty (left) and with an added quadratic penalty (right) for J vs. T0.

that the maximum value on the left side in figure J.1 is in a different location than on the right side. The maximum on the left side is located at very low TOF values, which are unrealistic for an actual mission. This observation is confirmed by the results of test 2 which indicate that low time of flight values result in high velocity mismatches upon departure and arrival, and hence are unfeasible trajectories. Applying the quadratic penalty results in the search space shown on the right side of figures J.1 to J.3. In these search spaces the maximum is located at more realistic time of flight values for an Earth-asteroid transfer. The fact that the results of test 2 and 3 do not exactly match the visualized space is due to the difference in the grid accuracy and the settings for the MC and the GA. apparently the MC in combination the GA finds better results than the grid search. Increasing the grid accuracy will probably lead to a peak in the search space closer to the values obtained with the MC and GA.

The second observation is the increase in contrast between good and bad solutions. The figures are all plotted on the same scale and same color map, so the results can be compared directly. For the search space including the quadratic penalty a large part of the search space has dropped below the axis limit of -10,000 and only the part of the search space close to the optimum is still visible. This makes it easier for an optimizer to find this optimal region. The three different views also show that in the part of the search space with objective values over -10,000 the shape is very irregular. This also agrees with the results of test 1 and 2 in figure 7.48. Those results show a strong increase in the standard deviation relative to the mean of the solutions, which indeed indicates an increase in irregularity in the search space. To show the increase in irregularity of the search space more clearly, the images in figure J.2 are plotted again in figure J.4, but on a scale starting from -20,000 instead of -10,000.

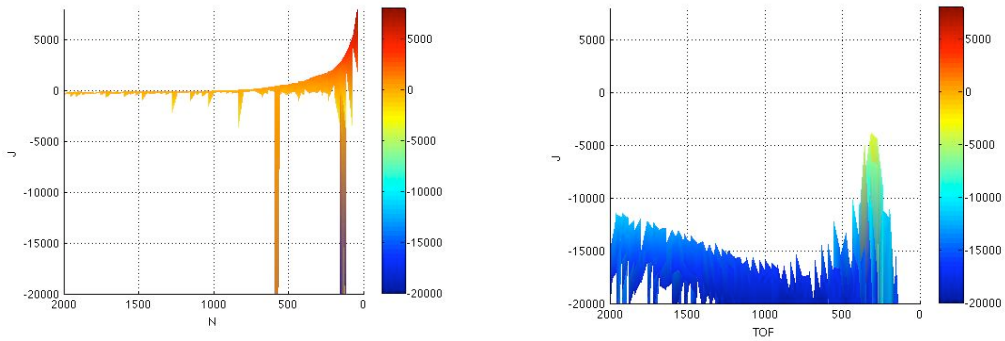

Figure J.4 Comparison of search space with mass equivalent penalty (left) and with an added quadratic penalty (right) for J vs. T0.

Visualization of Search Space of a Multileg Mission

The results of the grid search for the mission start date (T0) and the time of flight to the first asteroid (TOF) for the multiple leg transfer is shown in figures J.5 and J.6. To generate these images a cost function with a quadratic penalty for velocity mismatches over 1.2 km/s was applied. Figure J.5 shows a top view of the search space for different sections of the search space. The upper left corner shows the complete search space from the lower to the upper bound for T0 and TOF. The upper right picture is the results of a grid search performed on the part indicated by the green square in the upper left picture. It represents the 10% of the search space around the optimum solution. The lower left picture is a grid search

performed on the part indicated by the green square in the upper right picture. It represents the 3% of the search space around the optimum solution. Finally, the lower right picture shows the result of a grid search performed on the part of the search space indicated by the green square in the lower left picture. It represents the 0.5% of the search space around the optimum solution. The optimum solution is indicated by a green cross. A 3D image of the results in figure J.5 is shown in

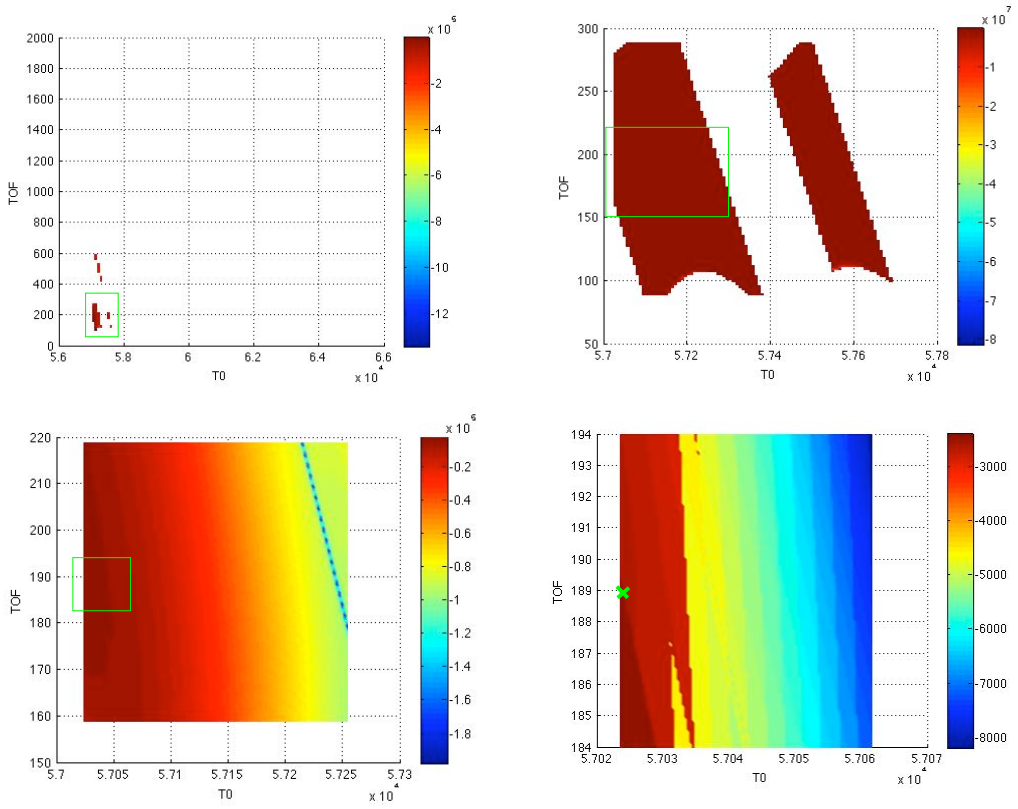

Figure J.5 Visualization of the search space for the continuous method of the asteroid sequence of the GTOC2 winner for T0 and TOF.

figure J.6. The first thing that becomes clear is that only a very limited part of the search space contains feasible solutions. This requires a method that is able to probe the search space thoroughly. The MC settings used in this report proved to be strong enough to identify these regions. The range of the objective values in the feasible regions themselves is large. There are a number of narrow spikes present. The ridge indicated by the green arrow is created by the penalty function. It is the jump as visualized schematically in figure 4.21.
The maximum value obtained by the grid search is -2416. This is close to the value found by the continuous method which was -2407 (see figure 7.18). It indicates that the continuous method is more accurate than the grid search.

In order to determine the influence of the grid accuracy and to determine if more narrow feasible solution regions exist a grid search was performed with a grid that is three times as small as the one used to generate figures J.5 and J.6. The results are summarized in figure J.7. On the left side the search space is shown with a grid accuracy of 100 intervals per variable. It is the same image as the upper left one in figure J.5. On the right side the result is presented for the grid search using 300 intervals per variable. Comparing the left image with the right image shows

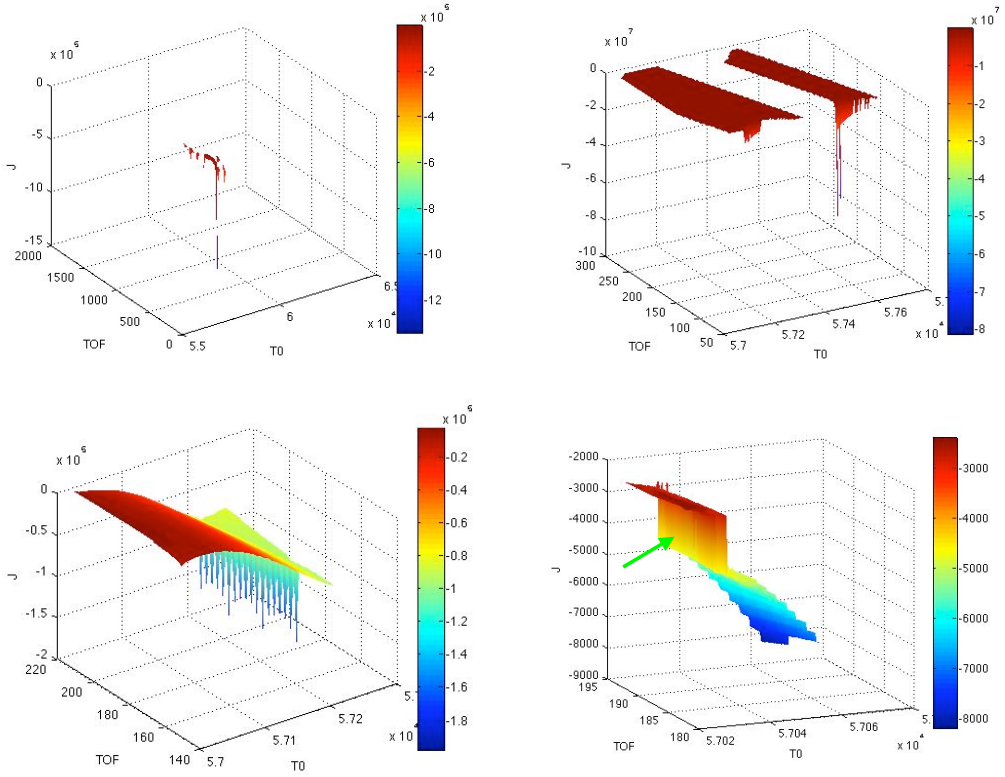

Figure J.6 3D representation of figure J.5.

that other narrow regions exist with feasible solutions that were not detected by the grid search that only used 100 intervals per variable. At the moment it is unclear if there are more regions that are even narrower than the ones found by the grid search using 300 intervals per variable. Another unanswered question at this point is whether or not the continuous method is seeing these narrow regions and discarding them because they are not optimal, or that the continuous method is not detecting these regions at all.

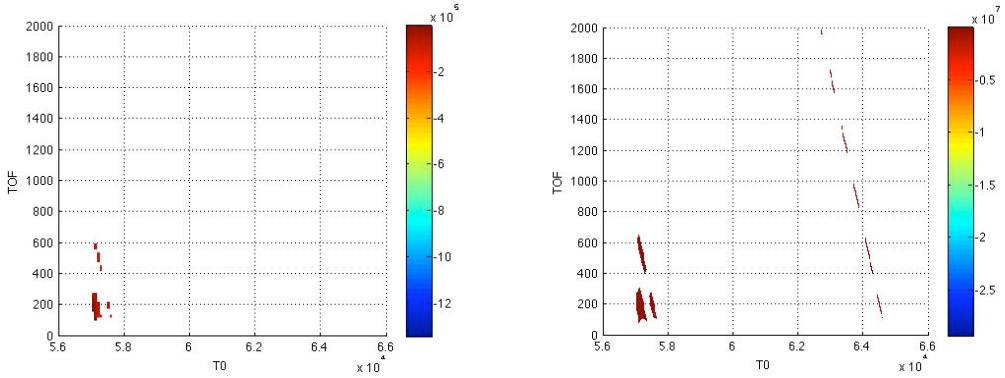

Figure J.7 Comparison of grid search with grid accuracy of 100 and 300.